March 2016

Self-Assembly and Stimuli Responsive Disassembly of Dendritic and Oligomeric Amphiphiles

Krishna Reddy Raghupathi

SELF-ASSEMBLY AND STIMULI RESPONSIVE DISASSEMBLY OF DENDRITIC AND OLIGOMERIC AMPHIPHILES

A Dissertation Presented

by

KRISHNA R. RAGHUPATHI

Submitted to the Graduate School of the
University of Massachusetts Amherst in partial fulfillment
of the requirements for the degree of

DOCTOR OF PHILOSOPHY

February 2016

Chemistry

SELF-ASSEMBLY AND STIMULI RESPONSIVE DISASSEMBLY OF DENDRITIC AND OLIGOMERIC AMPHIPHILES

A Dissertation Presented

by

Krishna R. Raghupathi

Approved as to style and content by:

_____

Sankaran Thayumanavan, Chair

_____

Richard W. Vachet, Member

_____

James Chambers, Member

_____

Susan C. Roberts, Member

_____

Craig T. Martin, Department Head

Chemistry Department

DEDICATION

To my Parents, Siblings, and my Wife

ACKNOWLEDGEMENTS

There so many wonderful people that I am very grateful to for their contribution, support, and guidance towards my PhD dissertation.

I would first like to thank my advisor Prof. Thayumanavan (Thai) without whom this dissertation was not possible. I am very grateful for his guidance, support, and encouragement in my research as well as professional development. I admire Prof Thai for his passion towards science, and for being a great inspiration to the group through leading by example.

I would like to thank my committee members, Prof. Vachet, Prof. Chambers, and Prof. Roberts, for their insights throughout my PhD, and especially their critical inputs during my PhD qualifiers. Also thanks to Dr. Weiguo Hu for giving me the opportunity to be a TA in NMR facility at UMass for four great years. I would also like to thank my master's research advisor Prof. Koodali for being a wonderful first mentor in my journey as a researcher and for being a constant source of inspiration. I would also like to thank Prof. Manna for being an excellent joint research advisor during the latter part of my master's, and for patiently teaching me several aspects of molecular biology.

A big thank you to all my collaborators Dr. Malar Azagarsamy, Jack Fuller, Uma Sridhar, Hui Wang, Poornima Rangadurai, Dr. Rajasekhar Ramireddy, Jing Guo, Jiaming Zhuang, and Dr. Subrahmanyam Ayyagari for their contributions. I should also thank two excellent undergraduate honors students Shilpa Vijayakumar and Kevin Byrne who pursued their thesis with me and contributed to my thesis greatly.

I am also thankful to visiting and summer students Oliver Roling, William Rowley, and Anshul Dhankher, who have contributed to my thesis.

I would also like to thank all current and past members of Thai Group and in particular Dendrimer Disassembly (Supramolecular Disassembly) sub group, Dr. Malar Azagarsamy, Dr. Volkan Yesilyurt, Dr. Rajasekhar Ramireddy, Dr. Deigo Amado Torres, Dr. Reuben Chacko, Dr. Andrea Delle Pelle, Dr. Bhooshan Popere, Dr. Balaji Ganapathi, Dr. Subrahmanyam Ayyagari, Dr. Mijanur Molla, Hui Wang, Kishore Raghupathi, Oyuntuya Munkhbat, Poornima Rangadurai, Uma Sridhar, and Vikash Kumar. I need to also thank my classmates in Thai Group Jiaming Zhuang, Ambata Poe, Jing Guo, and Judy Ventura who went through the challenges and excitements of graduate school along with me. Also special thanks to Karen Hakala who pampers the whole Thai Group with her delicious treats, and with warm welcoming presence.

I am also very thankful to my dearest friends from South Dakota, Satya Sai Sadhu, Sridhar Budhi, Nagaraj Chatiri, Hari Subramanian, Swetha Pothula for being great friends over the years. A special mention to my buddy Satya who has helped me so much in realizing my dream to pursue higher education in United States. Thanks for being a great friend, roommate, lab mate and above all one of a kind character.

Finally, nothing would have been possible for me without the love, care, and support of my wonderful family and extended family. My heartfelt gratitude to all the members of Raghupathi, Thopireddy, and Kontham families for being every step of the way in my journey. To my dearest wife Neelima; you have been with me for the professionally most challenging times but your presence has made it the most

blissful time as well; thank you very much for the support, friendship, and selfless love. To my lovely siblings Manga and Kishore; I have enjoyed everything we have done together, fun, games, sharing, complaining, mischief, and fighting. Many thanks to my grandparents Narsimha Reddy & Chandramma and Rami Reddy (late) & Susheela, for showing me the real example of hard work.

To my loving parents Vimala and Nagi Reddy; I am very lucky and proud to have you both in my life every single day. I am certain that you are very proud of me now as you are for every small step in my life. I admire greatly the unconditional love, and the sacrifices you both have made so that we have a better education and life. *Amma* and *Nanna,* this thesis is as much yours as mine; thank you for everything.

ABSTRACT

SELF-ASSEMBLY AND STIMULI RESPONSIVE DISASSEMBLY OF DENDRITIC AND OLIGOMERIC AMPHIPHILES

FEBRUARY 2016

KRISHNA R. RAGHUPATHI,

B.PHARMACY, OSMANIA UNIVERSITY

M.S., UNIVERSITY OF SOUTH DAKOTA

Ph.D., UNIVERSITY OF MASSACHUSETTS AMHERST

Directed by: Professor Sankaran Thayumanavan

Stimuli response is a fundamental process prevalent in all living systems, where a specific function (response) is generated in the presence of a given environmental cue (stimulus). Engineering materials for this process is often accomplished through another basic process, “self-assembly”. By understanding the key aspects of these processes scientists have developed a broad range of materials for a wide array of applications. This dissertation will primarily focus on developing stimuli responsive nanocarriers based on supramolecular assemblies of amphiphilic dendrimers and oligomers for safe transport and selective release of molecular cargo. Our concurrent goal is to also investigate several parameters which affect the molecular encapsulation and/or release through systematic structure property relationships.

Dendrimeric and Oligomeric amphiphiles are chosen as components of stimuli responsive assemblies, as they offer desirable assembly properties as

polymers (low CAC and better stability) combined with desired molecular characteristics as small molecules (uniformly disperse and reproducible). With amphiphilic dendron based assemblies: we have not only demonstrated their utility in stimuli responsive delivery using a biological (enzyme) and non-biological (temperature) stimulus, but also established the key assembly properties which dictate the nature of stimuli response. Specifically, we have deciphered the effect of unimer-aggregate equilibrium, kinetics of host and guest exchange, amphiphile molecular weight, and assembly size on stimuli responsive characteristics.

Oligomeric amphiphiles lack systematically branched architecture as dendrons, nonetheless they offer a good platform to study structure property correlations. We explore this aspect with temperature as well as photo responsive oligomeric amphiphiles. More importantly we have also shown that through rational molecular design variations (length and backbone) oligomeric amphiphile assemblies exhibit features similar to dendrimer amphiphiles. In addition to this, the ease of oligomer synthesis and the simplicity of molecular designs make them good candidates for a wide range of applications.

TABLE OF CONTENTS

Page

LIST OF FIGURES

Figure Page

LIST OF SCHEMES

CHAPTER 1

INTRODUCTION

Construction of functional materials at atomic or molecular level in nanoscale dimensions is termed as nanotechnology. The unique and interesting properties of materials at nanoscale dimensions have led to a broad range of applications such as in medicine, food, sensors, electronics, and fuels. Traditionally, the synthesis of these materials is accomplished either by a top-down or a bottom-up approach. Top-down approach as the name suggests, involves systematic scaling down of a macroscale material into much smaller nanoscale dimensions using progressively finer tools. This process however is limited to relatively larger geometries and also needs sophisticated equipment. On the other hand bottom approach uses molecular interactions such as hydrogen bonding, hydrophobic and hydrophilic effects, electrostatics, π- π stacking, van der waals, and coulomb forces to *self-assemble* the materials of interest into desired lengths and shapes.[1-3] This process is both faster and cost-effective, and with rational molecular design they are also very reproducible.

1.1 Supramolecular Self-Assembly

Self-Assembly is a fascinating and very prevalent process in nature ranging from length scales of nanoscale molecules to far-fetched galaxies. The fundamental driving force in all these entities is to establish an order through energy minimization. Supramolecular self-assembly is a spontaneous organization of

molecules driven by predominantly non-covalent forces as discussed earlier. The nature of these self-assembled structures is dictated by the inherent nature of the molecules, surrounding environment, and inter and/or intra molecular forces governing their assembly. Depending on these variations the self-assembled aggregates formed can be classified into micelles, reverse micelles, liposomes, lipid bilayers, self-assembled monolayers, etc.

Micelles are a class of supramolecular aggregates formed from self-assembly of amphiphilic molecules in aqueous solutions. The hydrophobic container properties of these aggregates have led to their use in fields such as detergents, sensing, drug delivery, and diagnostics. However the utility of micelles in these applications is better realized at minimal concentrations of amphiphiles due to factors such as toxicity and sensitivity in drug delivery and sensing respectively. This is achieved by the use of polymeric, dendrimeric, or oligomeric amphiphiles, which form micelles at low concentrations i.e. low CAC's (Critical Aggregation Concentrations).[4-6]

Micelles like other self-assembled aggregates are dynamic structures owing to the relatively weak nature of non-covalent interactions that drive their assembly. This makes them reversible structures where the fidelity of the aggregates is a fine balance between the forces which hold them together and the forces which disrupt them. This dynamic nature of the assemblies not only helps in the process of guest encapsulation and release but also provides a unique opportunity to tailor the stability of the aggregates depending on the specific application. For instance,

applications needing sustained release can prefer more stable assemblies, than the applications which necessitate burst release. This stability of the micelle assemblies can be tuned through, i). Amphiphile design (incorporation of functionalities which contribute to stability), ii). Molecular weight (greater stability with larger amphiphiles), or iii). Cross-linking (physical or chemical).

1.2 Stimuli Responsive Supramolecular Systems

Functional systems which respond to a certain change in environment with a specific stimulus are prevalent in nature from molecular to macroscopic levels. For example, regulation of blood glucose levels in the body through feedback regulation of insulin and glucagon can be deemed a stimuli responsive system at a molecular level. Similarly, nociception (processing of harmful stimuli) by nervous system is an example of stimuli response at macroscopic level. By understanding and mimicking the nature, several synthetic supramolecular systems are being studied for a broad range of applications such as controlled and/or targeted drug delivery, diagnostics, biosensors, tissue engineering, and coatings.

In the field of drug delivery significant strides have been made in diffusion based passive targeting i.e EPR (enhanced permeability and retention) effect,[7,8] and ligand recognition based active targeting. However, complete translation of these concepts into the clinic remains unfulfilled. An attractive alternative for this can be delivery systems which can respond to a specific stimulus and respond in a spatio-temporal fashion to release the drug payload. This is achieved by modifying the supramolecular assemblies such a way that they undergo a significant physical

and/or chemical transformation in response to a stimulus (specific change in environment). This transformation is expected to affect the fidelity of supramolecular assemblies in such a way that they gradually or suddenly (depending on specific need) lose their container properties and hence release the encapsulated cargo.

Depending on the source of stimulus, these responsive assemblies can be broadly classified into exogenous (external stimulus) and endogenous (internal stimulus). Exogenous stimuli refers to a stimulus which can be used as remote control to modulated the drug release, examples of such stimulus are Light, Magnetic field, Temperature, Ultrasound, and Electric field. Endogenous (internal) stimuli are based on microenvironments in cells and tissues such as pH, redox, sugars, enzymatic and non-enzymatic proteins.

1.2.1 Exogenous Stimulus

Among the several exogenous stimuli reported, temperature and light are the stimuli which are extensively studied owing to their wide applicability combined with the need for simpler apparatus.

1.2.1.1 Temperature Responsive Assemblies

Thermo/Temperature responsive systems are most widely studied class of stimuli responsive systems, where a small temperature change (most commonly elevated temperatures) results in a significant solubility change (*response*) of the colloidal aggregates. This change in solubility of colloidal assemblies affects their container properties resulting in the release of encapsulated guest molecules. These

systems are a significant improvement over *thermal therapy* where the temperature is increased locally at a cancer cells leading to their localized cell death.[9,10] Though straightforward this mode of therapy suffers from limitations such as prolonged exposure time, very high temperatures, and heat tolerance by cancer cells over time has limited its usage.[11-13]

Thermoresponsive assemblies are designed by incorporating a thermo-sensitive moiety as a hydrophilic or hydrophobic component of the constituting amphiphiles. Poly(N-isopropylacrylamide) (poly(NiPAM)) and poly ethylene glycol (PEG) have been investigated the most as thermos-sensitive components. These polymers undergo reversible phase transition at elevated temperatures termed as lower critical solution temperature (LCST),[14] and thereby affect the hydrophilic lipophilic balance (HLB) of the amphiphile. This change in HLB therefore affects the colloidal assembly leading to molecular release.

The phase transition behavior of poly(NiPAM) and PEG at LCST are perceived to be due to the differential hydration of these components as a function of temperature. At temperatures below LCST these polymers are extensively hydrated and therefore exist as random coil structures, however at LCST they result in formation of hydrophobic globules due to excessive dehydration. Nonetheless, as hydrogen bonding is a dynamic process, this phase transitions are reversible and reproducible. The LCST of these assemblies can also be precisely tuned by molecular weight variation of thermo-sensitive component or by varying the composition of other components in the amphiphile.

PEG containing assemblies in addition to their thermo-responsive behavior also have a cumulative advantage as drug delivery vehicles due to PEG's stealth property. Presence of PEG as a hydrophilic shell around the delivery vehicle protects it from the opsonization process and therefore increases its blood circulation time.[15,16] Increase in blood retention time significantly increases the accumulation of these assemblies at targeted site (cancer tissue) due to EPR effect. Localized thermal treatment at these sites therefore results in a good pharmacological action at that specific target. In addition to their use as drug delivery vehicle thermo-responsive systems are widely studied for their self-healing and sensing applications.

1.2.1.2 Light/Photo Responsive Assemblies

Light as a stimulus is an attractive tool owing to its non-invasiveness and the opportunity to achieve a remote control of the stimuli-response. The simplicity of stimulus and the flexibility to adjust its parameters such as wavelength, duration, and intensity has attracted much interest in developing several light-responsive molecular designs. Based on the structural and chemical transformation of the molecular designs in response to light, they can be classified as reversible and irreversible systems.

Reversible light responsive systems take advantage of the light induced isomerization of the responsive units which result in destabilization of the supramolecular assembly resulting in a microscopic response such as guest release or a macroscopic response such as sol-gel transformation. Photo isomerization of

azobenzene derivatives is widely studied in this regard; here irradiation at 300-380 nm and visible light results in *trans-cis* and *cis-trans* transformations respectively. For example liposomes formed by phosphocoline lipids with azobenzene group as a hydrophobic unit showed high drug encapsulation when in *trans* conformation, however irradiation of these assemblies resulted in disruption of liposome packing due to trans-cis isomerization, resulting in guest release.[17,18] Similarly trans-cis isomerization is also used to affect the HLB of the amphiphile in gene delivery.[19] Some other reversible photo isomers which are studied include azopyridine, stilbenes, and spiropyrans.

Irreversible light responsive assemblies on the other hand are achieved by incorporation of a light-sensitive aromatic protecting groups which cleaves upon light irradiation to affect the HLB, hence prompting a guest release. Nitrobenzyl esters are well studied in this class; a saturated hydrocarbon conjugated nitrobenzene group is used as a hydrophobic tail of the amphiphile, which is cleaved upon UV-irradiation hence affecting the HLB and the release of encapsulated contents.[20] Similarly, pyrenylmethyl esters were also studied as light cleavable hydrophobic functionalities; here pyrene cleavage of pyrene moiety which drives micellization is cleaved with 365 nm light source causing disassembly.[21] Other functional groups which irreversibly transform under light irradiation are malachite green, and 2-diazo-1,2-napthoquinone moieties.

Though light responsive assemblies are promising the systems which use UV and low wavelength visible light have drawbacks in their utility as drug delivery

vehicles; i). low penetration depth (due to scattering of low wavelength light by the soft tissues), and ii). UV light induced damage of healthy skin tissue. However, this can be resolved by using either (a). photo-sensitive groups which can respond to higher wavelength near infrared (NIR) radiation,[22] or by exploiting a two-photon technology which can be used with the existing systems that respond to UV light,[23] albeit without above mentioned limitations.

1.2.2 Endogenous Stimulus

Endogenous (internal) stimuli are a class of stimuli responsive drug delivery vehicles which respond to environment inherent to certain physiological conditions or a certain pathological state. Three of the most widely studied stimuli pH, redox, and enzyme stimuli are discussed below.

1.2.2.1 pH Responsive Assemblies

Physiological pH in the body is 7.4, and this is required for optimal function of enzymes and to maintain homeostasis. Except the gastro intestinal tract where the pH gradient tends to be rather drastic and sharp, the pH variations are very minimal at cellular and sub-cellular levels. However a sharp pH gradient does exist across the body at both cellular as well as systemic levels in certain pathological states. These abnormalities indicate an infected, inflamed, or malignant tissue, where the extracellular pH tends to be slightly acidic (5-7). On the other hand pH gradient after cellular uptake is also well defined with early endosome (5-6), late lysosome (4-5). These pH graduations (extracellular and intracellular) thus provide a great opportunity in drug delivery through smart molecular designs.

At a molecular level it can be perceived that assembly forming molecules containing ionizable functionalities such as amines, carboxylic acids are best suited for this purpose. Since the charge is directly associated with solubility, variations in pH can be used to prompt a charge generation or removal which affects the HLB significantly. Contrarily pH responsive assemblies are also designed using pH labile functionalities such as acetals, ketals, hydrazine, and imines to cause an irreversible change in HLB (Scheme 1.1)

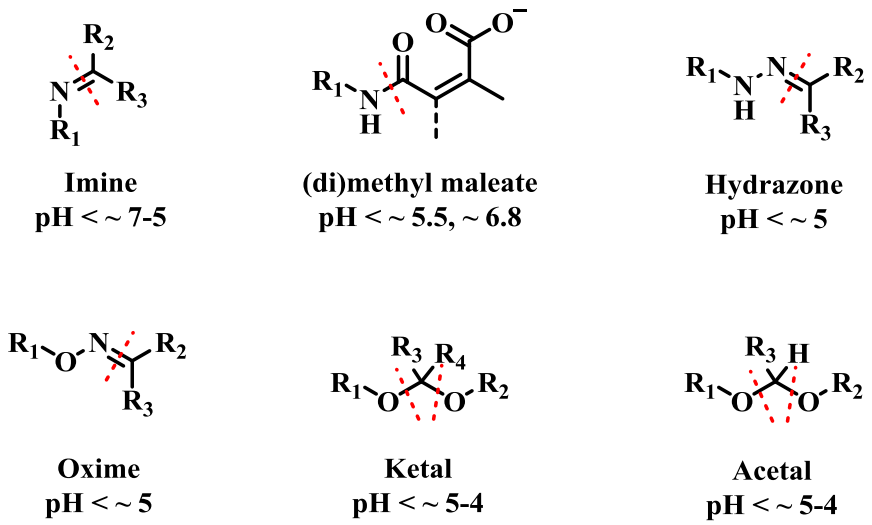

Scheme 1.1. pH cleavable functionalities and their pH sensitive range.

Several pH responsive systems are reported based on the above mentioned molecular design criteria on several platforms such as polymer-drug conjugates, micelles, polymerosomes, nanogels, and dendrimers. Among them dendrimers offer a promising platform due to the multivalent nature of pH sensitive units which can lead to a sharp change in assembly characteristics. Additionally, dendrimers and hyperbranched polymers are also explored as drug conjugates where the drug

molecules are covalently conjugated to the dendrons through pH cleavable units as prodrugs.

1.2.2.2 Redox Responsive Assemblies

Redox responsive systems utilize the huge disparity in of redox potential that exist in extracellular environment (~2 - 10 μM Glutathione (GSH)) *vs* the intracellular environment (~ 2 – 10 mM Glutathione). Additionally extracellular tumor microenvironments are also known to have significantly higher concentration of GSH in comparison to normal tissues. This provides an excellent opportunity for applications requiring intracellular delivery and tumor directed delivery respectively. Though there are several delivery platforms used for generation of redox responsive assemblies, most of the systems are exclusively based on disulfide linkages, which are prone to cleave in reducing environments.

Intracellular gene delivery is one of the widely explored classes of redox responsive systems where a plasmid DNA or siRNA (payload) is protected from extracellular components and cross the cell membrane to reach cytosol and thereby achieve significantly greater transfection efficiencies. This is done either by complexation/conjugation with positively charged polymers or by encapsulation in disulfide crosslinked micelles and liposomes. Similarly several researches have reported targeted release of anti-cancer drug payloads with disulfide crosslinked assemblies with a good control over the release kinetics.

1.2.2.3 Enzyme Responsive Assemblies

Amongst the endogenous stimuli responsive systems, enzymes/proteins can be considered primary imbalances as altered expression of enzymes such as proteases, glycosidases, acyl transferases and phospholipases are directly associated with several pathological conditions. Therefore designing supramolecular assemblies which can undergo morphological transformation in the presence of a specific enzyme gives a unique opportunity in the field of drug delivery owing to the highly specific nature of the enzyme transformations.

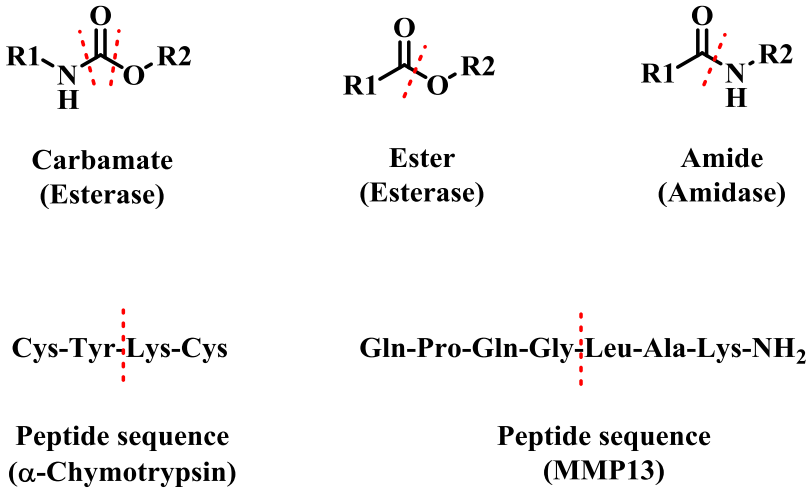

Scheme 1.2. Enzyme cleavage substrates and the cleavage site of enzymatic reaction.

While the molecular design of most stimuli responsive assemblies do not need significant emphasis on the spatial placement of the responsive functionalities, this factor is of greater importance in enzyme responsive assemblies considering the macromolecular nature of both the enzymes and supramolecular assemblies

(diffusion/collision limited). For example it has been reported that factors such as substrate accessibility[24] and assembly size[25] play a critical role in altering the kinetics of enzyme response and the subsequent molecular release. The common theme in the design is however to affect the HLB of supramolecular assembly by influencing the molecular interactions through a hydrolytic cleavage of enzyme substrates.

In drug delivery, enzyme responsive assemblies which can precisely deliver the payload in intracellular as well as extracellular compartments have been reported. Short peptide sequences which are designed and conjugated on to the supramolecular assemblies for Matrix metalloproteinase's (MMP's), α-Chymotrypsin, and Thermolysin are few examples of enzymes prompting extracellular drug release. On the other hand peptide sequences which can be phosphorylated by kinases (predominantly overexpressed in inflamed cells) and substrates which can be degraded by Cathepsin B(overexpressed in malignant tumors) are examples of intracellular delivery. Though significant literature has been report on enzyme mediated drug release, their utility *in vivo* still needs further evaluation to recognize the precise enzyme amounts to prompt drug release.

1.3 Stimuli Responsive Facially Amphiphilic Molecules

Amphiphilic molecules where the water soluble hydrophilic and water insoluble hydrophobic domains are separated by a rigid longitudinal axis are considered facially amphiphilic. Our group has reported a unique class of facially amphiphilic molecules with dendrimer architecture, composed of hydrophilic and

hydrophobic components in each repeat unit. This was achieved by using a biaryl based AB2 monomer as the core followed by iterative synthesis with corresponding AB2 monomers (aryl or biaryl) to achieve amphiphilic dendrons of different generations (proportional to number of iterations) where the amphiphilic functionalities are placed on each repeat unit.[26,27] We hypothesized that the inherent twist associated with the biaryl core and the macromolecular features of these molecules would make them facially amphiphilic.

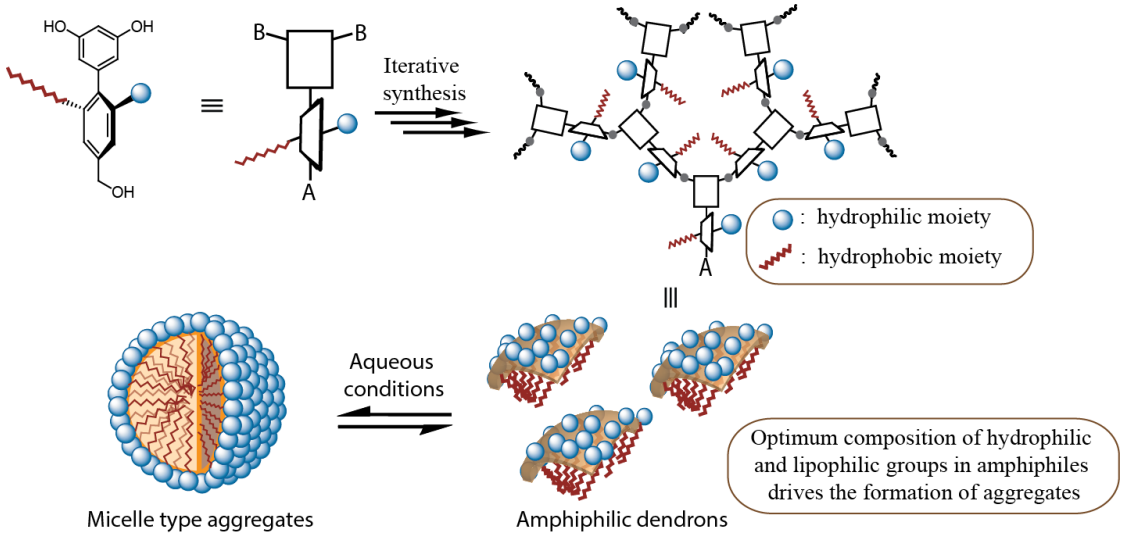

Figure 1.1. Facially amphiphilic dendron structure with biaryl AB2 core. Micelle type assemblies formed from these amphiphiles.

These dendrons spontaneously self-assemble to form micelle type aggregates at micromolar to sub-micromolar concentrations (low CAC's) and also sequester hydrophobic guest molecules in their interiors. It should be noted that the assemblies achieved from these amphiphiles (100 – 200 nm) were relatively large in comparison to conventional micelles, which was verified to be due to the lack of

conformational flexibility in the amphiphile backbone.[28] Nonetheless the unique supramolecular features of these dendrons such as low CAC's, container property, and uniformly disperse nature (molecular weights) offer an excellent opportunity to study structure-property relationships in regards to the importance of precise molecular designs in several applications.

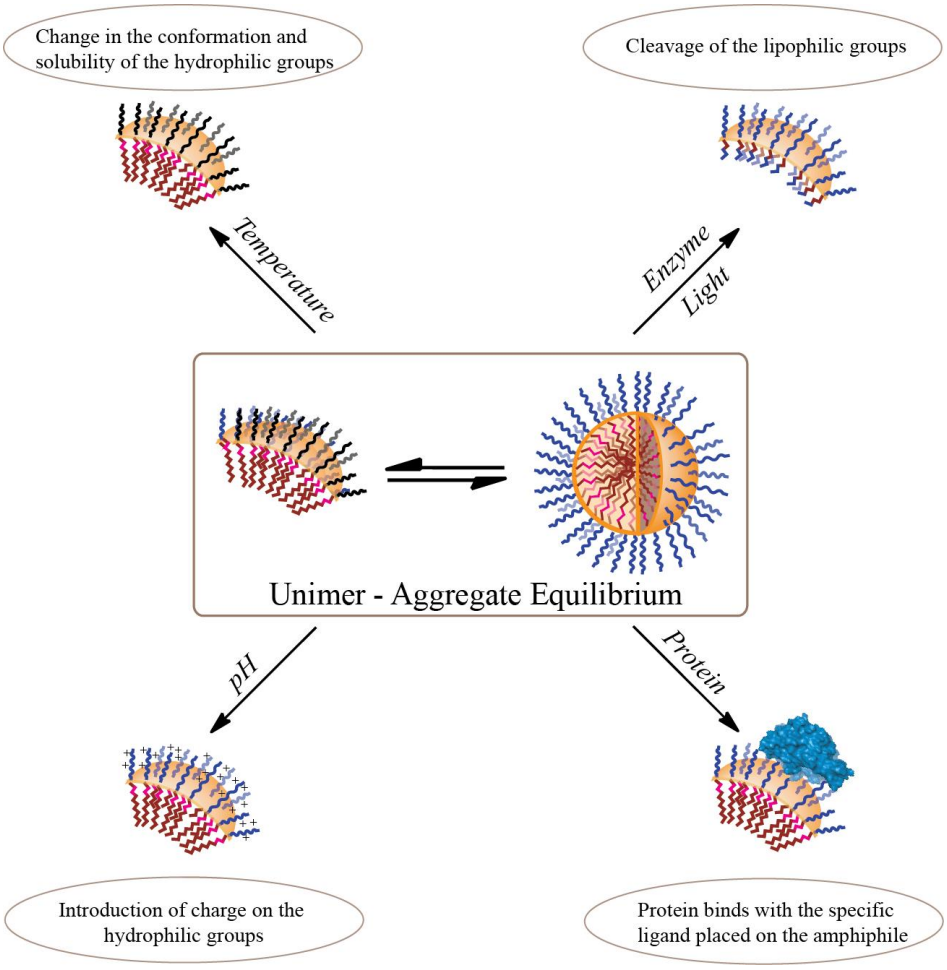

Figure 1.2. Schematic representation showing the role of unimer-aggregate equilibrium in stimuli responsive facially amphiphilic dendron assemblies.

Unlike classical dendrimeric micelles (unimolecular micelles),[29,30] the aggregates formed from these dendrons are self-assembled thermodynamic structures, which are assumed to be in equilibrium with their corresponding unimeric amphiphiles. The nature of this equilibrium is therefore dictated by the stability of the aggregates. By designing the amphiphiles such that their assembly is adversely affected in the presence of a specific stimulus we have demonstrated a series of stimuli responsive systems as shown in Figure 1.2. The insights obtained from these studies were also applied to relevant facially amphiphilic polymeric and oligomeric designs developed in our laboratory.

1.4 Summary and Dissertation Overview

In this chapter, an introduction to stimuli responsive systems based on supramolecular self-assembly was discussed. Fabrication of functional nanomaterials through self-assembly directed bottom up approach is not only a faster process but also economically more feasible. By understanding the molecular forces which drive self-assembly combined with a rational molecular design, nanomaterials can be achieved with good precision. Considering the reversible nature of self-assembled structures, additional stabilization such as crosslinking is required in applications where the integrity of self-assembled structures need to be maintained.

In stimuli responsive applications, the reversible nature of supramolecular interactions is utilized to disrupt the self-assembly and achieve corresponding

molecular release in the presence of a specific stimulus. Based on the origin of stimulus, the stimuli used in drug delivery were classified as exogenous or endogenous. The significance of each stimulus, the molecular design parameters that need to be considered, and an overview of few reported examples were discussed. Stimuli responsive facially amphiphilic molecules and their unique properties owing to their peculiar molecular design and self-assembly properties were also discussed.

The focus of this dissertation is to understand the unimer-aggregate equilibrium in stimuli responsive facially amphiphilic dendron assemblies, followed by the translation of these principles into synthetically more feasible oligomeric designs. In Chapter 2, enzyme responsive assemblies with tunable guest release will be discussed. Photo crosslinking of dendron assemblies is explored to understand the role of unimer-aggregate equilibrium as well as to tune the molecular release. In Chapter 3, temperature responsive facially amphiphilic dendron assemblies which exhibit unique sub-LCST characteristics will be discussed. The effect of this sub-LCST phenomenon of host and guest exchange dynamics will be presented. In Chapter 4, the molecular design basis for the sub-LCST phenomenon is explored with a series of oligomeric molecular designs. The role of backbone rigidity in sub-LCST behavior of amphiphilic assemblies and factors which contribute to the backbone rigidity will be discussed. In Chapter 5, general conclusions of the dissertation followed by future directions to i). further understand the unimer-aggregate equilibrium with dendron assemblies and ii). photoresponsive assemblies using oligomeric amphiphiles will be disused.

1.5 References

1. Zhang, S., Fabrication of novel biomaterials through molecular self-assembly. *Nat Biotech* **2003,** *21* (10), 1171-1178.

2. Balzani, V.; Credi, A.; Raymo, F. M.; Stoddart, J. F., Artificial Molecular Machines. *Angew. Chem. Int. Ed.* **2000,** *39* (19), 3348-3391.

3. Farokhzad, O. C.; Langer, R., Impact of Nanotechnology on Drug Delivery. *ACS Nano* **2009,** *3* (1), 16-20.

4. Torchilin, V. P., Structure and design of polymeric surfactant-based drug delivery systems. *Journal of Controlled Release* **2001,** *73* (2-3), 137-172.

5. Jones, M.-C.; Leroux, J.-C., Polymeric micelles – a new generation of colloidal drug carriers. *Eur. J. Pharm. Biopharm.* **1999,** *48* (2), 101-111.

6. Savariar, E. N.; Aathimanikandan, S. V.; Thayumanavan, S., Supramolecular assemblies from amphiphilic homopolymers: Testing the scope. *J. Am. Chem. Soc.* **2006,** *128* (50), 16224-16230.

7. Kennedy, J. E., High-intensity focused ultrasound in the treatment of solid tumours. *Nat Rev Cancer* **2005,** *5* (4), 321-327.

8. Sasaki, K.; Medan, M. S.; Azuma, T.; Kawabata, K.-i.; Shimoda, M.; Umemura, S.-i., Effect of Echo-Guided High-Intensity Focused Ultrasound Ablation on Localized Experimental Tumors. *J Vet Med Sci.* **2006,** *68* (10), 1069-1074.

9. Moseley, P. L., Heat shock proteins and heat adaptation of the whole organism. *J. Appl. Physiol.* **1997,** *83* (5), 1413-1417.

10. Dewhirst, M. W.; Viglianti, B. L.; Lora-Michiels, M.; Hanson, M.; Hoopes, P. J., Basic principles of thermal dosimetry and thermal thresholds for tissue damage from hyperthermia. *Int. J. Hyperthermia.* **2003,** *19* (3), 267-294.

11. Boutris, C.; Chatzi, E. G.; Kiparissides, C., Characterization of the LCST behaviour of aqueous poly(N-isopropylacrylamide) solutions by thermal and cloud point techniques. *Polymer* **1997,** *38* (10), 2567-2570.

12. Aathimanikandan, S. V.; Savariar, E. N.; Thayumanavan, S., Temperature-sensitive dendritic micelles. *J. Am. Chem. Soc.* **2005,** *127* (42), 14922-14929.

13. Hocine, S.; Li, M.-H., Thermoresponsive self-assembled polymer colloids in water. *Soft Matter* **2013,** *9* (25), 5839-5861.

14. Knop, K.; Hoogenboom, R.; Fischer, D.; Schubert, U. S., Poly(ethylene glycol) in Drug Delivery: Pros and Cons as Well as Potential Alternatives. *Angew. Chem. Int. Ed.* **2010,** *49* (36), 6288-6308.

15. Maeda, H.; Wu, J.; Sawa, T.; Matsumura, Y.; Hori, K., Tumor vascular permeability and the EPR effect in macromolecular therapeutics: a review. *J. Controlled Release.* **2000,** *65* (1-2), 271-284.

16. Maeda, H.; Bharate, G. Y.; Daruwalla, J., Polymeric drugs for efficient tumor-targeted drug delivery based on EPR-effect. *European Journal of Pharmaceutics and Biopharmaceutics* **2009,** *71* (3), 409-419.

17. Lu, J.; Choi, E.; Tamanoi, F.; Zink, J. I., Light-activated nanoimpeller-controlled drug release in cancer cells. *Small* **2008,** *4* (4), 421-426.

18. Yuan, Q.; Zhang, Y. F.; Chen, T.; Lu, D. Q.; Zhao, Z. L.; Zhang, X. B.; Li, Z. X.; Yan, C. H.; Tan, W. H., Photon-Manipulated Drug Release from a Mesoporous Nanocontainer Controlled by Azobenzene-Modified Nucleic Acid. *Acs Nano* **2012,** *6* (7), 6337-6344.

19. Liu, Y. C.; Le Ny, A. L. M.; Schmidt, J.; Talmon, Y.; Chmelka, B. F.; Lee, C. T., Photo-Assisted Gene Delivery Using Light-Responsive Catanionic Vesicles. *Langmuir* **2009,** *25* (10), 5713-5724.

20. Yesilyurt, V.; Ramireddy, R.; Thayumanavan, S., Photoregulated Release of Noncovalent Guests from Dendritic Amphiphilic Nanocontainers. *Angew. Chem.-Int. Edit.* **2011,** *50* (13), 3038-3042.

21. Jiang, J. Q.; Tong, X.; Zhao, Y., A new design for light-breakable polymer micelles. *J. Am. Chem. Soc.* **2005,** *127* (23), 8290-8291.

22. You, J.; Shao, R. P.; Wei, X.; Gupta, S.; Li, C., Near-Infrared Light Triggers Release of Paclitaxel from Biodegradable Microspheres: Photothermal Effect and Enhanced Antitumor Activity. *Small* **2010,** *6* (9), 1022-1031.

23. Goodwin, A. P.; Mynar, J. L.; Ma, Y. Z.; Fleming, G. R.; Frechet, J. M. J., Synthetic micelle sensitive to IR light via a two-photon process. *J. Am. Chem. Soc.* **2005,** *127* (28), 9952-9953.

24. Bosma, A. Y.; Ulijn, R. V.; McConnell, G.; Girkin, J.; Halling, P. J.; Flitsch, S. L., Using two photon microscopy to quantify enzymatic reaction rates on polymer beads. *Chem Commun.* **2003,** (22), 2790-2791.

25. Thornton, P. D.; McConnell, G.; Ulijn, R. V., Enzyme responsive polymer hydrogel beads. *Chem Commun.* **2005,** (47), 5913-5915.

26. Bharathi, P.; Zhao, H. D.; Thayumanavan, S., Toward globular macromolecules with functionalized interiors: Design and synthesis of dendrons with an interesting twist. *Org. Lett.* **2001,** *3* (12), 1961-1964.

27. Thayumanavan, S.; Bharathi, P.; Sivanandan, K.; Vutukuri, D. R., Towards dendrimers as biomimetic macromolecules. *CompteC. R. Chimie.* **2003,** *6* (8-10), 767-778.

28. Ambade, A. V.; Aathimanikandan, S. V.; Van der Poll, D.; Thayumanavan, S., Smaller building blocks form larger assemblies: Aggregation behavior of biaryl-based dendritic facial amphiphiles. *J. Org. Chem.* **2007,** *72* (22), 8167-8174.

29. Liu, M. J.; Kono, K.; Frechet, J. M. J., Water-soluble dendritic unimolecular micelles: Their potential as drug delivery agents. *J. Controlled Release.* **2000,** *65* (1-2), 121-131.

30. Hawker, C. J.; Wooley, K. L.; Frechet, J. M. J., Unimolecular Micelles and Globular Amphiphiles - Dendritic Macromolecules as Novel Recyclable Solubilization Agents. *J. Chem. Soc., Perkin Trans. 1* **1993,** (12), 1287-1297.

CHAPTER 2

GUEST RELEASE CONTROL IN ENZYME SENSITIVE, AMPHIPHILIC DENDRIMER BASED NANOPARTICLES THROUGH PHOTOCHEMICAL CROSSLINKING

2.1 Introduction

For supramolecular assemblies to have a broad impact, it is essential that they not only sequester guest molecules, but also release these bound guest molecules in response to a specific trigger. Among supramolecular assemblies, micelles have attracted great interest due to their ability to sequester lipophilic guest molecules in an aqueous environment.[1-5] This ability, combined with the fact that micellar assemblies are often nanoscopic in size, renders these assemblies of interest in a variety of applications, including drug delivery.[6-11] To this end, there have been several reports on stimuli-responsive micellar assemblies that respond to variations in pH, redox conditions, light, and temperature.[12-25] Assemblies that respond to variations in enzymatic activity, though not as prominent in the literature,[26-31] are also of great interest, because aberrations in enzymatic activity or protein concentration are the primary biological imbalances associated with many diseases.[32-34]

Amphiphilic assemblies generated from macromolecules, such as polymers and dendrimers, exhibit added advantages as stimuli-responsive systems, since these assemblies exhibit low critical aggregate concentrations (CAC) and high inherent stabilities.[35-38] Dendrimers are particularly interesting, allowing for precise control over molecular weights, thus providing a unique opportunity for developing fundamental structure–property correlations.[7] Enzyme-responsive dendrimers have been reported, wherein an enzyme-induced cleavage of a bond triggers a cascade of events that results in the covalent disassembly of the dendritic molecules.[27,46-50] In these cases, the molecules, to be released in response to the enzymatic reaction, are covalently attached to the dendrimer. It is interesting to develop strategies in which there is no necessity for covalently modifying the guest molecules to be released, as they allow for using a broad range of lipophilic guest molecules. Our research group has recently reported on such a possibility using our facially amphiphilic dendrimers as the host scaffold.[51] In this system, the guest molecules are non-covalently sequestered within the dendrimer assembly, and are then released in response to an enzymatic reaction, because of the change in the hydrophilic–lipophilic balance (HLB) caused by the cleavage of the substrate functionality. In that preliminary communication, we have demonstrated some degree of control over the guest release that can be obtained by varying the dendron generation. However, the tunability in the release rate was relatively limited. Thus, we have been interested in developing an approach where systematic control over guest-molecule release can be conveniently achieved. Herein, with the aid of photochemical reactions, we demonstrate that the tunability in the guest-molecule

release can be achieved by controlling the availability of the substrate functionalities in the dendrimers to the enzymes. We arrived at this strategy by seeking a correlation between the enzymatic reaction that causes the amphiphilic dendrimer to lose its hydrophilic-lipophilic balance and the release of non-covalently encapsulated guest molecules. We detail our findings on both of these aspects in this manuscript.

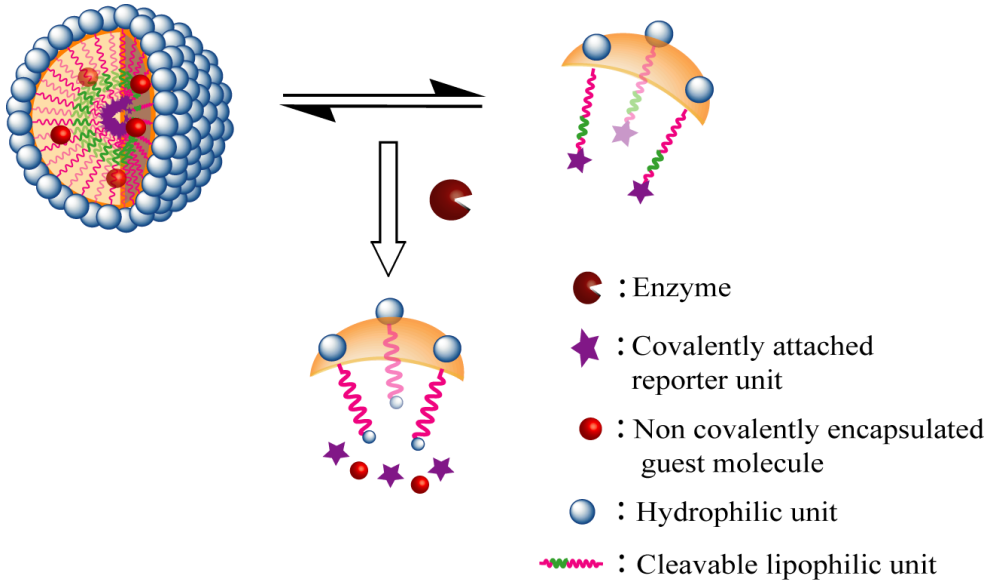

Figure 2.1. Schematic representation of enzyme induced release of covalently attached reporter units and non-covalently encapsulated guest molecules.

2.2 Molecular Design and Synthesis

To understand the correlation between the extent of enzyme-induced bond cleavage and the guest-molecule release, it is important that we introduce a reporter element in our dendrons, in which the cleavage reaction is reliably analyzed along with the release of the non-covalently encapsulated guest molecules (Figure 2.1). Fluorescence is a convenient and sensitive technique for this purpose. In our molecular design, it is essential that the enzyme-induced cleavage reaction

disconnects the lipophilic component of the amphiphilic dendrimer thus resulting in a more hydrophilic functionality at the dendron end. This change forms the basis for the stimulus-induced change in HLB, which will result in the release of the guest molecules. Therefore, we searched for a lipophilic fluorophore that is rendered non-fluorescent when attached to the dendron, but becomes fluorescent upon liberation from the dendritic backbone due to the enzymatic reaction. The hydroxycoumarin derivative, 4-methylumbelliferone (MUF), is highly fluorescent; however, the ester derivative of this molecule is not fluorescent.[52-54] Therefore we sought to utilize the esterase-induced cleavage of the ester functionality in molecule **A** (Figure 2.2), as the fluorescence reporting event. However, we found the hydrolytic stability of the phenolic ester in **A** to be poor even in the absence of the enzyme. Since it has been reported that the alkoxy coumarins are also non-fluorescent, we utilized the acetal-modified coumarin ester **B**. In this case, the esterase-induced cleavage of the ester would produce a hemiacetal, which is expected to decompose in situ to afford the fluorescent molecule MUF. When **B** was subjected to an enzymatic cleavage reaction, the solution indeed turned highly fluorescent with time, indicating the formation of MUF.

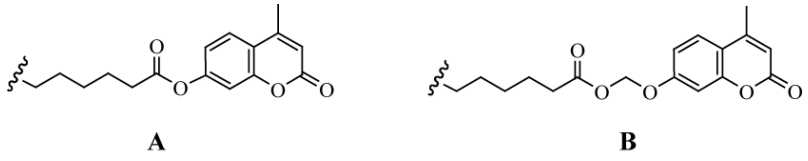

Figure 2.2. Coumarin based substrates for enzymatic cleavage.

We envisaged the use of the 1,3-dipolar Huisgen cycloaddition reaction, popularly referred to as click reaction, to attach the fluorophore precursor to the dendritic backbone. Accordingly, our target dendron structure is shown as structure **1** (Scheme 2.1). In this structure, the pentaethyleneglycol unit forms the hydrophilic functionality of the dendritic molecule, while the coumarin derivative constitutes the lipophilic component. We anticipated that the enzymatic cleavage of the ester bonds in dendron **1** by porcine liver esterase (PLE), should afford the carboxylic acid based dendron product **2** that contains hydrophilic functionalities at either face of the dendron and thus would lose its ability to non-covalently sequester hydrophobic guest molecules (Scheme 2.1).

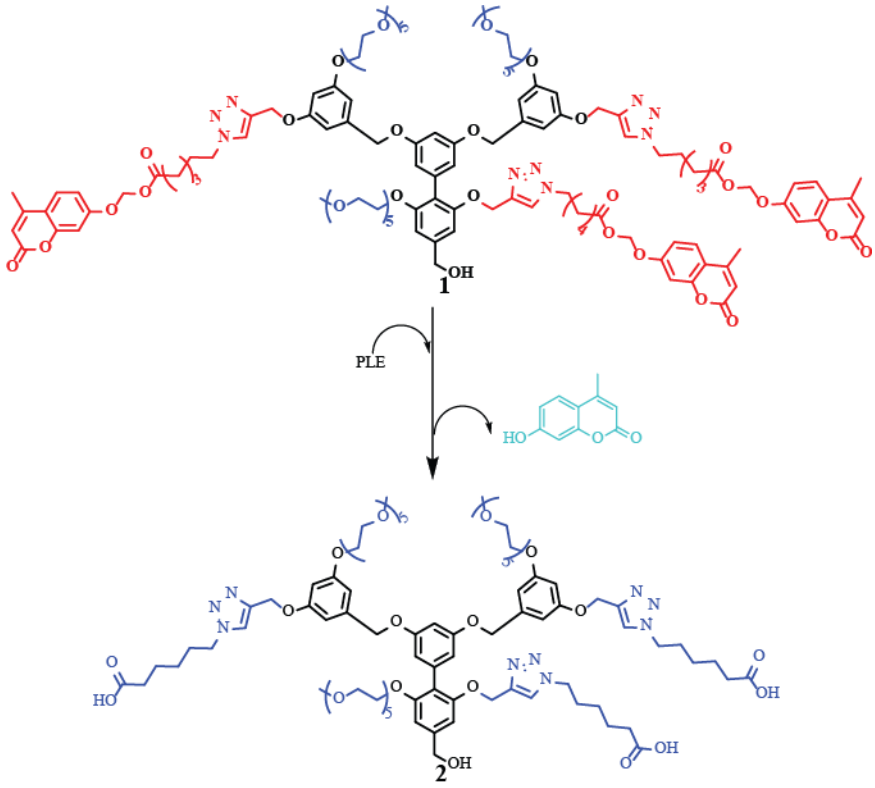

Scheme 2.1. Enzymatic action on target dendron **1**.

Synthesis of molecule **1** was approached in a modular fashion. The dendritic precursor to target molecule **1** is represented by molecule **5** in Scheme 2.2. Molecule **5** was assembled from the biaryl building block unit **3** and peripheral unit **4**. We have previously reported the synthesis of the biaryl building block **3** containing the pentaethyleneglycol and propargyl functionalities.[9] The reaction between **3** and **4** was carried out under potassium carbonate conditions to obtain **5** which was then treated with the acetal-functionalized coumarin **6** containing an azide moiety to obtain the targeted dendron **1** in 70% yield under click chemistry conditions.[55-58] Compound **6** was obtained from a reaction between MUF, dibromomethane, and 6-azidohexanoic acid in 36% yield (Scheme 2.2).

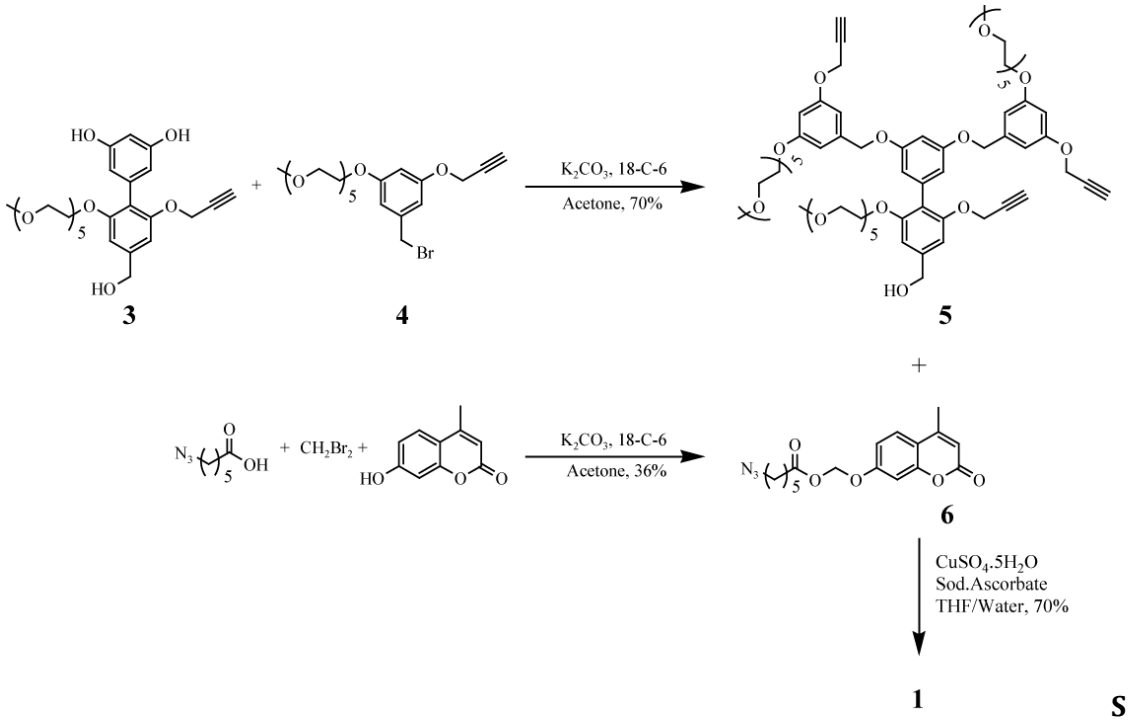

Scheme 2.2. Synthesis of target dendron **1**.

2.3 Characterization of the Assembly

We were first interested in confirming the micelle-type assemblies formed by G1 dendron **1**. We have previously reported that the most drastic change in the critical aggregation concentration (CAC) occurred from the monomer to G1-dendron; the CAC gain from the G1 to G2 dendron was relatively small.[31,51,59] Therefore, we focused on the simpler G1 dendron for the studies outlined here. It is essential, however, that we confirm that the CAC for the G1 dendron **1** synthesized here is indeed in the micromolar range. We decided to determine the CAC of **1** by using the same lipophilic molecule that will be used for observing the non-covalent guest release. To concurrently analyze the release of the non-covalently sequestered guest molecule, it is essential that the photophysical features of the guest dye molecule are very different from that of the coumarin derivatives. Accordingly, we chose 1,1′-dioctadecyl-3,3,3′3′-tetramethylindo carbocyanine perchlorate (DiI) as the guest molecule, which absorbs at 530 nm and emits at 573 nm. DiI is a hydrophobic molecule and is therefore not soluble in water by itself. However, when it is embedded in the hydrophobic interior of the micelles in aqueous solution, a finite concentration of this dye molecule would be present in the aqueous solution (Figure 2.3a).

The CAC for the assembly was determined from the plot of fluorescence response of DiI as a function of the dendron concentration.[14] A sudden change in the emission intensity of DiI was observed around 9.40 μM concentration of G1; this can be attributed to the onset of micelle formation (Figure 2.3b). To confirm the formation of the micellar assemblies, dynamic light scattering (DLS) experiments

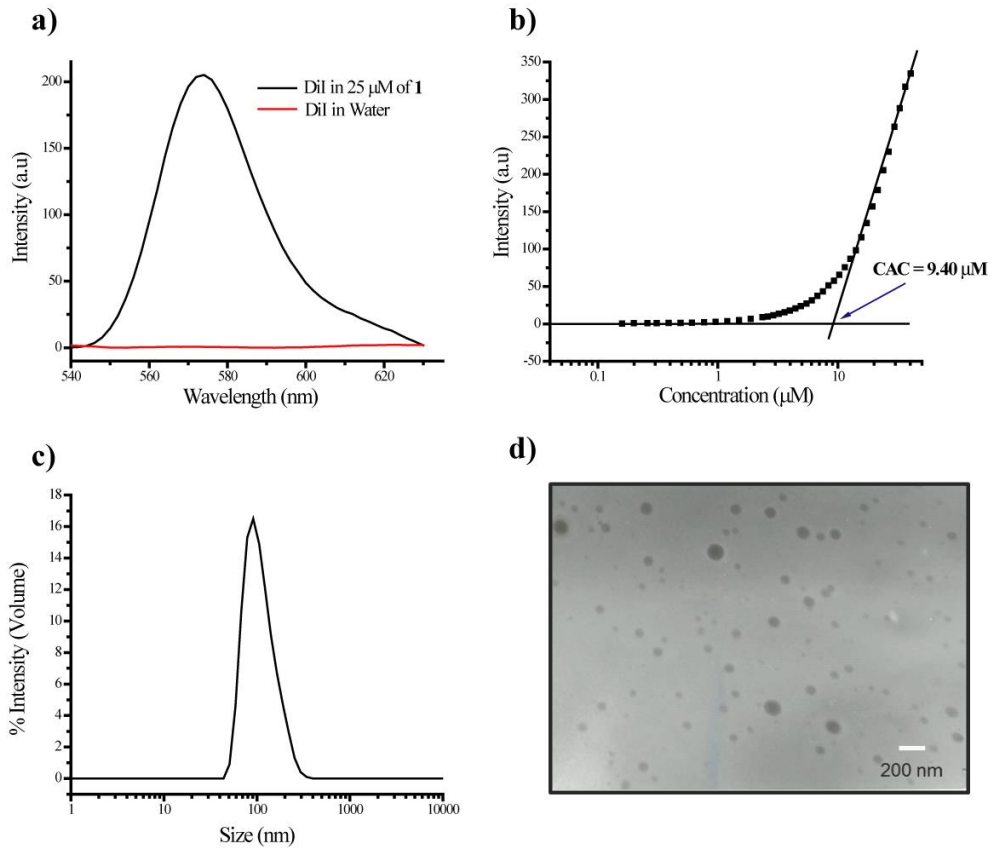

Figure 2.3. Micelle-type assembly. a) Emission spectrum of an aqueous solution of DiI in the presence and absence of G1 dendron **1** (l_{ex}=530 nm), b) CAC calculation for **1** by plotting fluorescence intensity of DiI vs. concentration of G1 dendrimer (l_{ex}=530 nm; l_{em}=573 nm), c) size of the assembly determined by DLS at 10 μM concentration of **1**, d) TEM image of G1 dendron **1** confirming formation of assemblies.

were conducted at 10 μM concentration of G1 dendron **1**. The excellent correlation function obtained in these measurements suggests that these micellar aggregates have an average hydrodynamic radius of 120 nm and a narrow polydispersity (Figure 2.3c). Note that this is a rather large size for a micellar assembly from these dendrimers. We believe that these are micelle-type aggregates, rather than a classical micelle. The reason for suggesting that these are indeed micelle-type aggregates is that these sequester lipophilic guest molecules and the lipophilicity of their interiors is similar to that observed in classical micellar assemblies (when

tested using fluorescent probes).[19,31,51] The studies, outlined below, were all conducted at 25 μM concentration of G1 dendron **1** (well above its CAC) in 50 mM HEPES buffer at pH 7.2. At this concentration, the dendrons assemble to form the micelle-type aggregates of similar size even in the buffer, as confirmed by DLS. The formation of the assemblies was also confirmed in the dry state by TEM (Figure 2.3d).

2.4 Enzyme Sensitive Behavior of Dendrimer Assemblies

One of the main objectives of this study is to understand the correlation between the guest-molecule release and the extent of enzymatic cleavage. To realize this objective, it is essential that we first understand the rate of enzymatic cleavage alone, before we test its correlation with the rate of guest-molecule release. To accomplish this, we have designed our dendrimer such that the enzymatic cleavage of the substrate will result in liberation of the fluorescent MUF. As a proof of concept, the enzyme sensitive nature of these dendrimers was tested by treating 25 μM dendrimer with 0.2 μM of the enzyme porcine liver esterase. The extent of enzymatic cleavage was then measured by monitoring the fluorescence of the enzyme-cleaved MUF by exciting it at 365 nm. The fluorescence intensity of MUF increased constantly with time and reached a saturation point at about 400 min (Figure 2.4a). The fluorescence turn-on from this reaction was evident even upon visual inspection of the solution (Figure 2.4b). This result confirms that this dendrimer is indeed sensitive to the enzyme and also that the extent of enzymatic cleavage can be monitored through the fluorescence turn-on of MUF.

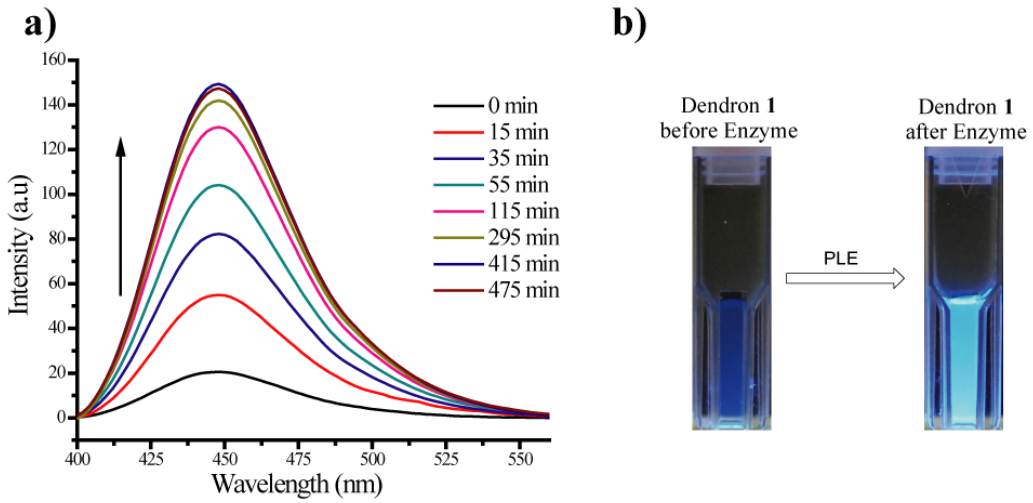

Figure 2.4. Turn-on fluorescence of coumarin (MUF) following the enzymatic action represented by a) emission spectra (l_{ex}=365 nm), b) photograph showing a visual evidence of the fluorescence turn-on upon substrate cleavage.

The MUF fluorescence not only provides a firsthand report of the enzymatic event, but also indicates the extent of imbalance brought into the micellar aggregate. This is because when the enzyme cleaves the hydrophobic substrate, the lipophilic termini are converted to carboxylic acid functionalities, thereby affecting the HLB. This resultant change in HLB can be observed by conveniently monitoring the

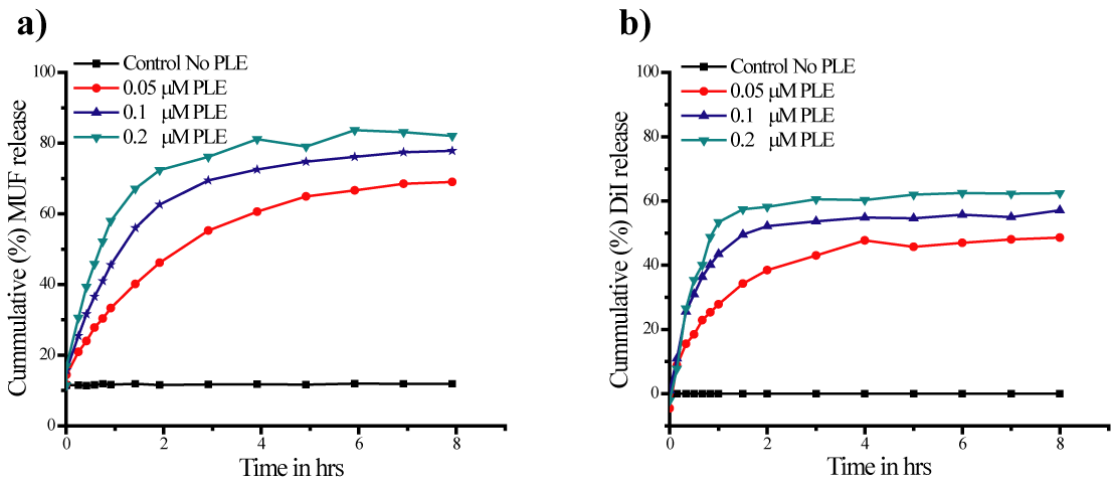

Figure 2.5. Enzyme concentration dependent release of a) MUF, and b) DiI.

release of the pre-encapsulated (non-covalently sequestered) guest molecules. To test this hypothesis, guest molecule DiI was non-covalently encapsulated in a 25 μM dendrimer solution in 50 mM HEPES Buffer. This dendrimer solution was treated with increasing concentrations (0.05 μM, 0.1 μM, and 0.2 μM) of PLE and the release of MUF and DiI were monitored by exciting at 365 nm and 530 nm, respectively. It can be noted from Figure 2.5 that the percentage release of both MUF and DiI increased proportionally with the enzyme concentration. This indicates that the change in HLB (indicated by DiI release) is indeed directly proportional to the extent of enzymatic cleavage (indicated by the MUF release), thereby suggesting a clear correlation between these two processes. Also, though enzymatic cleavage affects the HLB and causes the release of non-covalent guest molecule (DiI), it should be noted that there exists a residual assembly from the product dendron, as observed by DLS. Albeit with much lesser efficiency, due to the altered HLB, these residual aggregates are capable of retaining some of the guest molecules, as seen from the incomplete release of the DiI.

2.5 Photo-crosslinking of the Dendritic Micelles

While the observed difference in release rate can be attributed to differences in the enzymatic activity, it is desirable that we exert control over the extent of enzymatic reaction and the ensuing guest-molecule release, based on the inherent molecular characteristics of the supramolecular assembly. The difference in dendron generation has been shown to provide some control over release kinetics,[51] but it does not exhibit the level of systematic control desired. To develop such a possibility, we first examined the two limiting mechanistic possibilities for

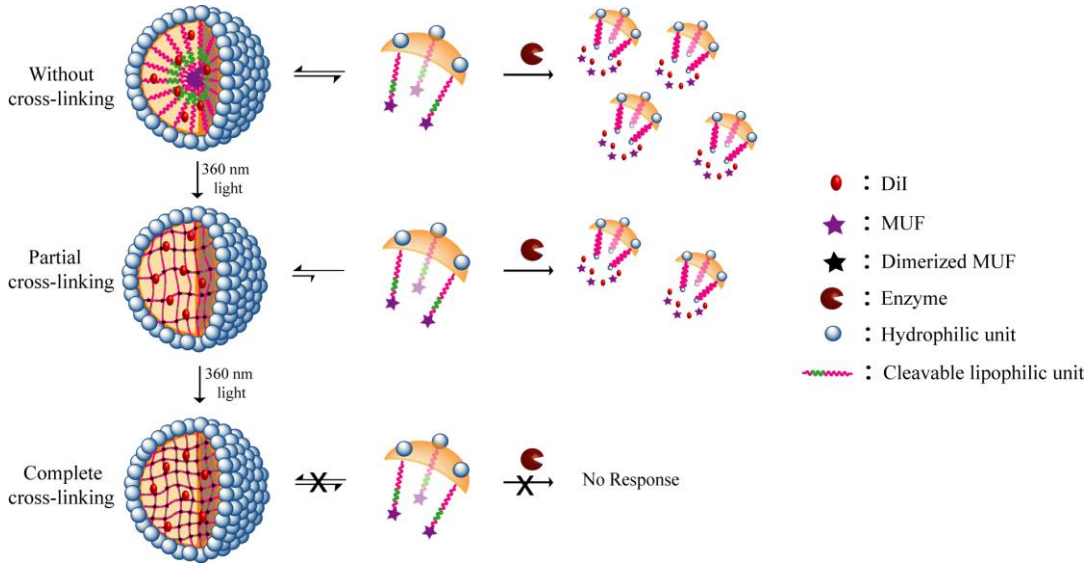

Figure 2.6. Schematic representation, showing the effect of aggregate–monomer equilibrium on enzymatic action.

the enzymatic reaction upon the substrate containing dendrons: 1) the enzyme transiently penetrates into the micellar interior to access the lipophilic substrate functionality or 2) the enzyme gains access to the substrate through the monomer–aggregate equilibrium, in which the monomeric state of the dendrons provide clear access to the substrate functionalities. We conceived that it is unlikely that the enzyme will access the lipophilic interior of a rather large micellar aggregate since the energetic penalty for such a step would be high. Therefore, scenario 2 (i.e., presentation of monomeric dendron through monomer–aggregate equilibrium) seems to be a more reasonable pathway for the observed enzyme-based guest release. With this assumption, we hypothesized that limiting the availability of the monomeric aggregates in solution should significantly affect the enzymatic reaction and thus the release kinetics.

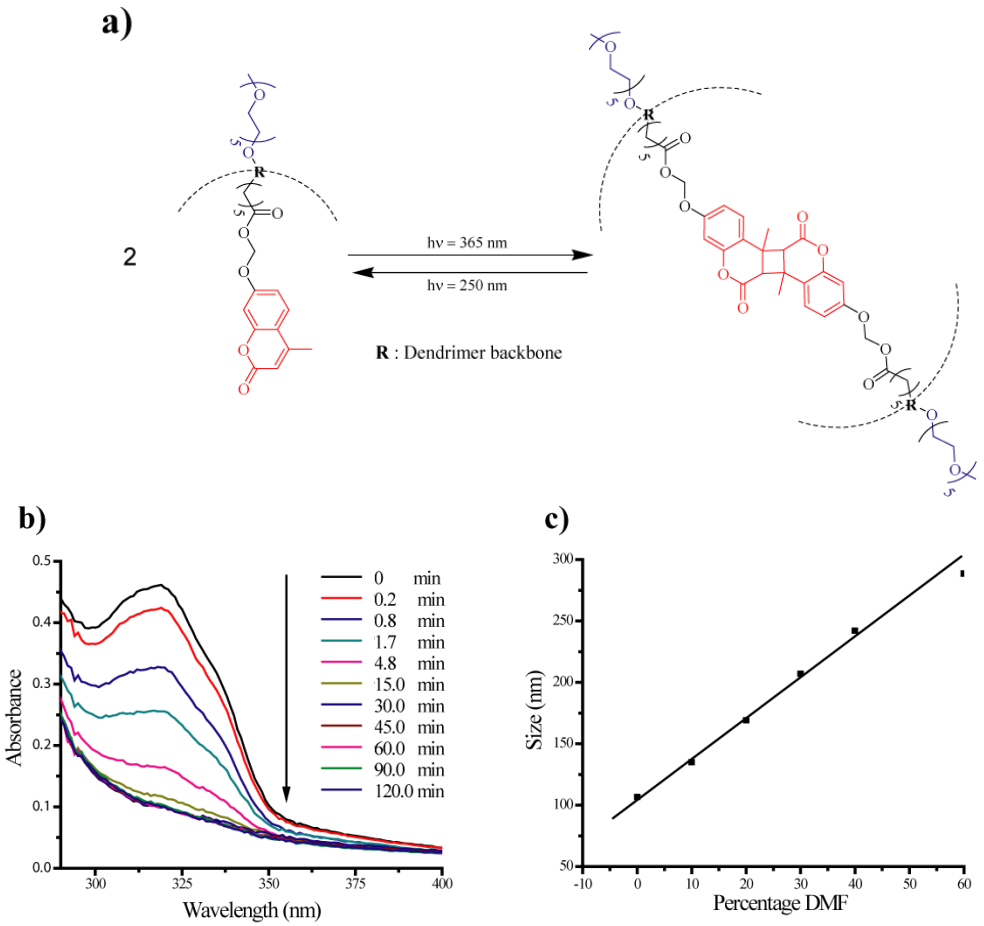

Figure 2.7. a) Reversible photodimerization of coumarin units (dimerized structure inferred from decrease in absorbance at 320 nm[16a] , b) UV absorption spectra indicating the increase in crosslinking density with increasing irradiation (365 nm) time, c) plot showing the swelling behavior of the crosslinked assemblies at 25 μM dendrimer concentration by varying the percentage of DMF.

One possible way of limiting the availability of the dendron in its monomeric state in solution would involve crosslinking the micellar interior in its aggregated state. As the degree of crosslinking increases, the availability of the dendrons in their monomeric state should decrease. We show three different scenarios in Figure 2.6: 1) no crosslinking, 2) low crosslinking density, 3) high crosslinking density. We decided to utilize the coumarin functionality to controllably crosslink the aggregates formed by the dendron. Photodimerization of coumarin functionalities by [2+2]

cycloaddition reaction is well known[60-63] (Figure 2.7a). For effective crosslinking of these aggregates, we need at least three coumarin functionalities per molecule involved in the assembly. Molecule **1** is the simplest dendritic structure that presents three units. It is also interesting to note that the presence of only three units presents the opportunity to more precisely correlate the extent of the reaction with dendrons available in the monomer–aggregate equilibrium. In the case of dendrons with a higher number of coumarin units, a small percentage of reaction can cause extensive crosslinking of the overall structure. This is another reason for our choice of a simple G1 dendron for these studies (in addition to the observation of the best CAC gain upon going from G0 to G1, rather than from G1 to G2).

Crosslinking was achieved by irradiating a solution of **1** at 365 nm. It is known that hydrophobic environments greatly enhance the rate of coumarin dimerization.[63] Since this is the case with our system, we anticipated the crosslinking reaction to be efficient. We observed that the required irradiation times for crosslinking are rather short and that the extent of crosslinking can also be tuned by simply varying the irradiation time. As shown in Figure 2.7b, the absorption peak at 320 nm, corresponding to the coumarin units in **1**, decreases with increasing irradiation time and reaches saturation at approximately 30 min of irradiation. The extent of crosslinking at different irradiation times was estimated using the initial absorbance at 320 nm (that is, at t=0 with no irradiation) as 0% crosslinked and the absorbance at saturation as 100% crosslinked (that is, at t=30 min of irradiation (Figure 2.9).

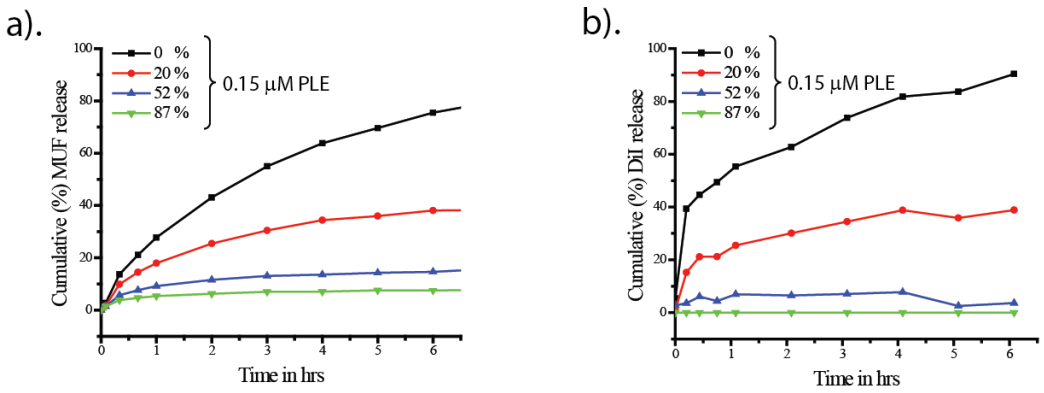

Figure 2.8. Temporal release of a) MUF and b) DiI (normalized), at different crosslinking densities.

To test if the observed photochemical transformation had resulted in crosslinking of the micellar aggregates, the stability of these nanostructures was tested. It is known from our previous studies that these facially amphiphilic dendrimers tend to lose their ability to aggregate, when subjected to a non-aqueous polar medium such as dimethylformamide (DMF).[64] Thus, the stability of the dendritic aggregates formed from the non-crosslinked dendron **1** and crosslinked dendron solutions with varying percentages of DMF were investigated using DLS. As expected, the non-crosslinked dendron solutions exhibited very poor correlation function in DLS and a broad PDI with just 20% of DMF, confirming the instability of the amphiphilic aggregate in this medium (Figure 2.10). On the other hand, the crosslinked dendritic solutions (all solutions had a final concentration of 25 μM of the dendron **1** with varying DMF/H_2O ratio) did not lose their aggregation behavior even at 60% DMF. In addition, the DLS also showed excellent correlation function and a narrow PDI, independent of the percentage of DMF. These observations confirm that the photochemical irradiation indeed crosslinks the dendritic micellar interiors. As

would be expected of a crosslinked nanostructure, these crosslinked particles did show a linear increase in size with increasing percentage of DMF (Figure 2.7c) which might be due to swelling.

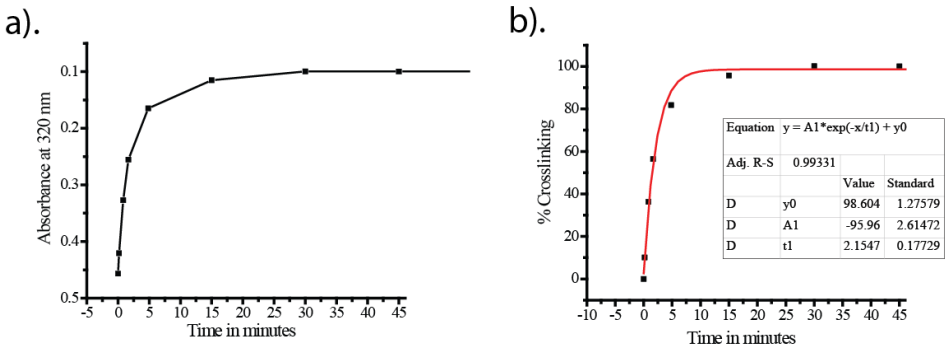

Figure 2.9. (a) Plot showing decrease in absorbance at 320 nm with increasing irradiation time. (b) Percentage crosslinking calculated by considering absorbance at 0 and 30 minutes as 0 and 100 percent crosslinking respectively.

Upon validation of the variation in crosslinking density based on the irradiation time, we were interested in testing whether there would be a differential availability of the dendrons for enzymatic reaction. Accordingly, we subjected a 25 μM solution of the dendrons to photochemical irradiation (365 nm) for different times to obtain the nanoaggregates with 0, 20, 52, and 87 % crosslinks (Figure 2.8). First, we tested the release of MUF in response to the enzyme and observed a clear correlation between the extent of crosslinking and MUF release from these dendritic assemblies. For instance, only a small percent release of MUF was observed with 87% crosslinked nanoaggregates even after 6 h, while 80% of MUF was released with uncrosslinked nanoaggregates. This observation has an important caveat; note that if the enzyme molecules were to access the interior of the dendron and cleave the ester bonds of the dimerized coumarin, then the fluorescence from MUF would not be observed, since the hydroxy version of the dimerized coumarin does not

fluoresce at this wavelength. This observation simply suggests that the extent of MUF release is controlled by different irradiation times. However, if we concurrently examine the release of the noncovalently sequestered guest molecule, DiI, further insights can be gained.

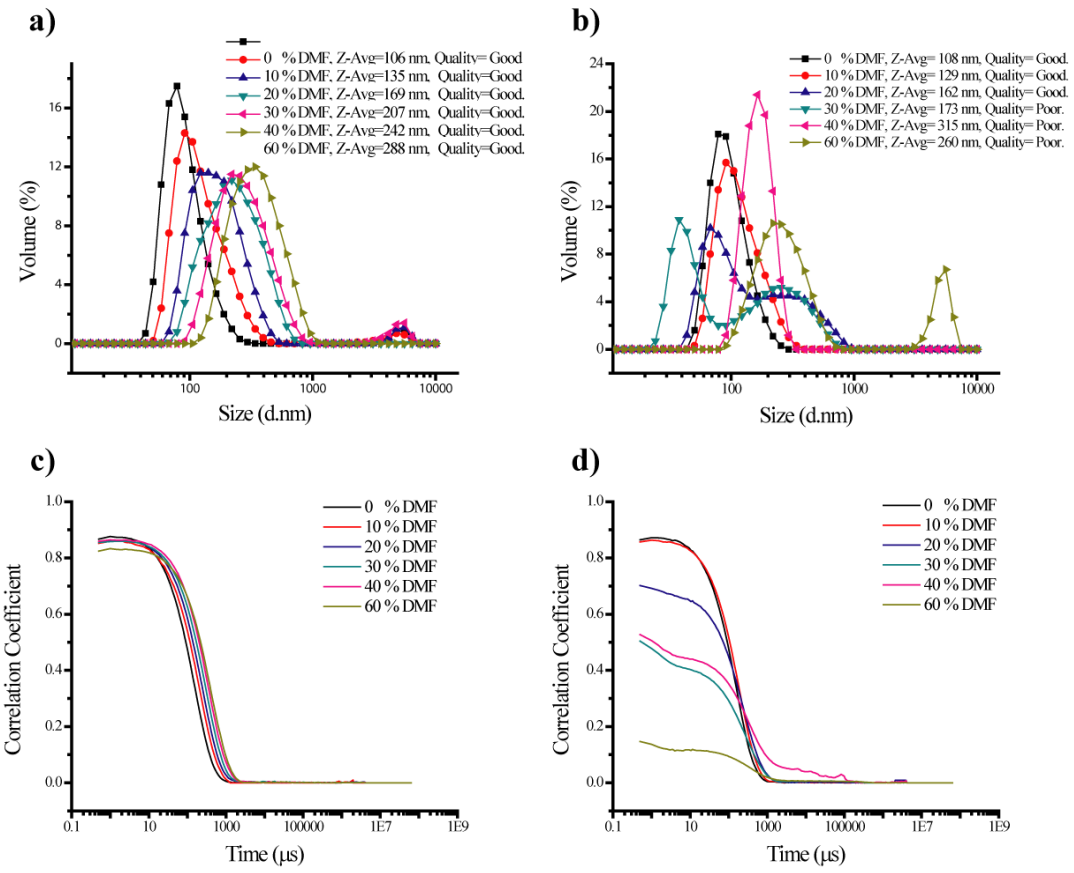

Figure 2.10. (a) DLS plot showing increase in the size of crosslinked aggregates with increase in the concentration of DMF. (b) Plot showing variation in the size of aggregates (non-crosslinked) with increase in concentration of DMF. (c) Crosslinked aggregates showing excellent correlation function independent of the DMF concentration. (d) Micellar aggregates (non-crosslinked) showing poor correlation function with increase in DMF concentration.

Note that if the enzyme were able to access the interior of the micelle and cleave the ester bonds, this cleavage reaction would simultaneously uncrosslink the dendritic aggregates and thus cause changes in HLB, independent of the crosslinking

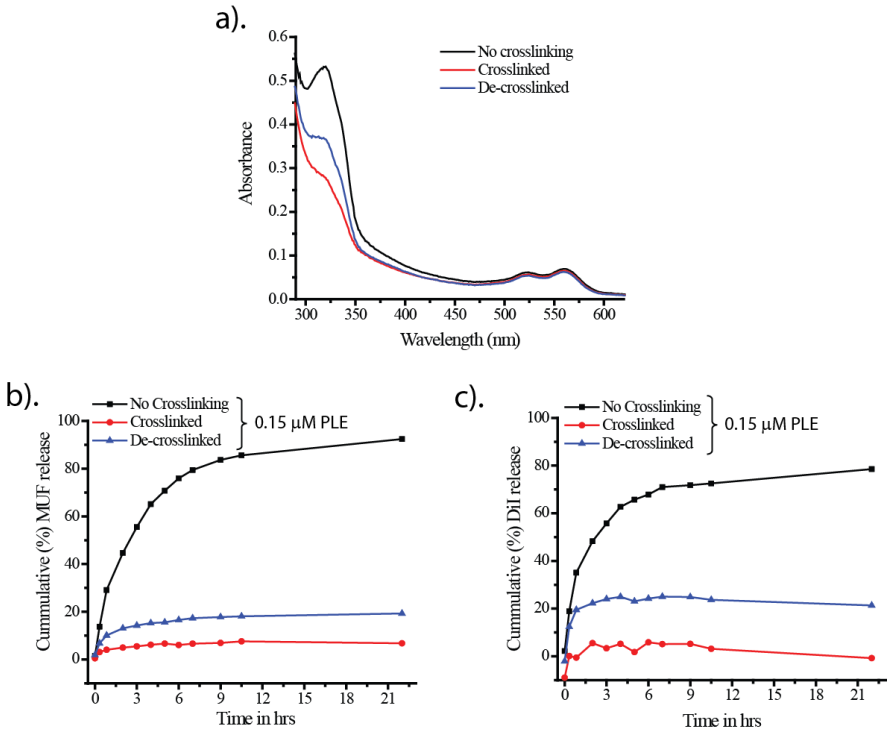

Figure 2.11. Decrosslinking and the dye-release studies. a) Absorption spectra showing partial recovery of non-crosslinked coumarin, b) time dependent MUF release, and c) DiI release.

density. These changes in HLB should then cause the amphiphilic aggregates to release the non-covalently sequestered guest molecules. On the other hand, if the enzymes do not have access to the interior of these particles, there should be a clear correlation between the previously observed MUF release and the release of the non-covalently sequestered DiI molecules. To differentiate these possibilities, we examined the release of DiI molecules from these assemblies by subjecting the 25 µM solutions of **1** to PLE. Here also, a very small percent release of DiI was observed in the case of the 87% crosslinked structure in 6 h, compared to about 83% release from the uncrosslinked structure over the same time period. The structures with intermediate crosslink densities exhibit intermediate release profiles. These observations support our assertion that the enzyme does not have access to the

interior of these assemblies. The utilization of the monomer–aggregate equilibrium to execute the enzymatic reaction and thus affect the HLB of the dendrons in solution seems to be the most reasonable alternate mechanism.

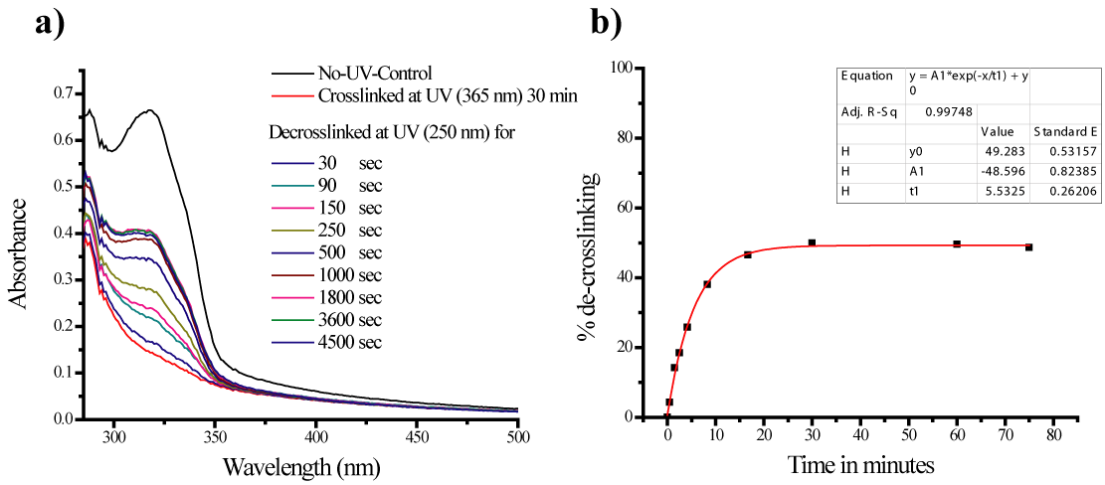

Figure 2.12. (a) UV absorption spectra indicating the recovery of absorption at 320 nm upon irradiation at 250 nm wavelength. (b) Plot showing percentage de-crosslinking with increase in irradiation time with 250 nm light.

This observation can be further augmented by reversibly enriching the monomer to aggregate concentration through the decrosslinking of crosslinked aggregates. This should then allow more accessible dendrons (in monomeric form) to the enzyme, and thereby show enhanced guest release. The decrosslinking of crosslinked aggregates was achieved through photochemical irradiation of the crosslinked aggregates at 254 nm wavelength. However it is known from the literature[65] that irradiation at 254 nm not only causes photocleavage of dimerized coumarin but also the photodimerization and finally reaches the equilibrium (photostationary state). This limits the recovery of the uncrosslinked dendrons to a maximum of about 50%.[65-68] The extent of decrosslinking at (250 nm) was

calculated by considering the absorbance at 320 nm before and after irradiation (365 nm) as 100 and 0%, respectively (Figure 2.12).

As the decrosslinking efficiency was limited to approximately 50%, it is important to note that significant number of crosslinkers are still intact in the crosslinked aggregate and these should be sufficient for retaining the majority of trapped guest molecules. To test this scope, dye-release experiments were conducted on three sets of 25 μM G1 dendrimer solutions: 1) no crosslinking, 2) crosslinked, 3) decrosslinked following initial crosslinking. The absorption spectra depicting these three cases are shown in Figure 2.11a; the re-emergence of the peak at 320 nm wavelength corresponds to the decrosslinking of the dimerized (crosslinked) MUF. These solutions were then subjected to the enzyme PLE and the dye release was monitored. In the case of covalently attached MUF, the non-crosslinked and crosslinked samples showed 90% and 5% release respectively, whereas about 20% release was observed in the case of decrosslinked sample (Figure 2.11b). A similar trend was observed for the non-covalently encapsulated DiI (Figure 2.11c). This observation therefore further validates that the enzyme does access the substrate in the monomeric form, provided through the monomer aggregate equilibrium. However, it is also important to note another possibility in which an individual monomer unit (present in the aggregate) transiently presents the lipophilic units at the surface of the aggregate, during which the enzyme can accesses its substrate functionality. At this time, we are unable to distinguish this possibility with the one based on the monomer–aggregate equilibrium.

2.6 Conclusions

We have designed and synthesized a dendritic molecule containing lipophilic fluorescent precursor functionality, which can self-assemble in aqueous solution to form nanoscopic micelle-like aggregates. Subjecting these dendrons to an enzymatic reaction releases a fluorophore, which has been utilized to monitor the release rate of the lipophilic fluorophore from the dendritic backbone. Since this enzymatic reaction also causes a change in the hydrophilic–lipophilic balance in the dendrons, the amphiphilic supramolecular nanostructures lose their micellar nature in response to the enzyme stimulus. Monitoring the release of non-covalently sequestered guest molecules during the deformation of the assembly suggests that there is a clear correlation between covalent bond cleavage and guest-molecule release. This observation led us to test the possibility of utilizing these dendrons for controlling the release of the guest molecules by limiting the extent of dendron availability in a monomer–aggregate equilibrium. We utilized the photochemical dimerization of coumarin to test this possibility. Indeed, we observed that the extent of guest-molecule release can be precisely controlled by manipulating the extent of crosslinking in these nanoassemblies. These observations also allowed us to rule out the possibility of enzymes accessing the interior of the micellar aggregates to execute the enzymatic reaction. We believe that the molecular-design strategies that emerge from these observations can impact a variety of areas, particularly those involving controlled molecular release.

2.7 Experimental Details

2.7.1 Synthesis and Characterization

All chemicals and reagents were purchased from commercial sources and were used as received, unless otherwise mentioned. Compounds 3 and 4 were synthesized following the previously reported procedures. ^{1}H-NMR spectra were recorded on 400 MHz Bruker NMR spectrometer using the residual proton resonance of the solvent as the internal standard. Chemical shifts are reported in parts per million (ppm). When peak multiplicities are given the following abbreviations are used: s, singlet; d, doublet; t, triplet; m, multiplet. 13C-NMR spectra were proton decoupled and measured on a 100 MHz Bruker spectrometer using carbon signal of the deuterated solvent as the internal standard.

2.7.1.1 Synthesis of compound 6

4-Methylumbelliferone (3.36 g, 19.09 mmol), dibromomethane (6.64 g, 38.20 mmol), K_2CO_3 (5.80 g, 42.00 mmol), and 18-crown-6 (0.84 g, 3.18 mmol) were mixed together in acetone (125 mL) and refluxed for 1 h under argon, azido hexanoic acid (2.50 g, 15.90 mmol), and dibromomethane (3.31 g, 19.04 mmol) were then added and refluxed for 15 h. The reaction mixture was concentrated in vacuo and the residue was dissolved in water and extracted twice with ethyl acetate, the combined extracts were then dried over anhydrous Na2SO4. Upon evaporation of the solvent, the crude product was purified by silica gel column chromatography (using combiflash) to afford 1.99 g (36%) of product 6. ^{1} H NMR (400 MHz, CDCl3) δ 7.54 (d, J = 8 Hz, 1H), 7.01 (s, 1H), 6.97 (d, J = 8 Hz, 1H), 6.20 (s, 1H), 5.82 (s, 2H), 3.23 (t, J = 16 Hz, 2H), 2.42 (s, 3H), 2.40 (t, J = 12 Hz, 2H), 1.69 – 1.55 (m, 4H), 1.40

(m, 2H); ^{13}C NMR (100 MHz CDCl3) δ 172.2, 161, 159.6, 155, 152.4, 126, 115.3, 113.3, 113.1, 103.5, 84.7, 51.2, 34, 28.6, 26.2, 24.2, 18.8. FAB/MS m/z (r.i) (M+ 49), 189 (72), 177 (100).

2.7.1.2 Synthesis of compound 5

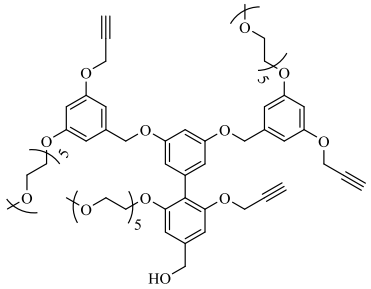

Compund **5** was synthesized using previously reported procedure.[51]

2.7.1.3 Synthesis of compound 1

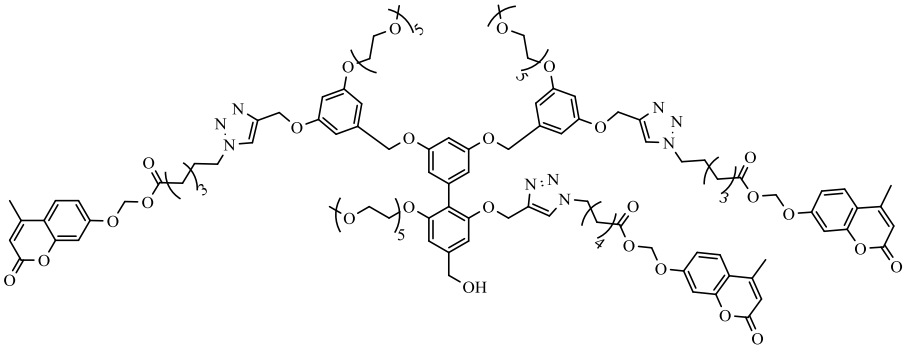

The dendritic acetylene compound 5 (30 mg, 0.023 mmol), and azide compound 6 (71 mg, 0.2 mmol) were dissolved in THF/H_2O (1:1) solvent mixture. To that was added $CuSO_4.5H_2O$ (2.9 mg, 0.011 mmol), sodium ascorbate (2.3 mg, 0.011 mmol) and heated to 50^o C for 36 h. The reaction mixture was then concentrated in vacuo to remove THF and extracted twice with ethyl acetate; the combined extracts were then dried over anhydrous Na2SO4. Upon evaporation of the solvent the crude mixture is purified by silica gel column chromatography to

afford 37 mg of product 1. ^{1}H NMR (400 MHz, $CDCl_3$) δ 7.59 – 7.49 (m, 5H), 7.20 (s, 1H), 6.97 – 6.91 (m, 6H), 6.64 – 6.46 (m, 12H), 6.15 – 6.13 (m, 3H), 5.79 -5.75 (m, 6H), 5.12 – 4.67 (m, 12H), 4.30 – 4.27 (t, J = 12 Hz, 4H), 4.13 – 4.05 (m, 9H), 3.82 – 3.80 (m, 5H), 3.69 – 3.49 (m, 55 H), 3.35 – 3.33 (m, 9H), 2.38 – 2.28 (m, 15 H), 1.88 – 1.24 (m, 24H). ^{13}C NMR (100MHz CDCl3) δ 171.42, 171.39, 160.35, 158.84, 158.37, 155.78, 154.29, 151.82, 143.88, 143.21, 142.10, 139.03, 135.37, 125.36, 125.34, 122.25, 121.92, 118.86, 114.59, 112.63, 112.34, 112.28, 109.89, 105.79, 104.69, 102.77, 102.75, 100.39, 100.27, 84.09, 71.33, 70.00, 69.90, 69.86, 69.06, 66.92, 64.48, 62.87, 61.39, 58.45, 49.46, 49.30, 33.10, 33.04, 31.01, 29.29, 29.07, 25.23, 23.31, 23.24, 18.11, 13.55; MALDI–ToF m/z calculated for $C_{120}H_{150}N_9O_{39}^{-}$ Na^{+} : 2368.5; found 2368.0.

2.7.2 Dynamic Light Scattering

The size distribution of the micelles was determined by Nano series Nano-ZS (Malvern Instrument) Zetasizer. In a typical experiment a stock solution of 100 μM dendrimer was prepared in milli-Q water by stirring the solution overnight inside the refrigerator. The resultant solution was then diluted to 25 μM with 50 mM HEPES buffer (pH 7.2). This solution was then filtered through 0.22 μm filter and the size of the micelles was measured at room temperature.

2.7.3 Spectroscopic Measurements

UV-Visible spectra were collected using a Cary 100 Spectrophotometer. Emission spectra were recorded on a JASCO (FP-6500) spectrofluorimeter using 1 mL disposable fluorescence cuvettes. The emission spectra for DiI were recorded by exciting at 530 nm, with the excitation and emission bandwidth set at 3 and 5 nm

respectively. On the other hand MUF was excited at 365 nm, with excitation and emission bandwidth set at 3 and 3 respectively.

2.7.4 Encapsulation of Guest Molecules

To a vial pre-weighed with required amount of dendrimer was added 50 μL of 1mg/mL DiI (in acetone), followed by evaporating the acetone with mild blow of Argon. To this was added milli-Q water to make the desired concentration of dendrimer and stirred at 5o C in a refrigerator for 48 hrs. The resultant solution is then passed through 0.22 μm filter to remove the non-encapsulated DiI, followed by stirring the solution at room temperature for 2 hours to remove any residual acetone present in the solution. This stock solution was accordingly diluted with 50mM HEPES Buffer (pH 7.2) to achieve required concentration of the dendrimer.

2.7.5 Dye Release

To the 1 mL of dendrimer stock solution encapsulated with DiI was added HEPES buffer (50 mM, pH = 7.2) to make the desired concentration of dendrimer solution. To this dendrimer solution was added varying amounts of 100 μM PLE stock solution (50 mM HEPES, pH = 7.2) and mixed well. The emission spectra of MUF and DiI were then recorded at every time interval by exciting at 365 nm and 530 nm respectively. The MUF, and DiI release were monitored using the emission intensities observed at 448 nm, and 573 nm respectively. The percentage release of MUF was calculated by considering the saturation point in the sample with highest PLE concentration (0.2 μM) as 100 percent release, whereas the percentage release of DiI was calculated by considering the control (with no enzyme) as zero percent release. The temperature was maintained at 25 ^{o} C throughout the experiment.

2.7.6 Photo crosslinking of Dendron Aggregates

Aqueous dendrimer solution in a scintillation vial was placed under a XX-15LW Bench Lamp (UVP) with UV light (λ ~ 365nm) at a 9.5 cm distance. The degree of crosslinking was varied by changing the time of exposure (Figure 2.10a). The percentage crosslinking is then determined form the exponential curve fitting as shown in the Figure 2.12b. The optimum time needed for complete crosslinking was observed to be 30 minutes.

2.7.7 Stability of the Crosslinked Aggregates

The stability of the crosslinked and non-crosslinked dendrimer aggregates was determined by testing their aggregation stability upon exposure to the increasing concentrations of a non-aqueous polar medium DMF. It can be observed from Figure S2.b,d that the non-crosslinked aggregates are polydisperse and have very poor correlation coefficients with just 20 % DMF. On the other hand, the Figure 2.11. (a) Plot showing decrease in absorbance at 320 nm with increasing irradiation time. (b) Percentage crosslinking calculated by considering absorbance at 0 and 30 minutes as 0 and 100 percent crosslinking respectively. Crosslinked aggregates showed enhanced stabilities with excellent correlation coefficients (Figure 2.10.a, c) even at 60 % DMF.

2.7.8 De-Crosslinking of the Crosslinked Aggregates

To test the scope of reversibly de-crosslinking the crosslinked aggregates, aqueous dendrimer solution was initially crosslinked at 365 nm following the procedure mentioned above. This crosslinked solution was then placed under a XX-15LW Bench Lamp (UVP) with UV light (λ ~ 250 nm) at a 9.5 cm distance. The degree of de-

crosslinking is then monitored through the gain in absorbance observed at 320 nm. It can be observed from Figure S3.a that the absorbance at 320 nm saturates after 30 minutes of irradiation. The degree of de-crosslinking was then calculated through exponential curve fitting by considering the absorbance at 320 nm of completely crosslinked sample (i.e after 30 min of irradiation at 365 nm) as 0 percent de-crosslinking and absorbance of the non-crosslinked sample (i.e no UV irradiation) as 100 percent de-crosslinking.

2.8 NMR Spectra

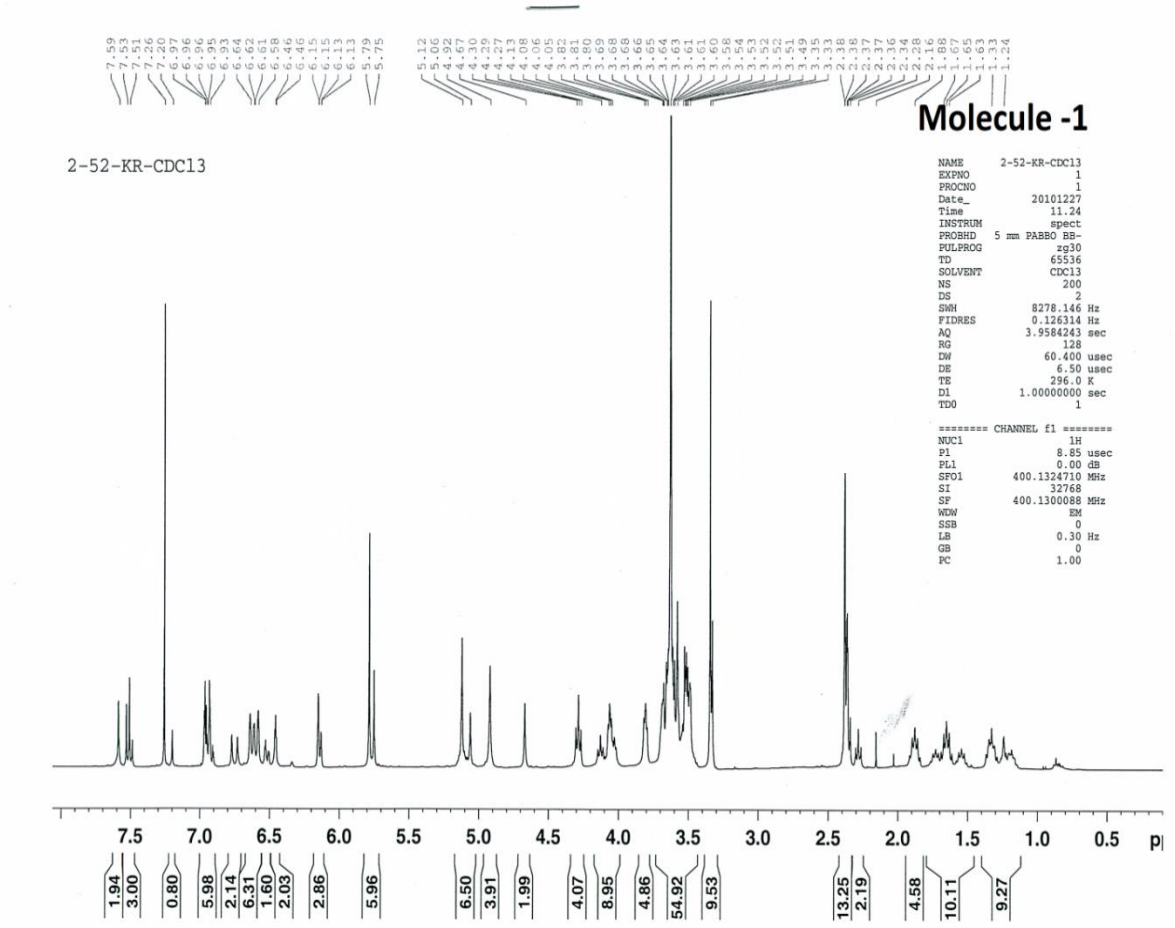

2.9 References

1. Liu, M. J.; Kono, K.; Fréchet, J. M. J., Water-soluble dendritic unimolecular micelles: Their potential as drug delivery agents. *J. Control. Release* **2000,** *65* (1-2), 121-131.

2. Gohy, J. F.; Hofmeier, H.; Alexeev, A.; Schubert, U. S., Aqueous micelles from supramolecular graft copolymers. *Macromol. Chem. Phys.* **2003,** *204* (12), 1524-1530.

3. Zhong, S.; Cui, H. G.; Chen, Z. Y.; Wooley, K. L.; Pochan, D. J., Helix self-assembly through the coiling of cylindrical micelles. *Soft Matter* **2008,** *4* (1), 90-93.

4. Bae, Y.; Kataoka, K., Intelligent polymeric micelles from functional poly(ethylene glycol)-poly(amino acid) block copolymers. *Adv. Drug Delivery Rev.* **2009,** *61* (10), 768-784.

5. Kabanov, A. V.; Nazarova, I. R.; Astafieva, I. V.; Batrakova, E. V.; Alakhov, V. Y.; Yaroslavov, A. A.; Kabanov, V. A., Micelle Formation and Solubilization of Fluorescent-Probes in Poly(Oxyethylene-B-Oxypropylene-B-Oxyethylene) Solutions. *Macromolecules* **1995,** *28* (7), 2303-2314.

6. Peer, D.; Karp, J. M.; Hong, S.; FaroKhzad, O. C.; Margalit, R.; Langer, R., Nanocarriers as an emerging platform for cancer therapy. *Nat. Nanotechnol.* **2007,** *2* (12), 751-760.

7. Oh, K. T.; Bronich, T. K.; Kabanov, A. V., Micellar formulations for drug delivery based on mixtures of hydrophobic and hydrophilic Pluronic((R)) block copolymers. *J. Controlled Release.* **2004,** *94* (2-3), 411-422.

8. Oh, K. T.; Bronich, T. K.; Kabanov, A. V., Micellar formulations for drug delivery based on mixtures of hydrophobic and hydrophilic Pluronic((R)) block copolymers. *J. Controlled Release.* **2004,** *94* (2-3), 411-422.

9. Allen, T. M.; Cullis, P. R., Drug delivery systems: Entering the mainstream. *Science* **2004,** *303* (5665), 1818-1822.

10. Kataoka, K.; Kwon, G. S.; Yokoyama, M.; Okano, T.; Sakurai, Y., Block-Copolymer Micelles as Vehicles for Drug Delivery. *J. Controlled Release.* **1993,** *24* (1-3), 119-132.

11. Bachelder, E. M.; Beaudette, T. T.; Broaders, K. E.; Dashe, J.; Frechet, J. M. J., Acetal-derivatized dextran: An acid-responsive biodegradable material for therapeutic applications. *J. Am. Chem. Soc.* **2008,** *130* (32), 10494-10495.

12. Gillies, E. R.; Frechet, J. M. J., pH-responsive copolymer assemblies for controlled release of doxorubicin. *Bioconjugate Chem.* **2005,** *16* (2), 361-368.

13. Chen, W.; Meng, F. H.; Li, F.; Ji, S. J.; Zhong, Z. Y., pH-Responsive Biodegradable Micelles Based on Acid-Labile Polycarbonate Hydrophobe: Synthesis and Triggered Drug Release. *Biomacromolecules* **2009,** *10* (7), 1727-1735.

14. Klaikherd, A.; Nagamani, C.; Thayumanavan, S., Multi-Stimuli Sensitive Amphiphilic Block Copolymer Assemblies. *J. Am. Chem. Soc.* **2009,** *131* (13), 4830-4838.

15. Rijcken, C. J. F.; Soga, O.; Hennink, W. E.; Nostrum, C. F. v., Triggered destabilisation of polymeric micelles and vesicles by changing polymers polarity: An attractive tool for drug delivery. *J. Controlled Release* **2007,** *120* (3), 131-148.

16. Alvarez-Lorenzo, C.; Bromberg, L.; Concheiro, A., Light-sensitive Intelligent Drug Delivery Systems. *Photochem. Photobiol.* **2009,** *85* (4), 848-860.

17. Babin, J.; Pelletier, M.; Lepage, M.; Allard, J. F.; Morris, D.; Zhao, Y., A New Two-Photon-Sensitive Block Copolymer Nanocarrier. *Angew. Chem. Int. Ed.* **2009,** *48* (18), 3329-3332.

18. Aathimanikandan, S. V.; Savariar, E. N.; Thayumanavan, S., Temperature-sensitive dendritic micelles. *J. Am. Chem. Soc.* **2005,** *127* (42), 14922-14929.

19. Chilkoti, A.; Dreher, M. R.; Meyer, D. E.; Raucher, D., Targeted drug delivery by thermally responsive polymers. *Adv. Drug Delivery Rev.* **2002,** *54* (5), 613-630.

20. Ghosh, S.; Yesilyurt, V.; Savariar, E. N.; Irvin, K.; Thayumanavan, S., Redox, Ionic Strength, and pH Sensitive Supramolecular Polymer Assemblies. *J. Polym. Sci., Part A: Polym. Chem* **2009,** *47* (4), 1052-1060.

21. Kim, E.; Kim, D.; Jung, H.; Lee, J.; Paul, S.; Selvapalam, N.; Yang, Y.; Lim, N.; Park, C. G.; Kim, K., Facile, Template-Free Synthesis of Stimuli-Responsive Polymer Nanocapsules for Targeted Drug Delivery. *Angew. Chem. Int. Ed.* **2010,** *49* (26), 4405-4408.

22. He, J.; Tong, X.; Zhao, Y., Photoresponsive Nanogels Based on Photocontrollable Cross-Links. *Macromolecules* **2009,** *42* (13), 4845-4852.

23. Yamaguchi, S.; Matsumoto, S.; Ishizuka, K.; Iko, Y.; Tabata, K. V.; Arata, H. F.; Fujita, H.; Noji, H.; Hamachi, I., Thermally responsive supramolecular nanomeshes for on/off switching of the rotary motion of F-1-ATPase at the single-molecule level. *Chem. Eur. J.* **2008,** *14* (6), 1891-1896.

24. Ruel-Gariépy, E.; Leroux, J.-C., In situ-forming hydrogels—review of temperature-sensitive systems. *Eur. J. Pharm. Biopharm.* **2004,** *58* (2), 409-426.

25. Bae, Y.; Fukushima, S.; Harada, A.; Kataoka, K., Design of environment-sensitive supramolecular assemblies for intracellular drug delivery: Polymeric micelles that are responsive to intracellular pH change. *Angew. Chem. Int. Ed.* **2003,** *42* (38), 4640-4643.

26. Ulijn, R. V., Enzyme-responsive materials: a new class of smart biomaterials. *J. Mater. Chem.* **2006,** *16* (23), 2217-2225.

27. Amir, R. J.; Shabat, D., Self-immolative dendrimer biodegradability by multi-enzymatic triggering. *Chem. Commun.* **2004,** (14), 1614-1615.

28. Jeong, Y.; Joo, M. K.; Bahk, K. H.; Choi, Y. Y.; Kim, H. T.; Kim, W. K.; Lee, H. J.; Sohn, Y. S.; Jeong, B., Enzymatically degradable temperature-sensitive polypeptide as a new in-situ gelling biomaterial. *J. Controlled Release.* **2009,** *137* (1), 25-30.

29. Amir, R. J.; Zhong, S.; Pochan, D. J.; Hawker, C. J., Enzymatically Triggered Self-Assembly of Block Copolymers. *J. Am. Chem. Soc.* **2009,** *131* (39), 13949-13951.

30. Saavedra, J. E.; Shami, P. J.; Wang, L. Y.; Davies, K. M.; Booth, M. N.; Citro, M. L.; Keefer, L. K., Esterase-sensitive nitric oxide donors of the diazeniumdiolate family: In vitro antileukemic activity. *J. Med. Chem.* **2000,** *43* (2), 261-269.

31. Azagarsamy, M. A.; Yesilyurt, V.; Thayumanavan, S., Disassembly of dendritic micellar containers due to protein binding. *J. Am. Chem. Soc.* **2010,** *132* (13), 4550-4551.

32. Wilson, K. E.; Langdon, S. P.; Lessells, A. M.; Miller, W. R., Expression of the extracellular matrix protein tenascin in malignant and benign ovarian tumours. *Br. J. Cancer.* **1996,** *74* (7), 999-1004.

33. Samantaray, S.; Sharma, R.; Chattopadhyaya, T. K.; Gupta, S. D.; Ralhan, R., Increased expression of MMP-2 and MMP-9 in esophageal squamous cell carcinoma. *J. Cancer. Res. Clin.* **2004,** *130* (1), 37-44.

34. Klein, H. L., The consequences of Rad51 overexpression for normal and tumor cells. *DNA Repair* **2008,** *7* (5), 686-693.

35. Newkome, G. R.; Moorefield, C. N.; Baker, G. R.; Johnson, A. L.; Behera, R. K., Chemistry of Micelles .11. Alkane Cascade Polymers Possessing Micellar Topology - Micellanoic Acid-Derivatives. *Angew. Chem. Int. Ed.* **1991,** *30* (9), 1176-1178.

36. Hawker, C. J.; Wooley, K. L.; Frechet, J. M. J., Unimolecular Micelles and Globular Amphiphiles - Dendritic Macromolecules as Novel Recyclable Solubilization Agents. *J. Chem. Soc., Perkin Trans. 1* **1993,** (12), 1287-1297.

37. Fleischer, G., Micellization in Aqueous-Solution of a Poly(Ethylene Oxide) Poly(Propylene Oxide) Poly(Ethylene Oxide) Triblock Copolymer Investigated with Pulsed Field Gradient Nmr. *J. Phys. Chem.* **1993,** *97* (2), 517-521.

38. Savariar, E. N.; Aathimanikandan, S. V.; Thayumanavan, S., Supramolecular assemblies from amphiphilic homopolymers: Testing the scope. *J. Am. Chem. Soc.* **2006,** *128* (50), 16224-16230.

39. Hecht, S.; Frechet, J. M. J., Dendritic encapsulation of function: Applying nature's site isolation principle from biomimetics to materials science. *Angew. Chem. Int. Ed.* **2001,** *40* (1), 74-91.

40. Medina, S. H.; El-Sayed, M. E. H., Dendrimers as Carriers for Delivery of Chemotherapeutic Agents. *Chemical Reviews* **2009,** *109* (7), 3141-3157.

41. Ambade, A. V.; Savariar, E. N.; Thayumanavan, S., Dendrimeric micelles for controlled drug release and targeted delivery. *Mol. Pharmaceutics.* **2005,** *2* (4), 264-272.

42. Astruc, D.; Boisselier, E.; Ornelas, C., Dendrimers designed for functions: From physical, photophysical, and supramolecular properties to applications in sensing, catalysis, molecular electronics, photonics, and nanomedicine. *Chem. Rev.* **2010,** *110* (4), 1857-1959.

43. Thayumanavan, S.; Bharathi, P.; Sivanandan, K.; Vutukuri, D. R., Towards dendrimers as biomimetic macromolecules. *C.R. Chim.* **2003,** *6* (8-10), 767-778.

44. Grayson, S. M.; Frechet, J. M. J., Convergent dendrons and dendrimers: from synthesis to applications. *Chem. Rev.* **2001,** *101* (12), 3819-3867.

45. Frechet, J. T., Donald, *Dendrimers and Other Dendritic Polymers*. John Wiley & Sons Ltd: Hoboken, N. J., 2001; p 688.

46. de Groot, F. M. H.; Albrecht, C.; Koekkoek, R.; Beusker, P. H.; Scheeren, H. W., "Cascade-release dendrimers" liberate all end groups upon a single triggering event in the dendritic core. *Angew. Chem. Int. Ed.* **2003,** *42* (37), 4490-4494.

47. Avital-Shmilovici, M.; Shabat, D., Self-immolative dendrimers: A distinctive approach to molecular amplification. *Soft Matter* **2010,** *6* (6), 1073-1080.

48. Amir, R. J.; Shabat, D., Domino dendrimers. In *Polymer Therapeutics I: Polymers as Drugs, Conjugates and Gene Delivery Systems*, **2006**; Vol. 192, pp 59-94.

49. Niederhafner, P.; Sebestik, J.; Jezek, J., Glycopeptide dendrimers. Part II. *J. Pept. Sci.* **2008,** *14* (1), 44-65.

50. Bensel, N.; Reymond, M. T.; Reymond, J. L., Pivalase catalytic antibodies: Towards abzymatic activation of prodrugs. *Chem. Eur. J.* **2001,** *7* (21), 4604-4612.

51. Azagarsamy, M. A.; Sokkalingam, P.; Thayumanavan, S., Enzyme-triggered disassembly of dendrimer-based amphiphilic nanocontainers. *J. Am. Chem. Soc.* **2009,** *131* (40), 14184-14185.

52. Wang, L. P.; Yang, X. F.; Zhao, M. L., A 4-Methylumbelliferone-based Fluorescent Probe for the Sensitive Detection of Captopril. *J. Fluoresc.* **2009,** *19* (4), 593-599.

53. Uttamapinant, C.; White, K. A.; Baruah, H.; Thompson, S.; Fernandez-Suarez, M.; Puthenveetil, S.; Ting, A. Y., A fluorophore ligase for site-specific protein labeling inside living cells. *PNAS* **2010,** *107* (24), 10914-10919.

54. Yang, X. F.; Wang, L. P.; Zhao, M. L.; Qi, H. P.; Wu, Y., A 4-Methylumbelliferone-based Fluorescent Probe for Sodium New Houttuyfonate. *Chin. J. Chem.* **2010,** *28* (8), 1469-1474.

55. Knop, K.; Hoogenboom, R.; Fischer, D.; Schubert, U. S., Poly(ethylene glycol) in Drug Delivery: Pros and Cons as Well as Potential Alternatives. *Angew. Chem. Int. Ed.* **2010,** *49* (36), 6288-6308.

56. Carlmark, A.; Hawker, C. J.; Hult, A.; Malkoch, M., New methodologies in the construction of dendritic materials. *Chem. Soc. Rev.* **2009,** *38* (2), 352-362.

57. Helms, B.; Mynar, J. L.; Hawker, C. J.; Frechet, J. M. J., Dendronized linear polymers via "click chemistry". *J. Am. Chem. Soc.* **2004,** *126* (46), 15020-15021.

58. Wang, Q.; Chittaboina, S.; Barnhill, H. N., Advances in 1,3-dipolar cycloaddition reaction of azides and alkynes - A prototype of "click" chemistry. *Lett. Org. Chem.* **2005,** *2* (4), 293-301.

59. Gomez-Escudero, A.; Azagarsamy, M. A.; Theddu, N.; Vachet, R. W.; Thayumanavan, S., Selective peptide binding using facially amphiphilic dendrimers. *J. Am. Chem. Soc.* **2008,** *130* (33), 11156-11163.

60. Muthuramu, K.; Ramamurthy, V., Photo-Dimerization of Coumarin in Aqueous and Micellar Media. *J. Org. Chem.* **1982,** *47* (20), 3976-3979.

61. Gnanaguru, K.; Ramasubbu, N.; Venkatesan, K.; Ramamurthy, V., A Study on the Photochemical Dimerization of Coumarins in the Solid-State. *J. Org. Chem.* **1985,** *50* (13), 2337-2346.

62. Trenor, S. R.; Shultz, A. R.; Love, B. J.; Long, T. E., Coumarins in polymers: From light harvesting to photo-cross-linkable tissue scaffolds. *Chem. Rev.* **2004,** *104* (6), 3059-3077.

63. Muthuramu, K.; Ramamurthy, V., Selectivity in Chemical-Reactions in Micellar Media - Photodimerization of Substituted Coumarins in Micelles. *Indian J. Chem., Sect B* **1984,** *23* (6), 502-508.

64. Azagarsamy, M. A.; Krishnamoorthy, K.; Sivanandan, K.; Thayumanavan, S., Site-Specific Installation and Study of Electroactive Units in Every Layer of Dendrons. *J. Org. Chem.* **2009,** *74* (24), 9475-9485.

65. Chen, Y.; Chen, K. H., Synthesis and reversible photocleavage of novel polyurethanes containing coumarin dimer components. *J. Polym. Sci., Part A: Polym. Chem* **1997,** *35* (4), 613-624.

66. Chen, Y.; Chou, C. F., Reversible photodimerization of coumarin derivatives disersed in poly (vinyl acetate). *J. Polym. Sci., Part A: Polym. Chem* **1995,** *33* (16), 2705-2714.

67. Chen, Y.; Chen, K. H., Synthesis and reversible photocleavage of novel polyurethanes containing coumarin dimer components. *J. Polym. Sci., Part A: Polym. Chem* **1997,** *35* (4), 613-624.

68. Chujo, Y.; Sada, K.; Saegusa, T., A novel nonionic hydrogel from 2-methyl-2-oxazoline, 3 polyoxazoline having a coumarin as a pendant group - synthesis and photogelation. *Macromolecules* **1990,** *23* (10), 2693-2697.

CHAPTER 3

TEMPERATURE-SENSITIVE TRANSITIONS BELOW LCST IN AMPHIPHILIC DENDRITIC ASSEMBLIES: HOST-GUEST IMPLICATIONS

Adapted with permission from Jack M. Fuller,† Krishna R. Raghupathi,† Rajasekhar R. Ramireddy, Ayyagari V. Subrahmanyam, Volkan Yesilyurt, and S. Thayumanavan. Guest release control in enzyme sensitive, amphiphilic dendrimer based nanoparticles through photochemical crosslinking. *Journal of the American Chemical Society* **2013**, *135*, 8947 – 8954.

3.1 Introduction

Stimuli-sensitive supramolecular assemblies have captured our attention, because of their impact on a variety of applications, including biosensing, drug delivery, and diagnostics.[1-9] It is often desirable, in many of these applications, that the surface moieties interfacing with the aqueous milieu do not exhibit any nonspecific binding characteristics. Oligo- and poly(ethylene glycol) based hydrophilic functional groups have been quite popular in this context.[10-13] In addition to the desirable nonspecific binding features, these functional groups are also capable of imparting temperature-sensitive character to a supramolecular assembly.[14-17] Considering the prevalence of ethylene glycol based functional groups in biomaterials, it is critical that we understand the factors which underlie the thermal sensitivity. It is widely accepted that the thermal sensitivity arises from the fact that the degree of hydrogen bonding between the ethylene glycol moieties and

water is inversely proportional to the temperature.[14,18,19] This feature has been observed in the form of macroscopic phase changes, where a polymer or a supramolecular assembly phase separates from the aqueous phase in response to increased temperature. This phase transition is reported as the molecule's lower critical solution temperature (LCST) or the cloud point.[20,21] Molecules are soluble below their cloud point but will precipitate above this temperature due to weakened hydrogen bonding with the aqueous medium. In effect, ethylene glycol units become less hydrated (i.e., less hydrophilic) in an elevated thermal environment, resulting in increased intermolecular aggregation and ultimately precipitation. Numerous reports describe cloud-point-mediated triggers in drug delivery,[22-24] sensing,[25-27] and catalysis[28-30] as precipitation-mediated responses. While the cloud-point phase transition is an easily observed macroscopic phenomenon, we have found no studies investigating the thermal properties of these molecules below their cloud point. This is especially important in amphiphilic assemblies that feature these temperature-sensitive functional groups, because the change in hydrophilic–lipophilic balance (HLB) above and below the LCST results in dramatically altered supramolecular structures. Since the fidelity of an amphiphilic assembly depends on the HLB,[31-33] if there is a temperature-dependent effect prior to the macroscopic phase change in its building blocks, then it will likely alter the assembly itself. Here, we report such a phenomenon in facially amphiphilic dendrons.[34,35] Specifically, we have observed a sub-LCST transition in which the molecular organization, host–guest encapsulation properties, and dynamics of the supramolecular assemblies are affected by temperature (Figure 3.1). In this paper,

we explore the previously unreported thermoresponsive behavior as demonstrated by temperature-dependent dynamic light scattering (DLS), dynamic FRET-based guest exchange, and host exchange, as monitored by an excimer-based fluorescence probe. This work provides insight into the self-assembly and thermoresponsive properties of ethylene glycol containing molecules by experimentally revealing a sub-LCST dynamic to static supramolecular transition.

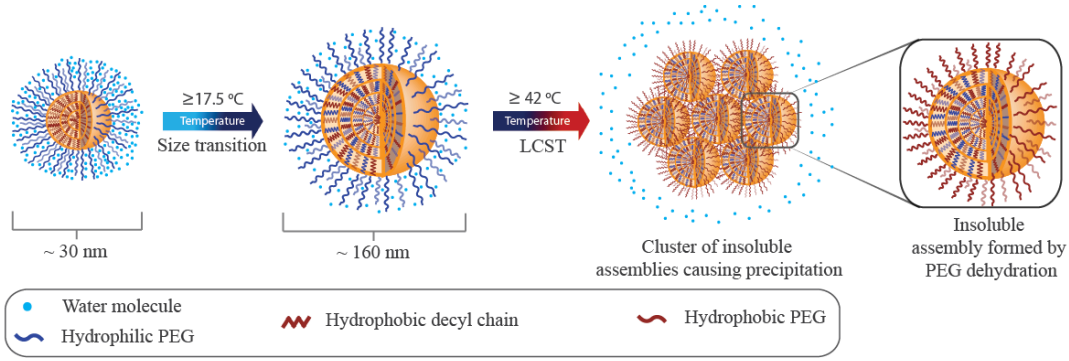

Figure 3.1. Schematic representation of the proposed sub-LCST supramolecular transition at ~ 17.5 °C and *LCST* at ~ 42 °C respectively.

We chose oligo(ethylene glycol) (OEG)-containing facially amphiphilic dendrons (Scheme 3.1) for this study, because (i) these dendrons are known to exhibit LCST behavior,[17] (ii) the monodisperse nature of the dendrons[33,36-39] provides the opportunity to systematically vary the structure of the building blocks of the amphiphilic assembly and investigate its effect upon the temperature-dependent host characteristics, and (iii) the amphiphilic assemblies from these dendrons can act as hosts for noncovalently binding guest molecules.

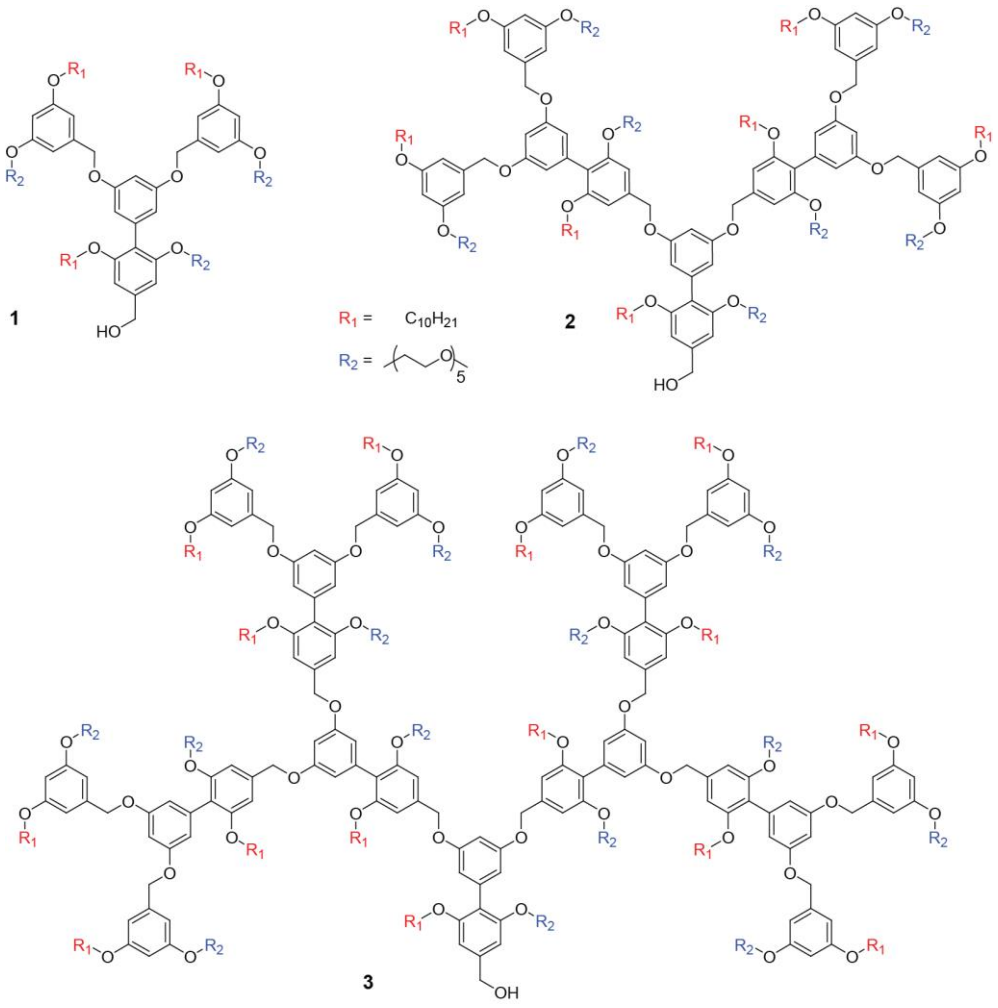

Scheme 3.1. Structure of temperature sensitive facially amphiphilic dendrons

3.2 Molecular Designs and Aggregation Properties

Facially amphiphilic dendrons, with a five-repeat OEG unit as the hydrophilic moiety and a decyl group as the lipophilic moiety, have been shown to organize into spherical assemblies in the aqueous phase.[17] Host–guest studies revealed that these assemblies contain a hydrophobic interior for sequestering lipophilic guest molecules, reminiscent of micelle-like structures. However, size measurements using dynamic light scattering (DLS) and transmission electron microscopy (TEM) reveal that these are about 160 nm in diameter at 25 °C.[17] This rather large size, for

a micellar assembly, and the facially amphiphilic structure of the dendrons led us to assume that the hydrophobic interior (as probed by the microenvironment of fluorescent guest molecules) is composed of lipophilic alkyl and buried OEG moieties. This is understandable, because unhydrated OEG units are thought to be hydrophobic. Considering these possibilities, we were interested in investigating whether the temperature-dependent hydration of the OEG units would alter the HLB, where a greater number of OEG units are exposed to the solvent at lower temperatures.

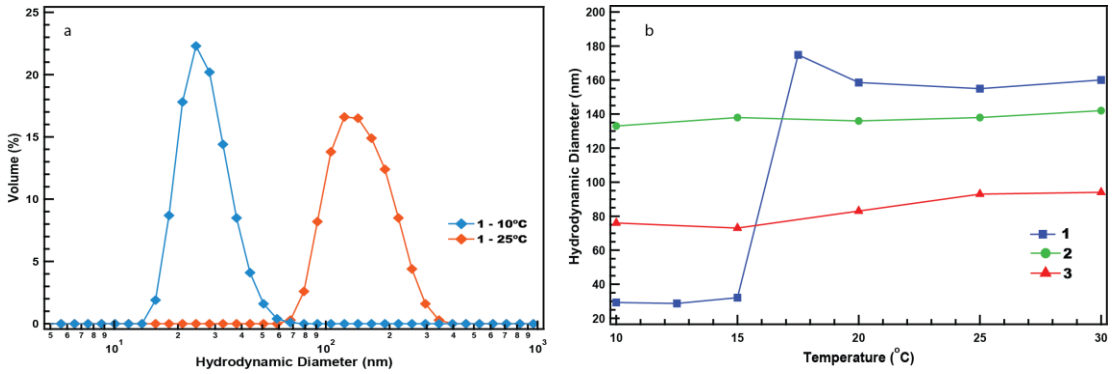

Figure 3.2. Temperature dependent size variations as observed by dynamic light scattering (DLS). a) A large change in the D_H of 1 was observed for 25 °C (160 nm) and 10 °C (30 nm) assemblies. b) The temperature responsiveness of dendrons **1**, **2**, and **3** were determined. Dendron **1** showed a sharp change in the hydrodynamic radius between 15 and 17.5 °C, while the assemblies from dendrons **2** and **3** were temperature insensitive.

To investigate this, we first measured the size of the assembly obtained from our first-generation facially amphiphilic dendron **1**, using DLS at 10 °C. Indeed, we found that the size of the amphiphilic assembly formed from the dendron is much smaller (~30 nm), in comparison to that observed at ambient temperature (~160 nm) (Figure 3.2a). Considering this observation, we carried out systematic temperature-dependent DLS studies for the dendron **1**. The results from these

studies highlight a sharp transition in the size of the aggregate between 15 and 17.5 °C (Figure 3.2b). The PDI values of all assemblies were between 0.110 and 0.306 with correlation functions of >0.82. The correlation functions were slightly lower (0.70 and 0.71) for the smaller assemblies at the two lowest temperatures studied, 10 and 12.5 °C (Figure 3.5). Note that the classical cloud point or the LCST transition for this molecule is 42 °C (Figure 3.9)[17] and there seems to be a previously unobserved transition at a lower temperature. Interestingly, when the second- and third-generation dendrons (**2** and **3**) were investigated, no temperature-dependent size change was observed at lower temperatures within the temperature ranges investigated; the LCST values of these dendrons were 32 and 31 °C, respectively.[17] Thus, the following are the noteworthy features of this preliminary finding: (i) dendron **1** exhibits a macrophase separation, resulting in an anisotropic mixture at 40 °C, the so-called LCST, (ii) below the LCST, some higher order aggregation does occur, but the assembly does not exhibit any macrophase separation, (iii) far below the LCST, there exists a second, sub-LCST transition, resulting in smaller aggregates presumably due to greater hydration of the OEG units, and (iv) this three-phase system is unique to **1**, in comparison to second- and third-generation dendrons (**2** and **3**). We speculate that the higher number of amphiphilic units that are covalently tethered in these dendrons results in a larger energetic penalty for reorganizing the assembly formed at ambient temperature, thus preventing a sub-LCST transition.[40,41] It is critical then to understand the dynamic nature of the supramolecular assembly from the first-generation dendron, in comparison to the second- and third-generation facially amphiphilic dendrons.

3.3 Temperature Dependent Host Exchange

At first glance, it seems obvious that a size change with decreasing temperature should dictate that the dendron host also exchanges. Note that our previous experiments do suggest that there would be a change in the size upon decrease in temperature. However, once an assembly is at a particular temperature, we do not know whether or not the host molecule rapidly exchanges among the amphiphilic assemblies. Therefore, it is interesting to investigate whether host exchange dynamics is dependent on temperature. For this purpose, we synthesized a G1 dendron (**6**; Scheme 3.2) with a pyrene moiety "clicked" at its focal point. Dendron **6** forms an assembly much like that of **1**, with the exception that we now have a covalently bound fluorescent probe at the interior of the aggregate with which we can monitor thermosensitivity of the host exchange. In the amphiphilic supramolecular assembly, pyrene units would be forced into close proximity. This

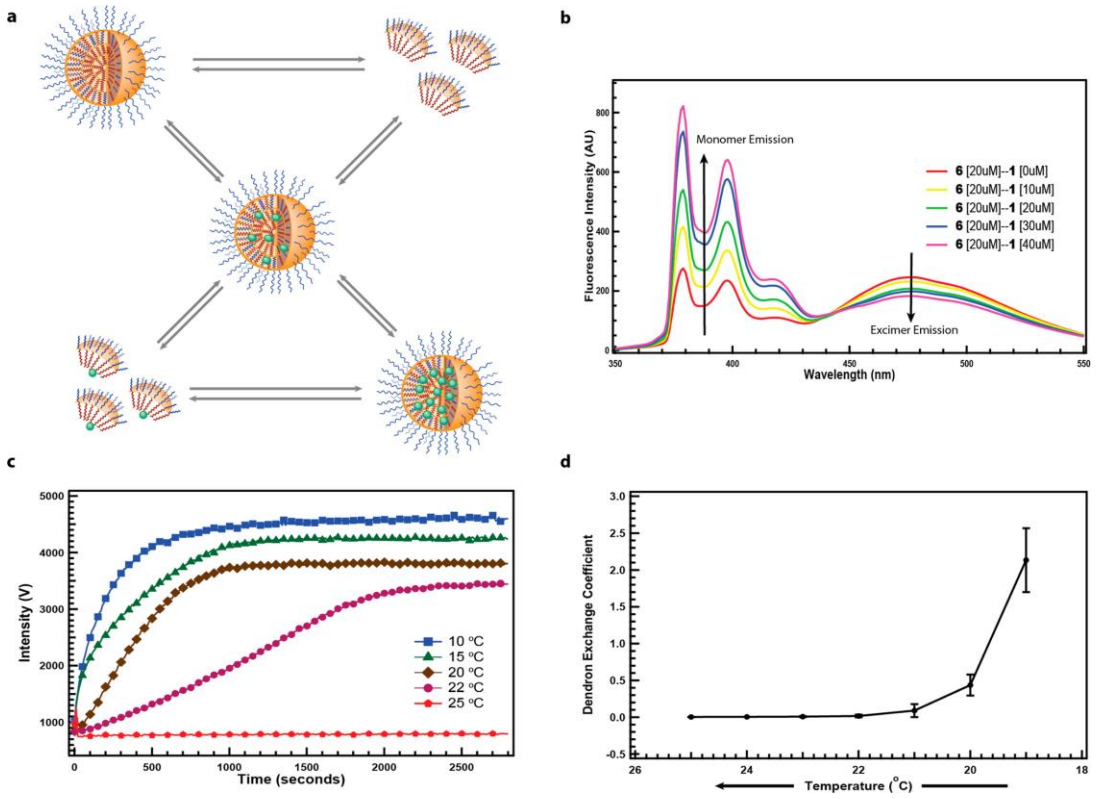

Figure 3.3. Dendron exchange via mixed micellar assemblies. Exchange rates are extracted using a covalently linked pyrene probe 6 in a mixed assembly experiment. (a) Dendritic supramolecular assemblies are in equilibrium with individual dendrons in solution; mixing 1 and 6 results in a mixed assembly (1*6), where the effective concentration of pyrene units will be reduced. (b) The change in the excimer/monomer ratio upon 1*6 formation allows us to directly monitor dendron exchange via time-lapse fluorescence measurements. (c) Mixing solutions of 1 and 6 at multiple temperatures while monitoring the pyrene monomer emission shows a distinct change in dendron exchange rates. (d) Ramping the temperature by 1 °C increments from 25 to 19 °C shows the dramatic change in the equilibrium between supramolecular assemblies and individual dendron units in solution. The change in assembly dynamics, coupled with the change in hydrodynamic radius, suggests the presence of two organizationally distinct assemblies below the LCST of the material.

state can be probed through the formation of an excited state dimer (excimer), which spectroscopically reveals itself through a broad emission peak with a large Stokes shift. If we mix the dendron **6** with the pyrene-less dendron **1** and if there were a rapid exchange of the dendron molecules among the aggregates, then the concentration of the pyrene units within an aggregate will decrease (Figure 3.3a).

This decrease should result in reduced excimer emission and a corresponding increase in the emission that corresponds to the pyrene monomer. To first investigate the viability of this experiment, we first mixed different concentrations of dendron **1** with a 20 μM solution of **6** and monitored the pyrene fluorescence. Note that the pyrene excimer emission indeed decreases with a concurrent increase in the monomeric emission, when the concentration of **1** is increased in the solution (Figure 3.3b).

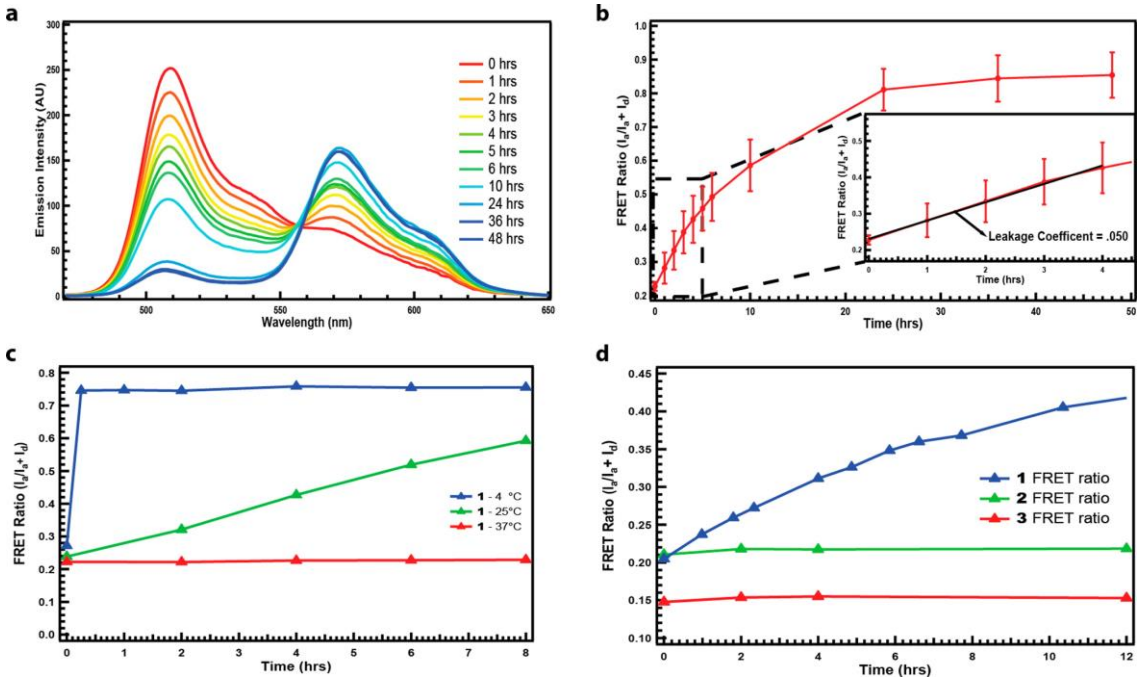

Figure 3.4. (a) Excitation of DiO at 450 nm results in FRET, when a mixed assembly is present. (b) The leakage coefficient (Λ) is derived from the acceptor−donor ratio as the slope of the FRET ratio (see inset for linear region of dye exchange). (c) The temperature sensitivity of **1** was shown to have an inverse effect on the guest exchange dynamics with exchange at 4 °C complete within 10 min and virtually no exchange observed at 37 °C. (d) Guest molecule mixing studies were performed with 1−3 to test any generation dependence on the exchange rates. Exchange was only observed for the first-generation dendron **1**.

To allow for a direct correlation between dendron exchange rates and temperature sensitivity, we used time-lapse fluorescence, where we monitored the increase in monomer emission with time. Solutions of **1** and **6** (25 μM) were brought to the target temperature (±1 °C) for 30 min prior to mixing. The solutions were then combined in the fluorescence cuvette holder at a pre-equilibrated temperature. The emission intensity at 379 nm (monomeric pyrene) was monitored with one measurement every 10 s (Figure 3.3c). The peak intensity at 379 nm increased rapidly, when the temperature was 10 °C. On the other hand, there was no change in the emission intensity at 25 °C. In other words, the dynamics of host exchange is faster at lower temperatures. If our hypothesis that the higher

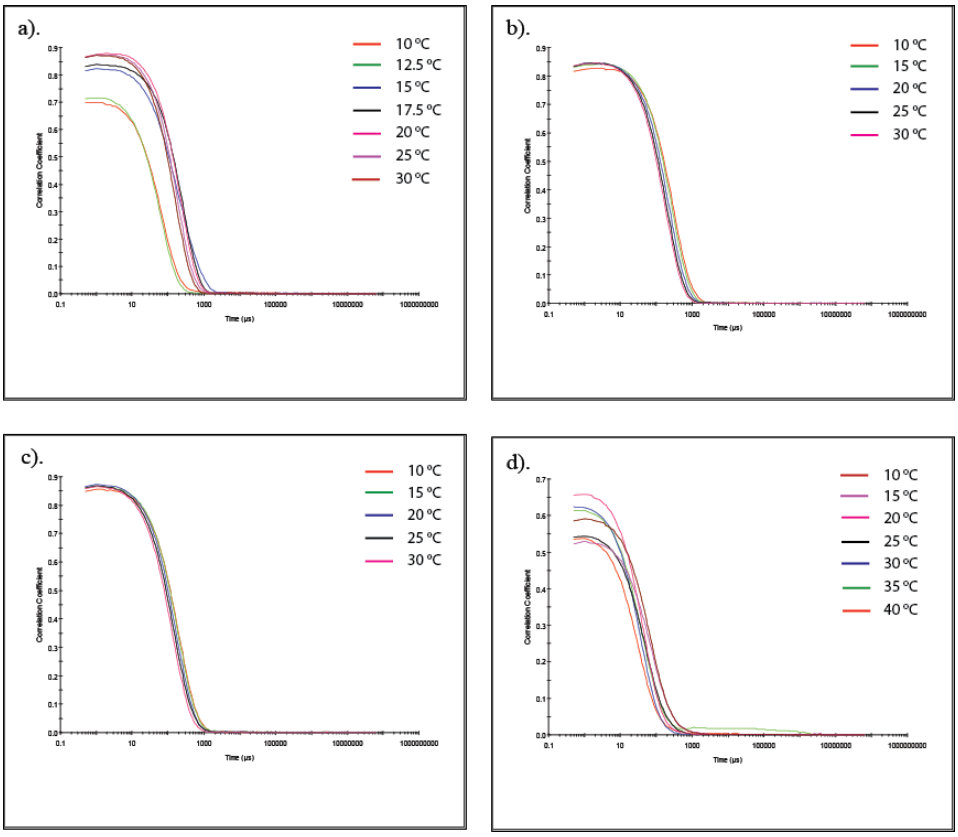

Figure 3.5. . Correlograms of G1(a), G2(b), G3(c) OEG dendrimers and G1 zwitterionic dendrimer(d) as determined by DLS.

generation dendrons pay a larger energetic penalty for dissociating from the amphiphilic aggregate were correct, then those two dendrons should not exhibit host exchange at any temperature (or exhibit this behavior at even lower temperatures). Indeed, dendrons **2** and **3** did not exhibit any exchange over the temperature range of 10–25 °C, when the experiments were carried out with a mixture of these dendrons with the dendron **6** (Figure 3.8). These results further support the tighter association of the host molecules in the higher generation dendrons.

In analyzing the data in Figure 3.3c, we noticed not only that there was a strong temperature dependence upon the dendron exchange but also that the transition from a non-exchanging mixture to an exchanging mixture was rather sharp between 22.5 and 20 °C. Assuming first order, we calculated the rate constants at these temperatures using their half-lives and found that there was a significant increase in rate from 22.5 to 20 °C, where the rate constants obtained at these temperatures were 8.5468×10^{-4} and 2.6557×10^{-3} s^{-1}, respectively. The rate further increases with decreasing temperature and reaches 8.557×10^{-3} s^{-1} at 10 °C, which is an order of magnitude higher than the rate observed at 22.5 °C (Figure 3.10). To independently investigate the sharpness of the transition observed in Figure 3.3c, from a static to a dynamic assembly, the temperature of a single mixed micelle solution was decreased from 25 to 19 °C by 1 °C increments. The **1*6** solution was allowed to equilibrate at each temperature, and the exchange coefficients were calculated. The transition from negligible dendron exchange to a very rapidly exchanging assembly occurs over a ~2 °C range (Figure 3.3d). The

slight discrepancy in the transition temperature range from the temperature ramping experiments and constant temperature mixing experiments is attributed to the possible difference in pre-equilibration times. Finally, to understand if the increase in dynamics of host exchange observed at lower temperatures (Figure 3.3c) is associated with any sub-LCST size transition, variable-temperature DLS was performed with assemblies from **6** and **1*6**. Surprisingly, assembly from **6** alone did not show a size transition at lower temperatures, presumably due the increased hydrophilicity in lipophilic chain due to pyrene. However, assembly from **1*6** did show a temperature-dependent size transition, suggesting that the host **6** is indeed also dynamic at lower temperatures (Figure 3.11).

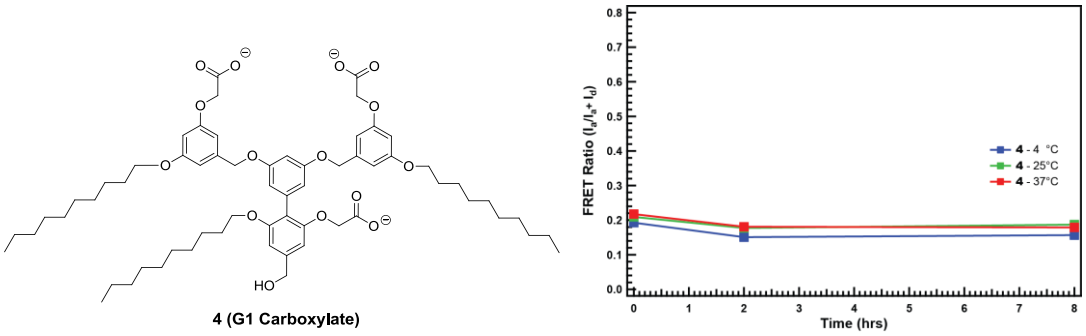

Figure 3.6. G1 carboxylate dendrimer (4) was shown to have high encapsulation stability at low temperatures by the lack of FRET evolution at all temperatures.

3.4 Temperature Dependent Guest Exchange

Considering the temperature-dependent assembly behavior, as well as host exchange, we were interested in investigating the implications of this behavior in guest exchange. We neither anticipated nor observed any significant difference in the extent of encapsulation of guest molecules based on minor temperature variations in the assembly. However, we were interested in identifying the

implications of the temperature-dependent changes in the amphiphilic assembly upon the dynamics of guest exchange between the host and the bulk solvent, which is referred to as the encapsulation stability.[42] Note that the host–guest interactions in these amphiphilic assemblies are driven by solvophobic interactions. Therefore, if the solvation of the host molecule were to differ with temperature, then it should follow that the encapsulation stability would also be different.

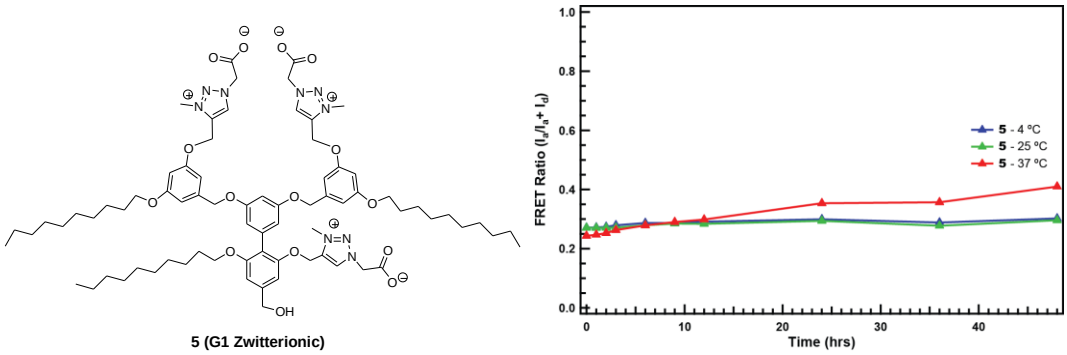

Figure 3.7. G1 zwitterionic dendrimer (5) was shown to have high encapsulation stability at low temperatures by the lack of FRET evolution at 4 ^{0}C and 25 ^{0}C. Some guest exchange was seen at 37 ^{0}C, most likely due to an increase in guest leakage by an increase in diffusion. This highlights the importance of oligoethylene glycol hydration on the observed inverse temperature sensitive dynamics of guest exchange.

That is, the dynamics of guest exchange should be higher at lower temperatures, since the dendron becomes more hydrophilic at lower temperature. In terms of the general relationship between dynamics and temperature, this seems counterintuitive at first. However, when we account for the solvation of the host, this seems possible. The dynamics of guest exchange and thus the leakage coefficient can be measured using a recently developed fluorescence resonance energy transfer (FRET) based method.[42] Briefly here, two different solutions of the host–guest assembly are generated: one containing a FRET donor dye as the guest molecule and the other containing the corresponding FRET acceptor guest molecule.

When these two solutions are mixed, if there is a rapid guest exchange the FRET donor and acceptor guest molecules will result in the same supramolecular assembly; this can be discerned by a decrease in the donor emission with a concurrent increase in the acceptor emission, when the donor molecule is excited. If there is no guest exchange, there should be no evolution of the relative emission intensities with time.

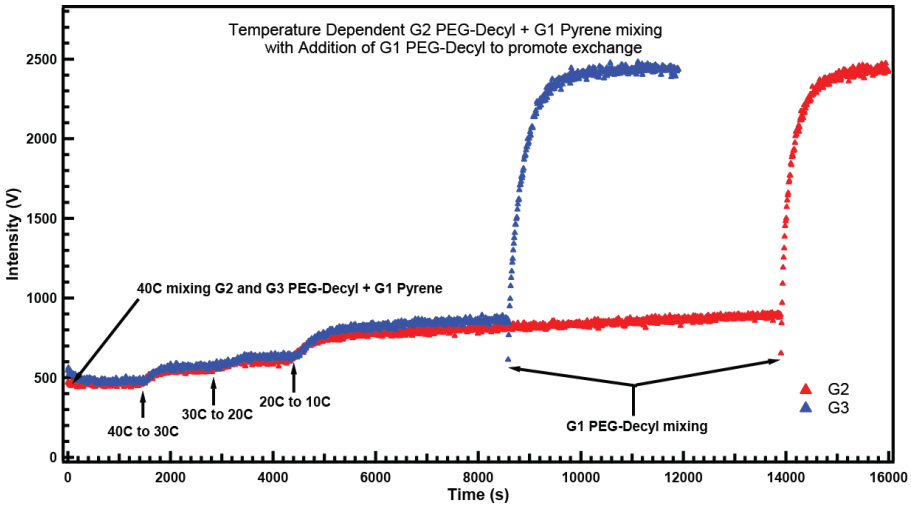

Figure 3.8. The emission of pyrene at 379 nm was followed over time. There is no significant exchange of 2 or 3 with 6 as shown by the lack of a sustained increase in the emission at 379 nm (pyrene monomer emission). The increase in fluorescence intensity with the decreasing temperature is a phenomenon observed for all fluorescent molecules in our dendritic assembly and does not correspond to a dendron host exchange process. Rapid exchange of dendrons is observed upon the addition of 1 to the system as seen by the dramatic increase in emission as observed with 1*6 formations.

In our experiments, we used 3,3′-dioctadecyloxacarbocyanine perchlorate (DiO, FRET donor) and 1,1′-dioctadecyl-3,3,3′,3′-tetramethylindocarbocyanine perchlorate (DiI, FRET acceptor) as the lipophilic FRET pair. The dye molecules were encapsulated in **1** in separate solutions, referred to as **1**-DiO and **1**-DiI. The two solutions were then mixed, and the evolution of FRET was monitored over time

(Figure 3.4a). Indeed, when the DiO molecule was selectively excited in the solution, the emission intensity from DiO decreased with time, while the emission from DiI increased. The leakage coefficient (Λ), which is the slope of the linear fit of the FRET ratio over time at initial times, was found to be Λ = 0.05 for **1** at 25 °C (Figure 3.4b). The FRET ratio is defined as $I_a/(I_a + I_d)$, where I_a and I_d are the intensities of the acceptor and donor emissions at their respective emission maxima.[42,43]

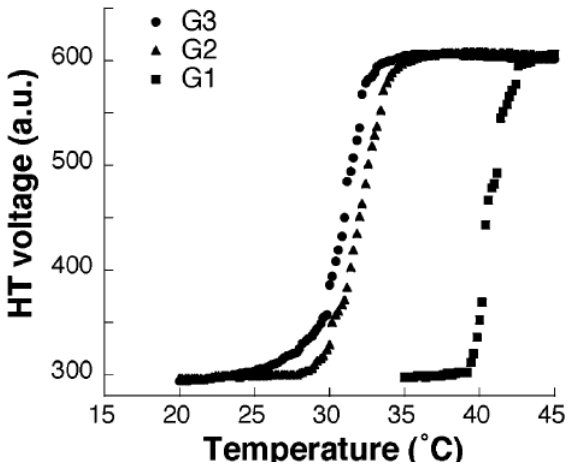

Figure 3.9. Temperature-dependent macroscopic phase change observed by increase in high tension voltage, triggered by precipitation-based scattering. The data in Figure 2c is reproduced from a previous publication for comparison.[17]

Temperature (K)	$t_{1/2}$ (s)	k (s^{-1})
283	81	8.5468×10^{-3}
288	120	5.776×10^{-3}
293	261	2.6557×10^{-3}
295.5	811	8.5468×10^{-4}

Figure 3.10. Rate constants for host exchange at different temperatures (283 K to 295.5 K). It can be seen that the rate increase by an order of magnitude going from 295.5 K to 283 K.

Considering our findings with temperature-dependent change in the size of the amphiphilic assembly, we investigated the dynamics of guest exchange in these assemblies at different temperatures. Mixing experiments utilizing **1**-DiO and **1**-DiI were first performed at 4 and 37 °C. Interestingly, an increase in the exchange dynamics of guest molecules was observed at 4 °C, as a complete guest exchange occurs in less than 10 min with $\Lambda > 1.897$. Conversely, essentially no FRET evolution was observed at 37 °C, which affords $\Lambda \leq 0.001$. Although exchange dynamics is typically expected to be faster at higher temperatures, note that the guest exchange is extremely rapid at lower temperatures and nonexistent at higher temperatures in this assembly in the aqueous phase. This is taken to indicate that the guest molecule exchange is heavily influenced by the hydration state of OEG for the first-generation dendron **1** (Figure 3.4c).

In order to further test our hypothesis that the temperature-dependent size changes and guest exchange dynamics are likely due to differences in hydration of the OEG units, we tested the temperature-dependent studies with two control dendrons, the carboxylate dendron **4** and the zwitterionic dendron **5**. These dendrons are structurally similar to **1**, except that the hydrophilic OEG unit is replaced with carboxylate and zwitterionic moieties, respectively. Both **4** and **5** self-assemble into micelle-like aggregates, which are capable of sequestering guest molecules. Dendron **4** was shown to be temperature insensitive with respect to both aggregate size and encapsulation stability (Figure 3.6). It should be noted that, as a polyelectrolyte, counterion effects could have significant effects on the solution properties of **4**. Dendron **5** addresses this concern, as it is a neutral zwitterionic

molecule that should not be affected by changes in temperature. Theoretically, both dendrons should be insensitive to any hydrogen-bonding effects, as the interfacial interaction with water is strong enough not to be affected in the temperature range of this study. We therefore expect no size change as a function of temperature or inverse temperature dependence on guest exchange. We were gratified to observe no difference in assembly size with temperature. Similarly, the FRET-based guest exchange studies with **5** revealed that no guest exchange is observed at room temperature or at lower temperatures. Slightly elevated guest exchange was observed for higher temperatures, most likely due to the classical increased diffusion at higher temperature (Figure 3.7).

Guest exchange experiments for the higher generation dendrons **2** and **3** showed no FRET evolution with time, indicating that the lipophilic guest molecules are stably encapsulated in these amphiphilic assemblies (Figure 3.4d). This exchange dynamics, or lack thereof, was found to be temperature insensitive, suggesting that the host properties of higher generation dendrons are not affected by the possible increased hydration of OEG. The insensitivity of the larger dendrons is most likely correlated to a larger energetic penalty of rearrangement, which has the effect of providing a stable hydrophobic environment for guest encapsulation. The difference in guest encapsulation stability of **1** can be explained by considering the two limiting scenarios for the dynamics of guest exchange. The first scenario is where the guest molecules are able to diffuse in and out of the assembly through Fickian diffusion, resulting in an unassisted guest exchange among the host molecules present in solution. The second scenario

involves a dynamic exchange of individual dendrons among the aggregates, where a dendron dissociates from an aggregate and the monomeric form then reassembles with one of the other aggregates. Here guest molecules, closely associated with an exchanging amphiphilic dendron, could be simultaneously transported until a recombination event occurs with another assembly. This process would also manifest itself as a guest exchange with respect to the FRET-based measurement. It is also important to note that these processes are not mutually exclusive. In addition, the latter scenario would be consistent with our hypothesis that the larger dendrons afford stable encapsulation, because there is a larger energetic penalty for molecular rearrangement.

The dynamic and static nature of dendrons observed from the host exchange as well as the guest exchange experiments below and above a specific temperature could be viewed as a sub-LCST transition, on the basis of a phenomenon that occurs well below the macrophase separation temperature defined by the LCST (Figure 3.1). The presence of a sub-LCST in this system and the effect it has upon the host–guest capabilities of the dendron assembly illustrate the importance of the temperature-mediated properties of OEG-based supramolecular assemblies. Further computational and spectroscopic studies on these systems are warranted for an even greater understanding of the underlying physical properties affecting OEG hydration and supramolecular behavior.

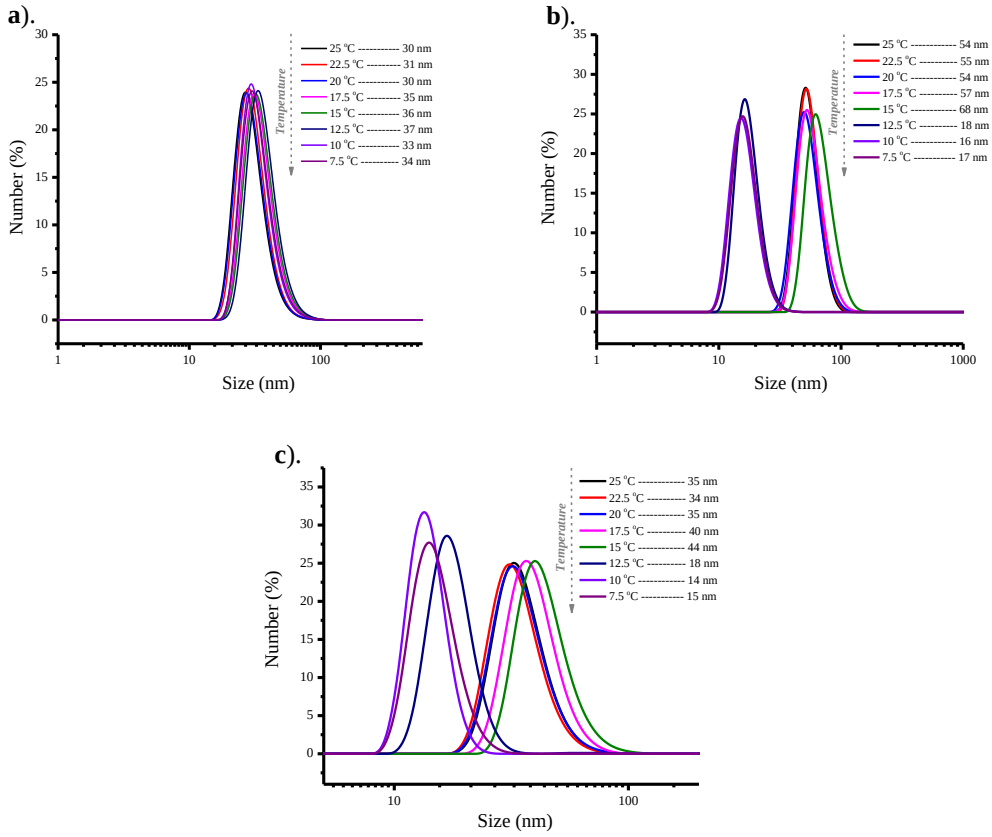

Figure 3.11. Variable temperature DLS of **a)**. **6** , **b)**. **1** , and **c)**. 1:1 mixture of **1** and **6**

3.5 Conclusions

A study of amphiphilic supramolecular assemblies, containing OEG units as hydrophilic functionalities, at temperatures below their LCST reveals that there is also a possibility of sub-LCST transitions in these supramolecular assemblies. We found the following. (i) The size of the supramolecular assemblies can significantly change in response to temperature variations. This is attributed to the enhanced hydration of the OEG units in the amphiphilic dendron. (ii) The size change and the ensuing temperature-dependent variations in the host–guest properties of the dendrons is unique to the first-generation dendron. Structurally similar, but larger,

second- and third-generation dendrons do not exhibit these features. We speculate that the higher number of amphiphilic units that are covalently tethered in these dendrons results in a larger energetic penalty for reorganizing the assembly formed at ambient temperature. (iii) Concurrent with the temperature-dependent size change, the guest encapsulation stability of the dendrons also decreases with decreasing temperature. While guest molecules are stably encapsulated at ambient temperature, the dynamics of guest exchange is much faster at lower temperatures. (iv) In addition to the rapid guest exchange at lower temperatures, the dendritic host also rapidly exchanges at low temperatures. When analyzing the temperature at which the dendritic host transitions from being in a static assembly to a dynamic one, we identified that there is a rather sharp transition temperature, which we call a sub-LCST transition temperature (Figure 1). The fact that this temperature-dependent host exchange dynamics is present in **1**, but not in **2** and **3**, further supports the hypothesis that there is a larger energetic penalty for reorganizing the assembly in higher generation dendrons. Amphiphilic assemblies have been of interest for a variety of applications. Ethylene glycol based amphiphilic systems are often targeted for biological applications, because these systems are known to provide enhanced circulation times and nonfouling hydrophilic surfaces.[13,44,45] The commonly anticipated temperature-dependence feature in these assemblies involves the macroscopic phase separation of these assemblies from solution, often described as the LCST. The findings here that there can be temperature-dependent transitions in these amphiphilic assemblies well below their LCST and that these sub-LCST transitions have a significant impact on the host–guest properties of the

assemblies, will have important implications in the design and utility of such amphiphilic molecules in these applications.

3.6 Experimental Details

3.6.1 Synthesis and Characterization

All chemicals and reagents were purchased from commercial sources and were used as received, unless otherwise mentioned. Compound **C** was synthesized following the previously reported procedure.[1] ^{1}H-NMR spectra were recorded on 400 MHz Bruker NMR spectrometer using the residual proton resonance of the solvent as the internal standard. Chemical shifts are reported in parts per million (ppm). When peak multiplicities are given the following abbreviations are used: s, singlet; d, doublet; t, triplet; m, multiplet. ^{13}C-NMR spectra were proton decoupled and measured on a 100 MHz Bruker spectrometer using carbon signal of the deuterated solvent as the internal standard.

3.6.1.1 Synthesis of Compound A

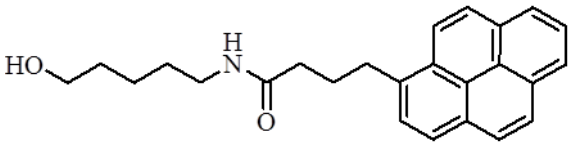

Pyrenebutyric acid (1.25 g, 4.34 mmol), 4-dimethylaminopyridine (0.158 g, 1.29 mmol), N-(3-dimethylaminopropyl)-N′-ethylcarbodiimide (0.995 g, 5.19 mmol), and triethylamine (0.526 g, 5.2 mmol) were mixed together in dry DMF for 15 minutes under argon atmosphere at 0 ^{o}C, to this reaction mixture was added 5-aminopentanol (0.447 g, 4.33 mmol) drop wise and stirred at 0 ^{o}C - room

temperature for 5 hours. The reaction mixture was then diluted with ethyl acetate and extracted with water three times to remove DMF from the organic extract; this extract was then dried over anhydrous Na_2SO_4. The solvent was then evaporated under vacuo and the crude product obtained was purified by silica gel column chromatography (using combiflash) to afford 1.16 g (72 %) of product. NMR and MS data. ^{1}H-NMR (400 MHz, $CDCl_3$) δ 8.30 (d, J = 8 Hz, 1H), 8.18-8.15 (m, 2H), 8.12 (m, 1H), 8.10 (s, 1H), 8.03 (s, 2H), 8.01 (t, J = 8 Hz, 1H), 7.87-7.85 (d, J = 8 Hz, 1H), 5.37 (s, 1H), 3.63 (t, J = 8 Hz, 2H), 3.41 (t, J = 4 Hz, 2H), 3.27 (q, J = 8 Hz, 2H), 2.29 – 2.18 (m, 4H), 1.57 – 1.34 (m, 6H). ^{13}C-NMR (100 MHz; $CDCl_3$): δ 172.6, 135.8, 131.4, 130.8, 129.9, 128.7, 127.4, 127.4, 127.3, 126.7, 125.8, 125.0, 124.9, 124.9, 124.7, 123.3, 39.3, 36.0, 32.7, 32.1, 29.4, 27.4, 23.0. FAB/MS m/z calculated for $C_{25}H_{27}NO_2$ 374.21200; measured 374.21122.

3.6.1.2 Synthesis of Compound B

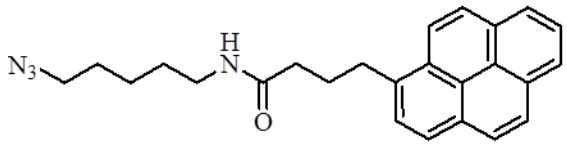

To compound **A** (0.5 g, 1.34 mmol) dissolved in THF was added triethylamine (0.16 g, 1.6 mmol) and stirred for 10 minutes at room temperature, to this was added methanesulfonyl chloride (0.31 g, 2.68 mmol) and stirred at room temperature for another 4 hours. After confirming the conversion of compound **A** to corresponding mesylate through thin layer chromatography, solvent (THF) is evaporated under vacuo to obtain a crude mesylate of compound **A**. This crude mixture was then dissolved in acetonitrile and to this was added sodium azide (0.17 g, 2.68 mmol) followed by refluxing the reaction mixture at 65 ^{o}C for 12 hours. The

solvent was then evaporated under vacuo and the crude product obtained was purified by silica gel column chromatography (using combiflash) to afford 0.53 g (95 %) of product. ^{1}H-NMR (400 MHz; $CDCl_3$): δ 8.28 (d, J = 8 Hz, 1H), 8.16 (d, 2H), 8.09 (d, J = 8 Hz, 2H), 8.04 - 7.96 (m, 3H), 7.83 (d, J = 8 Hz, 1H), 5.40 (s, 1H), 3.36 (t, J = 8 Hz, 1H), 3.20 – 3.17 (m, 4H), 2.25 - 2.15 (m, 4H), 1.54 – 1.25 (m, 8H). ^{13}C - NMR (100 MHz; $CDCl_3$): δ 172.5, 135.8, 131.4, 130.8, 129.9, 128.7, 127.4, 127.3, 127.3, 127.0, 126.7, 125.8, 125.0, 124.9, 124.9, 124.7, 123.3, 51.3, 39.3, 36.0, 32.7, 29.5, 28.7, 27.4, 26.4, 26.3. FAB/MS m/z calculated for $C_{25}H_{26}N_4O$ 413.23; measured 413.24.

3.6.1.3 Synthesis of Compound C

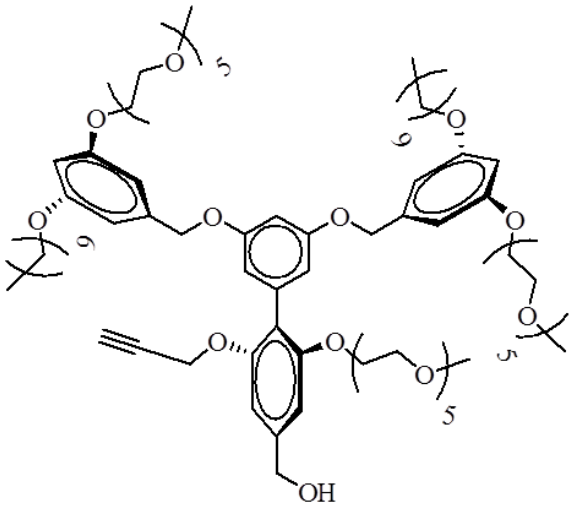

Compound **C** is synthesized by previously reported procedure[1] from our group. ^{1}H-NMR (400 MHz; acetone-d6): δ 6.87 (s, 1H), 6.80 (s, 1H), 6.66 – 6.59 (m, 7H), 6.46 (t, J = 2.2 Hz, 2H), 5.62 (s, 2H), 5.05 (s, 4H), 4.67 – 4.65 (m, 4H), 4.14 – 4.12 (m, 4H), 4.08 – 4.05 (m, 2H), 3.99 (t, J = 6.5 Hz, 4H), 3.82-3.80 (m, 4H), 3.67-3.43 (m, 54H), 3.27 (s, 9H), 3.01 (t, J = 2.4 Hz, 1H), 2.83 – 2.79 (m, 3H), 2.09 (s, 3H), 1.80-1.73 (m, 4H), 1.48 - 1.28 (m, 32H), 0.90 – 0.86 (m, 6H). ^{13}C-NMR (100 MHz; acetone-d6): δ 160.5, 160.3, 159.1, 156.9, 155.6, 143.7, 143.7, 140.0, 136.1, 118.9, 110.5, 105.9,

105.7, 104.5, 104.4, 100.6, 100.3, 79.2, 75.9, 71.7, 70.5, 70.5, 70.4, 70.3, 70.3, 70.3, 70.2, 70.1, 69.5, 69.4, 69.2, 68.6, 67.7, 67.5, 63.8, 63.7, 57.9, 55.9, 54.0, 31.7, 25.9, 22.4, 13.5; MALDI-TOF m/z calculated for $C_{83}H_{13}2O_{24}$ + Na : 1536.91; found 1537.49.

3.6.1.4 Synthesis of Compound 6

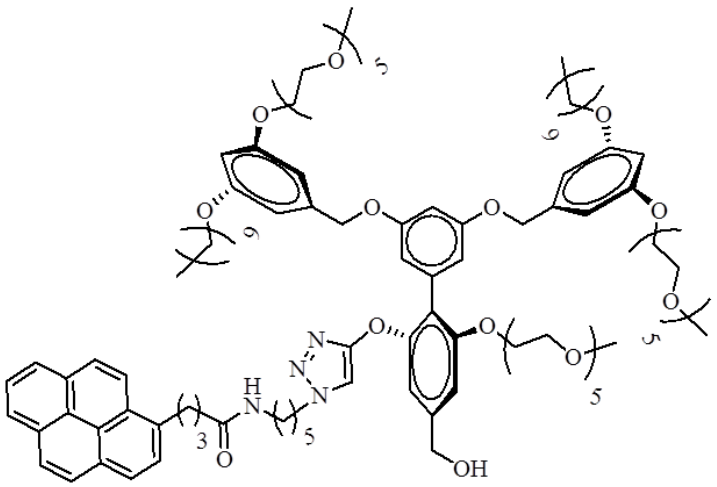

The dendritic acetylene compound **C** (50 mg, 0.033 mmol), and azide compound **B** (26 mg, 0.066 mmol) were dissolved in 1:1 THF/H2O mixture. To this was added $CuSO_4.5H_2O$ (4.1 mg, 0.0165 mmol), sodium ascorbate (3.26 mg, 0.0165 mmol) and stirred at room temperature for 24 hours. The reaction mixture was then concentrated in vacuo to remove THF and extracted twice with ethyl acetate; the combined extracts were then dried over Na_2SO_4. Upon evaporation of the solvent the crude mixture is purified by silica gel column chromatography to afford 40 mg of product **5**. ^{1}H-NMR (400 MHz; acetone-d6): δ 8.43 (d, J = 9.3 Hz, 1H), 8.24 – 8.15 (m, 4H), 8.08 (d, J = 1.2 Hz, 2H), 8.02 (t, J = 7.6 Hz, 1H), 7.92 (d, J = 8 Hz, 1H), 7.65 (s, 1H), 7.00 (t, J = 2.2 Hz, 1H), 6.92 (s, 1H), 6.79 (s, 1H), 6.70 – 6.65 (m, 6H), 6.59 (t, J = 2.2 Hz, 1H), 6.43 (t, J = 2.2 Hz, 2H), 5.11 (s, 2H), 5.01 (s, 4H), 4.66 – 4.65 (m, 2H), 4.37 (t, J = 5.5 Hz, 1H), 4.25 (t, J = 8 Hz, 2H), 4.13 – 4.04 (m, 7H), 3.95 (t, J = 4 Hz,

4H), 3.80 -3.35 (m, 64H), 3.26 – 3.25 (m, 9H), 3.19 – 3.13 (m, 2H), 2.31 (t, J = 7 Hz, 2H), 2.15 – 2.11 (m, 2H), 1.80 – 1.68 (m, 7H), 1.45 – 1.20 (m, 42H), 0.89 – 0.84 (m, 8H). ^{13}C-NMR (100 MHz; acetone-d6): δ 171.6, 160.4, 160.1, 158.9, 156.7, 156.2, 143.7, 143.5, 139.9, 136.6, 136.1, 131.3, 130.8, 129.7, 128.6, 127.4, 127.1, 126.4, 125.8, 124.8, 124.7, 124.6, 123.5, 123.0, 118.5, 110.4, 105.8, 105.0, 104.5, 104.1, 100.5, 100.1, 71.6, 70.4, 70.3, 70.2, 70.2, 70.2, 70.1, 70.1, 70.0, 69.4, 69.3, 69.1, 68.3, 67.6, 67.3, 63.7, 63.6, 62.5, 57.8, 49.4, 38.6, 35.2, 32.5, 31.6, 28.2, 25.9, 25.8, 25.7, 22.3, 13.3. MALDI-TOF m/z calculated for $C_{83}H_{132}O_{24}$ + K: 1950.22; found 1949.34.

3.6.1.5 Characterization of Zwitterionic Dendron 5

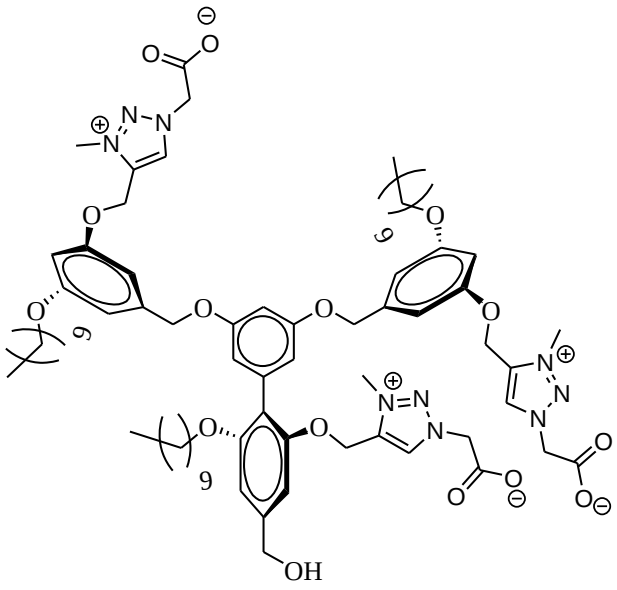

^{1}H-NMR (400 MHz; MeOD): δ 8.81 (s, 2H), 8.43 (s, 1H), 6.91 (s, 1H), 6.83 (s, 1H), 6.78 (s, 2H), 6.72 (s, 2H), 6.64 (t, J = 2.2 Hz, 1H), 6.61 (t, J = 2.2 Hz, 2H), 6.46 (d, J = 2.1 Hz, 2H), 5.45 (s, 4H), 5.27 (s, 2H), 5.22 (s, 4H), 5.08 (s, 2H), 5.04 (s, 4H), 4.67 (s, 2H), 4.37 (s, 6H), 3.98 (t, J = 6.36, 4H), 3.90 (t, J = 6.08, 2H), 3.81 (s, 3H), 1.81-1.74 (m, 4H), 1.57-1.45 (m, 4H), 1.59-1.19 (m, 40H), 0.94-0.84 (m, 9H). ^{13}C-NMR (100 MHz; MeOD): δ 168.6, 164.0, 162.9, 162.4, 148.2, 147.8, 143.1, 127.6,

113.7, 109.9, 109.2, 105.3, 104.3, 87.3, 87.2, 84.0, 83.9, 82.8, 82.6, 81.9, 81.8, 81.5, 81.1, 79.8, 78.7, 78.6, 77.4, 77.4, 73.3, 72.3, 71.6, 68.8, 67.5, 65.4, 64.2, 61.9, 56.1, 55.0, 35.3, 33.0, 32.9, 32.8, 32.7, 32.5, 31.4, 31.3, 29.5, 29.4, 26.1, 21.9, 17.5. MALDI-TOF m/z calculated for $C_{75}H_{106}N_9O_{15}$ [M++H]: 1373.69; found 1374.84.

3.6.2 Preparation of Dendrimer Solutions

Stock solutions of dendrimers were prepared by dissolving dendrimer in milli-Q purified water at 0.3 mg/mL. The solution was vortexed for 30 s, sonicated for one hour, and stirred at 4 °C overnight for one month without drastic changes in the aggregation properties. Subsequent dilutions were made to the target concentrations for FRET, mixed micelle, or DLS experiments.

3.6.3 Dye Loading and Fluorescence Parameters

FRET studies were performed on a Jasco-6500 spectrofluoremeter. Dye loading was performed thrice for each solution as follows: 3 μL of 1 mg/mL dye (DiO or DiI) in acetone was added to a 6 mL glass vial. The acetone was evaporated and 2 mL of dendrimer solution added, the mixture was sonicated for one hour, stirred at 4 °C for three hours, and filtered. Encapsulation efficiency was monitored by UV-vis absorbance on a Cary-100 scan UV-Vis spectrophotometer. Temperature dependent exchange experiments were controlled by storage of dendrimer solutions in a refrigerator at 4 °C, in a warm water bath for 25 °C, and a hot water bath for 37 °C. DiO was excited at 450 nm, DiO and DiI emission were monitored at 508 and 571 nm respectively for the calculation of leakage coefficients.

3.6.4 Dynamic Light Scattering

DLS was performed on a Malvern nano-zeta sizer instrument with a 637 nm laser source with non-invasive backscattering technology detected at 173^0. All sizes are reported as the hydrodynamic diameter (DH) and were repeated in triplicate. All samples were filtered to exclude any aggregates over 0.22 μm and maintained at ±0.1 °C with an equilibration time of seven minutes for each sample.

3.6.5 Time-lapse Fluorescence with Mixed Micelles

Time-lapse studies were performed on a Jasco FP-6500 fluorimeter with a xenon flash power supply and TC125 temperature controller. Solutions of 1 and 6 (25 μM) were pre-equilibrated at the target temperature ±1 °C for 30 min prior to mixing. 6 (0.5 mL) was added to a fluorescence cuvette in a thermoelectric cuvette holder and allowed to equilibrate. 1 (0.5 mL) was syringed directly into the fluorescence cuvette and the emission at 379 nm was monitored. Instrument settings were as follows: Ex-339 nm, em-379 nm. The system was maintained at the target temperature ±0.1 °C and stirred at low rpm. Each temperature mixing was performed in triplicate and an average exchange coefficient was calculated from the linear regression of the pyrene monomer emission versus time. Temperature ramping experiments were performed with the same mixing procedure as the described for the mixed micelle emission. Mixing was started at 25 °C and held for ≈15 min and then decreased by 1 °C increments. Each temperature was held for 15 min or until reaching a stable exchange rate.

3.7 NMR Spectra

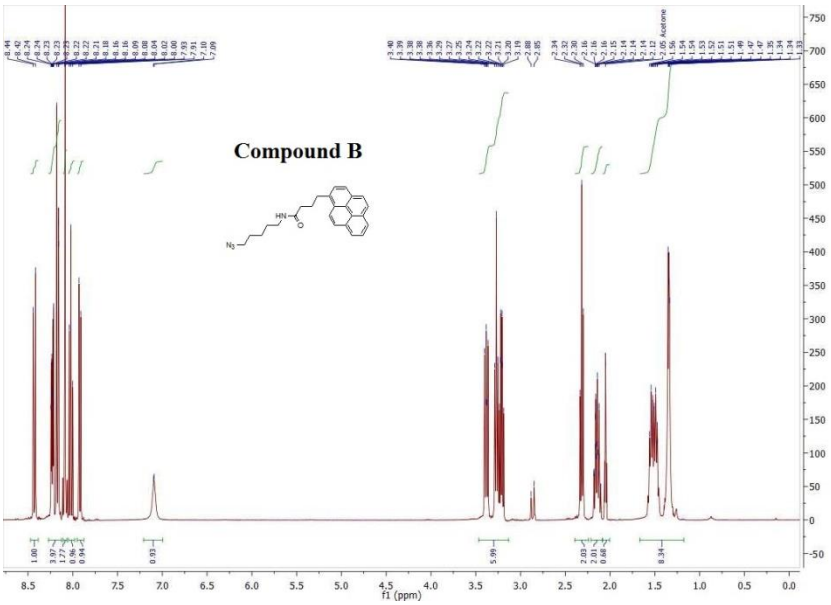

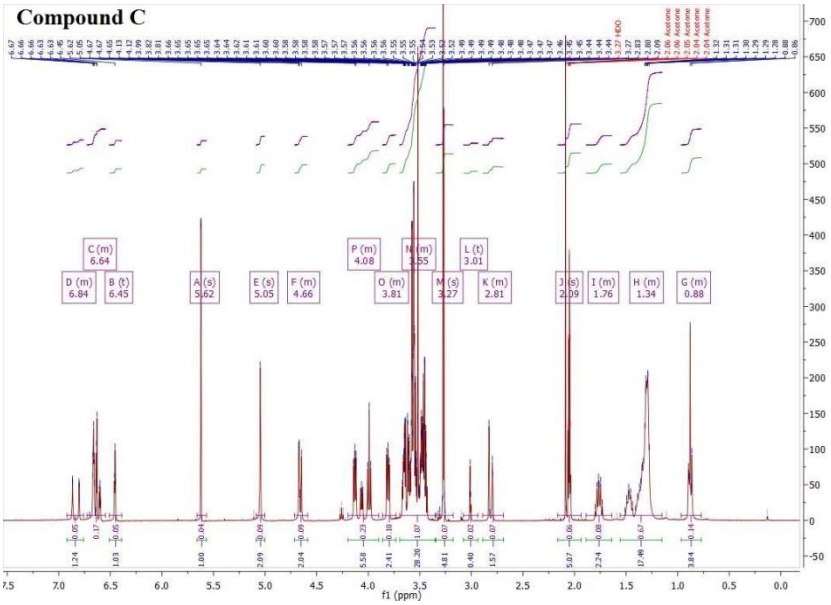

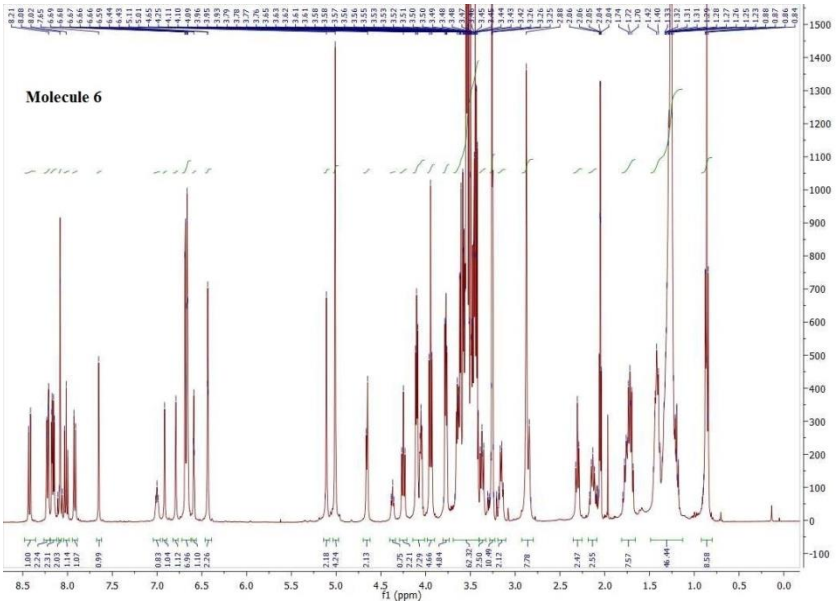

3.8 References

1. Beer, P. D.; Gale, P. A., Anion recognition and sensing: The state of the art and future perspectives. *Angew. Chem. Int. Ed.* **2001,** *40* (3), 486-516.

2. Song, J.; Cheng, Q.; Zhu, S. M.; Stevens, R. C., "Smart" materials for biosensing devices: Cell-mimicking supramolecular assemblies and colorimetric detection of pathogenic agents. *Biomed. Microdevices* **2002,** *4* (3), 213-221.

3. González, D. C.; Savariar, E. N.; Thayumanavan, S., Fluorescence Patterns from Supramolecular Polymer Assembly and Disassembly for Sensing Metallo- and Nonmetalloproteins. *J. Am. Chem. Soc.* **2009,** *131* (22), 7708-7716.

4. Gillies, E. R.; Jonsson, T. B.; Fréchet, J. M. J., Stimuli-responsive supramolecular assemblies of linear-dendritic copolymers. *J. Am. Chem. Soc.* **2004,** *126* (38), 11936-11943.

5. Jeong, B.; Bae, Y. H.; Lee, D. S.; Kim, S. W., Biodegradable block copolymers as injectable drug-delivery systems. *Nature* **1997,** *388* (6645), 860-862.

6. Bae, Y.; Fukushima, S.; Harada, A.; Kataoka, K., Design of environment-sensitive supramolecular assemblies for intracellular drug delivery: Polymeric micelles that are responsive to intracellular pH change. *Angew. Chem. Int. Ed.* **2003,** *42* (38), 4640-4643.

7. Benvin, A. L.; Creeger, Y.; Fisher, G. W.; Ballou, B.; Waggoner, A. S.; Armitage, B. A., Fluorescent DNA Nanotags: Supramolecular Fluorescent Labels Based on Intercalating Dye Arrays Assembled on Nanostructured DNA Templates. *J. Am. Chem. Soc.* **2007,** *129* (7), 2025-2034.

8. Cabral, H.; Nishiyama, N.; Kataoka, K., Supramolecular nanodevices: From design validation to theranostic nanomedicine. *Accounts Chem. Res.* **2011,** *44* (10), 999-1008.

9. Nystrom, A. M.; Wooley, K. L., The importance of Chemistry in Creating Well-Defined Nanoscopic Embedded Therapeutics: Devices Capable of the Dual Functions of Imaging and Therapy. *Accounts Chem. Res.* **2011,** *44* (10), 969-978.

10. Knop, K.; Hoogenboom, R.; Fischer, D.; Schubert, U. S., Poly(ethylene glycol) in Drug Delivery: Pros and Cons as Well as Potential Alternatives. *Angew. Chem. Int. Ed.* **2010,** *49* (36), 6288-6308.

11. Otsuka, H.; Nagasaki, Y.; Kataoka, K., PEGylated nanoparticles for biological and pharmaceutical applications. *Adv. Drug Delivery Rev.* **2003,** *55* (3), 403-419.

12. Alexis, F.; Pridgen, E.; Molnar, L. K.; Farokhzad, O. C., Factors affecting the clearance and biodistribution of polymeric nanoparticles. *Mol. Pharmaceutics* **2008,** *5* (4), 505-515.

13. Chen, H.; Yuan, L.; Song, W.; Wu, Z. K.; Li, D., Biocompatible polymer materials: Role of protein-surface interactions. *Prog. Polym. Sci.* **2008,** *33* (11), 1059-1087.

14. Lutz, J.-F.; Akdemir, O.; Hoth, A., Point by point comparison of two thermosensitive polymers exhibiting a similar LCST: Is the age of poly(NIPAM) over ? *J. Am. Chem. Soc.* **2006,** *128* (40), 13046-13047.

15. Qin, S.; Geng, Y.; Discher, D. E.; Yang, S., Temperature-controlled assembly and release from polymer vesicles of poly(ethylene oxide)-block-poly(N-isopropylacrylamide). *Adv. Mater.* **2006,** *18* (21), 2905-2909.

16. Lutz, J.-F., Thermo-Switchable Materials Prepared Using the OEGMA-Platform. *Adv. Mater.* **2011,** *23* (19), 2237-2243.

17. Aathimanikandan, S. V.; Savariar, E. N.; Thayumanavan, S., Temperature-sensitive dendritic micelles. *J. Am. Chem. Soc.* **2005,** *127* (42), 14922-14929.

18. Rackaitis, M.; Strawhecker, K.; Manias, E., Water-soluble polymers with tunable temperature sensitivity: Solution behavior. *J. Polym. Sci., Part B: Polym. Phys.* **2002,** *40* (19), 2339-2342.

19. Hammouda, B.; Ho, D.; Kline, S., SANS from Poly(ethylene oxide)/Water Systems. *Macromolecules* **2002,** *35* (22), 8578-8585.

20. Becer, C. R.; Hahn, S.; Fijten, M. W. M.; Thijs, H. M. L.; Hoogenboom, R.; Schubert, U. S., Libraries of Methacrylic Acid and Oligo(ethylene glycol) Methacrylate Copolymers with LCST Behavior. *J. Polym. Sci., Part A: Polym. Chem.* **2008,** *46* (21), 7138-7147.

21. Corti, M.; Minero, C.; Degiorgio, V., Cloud point transition in nonionic micellar solutions. *J. Phys. Chem.* **1984,** *88* (2), 309-317.

22. Chilkoti, A.; Dreher, M. R.; Meyer, D. E.; Raucher, D., Targeted drug delivery by thermally responsive polymers. *Adv. Drug Delivery Rev.* **2002,** *54* (5), 613-630.

23. Schmaljohann, D., Thermo- and pH-responsive polymers in drug delivery. *Adv. Drug Delivery Rev.* **2006,** *58* (15), 1655-1670.

24. Chung, J. E.; Yokoyama, M.; Yamato, M.; Aoyagi, T.; Sakurai, Y.; Okano, T., Thermo-responsive drug delivery from polymeric micelles constructed using block copolymers of poly(N-isopropylacrylamide) and poly(butylmethacrylate). *J. Controlled Release* **1999,** *62* (1–2), 115-127.

25. Kataoka, K.; Miyazaki, H.; Okano, T.; Sakurai, Y., Sensitive glucose-induced change of the lower critical solution temperature of poly[N,N-(dimethylacrylamide)-co-3-(acrylamido)-phenylboronic acid] in physiological saline. *Macromolecules* **1994,** *27* (4), 1061-1062.

26. Koopmans, C.; Ritter, H., Color Change of N-Isopropylacrylamide Copolymer Bearing Reichardts Dye as Optical Sensor for Lower Critical Solution Temperature and for Host−Guest Interaction with β-Cyclodextrin. *J. Am. Chem. Soc.* **2007,** *129* (12), 3502-3503.

27. Liu, T.; Liu, S., Responsive Polymers-Based Dual Fluorescent Chemosensors for Zn2+ Ions and Temperatures Working in Purely Aqueous Media. *Anal. Chem.* **2011,** *83* (7), 2775-2785.

28. Bergbreiter, D. E.; Case, B. L.; Liu, Y.-S.; Caraway, J. W., Poly(N-isopropylacrylamide) Soluble Polymer Supports in Catalysis and Synthesis. *Macromolecules* **1998,** *31* (18), 6053-6062.

29. Bergbreiter, D. E.; Caraway, J. W., Thermoresponsive Polymer-Bound Substrates. *J. Am. Chem. Soc.* **1996,** *118* (25), 6092-6093.

30. Kimura, M.; Kato, M.; Muto, T.; Hanabusa, K.; Shirai, H., Temperature-Sensitive Dendritic Hosts: Synthesis, Characterization, and Control of Catalytic Activity. *Macromolecules* **2000,** *33* (4), 1117-1119.

31. Mitchell, D. J.; Ninham, B. W., Micelles, vesicles and microemulsions. *J. Chem. Soc., Faraday Transactions 2.* **1981,** *77* (4), 601-629.

32. Schott, H., Hydrophilic-lipophilic balance, solubility parameter, and oil-water partition coefficient as universal parameters of nonionic surfactants. *J. Pharm. Sci.* **1995,** *84* (10), 1215-1222.

33. R. Ramireddy, R.; Raghupathi, K. R.; Torres, D. A.; Thayumanavan, S., Stimuli sensitive amphiphilic dendrimers. *New J. Chem.* **2012,** *36* (2), 340-349.

34. Bharathi, P.; Zhao, H. D.; Thayumanavan, S., Toward globular macromolecules with functionalized interiors: Design and synthesis of dendrons with an interesting twist. *Org. Lett.* **2001,** *3* (12), 1961-1964.

35. Vutukuri, D. R.; Basu, S.; Thayumanavan, S., Dendrimers with Both Polar and Apolar Nanocontainer Characteristics. *J. Am. Chem. Soc.* **2004,** *126* (48), 15636-15637.

36. Grayson, S. M.; Frechet, J. M. J., Convergent dendrons and dendrimers: from synthesis to applications. *Chem. Rev.* **2001,** *101* (12), 3819-3867.

37. Fischer, M.; Vögtle, F., Dendrimers: From design to application—A progress report. *Angew. Chem. Int. Ed.* **1999,** *38* (7), 884-905.

38. George R. Newkome, C. N. M., Fritz Vögtle., *Dendrimers and Dendrons: Concepts, Syntheses, Applications.* Wiley-VCH: 2001; p 635.

39. Donald A. Tomalia, J. B. C., Ulrik Boas, *Dendrimers, Dendrons, and Dendritic Polymers: Discovery, Applications, and the Future*. 1 ed.; Cambridge University Press: New York, United States of America, 2012; p 420.

40. Choi, S. H.; Lodge, T. P.; Bates, F. S., Mechanism of Molecular Exchange in Diblock Copolymer Micelles: Hypersensitivity to Core Chain Length. *Phys. Rev. Lett.* **2010,** *104* (4).

41. Waton, G.; Michels, B.; Zana, R., Dynamics of Micelles of Polyethyleneoxide-Polypropyleneoxide-Polyethyleneoxide Block Copolymers in Aqueous Solutions. *J. Colloid Interface Sci.* **1999,** *212* (2), 593-596.

42. Jiwpanich, S.; Ryu, J.-H.; Bickerton, S.; Thayumanavan, S., Noncovalent Encapsulation Stabilities in Supramolecular Nanoassemblies. *J. Am. Chem. Soc.* **2010,** *132* (31), 10683-10685.

43. Nir, E.; Michalet, X.; Hamadani, K. M.; Laurence, T. A.; Neuhauser, D.; Kovchegov, Y.; Weiss, S., Shot-noise limited single-molecule FRET histograms: Comparison between theory and experiments. *J. Phys. Chem. B* **2006,** *110* (44), 22103-22124.

44. Yebra, D. M.; Kiil, S.; Dam-Johansen, K., Antifouling technology - past, present and future steps towards efficient and environmentally friendly antifouling coatings. *Prog. Org. Coat.* **2004,** *50* (2), 75-104.

45. Banerjee, I.; Pangule, R. C.; Kane, R. S., Antifouling Coatings: Recent Developments in the Design of Surfaces That Prevent Fouling by Proteins, Bacteria, and Marine Organisms. *Adv. Mater.* **2011,** *23* (6), 690-718.

CHAPTER 4

INFLUENCE OF BACKBONE CONFORMATIONAL RIGIDITY IN TEMPERATURE-SENSITIVE AMPHIPHILIC SUPRAMOLECULAR ASSEMBLIES

Adapted with permission from Krishna R. Raghupathi, Uma Sridhar, Kevin Byrne, Kishore Raghupathi, S. Thayumanavan. Influence of backbone conformational rigidity in temperature-sensitive amphiphilic supramolecular assemblies. *Journal of the American Chemical Society* **2015**, *137*, 5308 – 5311.

4.1 Introduction

Stimuli responsive systems have garnered significant attention due to their utility in several applications such as drug delivery, sensing, tissue engineering, and diagnostics.[1-5] Self-assembling systems such as micelles and liposomes have been quite popular in this context, as the morphology of these assemblies can provide an observable response to a specific environmental change.[1,6-8] Among various stimuli, temperature has been of interest, where the thermo-responsive components of the assembly undergo a phase transition at a specific temperature, commonly referred to as cloud point or lower critical solution temperature (LCST).[9-18] Among thermo-sensitive components, oligo(ethylene glycol) (OEG) and poly(ethyleneglycol) (PEG) based systems have been subjects of exploration in recent years.[19-21] The LCST of OEG containing amphiphilic assemblies is the result of the fact that OEG units are only hydrophilic, because they hydrogen bond with water molecules.[22-24] When the temperature of the solution is increased, the OEG units become hydrophobic

because of the temperature-induced decrease in hydrogen bonding. This change in the hydrophilicity of the molecule is the reason for the observed LCST transitions. The structure-property correlations studied with temperature-sensitive polymers are most often studied as a phenomenon that involves a noticeable macroscopic phase change at higher temperatures.[9-18] It has been recognized only recently that there exists interesting morphological transition in these amphiphilic aggregates at temperatures below the typical LCST, the so-called sub-LCST transition.[25] In our efforts to understand the underlying structural requirements that endow molecules with sub-LCST characteristics (Figure 4.1), we have uncovered an interesting effect of the shape of the amphiphile on their aggregation state and their temperature sensitive behavior. We disclose these preliminary findings in this manuscript.

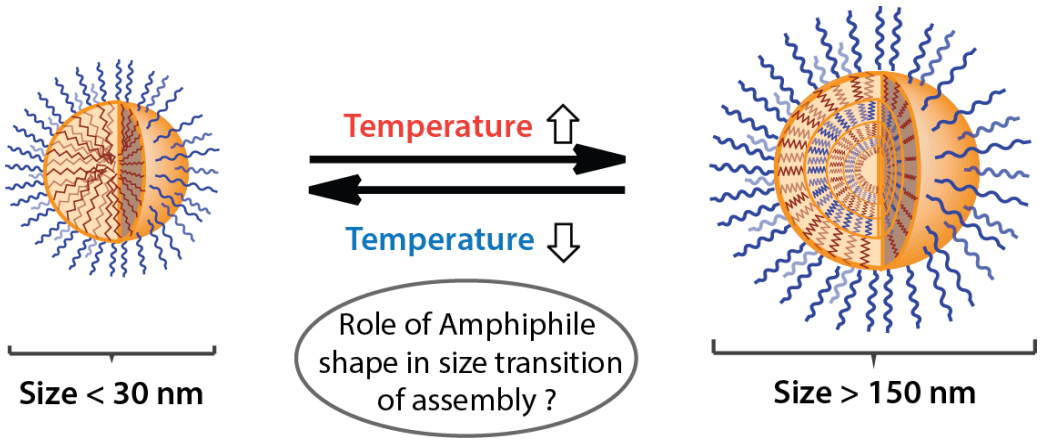

Figure 4.1. Schematic representation of temperature dependent size transition of amphiphilic assemblies, and the potential role of amphiphile shape in this phenomenon.

4.2 Role of PEG in Size Transition Phenomenon

The molecule in which the sub-LCST phenomenon was previously observed is shown as structure **1** in Scheme 4.1. We started with a simple hypothesis that the presence of OEG moieties in molecule **1** and its ability to self-assemble to form

amphiphilic aggregates are the key criteria for the observed sub-LCST behavior. If this were the case, then other ethylene glycol based amphiphiles, which do form amphiphilic assemblies in water, should also exhibit similar features. We tested this hypothesis by studying several PEG containing amphiphiles: Tween-20, Brij-35, Triton-X-100, and Brij-L4. A simple size analysis of these assemblies at different temperatures suggests that these molecules do not have the propensity to exhibit a sub-LCST transition, akin to that observed with molecule **1** (Figure 4.2). These results suggest that although the sub-LCST behavior is indeed a temperature responsive event, the presence of PEG moieties in the amphiphile alone is not a sufficient criterion for this phenomenon.

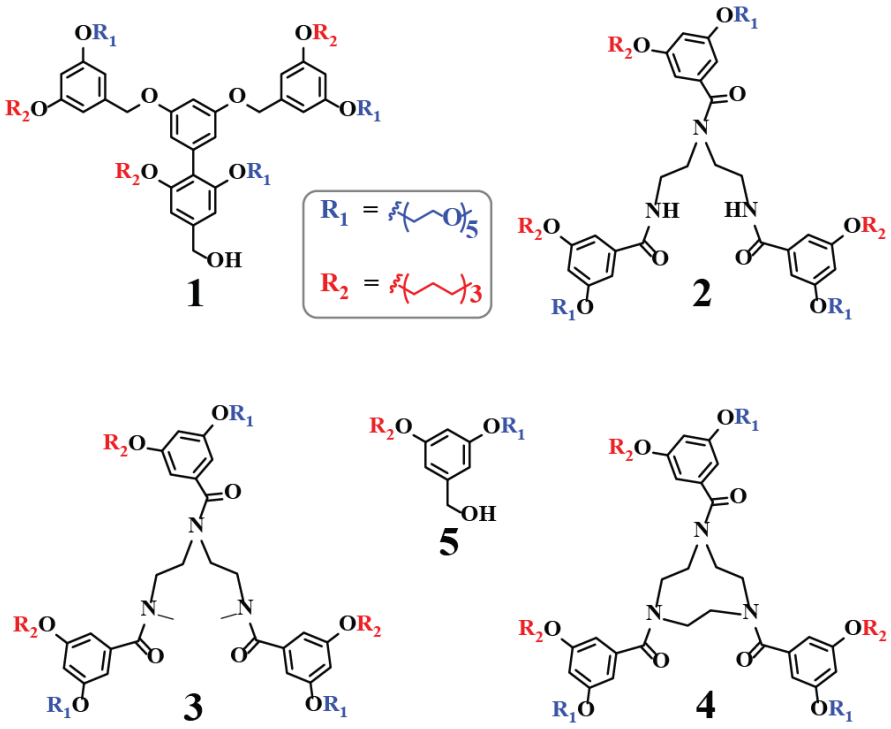

Scheme 4.1. Structures of temperature responsive trimeric (1, 2, 3, and 4) and monomeric (5) used in this study.

Next, we tested the possibility that the functional group composition inherent to molecule **1** (*e.g.* pentaethylene glycol and decyl unit as the amphiphile combination) that dictates this behavior. We have already shown that the second generation dendron with the same amphiphilic units do not exhibit this behavior.[25] We attributed this observation to a frozen aggregate formed by the higher generation amphiphile. To fully test this possibility however, it is essential that we also test the lower generation amphiphile containing the same amphiphilic units. Accordingly, we synthesized molecule **5**, which exhibited an LCST phase transition at ~35 °C, but no sub-LCST features were observed in this molecule (Figure 4.3).

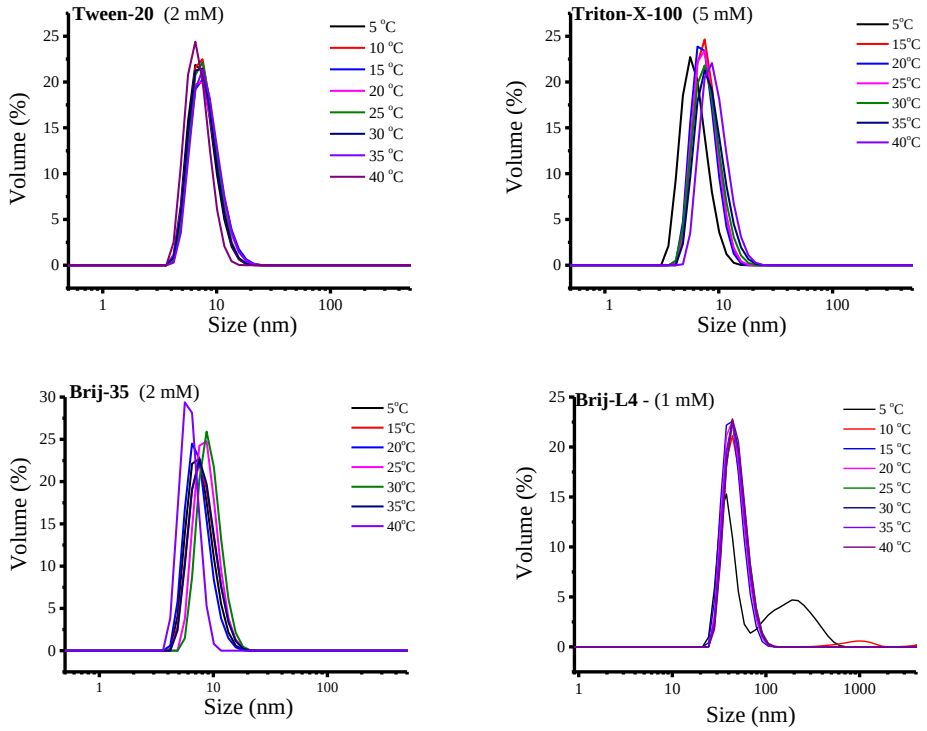

Figure 4.2. Temperature dependent size analysis (DLS) of several PEG containing surfactant assemblies.

4.3 Hypothesis and Molecular Design

From the observations so far, we next hypothesized that the sub-LCST transition might be associated with the geometry of the functional groups presented, in addition to the presence of thermo-sensitive OEG moieties. Considering this, we next designed and synthesized two linear trimeric amphiphiles **2** and **3**, with similar amphiphilic functionalities as **1** (Scheme 4.1). Our rationale for choosing these two amphiphiles was to test if the assembly properties observed with **1** is due to its trimeric architecture. The difference between **2** and **3** lies simply in the nature of amide backbone. Molecule **2**, which is composed of two secondary amides and a tertiary amide, is expected to be slightly more hydrophilic and hence have better water solubility in comparison to molecule **3** which contains three tertiary amides. We envisioned that these two molecules would therefore also help us understand the role of amphiphile's backbone in obtaining the temperature-sensitive assembly characteristics observed with molecule **1**. The synthetic scheme and characterization of these amphiphiles is shown in Scheme 4.2.

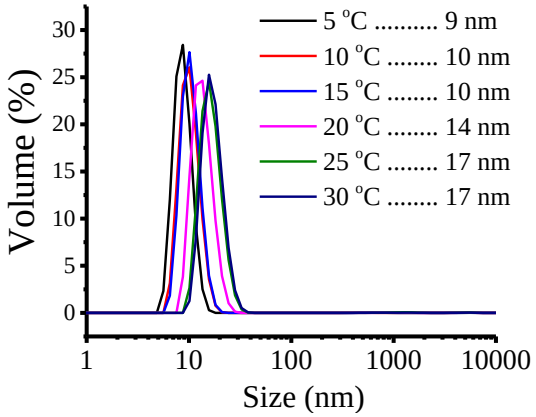

Figure 4.3. Temperature dependent size measurement of molecule **5** assembly by DLS.

We first tested the LCST of amphiphilic assemblies **2** and **3** by monitoring the turbidity with temperature (Figure 4.4) and found both their LCSTs to be ~45 °C. In addition, we also noticed that molecule **2** assembly showed a small change in turbidity at ~25 °C, well before reaching its LCST (Figure 4.4a). This indicated that there is a possible transition in the nanoscale assembly at temperatures below LCST. To understand this further, the size of these assemblies was measured at different temperatures using dynamic light scattering (DLS). Indeed, we found that the assembly from molecule **2** showed temperature dependent size transition at ~ 25 °C, consistent with the slight change in turbidity during the LCST measurements (Figure 4.5a & Figure 4.6).

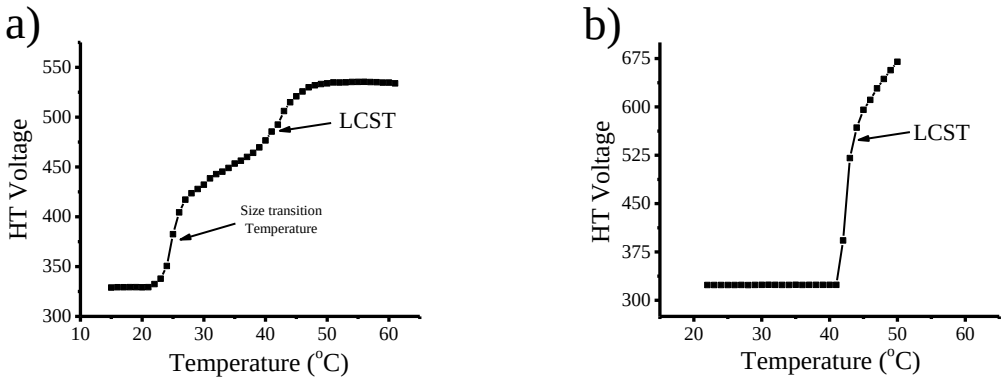

Figure 4.4. LCST measurements plotted as HT Voltage (*turbidity indicator*) vs Temperature, of (a) Molecule **2**, and (b) Molecule **3**

It is also noteworthy that the size transition observed with **2** is very sharp (± 2 °C) and reversible (Figure 4.7), underlining the utility of such property in thermoresponsive applications. Interestingly, on the other hand, assemblies from molecule **3** did not exhibit any sharp size transition (Figure 4.5c). The size of the assembly changed from about 18 nm at 40 °C to 7 nm at 15 °C. But, these size changes are not sharp at any particular temperature; they are rather small and

systematic changes. Since both **2** and **3** are trimeric amphiphiles with very similar structural features, the stark contrast in their assembly properties was indeed surprising. A simple-minded conclusion here is that these results indicate that the sub-LCST behavior is not applicable to all trimeric amphiphiles.

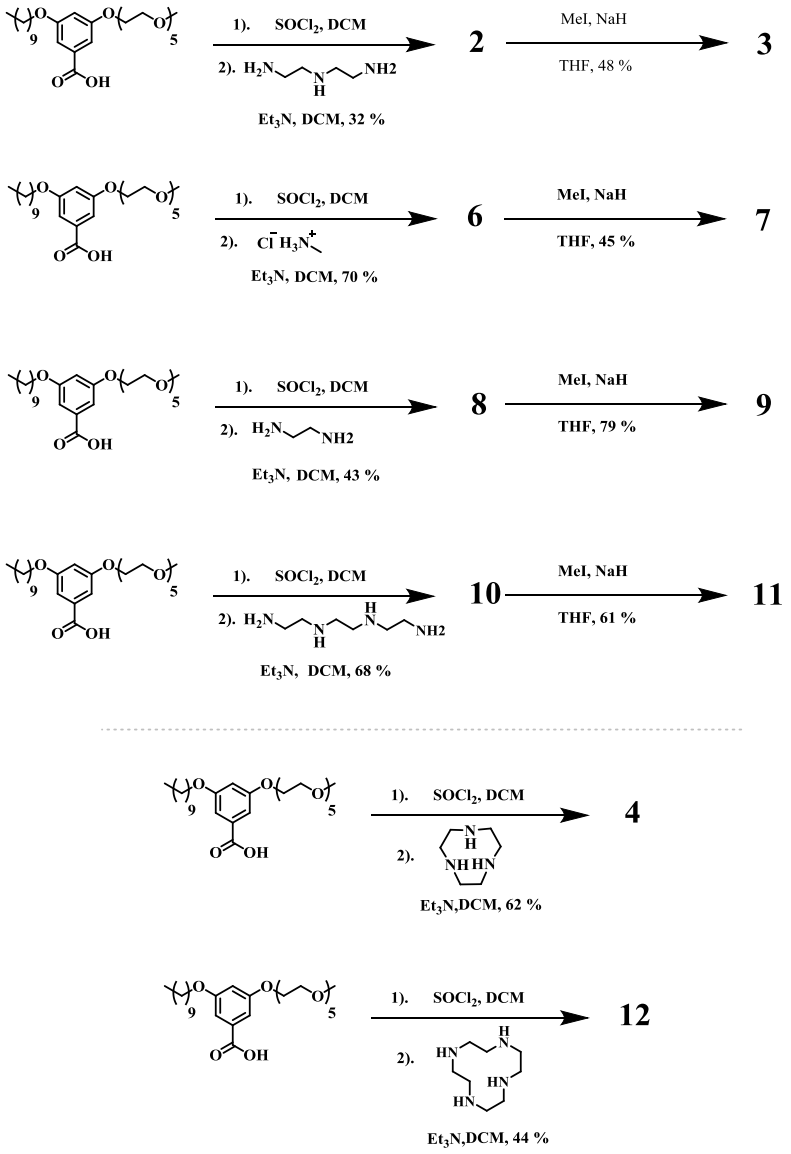

Scheme 4.2. Synthesis of Oligomers **2 – 4** & **6 - 12**.

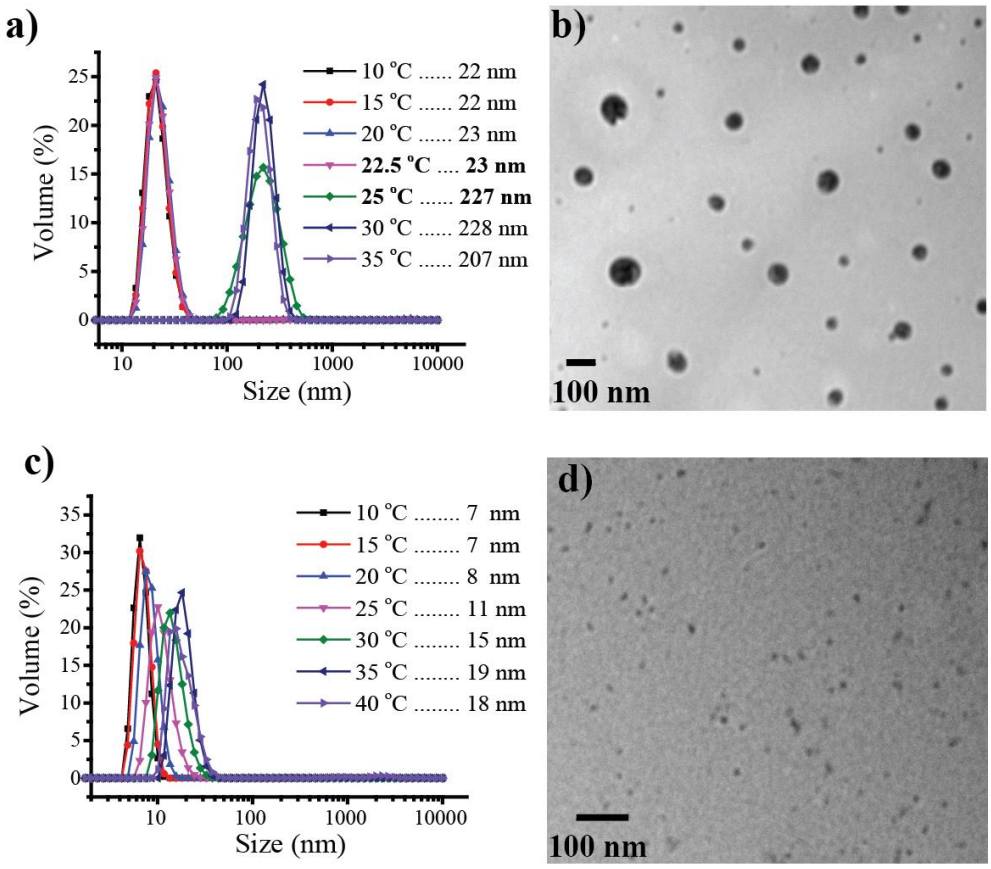

Figure 4.5. Temperature-dependent size variation as observed with dynamic light scattering (DLS) of (a) Molecule **2** and (c) Molecule **3** respectively. Corresponding TEM images of (b) **2** and (d) molecule **3** assemblies at 25 °C indicating formation of spherical assemblies.

4.4 Role of Amphiphile Backbone Rigidity and Hydrogen Bonding

Realizing that the only difference in molecular designs of **2** and **3** is the amide backbone, we were interested in investigating its role. Our initial hypothesis of the difference in hydrophilicity of the amide backbones could not explain this sub-LCST observation as molecule **3** (less hydrophilic backbone) surprisingly had much better solubility than molecule **2** at room temperature. Since the presence of secondary amides in **2** is not contributing to its solubility in water, we hypothesized a scenario where the molecule **2** is stabilized by intramolecular hydrogen bonding between the

two secondary amides at the termini, as shown in Figure 4.8. The reason for this hypothesis stems from the possibility that such a conformation would have molecule **2** assume a shape similar to that of molecule **1** (Figure 4.8), which could be the reason for the similarity in their temperature-sensitive assembly features. On the other hand, such a conformational stabilization is not possible in molecule **3** due to the lack of hydrogen bonding protons in its backbone, which could explain the deviation of its assembly properties.

Since all these studies are carried out in water, it is reasonable to question the existence of such intramolecular hydrogen bonding as water (bulk solvent) can effectively compete for hydrogen bonding. However the reasons for our assertion on the existence of such a possibility are: (*i*) Note that our initial assembly size is >200 nm. Considering that the observed aggregates are solid spheres and not water filled (as observed from TEM in Figure 4.5b, 4.6 and hydrophobic guest incorporation in Figure 4.9), these complex micelle-like aggregates have a high percentage of the amphiphiles within their solvent-excluded interior.

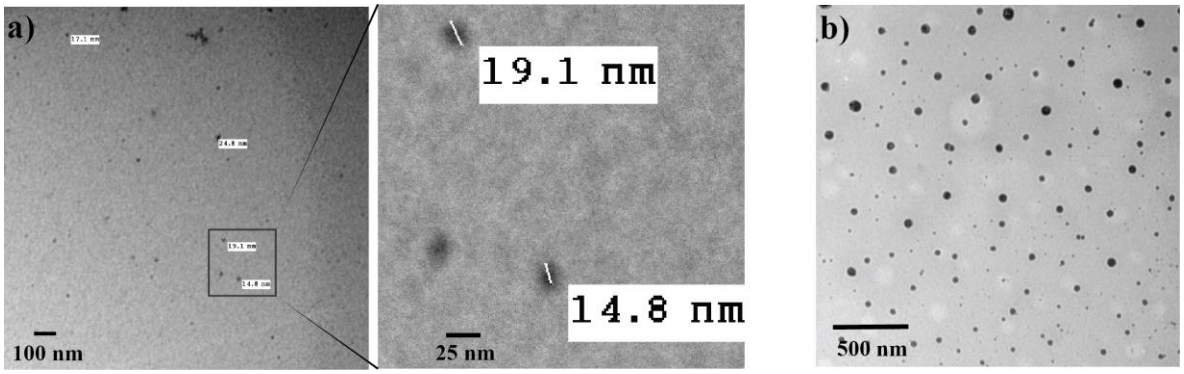

Figure 4.6. TEM images of Trimer **2** assemblies formed at (a) 18 ^{o}C and (b) 25 ^{o}C respectively.

This water-excluded environment is conducive for intramolecular hydrogen bond formation in natural and artificial systems.[26-28] (*ii*) Amide-amide hydrogen bond strengths have been found to be comparable or greater than amide-water hydrogen bond strengths.[29-31] These factors prompted us to first investigate the possibility of intramolecular hydrogen bonding in **2**. However, this proved to be hard to decipher, because molecule **2** exists as nanoscopic assembly in water and NMR peaks were not easily discernible. It is understandable that the buried amides in a large aggregate are particularly difficult to visualize, because of low segmental mobility.

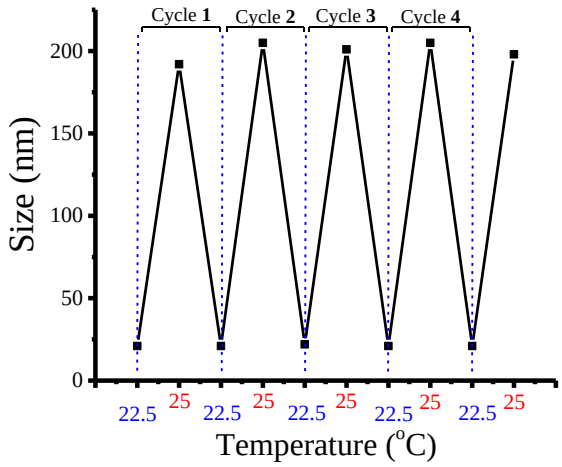

Figure 4.7. Reversibility of the size transition in Molecule 2 assembly as measured by DLS.

We were however interested in evaluating whether molecule **2** is capable of intramolecular hydrogen bonding. We utilized a nonpolar solvent for this purpose, as the internal environment of the assembly is nonpolar. Thus, we studied the hydrogen bonding possibilities in **2** in CD_2Cl_2 using NMR. The ^1H NMR spectra of molecule **2** showed a downfield shift of amide protons clearly indicating the

presence of hydrogen bonding. To decipher if this is due to intramolecular hydrogen-bonding rather the possible intermolecular hydrogen bonding, we monitored the chemical shifts of amide protons at several concentrations. We found that the hydrogen bonding in molecule **2** is indeed intramolecular, as the chemical shifts of the amide protons were independent of concentration change (Figure 4.10).

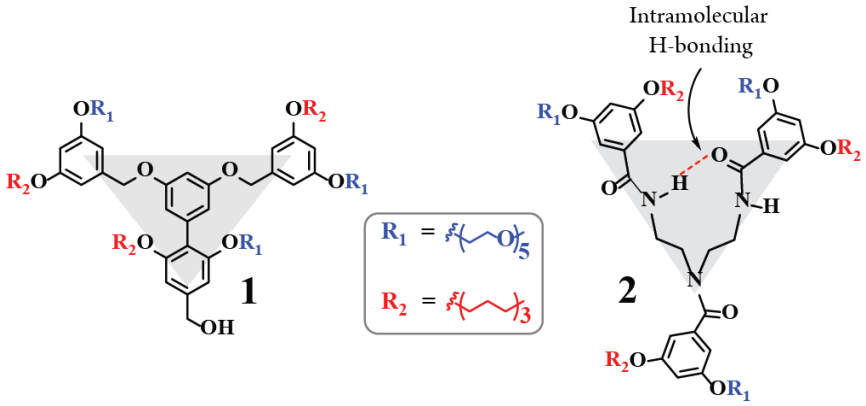

Figure 4.8. Similarity in the shape of dendron amphiphile **1**, and hypothetical representation of hydrogen bond stabilized trimer **2**.

If the intramolecular hydrogen bonding were indeed present in **2**, the molecule is likely to be conformationally more rigid and thus be more similar to **1** in the relative placements of the amphiphilic moieties within the trimer (Figure 4.8). To test this hypothesis, we designed and synthesized molecule **4**, which should have similar amphiphile shape as the conformationally rigid version of **2**, but is structurally similar to **3** in that it does not have any secondary amides (Figure 4.11). In fact, the only difference between these molecules is that the terminal methyl groups of **3** have been tied together to form **4**. Interestingly, size characterization of molecule **4** at different temperatures by DLS has revealed that this molecule also exhibits a rather drastic and sharp size transition feature at ~ 23 ^{o}C (Figure 4.11).

Considering that **4** is structurally similar to **3**, but conformationally similar to the proposed intramolecularly hydrogen bonded **2**, and considering that its assembly behavior is similar to that of **2**, these results signify the importance of conformational rigidity for the observed sub-LCST transition.

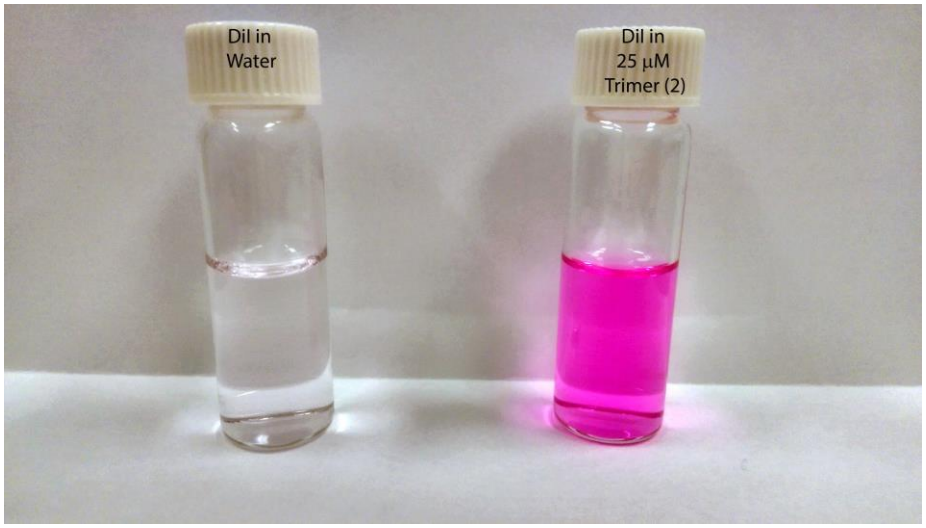

Figure 4.9. Picture of micelle solution formed from molecule **2** (right), indicating encapsulation of hydrophobic guest molecules (DiI).

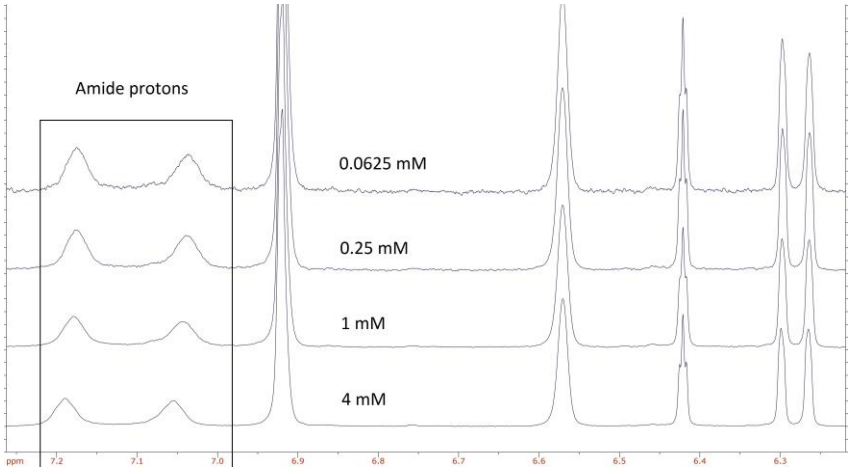

Figure 4.10. ^{1}H NMR spectra of molecule **2** in CD_2Cl_2 at different concentrations, showing the chemical shifts of amide protons.

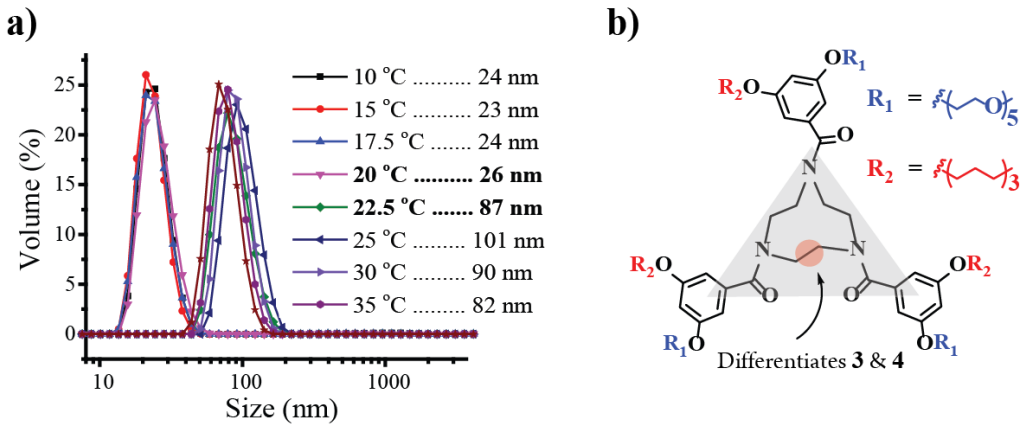

Figure 4.11. (a) Temperature-dependent size variation of molecule **3** assembly, from DLS. (b) Cyclic trimer (**3**) depicted with shape similar to **1** & **2**.

4.5 Effect of sub-LCST on Guest Encapsulation Stability

Finally, we were interested in understanding the implications of the sub-LCST behavior exhibited by **2** and **4** on the encapsulation stabilities of these assemblies. We have done this by analyzing the exchange dynamics of encapsulated guest molecules at different temperatures, using a recently reported fluorescence resonance energy transfer (FRET) based method.[32] Briefly, poor encapsulation stability should result in a dynamic exchange of encapsulated guest molecules, and therefore an exponential FRET evolution; in contrary there should be minimal or no evolution of FRET with time for assemblies with good encapsulation stability. We observed that both **2** and **4** assemblies show stable encapsulation at higher temperatures (Figure 4.12). However, significant increase in guest exchange was observed when the temperature approached their corresponding size transition points, 25 °C and 23 °C for **2** and **4** respectively (Figure 4.12). At first sight, this seems counterintuitive that the guest exchange dynamics is faster at lower temperature. Note however that these results simply suggest that the smaller

supramolecular assembly below the sub-LCST transition is a poorer host for guest encapsulation compared to the larger supramolecular assembly observed at higher temperatures. Since these are two different assemblies, the observations do not violate any laws of thermodynamics.

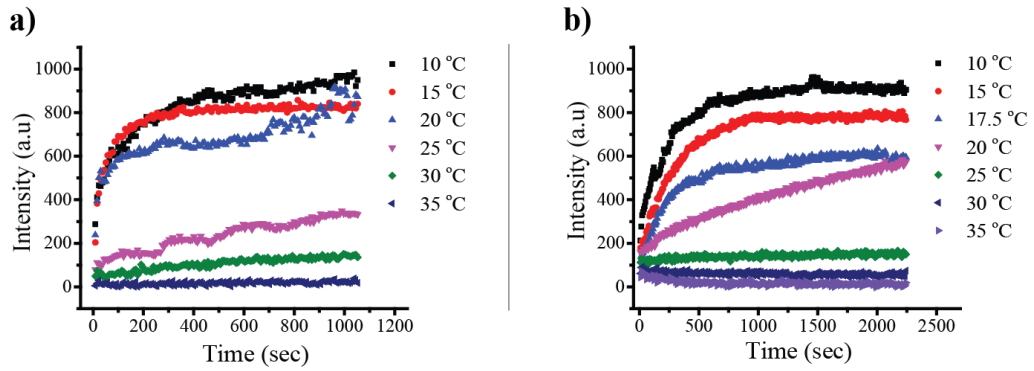

Figure 4.12. Guest exchange dynamics as a function of temperature in (a) Trimer **1**, and (b) Cyclic Trimer **4** assemblies respectively.

We interrogated molecule **3** for encapsulation stability as well. Note that there were small size changes with temperature in molecule **3** as well, which we dismissed as relatively insignificant. However, if there were any significant guest encapsulation differences with this molecule at different temperatures, these small changes can be significant. We found that assemblies from **3** exhibited spontaneous guest exchange irrespective of temperature as shown in Figure 4.13 (*i.e.* poor encapsulation stability at all temperatures). These results support our earlier hypotheses.

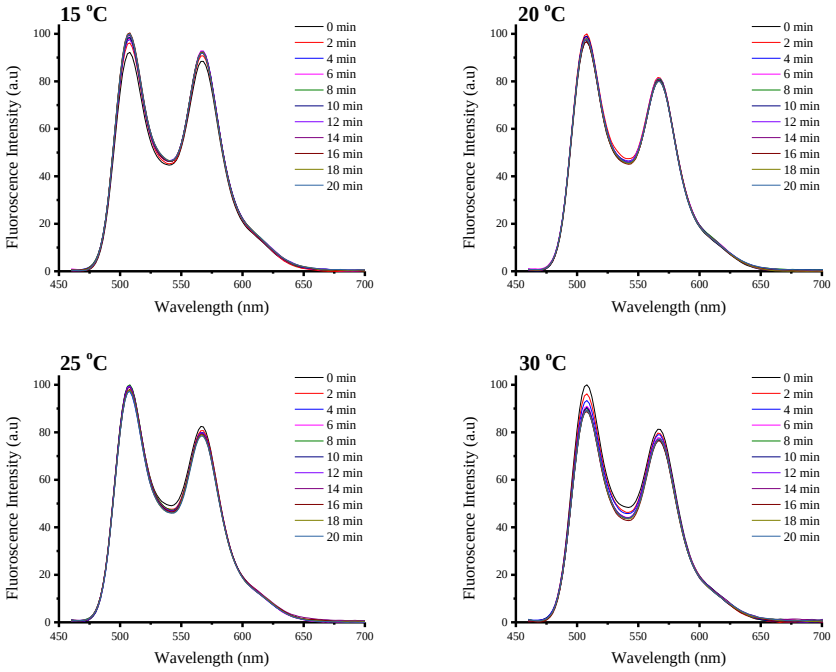

Figure 4.13. Fluorescence spectra of molecule **3** assembly after mixing (DiO and DiI containing assemblies), indicating spontaneous guest exchange irrespective of temperature change. The fluorescence intensity of DiI due to FRET did not change

4.6 Role of Amphiphile Multiplicity in sub-LCST Phenomenon

In previous sections we have discussed the role of amphiphile backbone and how the rigidity imparted to it through hydrogen bonding **2** or covalent bonding **4** imparts sub-LCST property to the resultant assembly. Though this study resulted in understanding several key fundamental parameters which influence the sub-LCST phenomenon, it was

limited to the amphiphiles only with a trimeric architecture. To investigate if this sub-LCST feature can be extended to oligomers of different amphiphile multiplicities, there is a need to extend the current repertoire of amphiphiles. Here we propose to do this by systematically studying the assembly properties of oligomers with variable number of amphiphilic units **5**, **7**, **9** (Scheme 4.3). As

discussed earlier (section 4.3), elimination of secondary amide lead to a significant change in assembly properties, in this context corresponding oligomers with methylation of terminal amides **6**, **8**, **10** were also designed. The synthesis of these amphiphiles is shown in Scheme 4.2 and, the characterization of is discussed in section 4.8.1.

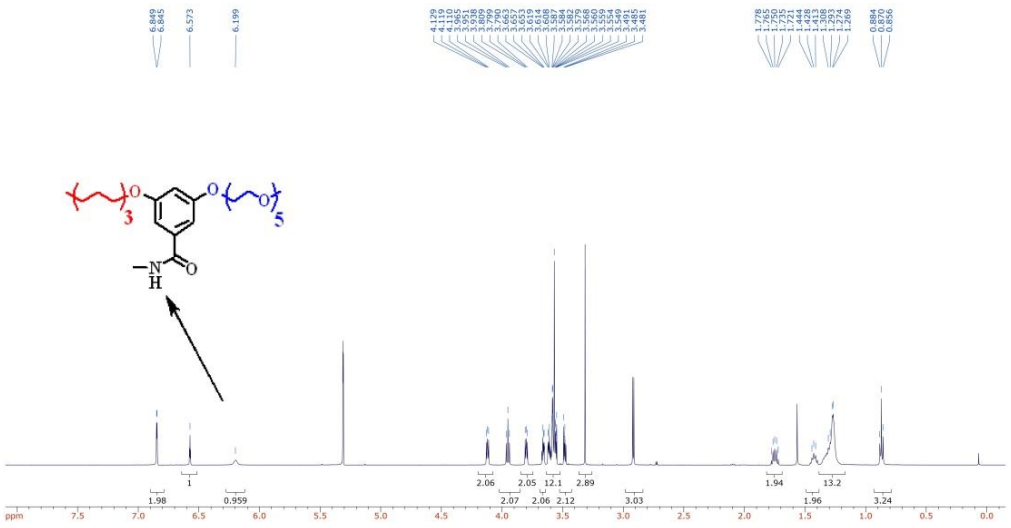

Figure 4.14. NMR spectrum of control molecule with just one amide functionality showing the corresponding amide proton at ~ 6.1 ppm

4.6.1 Case Study of Monomeric Amphiphiles

Since monomer **6** is essentially the basic amphiphilic component of all the higher order oligomeric amphiphiles, we first tested the assembly features of this amphiphile in the context of its temperature responsive behavior. We have observed that the monomer **6** exhibited an interesting low LCST, where the phase transition is observed at ~ 35 ^{o}C (Figure 4.15a). To further test if this assembly exhibits any sub-LCST features, we investigated the size of the assembly at several temperatures below LCST. As shown in Figure 4.15b, the increase in size of the

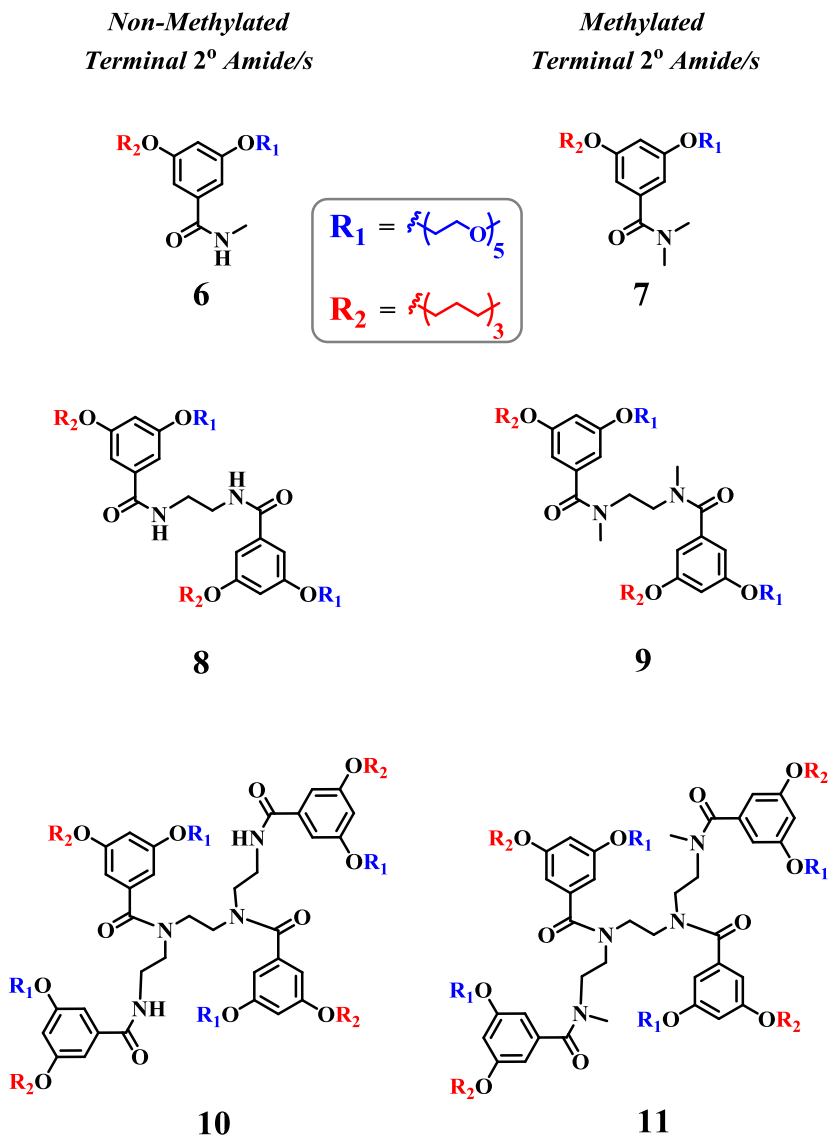

Scheme 4.3. Schematic of Amphiphiles with (**6**, **8**, **10**) and without H-bonding backbone (**7**, **9, 11**)

assemblies observed with temperature was rather systemic and lacked any size transition peculiar to the sub-LCST phenomenon. It should be noted that the molecule **6** also has a secondary amide which can hydrogen bond in intermolecular fashion with other corresponding amides or with the water molecules (solvent medium). We speculate if this low LCST observed (Figure 4.15a) is due to this feature, as the change in hydration with temperature of these amides can result in a

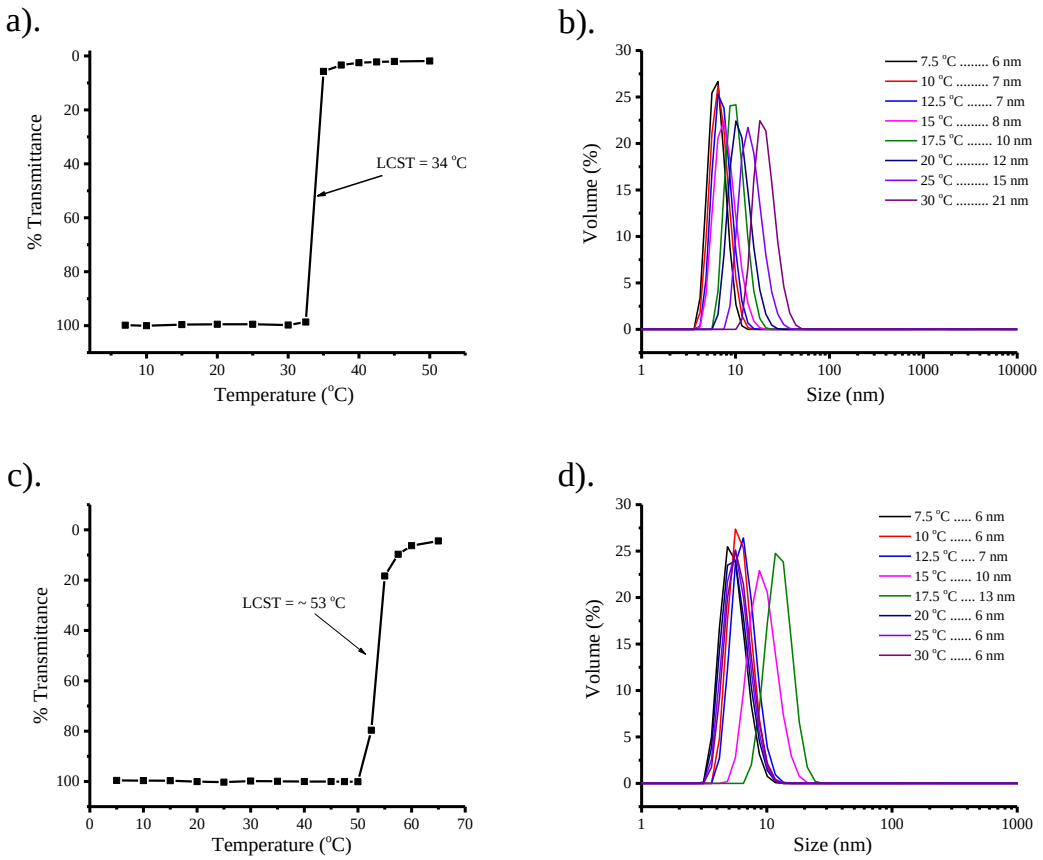

Figure 4.15. Temperature responsiveness of monomer 6 and methylated monomer **7** assembly, (a) LCST calculation using UV-Vis at 1mM concentration in water, (b) Size analysis using variable temperature DLS.

concomitant change in its solubility. To test this hypothesis we synthesized molecule **7** (elimination of H-bonding amide by methylation) and tested the LCST and the temperature responsive size of the assembly. Interestingly the molecule **7** assembly showed significantly higher LCST phase transition therefore suggesting that the presence of H-bonding amide is indeed responsible for lower LCST.

Additionally we have also observed that molecule **6** has a lower CMC in comparison to molecule **7**, possibly due to stabilization from H-bonding in the former assembly. Though a sub-LCST feature has not been observed in the case of monomeric amphiphiles, this study provided an understanding on the role of amide

functionality in influencing the stability as well as temperature responsive nature of the amphiphilic assemblies.

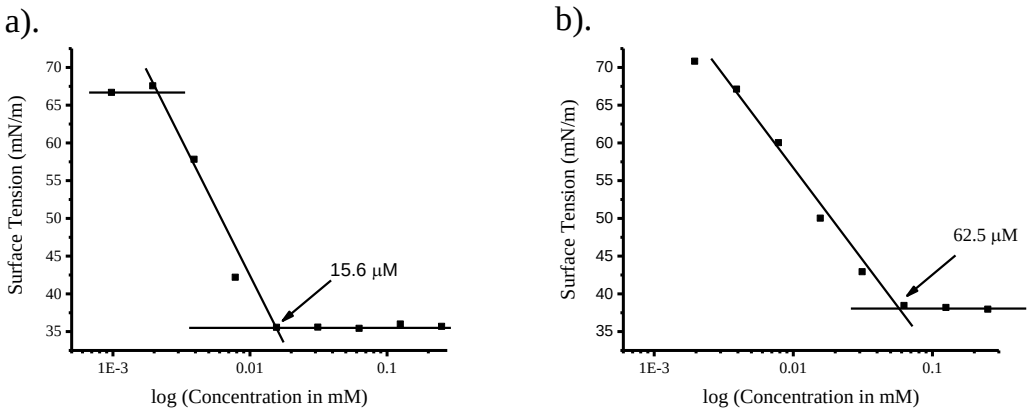

Figure 4.16. CMC of amphiphilic assemblies of (a) monomer **6** and (b) methylated monomer **7**

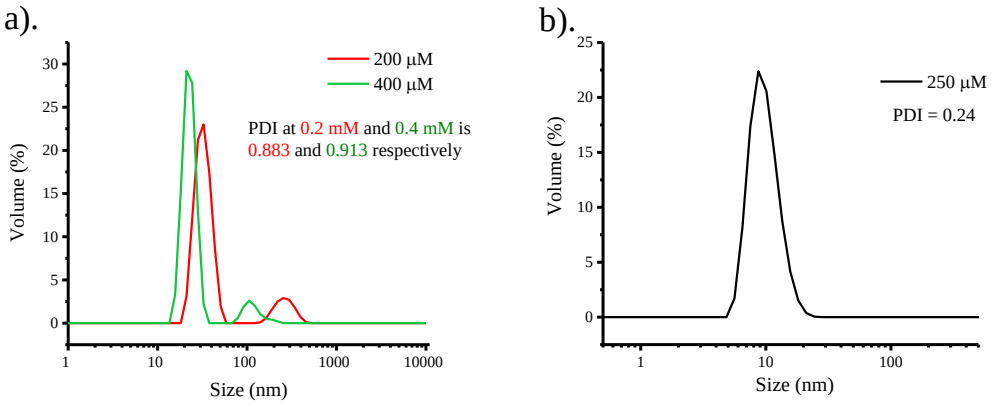

Figure 4.17. Size Analysis of amphiphilic assemblies of (a) monomer 6 and (b) methylated monomer 7

4.6.2 Case Study of Dimeric Amphiphiles

As observed in the above section the monomeric amphiphile **6** was composed of just one amide in its backbone, therefore eliminating the possibility of any intramolecular H-bonding induced rigidity as observed in the case of trimer **2**.

Nonetheless, this aspect can be tested with a dimeric amphiphile **8**, which also has two amides that can hydrogen bond intramolecularly. When assembly features of molecule **8** were studied we found that it had surprisingly poor solubility in water; even when solubilized with an aid of an organic solvent (miniscule amount of acetone) it did not form assemblies (noted from very poor correlation function in DLS) (Figure 4.17a). This is an interesting phenomenon because the monomer (smaller) as well as the trimeric (larger) amphiphiles **6** and **2** respectively, both formed assemblies and had better solubility in water. Nonetheless it should be noted that molecule **2** (hydrogen bonding) also had poor solubility in comparison to its methylated counterpart **3** as discussed in section 4.3. We contemplated if poor solubility of molecule **8** is also due to rigidity induced in its backbone through intramolecular hydrogen bonding. This assumption was supported by NMR spectra (section 4.9), where the amide protons have shifted significantly downfield (in comparison to molecule **6**) suggesting that they are H-bonded. This hypothesis was further tested by studying the assembly of dimeric amphiphile **9**, where the secondary amides are methylated to eliminate H-bonding possibility. We were delighted to observe that the solubility of **9** significantly increased, and also resulted in formation of stable assemblies (Figure 4.17b). Though the contrasting assembly features of **8** and **9** do suggest the presence of intramolecular hydrogen bonding in molecule **8**, at this point we were not able to deduce a reason for its poor water solubility and the absence of assembly. However we reason that the rigidity imparted into the backbone of molecule **8** through intramolecular hydrogen

bonding might limit the flexibility of the resulting amphiphile to form an assembly (Figure 4.18)

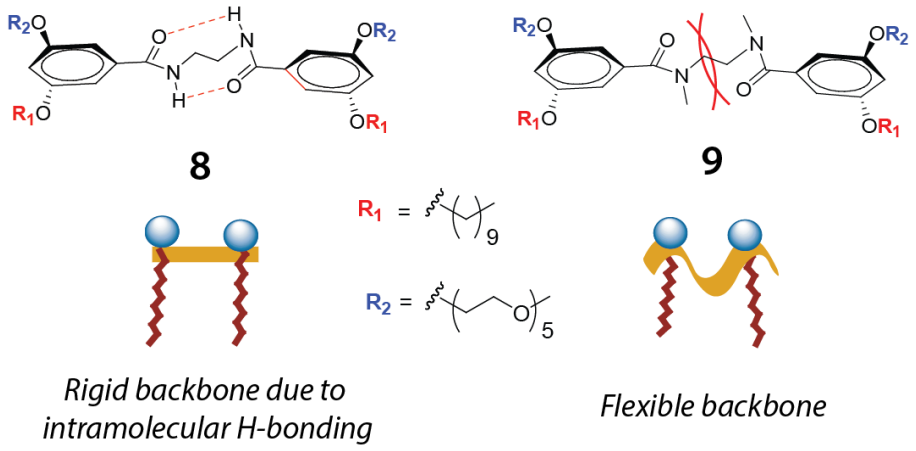

Figure 4.18. Hypothetical representation of rigidity in backbone of molecule **8** due to H-bonding and absence of such feature in molecule **9**

4.6.3 Case Study of Tetrameric Amphiphiles

Investigation of monomeric and dimeric amphiphiles has suggested that the presence of H-bonding amides can influence properties such as solubility, LCST, CMC, and assembly forming ability. However these shorter amphiphiles did not exhibit the unique sub-LCST phenomenon that was observed in trimeric amphiphiles (**1**, **2,** and **4**). To test if this can be achieved with higher order oligomers we have synthesized and tested the tetrameric amphiphile **10**. As shown in figure 4.19a, the molecule **10** indeed formed micelle type assemblies and also exhibited temperature dependent sub-LCST size transition. This observation highlighted that the sub-LSCT phenomenon is not exclusive to just the amphiphiles which are trimeric. Similar to molecule **2** we speculated that the sub-LCST observed in molecule **10** is also due to the backbone rigidity induced by H-bonding. This was

verified using molecule **11** where the amides are methylated to avoid H-bonding interactions. We were gratified to observe that molecule **11** also indeed did not exhibit sub-LCST size transition, therefore highlighting the role of rigidity in backbone even in the case of a tetramer.

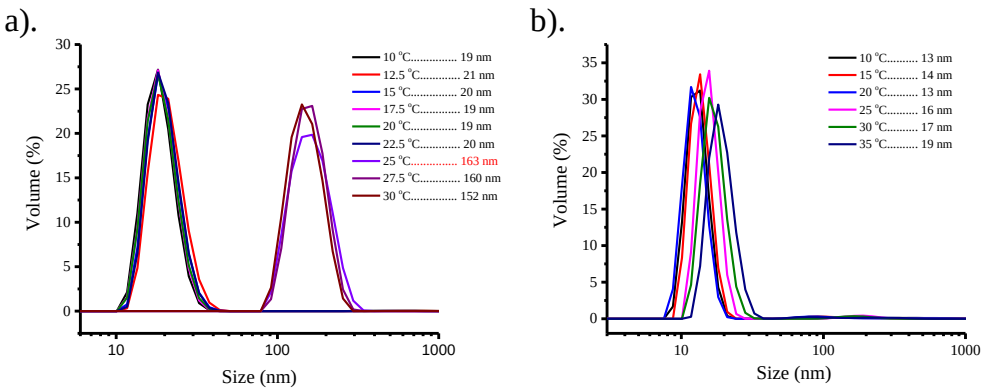

Figure 4.19. Temperature responsive size of Tetramer **10** (a) and Methylated tetramer **11** (b) assemblies using DLS.

To further test the role of amphiphile rigidity in sub-LCST, we synthesized molecule **12** which is identical to molecule **11**, except for a covalent bond connecting the terminal methyl groups. This should result in an amphiphile with rigid backbone and therefore resemble intramolecularly H-bonded tetramer **10** (Figure 4.20). Temperature dependent size of assemblies from amphiphile **12** did result in a size transition; however the magnitude of the size change is significantly smaller in comparison to sub-LCST transition in other amphiphiles (**1**, **2**, **4**, and **10**).

Similar to molecule **1**, **2**, and **4** assemblies we expected that the sub-LCST observed in molecule **10** should affect the encapsulation ability of its assembly. This was tested using FRET based method discussed earlier. As expected the assemblies

were leaky below sub-LCST temperature, but stably encapsulated the guest molecules at temperatures above sub-LCST (Figure 4.21).

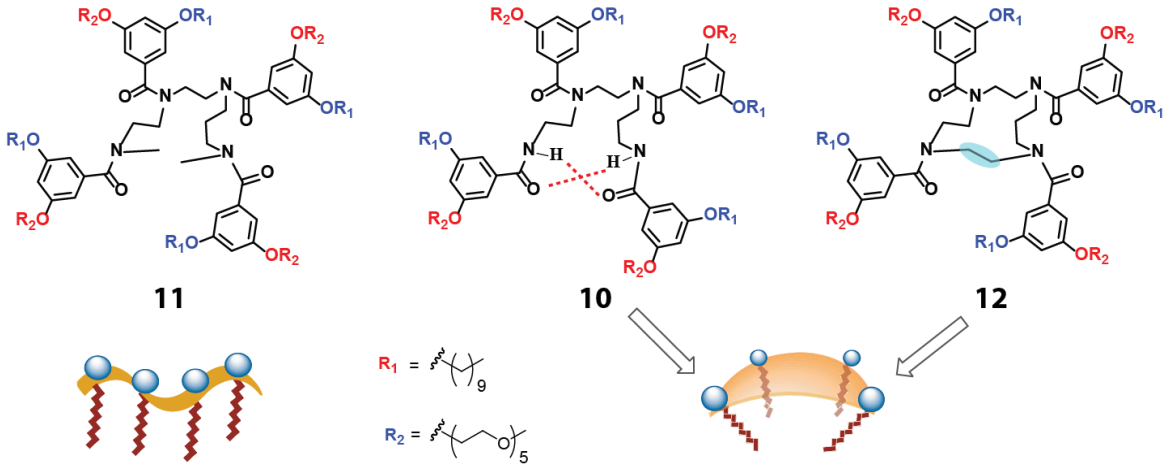

Figure 4.20. Tetrameric amphiphiles and their hypothetical amphiphile shape representation. Flexible backbone in case of **11**. Rigid backbone in case of H-bonded **10** and covalently bonded **12**.

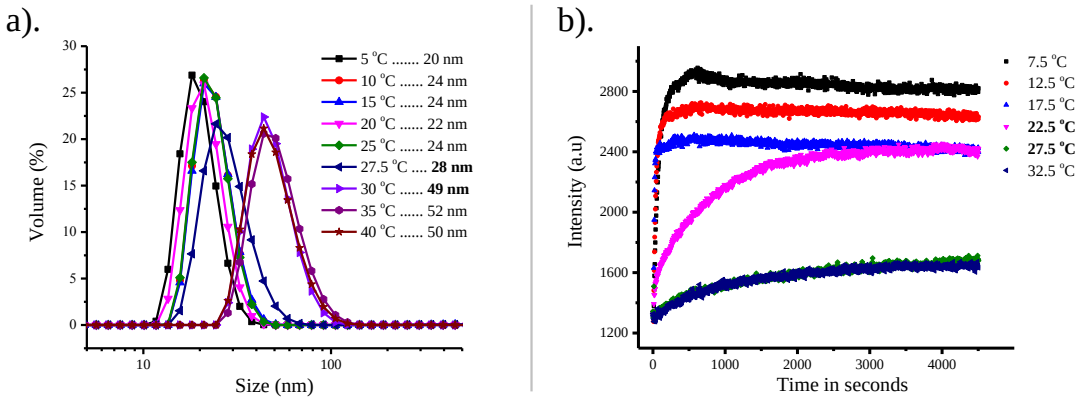

Figure 4.21. (a). Temperature dependent size analysis (DLS) of cyclic tetramer **12** assembly . (b). Guest encapsulation stability of molecule **10** assembly using FRET method.

4.7 Conclusions

In summary, we have investigated the structural requirements for oligomeric amphiphiles to exhibit a unique temperature sensitive transition below its LCST (sub-LCST). We find the mere presence of a temperature-responsive oligoethylene (or polyethylene) glycol unit does not endow molecules with sub-LCST behavior. Rigidity in the amphiphile backbone was found to be an essential criterion, in addition to the presence of OEG moieties. We also found that intramolecular hydrogen-bonding within the amphiphile can induce such rigidity in the amphiphile backbone. Guest encapsulation property of these assemblies was found to be significantly altered as a result of temperature responsive size change. We show that excellent guest encapsulation stability can be achieved at higher temperatures in assemblies from more rigidified amphiphiles. The reversibility and sharpness of the size change illustrates the applicability of this phenomenon in many temperature responsive applications. The supramolecular design parameters studied here can be translated in to more robust and biodegradable systems, which is one of the current foci in our laboratories.

4.8 Experimental Methods

4.8.1 Synthesis and Characterization

All chemicals and reagents were purchased from commercial sources and were used as received, unless otherwise mentioned. Compound **A** was synthesized following the previously reported procedure[20]. ^{1}H-NMR spectra were recorded on 400 MHz Bruker NMR spectrometer using the residual proton

resonance of the solvent as the internal standard. Chemical shifts are reported in parts per million (ppm). When peak multiplicities are given the following abbreviations are used: s, singlet; d, doublet; t, triplet; m, multiplet. ^{13}C-NMR spectra were proton decoupled and measured on a 500 MHz Bruker spectrometer with 125 MHz frequency by using carbon signal of the deuterated solvent as the internal standard. ^{1}H NMR of the methylated amphiphiles showed incorrect integrations and were rounded to the expected values. To clearly confirm the formation and purity of those products mass spectrometry was performed and reported.

4.8.1.1 Preparation of Jones Reagent

Chromium trioxide (7 g, 70 mmol) is dissolved in 10 mL of water in a 50 mL Erlenmeyer flask. The solution is then cooled using an ice bath followed by addition of 6.1 mL of concentrated sulfuric acid (18 M) slowly. The resultant solution is then diluted with 20 mL of water with constant stirring.

4.8.1.2 Synthesis of Acid Precursor

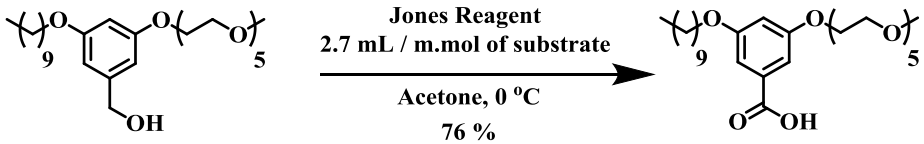

Compound **A** (0.77 g, 1.49 mmol) was dissolved in acetone and cooled using an ice bath. To this solution was added a cooled solution of Jones reagent (4 mL, 2.7 mL/mmol) drop wise, and stirred for 4 hours. Upon complete conversion of the reaction (checked by TLC (thin layer chromatography), the reaction mixture was filtered to remove a green precipitate formed. To this filtrate was added excess of

isopropyl alcohol and filtered again to remove any new precipitate formed. The reaction mixture was then concentrated in vacuo and the residue was dissolved in water and the pH of this aqueous phase was adjusted to pH < 3, followed by extracting twice with ethyl acetate, the combined extracts were then dried over anhydrous Na_2SO_4. Upon evaporation of the solvent, the crude product was purified by silica gel column chromatography (using combiflash) to afford 0.6 g (76%) of compound **B**. ^{1}H-NMR (400 MHz; Acetone-d_6): δ 7.17-7.16 (m, 2H), 6.75 (t, *J* = 2.3 Hz, 1H), 4.18 (t, *J* = 4.7 Hz, 2H), 4.04 (t, *J* = 6.5 Hz, 2H), 3.84 (t, *J* = 4.7 Hz, 2H), 3.68-3.54 (m, 14H), 3.47-3.45 (m, 2H), 3.28 (s, 3H), 1.82-1.75 (m, 2H), 1.53-1.45 (m, 2H), 1.41-1.28 (m, 14H), 0.88 (t, *J* = 6.9 Hz, 3H). 13-C NMR (125 MHz; Acetone): δ 170.9, 167.3, 161.27, 161.09, 133.3, 108.8, 108.6, 106.8, 72.7, 71.44, 71.29, 71.25, 71.06, 70.3, 68.92, 68.75, 60.5, 58.8, 32.6, 26.7, 25.7, 23.3, 20.8, 14.50, 14.36.

4.8.1.3 General procedure for synthesis of Oligomers 2 & 4

To a solution of compound **B** in methylene chloride was added excess of thionyl chloride and the mixture was refluxed for 4 hours. The reaction mixture was then concentrated in vacuo to remove unreacted excess of thionyl chloride. The crude acid chloride product obtained was then dried for an additional 2 hours under vacuo and redispered in methylene chloride. To this solution of acid chloride was then added appropriate equivalents of the corresponding amine and triethylamine and stirred at room temperature for 24 hours. The reaction mixture was then concentrated in vacuo and the residue was dissolved in water and extracted twice with ethyl acetate, the combined extracts were then dried over anhydrous Na_2SO_4.

Upon evaporation of the solvent, the crude product was purified by silica gel column chromatography (using combiflash) to obtain respective oligomer.

4.8.1.4 Molecule 2

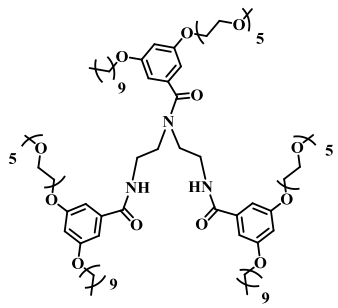

^{1}H-NMR (400 MHz; Acetone-d_6): δ 7.95 (s, 2H), 7.04 (s, 4H), 6.63 (s, 2H), 6.46-6.38 (m, 3H), 4.14 (s, 4H), 4.01-3.99 (m, 4H), 3.92-3.89 (m, 2H), 3.81-3.54 (m, 52H), 3.46 (t, *J* = 4.9 Hz, 6H), 3.28 (s, 9H), 1.76 (s, 4H), 1.70-1.63 (m, 2H), 1.46-1.31 (m, 48H), 0.88 (t, *J* = 6.7 Hz, 9H). 13-C NMR (125 MHz; Acetone-d_6): δ 172.7, 161.21, 161.05, 160.96, 160.7, 140.0, 106.7, 106.3, 105.7, 105.4, 105.0, 103.1, 72.6, 71.36, 71.21, 71.02, 70.2, 68.8, 68.6, 68.3, 58.8, 39.0, 23.3, 14.4. MALDI-ToF m/z 16657.316 ($C_{88}H_{151}N3O_{24}$+Na^+ requires 1657.0598)

4.8.1.5 Molecule 4

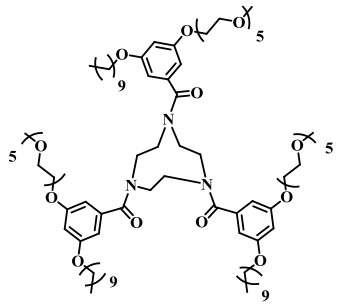

^{1}H-NMR (300 MHz; Acetone-d_6): δ 6.55-6.34 (m, 9H), 4.11 (t, *J* = 3.8 Hz, 6H), 3.95 (t, *J* = 6.3 Hz, 6H), 3.79-3.54 (m, 56H), 3.47-3.44 (m, 6H), 3.28 (s, 9H), 1.84-1.70

(m, 8H), 1.43-1.30 (m, 42H), 0.88 (t, *J* = 6.3 Hz, 9H). 13-C NMR (125 MHz; Acetone-d_6): δ 172.7, 161.37, 161.28, 161.0, 139.8, 106.4, 106.0, 105.5, 103.1, 72.7, 71.41, 71.30, 71.27, 71.08, 70.3, 68.8, 68.6, 58.8, 51.1, 23.4, 14.4. MALDI-ToF m/z 1683.766 ($C_{120}H_{206}N_4O_{32}$+Na^+ requires 1683.0698).

4.8.1.6 Molecule 3

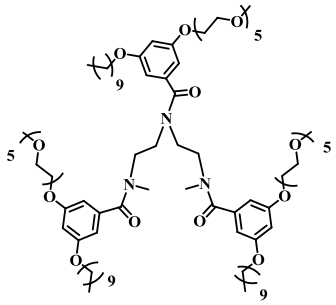

^{1}H-NMR (400 MHz; Acetone-d_6): δ 6.57-6.41 (m, 9H), 4.16-3.55 (m, 60H), 3.46 (t, *J* = 4.8 Hz, 6H), 3.28 (s, 9H), 3.06 (s, 3H), 2.66 (s, 3H), 1.79-1.65 (m, 6H), 1.33 (d, *J* = 75.8 Hz, 42H), 0.88-0.86 (m, 9H). 13-C NMR (125 MHz; Acetone-d_6): δ 172.0, 171.6, 161.21, 161.06, 161.00, 160.94, 160.74, 139.7, 106.32, 106.24, 106.11, 105.91, 105.54, 105.43, 103.70, 103.52, 103.1, 102.9, 72.6, 71.37, 71.32, 70.28, 70.13, 68.82, 68.72, 68.58, 68.43, 58.8, 23.3, 14.4. MALDI-ToF m/z 1685.493 ($C_{90}H_{155}N_3O_{24}$+Na^+ requires 1685.0898).

4.8.1.7 Molecule 5

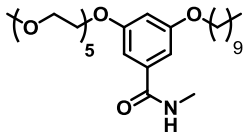

^{1}H-NMR (400 MHz; $CDCl_3$): δ 6.88 (d, *J* = 1.7 Hz, 2H), 6.58 (t, *J* = 2.0 Hz, 1H), 6.16 (bs, 1H), 4.14 (t, *J* = 4.7 Hz, 2H), 3.95 (t, *J* = 6.6 Hz, 2H), 3.84 (t, *J* = 4.7 Hz, 2H), 3.72-3.62 (m, 14H), 3.54 (m, 2H), 3.37 (s, 3H), 2.98 (d, *J* = 4.8 Hz, 3H), 1.76 (quintet, *J*

= 7.2 Hz, 2H), 1.43-1.27 (m, 14H), 0.88 (t, *J* = 6.8 Hz, 3H). ^{13}C NMR (125 MHz; $CDCl_3$): δ 168.1, 160.3, 159.9, 136.7, 105.7, 105.2, 104.5, 71.9, 70.78, 70.62, 70.59, 70.50, 69.7, 68.3, 67.7, 59.0, 31.9, 29.58, 29.57, 29.37, 29.33, 29.17, 26.9, 26.0, 22.7, 14.1. ESI-MS m/z 564.358 ($C_{29}H_{51}NO_8$ + Na^+ requires 564.349).

4.8.1.8 Molecule 6

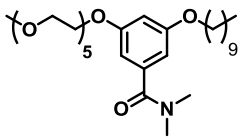

^{1}H-NMR (400 MHz; $CDCl_3$): δ 6.51 (m, 2H), 6.49 (m, 1H), 4.10 (t, *J* = 4.8 Hz, 2H), 3.92 (t, *J* = 6.6 Hz, 2H), 3.84 (t, *J* = 4.8 Hz, 2H), 3.73-3.63 (m, 14H), 3.54 (dd, *J* = 5.7, 3.6 Hz, 2H), 3.37 (s, 3H), 3.08 (s, 3H), 2.96 (s, 3H), 1.75 (dt, *J* = 14.4, 7.0 Hz, 2H), 1.44-1.33 (m, 14H), 0.88 (t, *J* = 6.8 Hz, 3H). ^{13}C NMR (125 MHz; $CDCl_3$): δ 171.4, 160.4, 159.9, 138.2, 105.8, 105.4, 102.7, 72.0, 70.92, 70.72, 70.69, 70.67, 70.62, 69.7, 68.4, 67.7, 59.1, 39.6, 35.4, 32.0, 29.68, 29.67, 29.48, 29.43, 29.28, 26.1, 22.8, 14.2. MALDI-ToF m/z 578.40 ($C_{30}H_{53}NO_8$+Na^+ requires 578.3698).

4.8.1.9 Molecule 7

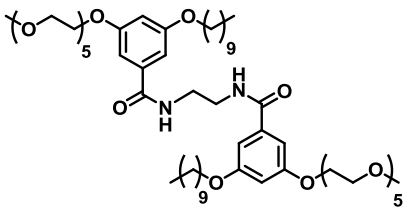

^{1}H-NMR (400 MHz; Acetone-d_6): δ 8.06 (bs, 2H), 7.05 (d, *J* = 2.0 Hz, 4H), 6.63 (t, *J* = 2.2 Hz, 2H), 4.16 (t, *J* = 4.7 Hz, 4H), 4.01 (t, *J* = 6.5 Hz, 4H), 3.82 (t, *J* = 4.7 Hz, 4H), 3.67-3.54 (m, 28H), 3.46 (dd, *J* = 5.8, 3.9 Hz, 4H), 3.27 (s, 6H), 1.78 (quintet, *J* =

7.2 Hz, 4H), 1.52-1.30 (m, 28H), 0.88 (t, *J* = 6.8 Hz, 6H). ^{13}C NMR (125 MHz; Acetone-d_6): δ 167.7, 161.2, 161.0, 137.8, 106.7, 106.4, 104.9, 72.6, 71.41, 71.28, 71.26, 71.23, 71.22, 71.04, 70.3, 68.8, 68.6, 58.8, 41.0, 23.3, 14.4. ESI-MS m/z 1103.7143 ($C_{58}H_{100}N_2O_{16}$ + Na^+ requires 1103.6997).

4.8.1.10 Molecule 8

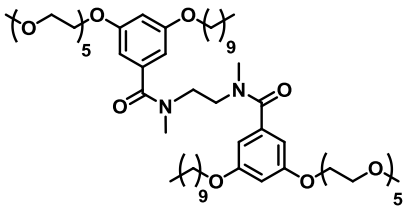

^{1}H-NMR (400 MHz; Acetone-d_6): δ 6.53-6.38 (m, 6H), 4.15-3.55 (m, 44H), 3.46 (dd, *J* = 5.8, 3.9 Hz, 4H), 3.28 (s, 6H), 3.05 (s, 6H), 1.77-1.67 (m, 4H), 1.48-1.30 (m, 28H), 0.88 (t, *J* = 6.6 Hz, 6H). ^{13}C NMR (125 MHz; Acetone-d_6): δ 171.4, 161.0, 160.8, 140.0, 106.1, 105.9, 103.1, 72.7, 71.4, 71.1, 70.2, 68.7, 68.5, 58.8, 44.8, 37.8, 23.3, 14.4. ESI-MS m/z 1131.7344 ($C_{60}H_{104}N_2O_{16}$ + Na^+ requires 1131.7298).

4.8.1.11 Molecule 9

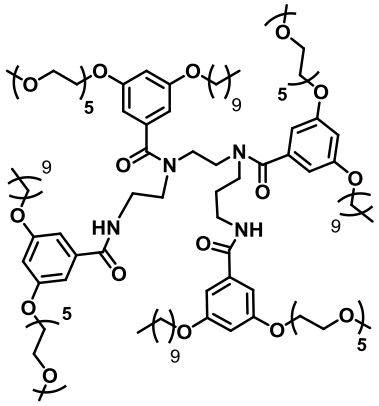

^{1}H-NMR (400 MHz; Acetone-d_6): δ 8.34 (bs, 1H), 7.83 (bs, 1H), 7.1- 7.07 (m, 4H), 6.63-6.37 (m, 8H), 4.14-3.46 (m, 88H), 3.29 (s, 12H), 1.76-1.45 (m, 64H), 0.90 (t, *J* = 6.1 Hz, 12H). ^{13}C NMR (125 MHz; Acetone-d_6): δ 171.9, 171.5, 161.07, 161.02,

160.8, 140.0, 139.5, 106.2, 105.95, 105.86, 105.5, 103.6, 103.0, 72.7, 71.3, 70.23, 70.16, 68.74, 68.60, 68.46, 58.8, 23.4, 14.4. MALDI-ToF m/z 2210.4948 ($C_{118}H_{202}N_4O_{32}$+Na^+ requires 2211.4198).

4.8.1.12 Molecule 10

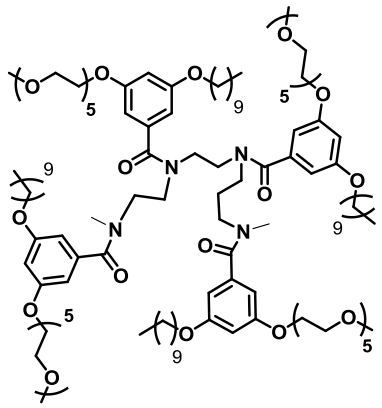

^{1}H-NMR (400 MHz; Acetone-d_6): δ 6.53-6.39 (m, 12H), 4.16-3.46 (m, 88H), 3.28 (s, 12H), 3.00 (s, 3H), 2.67 (s, 3H), 1.78-1.30 (m, 64H), 0.88 (d, *J* = 5.5 Hz, 12H). ^{13}C NMR (125 MHz; Acetone-d_6): δ 171.9, 171.5, 161.07, 161.02, 160.8, 140.0, 139.5, 106.2, 105.95, 105.86, 105.5, 103.6, 103.0, 72.7, 71.3, 70.23, 70.16, 68.74, 68.60, 68.46, 58.8, 23.4, 14.4. MALDI-ToF m/z 2237.464 ($C_{120}H_{206}N_4O_{32}$+H^+ requires 2238.3898).

4.8.1.13 Molecule 11

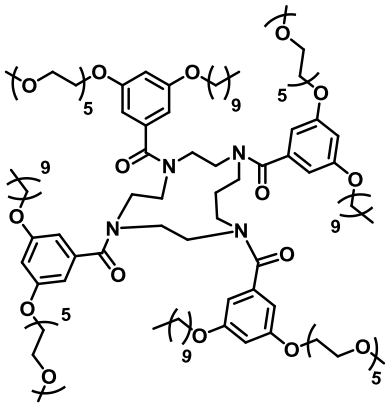

^{1}H-NMR (400 MHz; Acetone-d_6): δ 6.57-6.25 (m, 12H), 4.18-3.55 (m, 92H), 3.46 (t, *J* = 4.8 Hz, 8H), 3.28 (s, 12H), 1.76 (s, 8H), 1.47-1.29 (m, 56H), 0.88 (t, *J* = 5.8 Hz, 12H). MALDI-ToF m/z 2237.464 ($C_{120}H_{206}N_4O_{32}+H^+$ requires 2238.3898).

4.8.2 Dynamic Light Scattering

DLS was performed on a Malvern nano-zeta sizer instrument with a 637 nm laser source with non-invasive backscattering technology detected at 173^0. All sizes are reported as the hydrodynamic diameter (D_H) and were repeated in triplicate. All samples were prepared in water at pH 7 by brief sonication and vortexing at room temperature. Variable temperature DLS experiments were performed by equilibrating the aqueous solutions for 6 minutes at the respective temperature before the size measurements.

4.8.3 Guest Exchange experiments using FRET

FRET studies were performed on a PTI spectrofluorometer with a XenoFlash power supply and Quantum TC125 temperature control. Dye loading (DiI and DiO) in the micelles was always done at 1 wt % of the corresponding amphiphile as

follows: 20 µL of 0.5 mg/mL dye (DiO or DiI) in acetone was added to a 20 mL glass vial containing 1 mg of amphiphile (**2** or **4**), to this mixture was added additional 40 µL of acetone to homogeneously mix all the components. The acetone was then evaporated using a mild argon flow, followed by addition of calculated amount of water to make 25 µM amphiphile solutions. Temperature dependent guest exchange experiments were done as follows: 25 µM amphiphile (**2** or **4**) solution loaded with DiO was equilibrated at corresponding temperature in the fluorimeter cell for 6 minutes, similarly 25 µM amphiphile solution containing DiI was equilibrated at the same temperature outside using an ice bath or hot water bath for 6 minutes, upon equilibration DiI containing solution was briskly transferred into a 1 mL syringe and added to DiO containing solution. DiO was excited at 440 nm, and DiI emission was monitored at 567 nm at different time points using time-lapse fluorescence measurements.

4.9 NMR Spectra

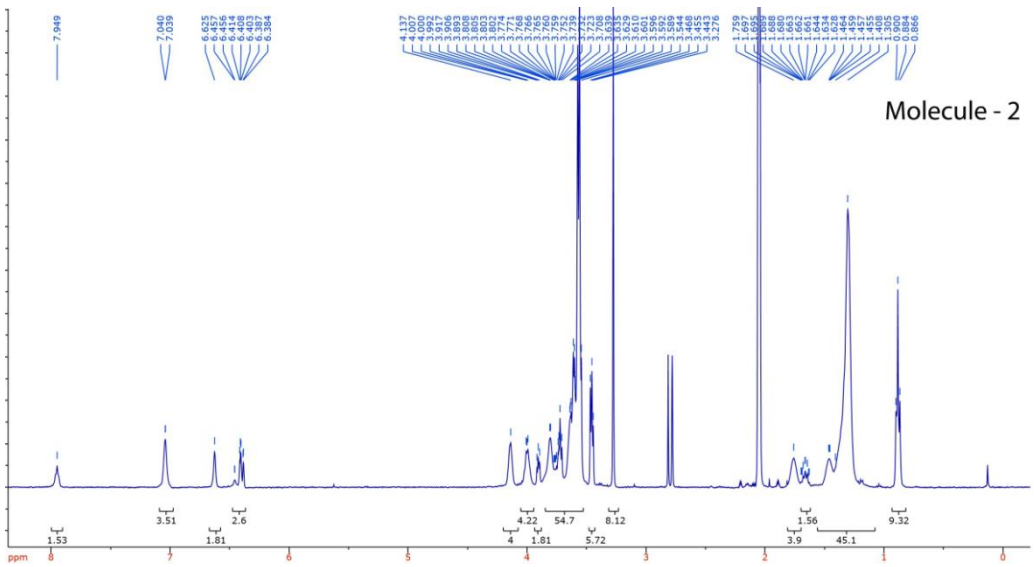

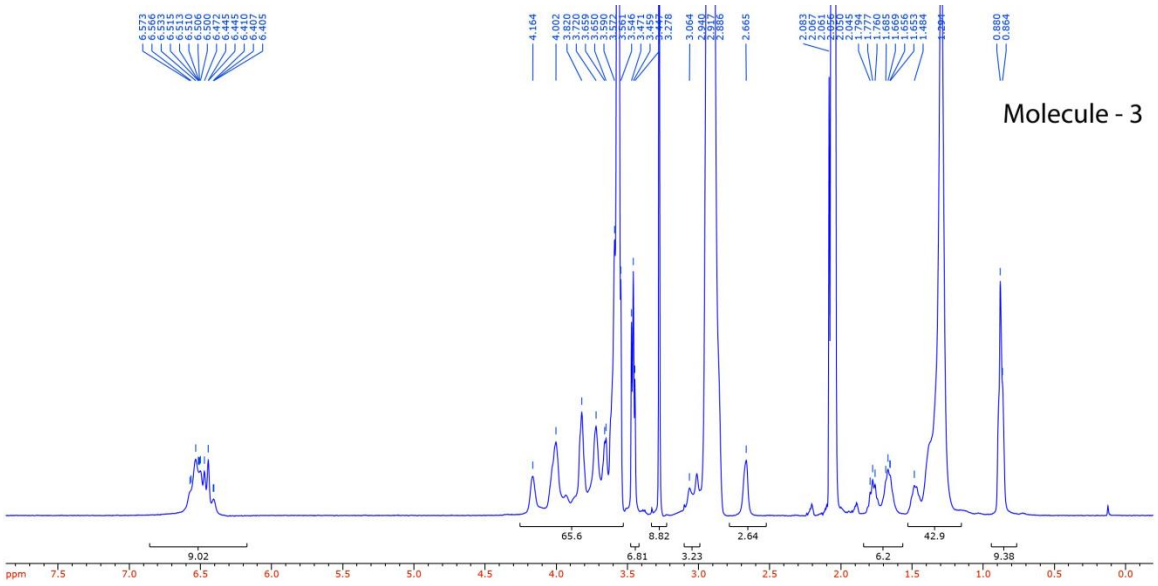
Molecule - 3

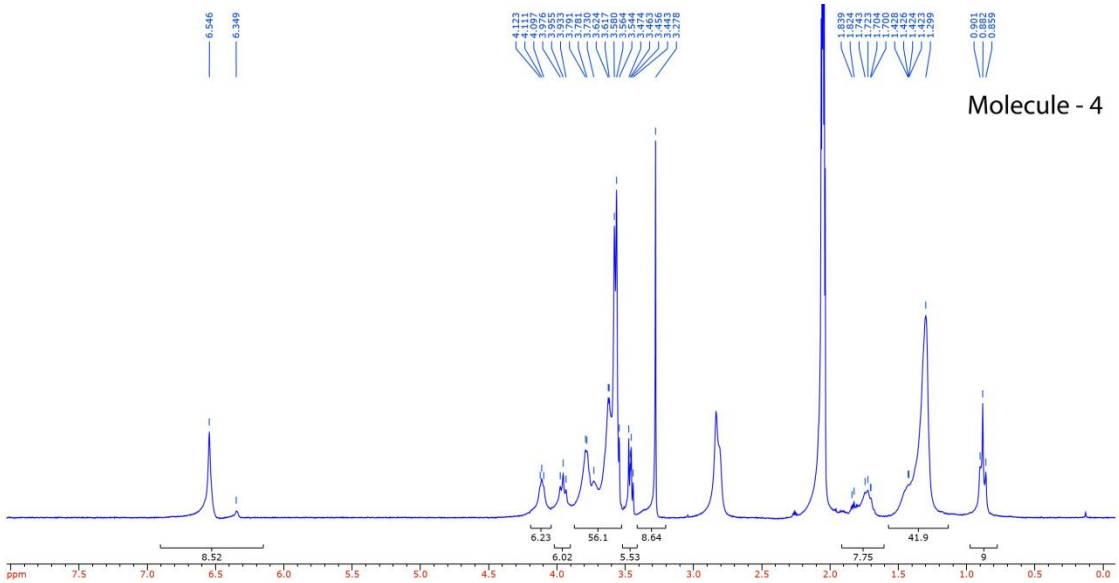
Molecule - 4

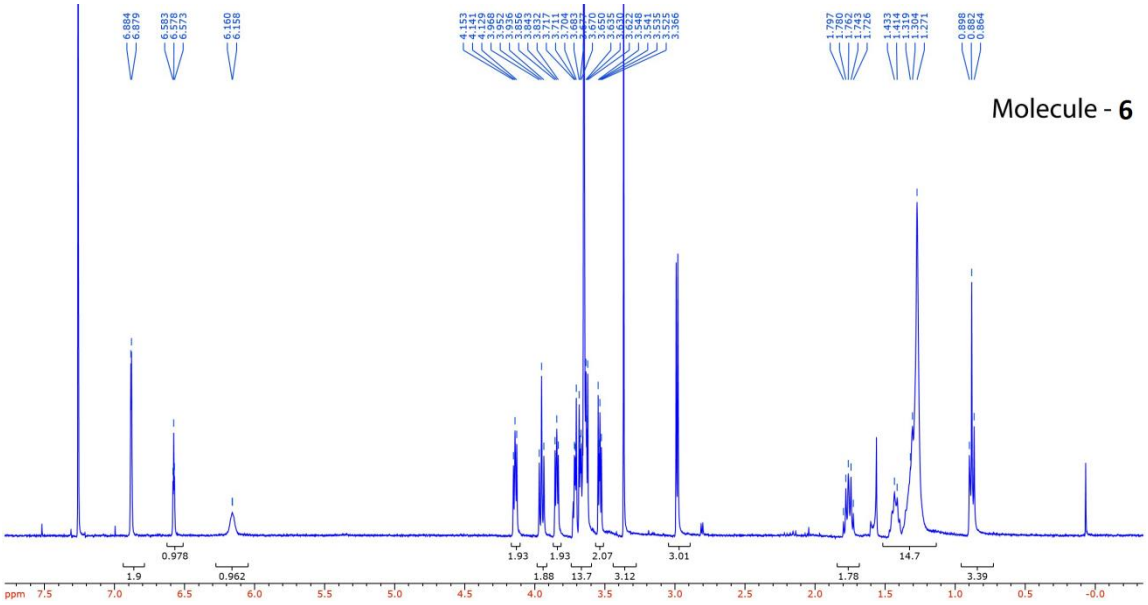
Molecule - 6

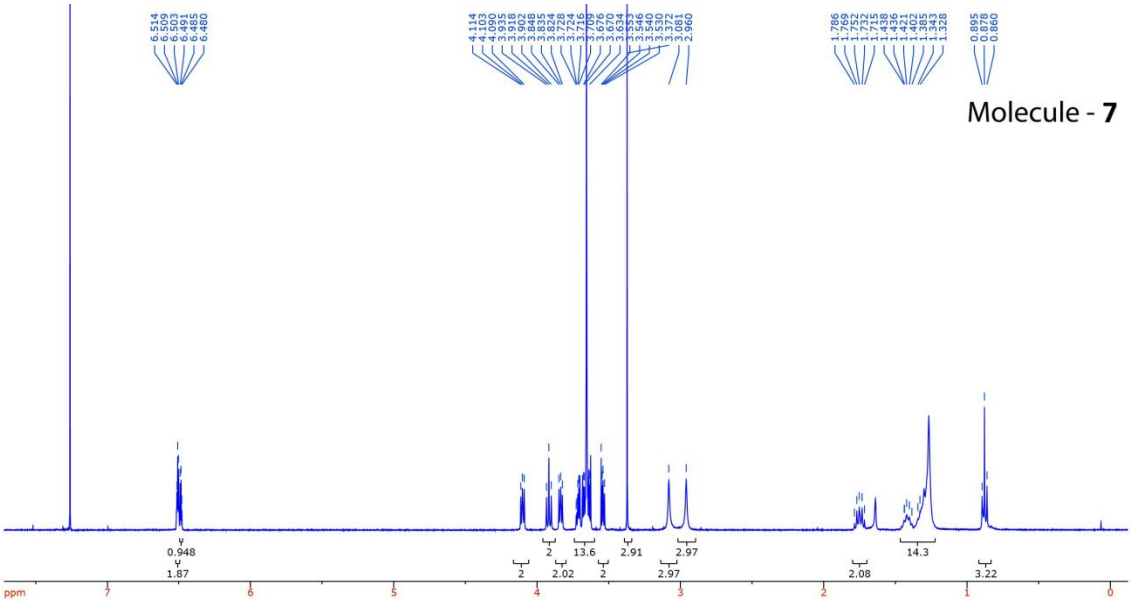
Molecule - 7

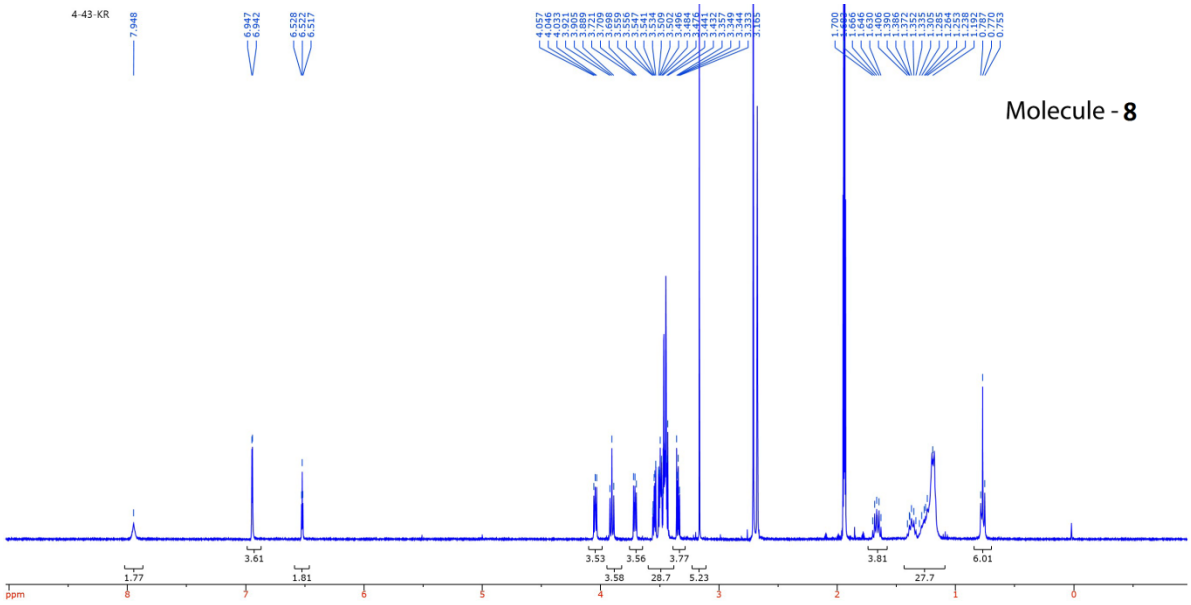
4-43-KR
Molecule - 8

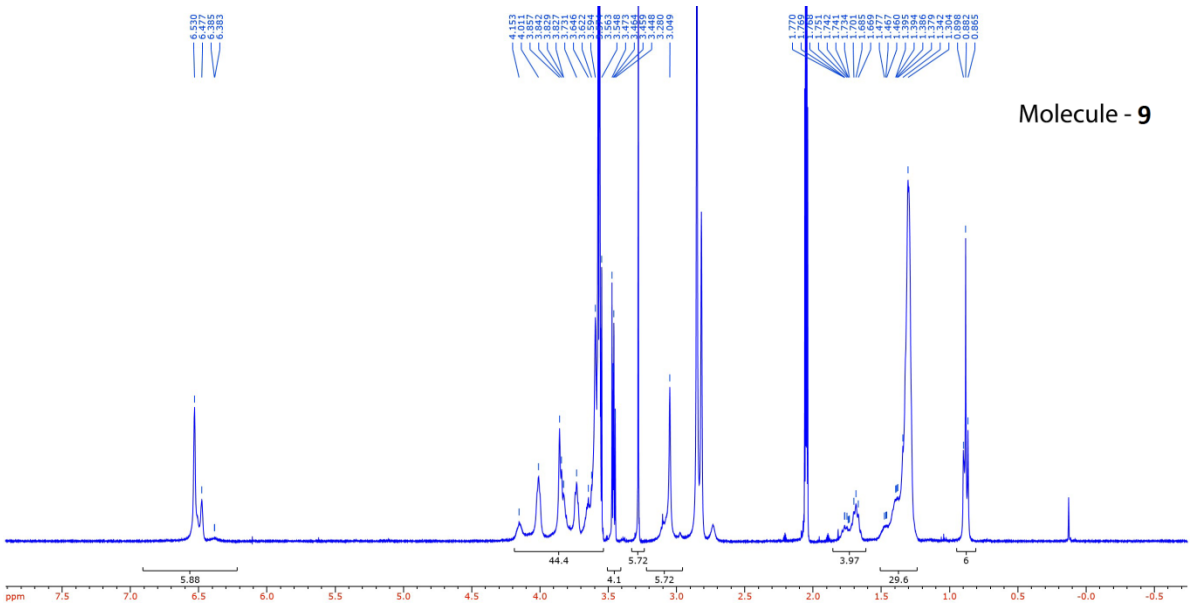
Molecule - 9

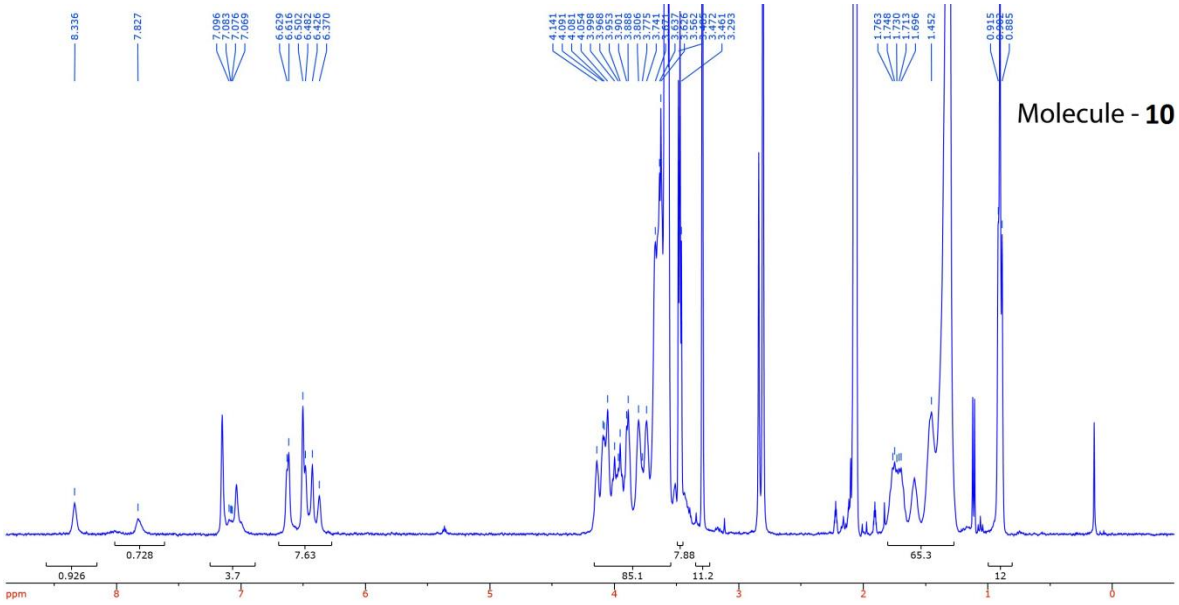
Molecule - **10**

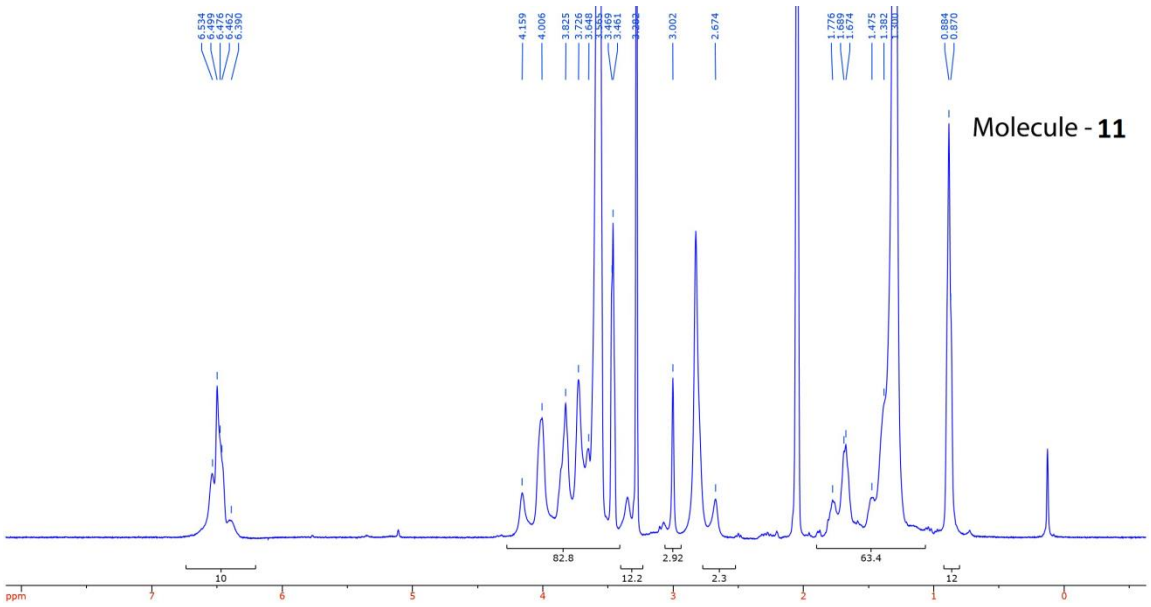
Molecule - **11**

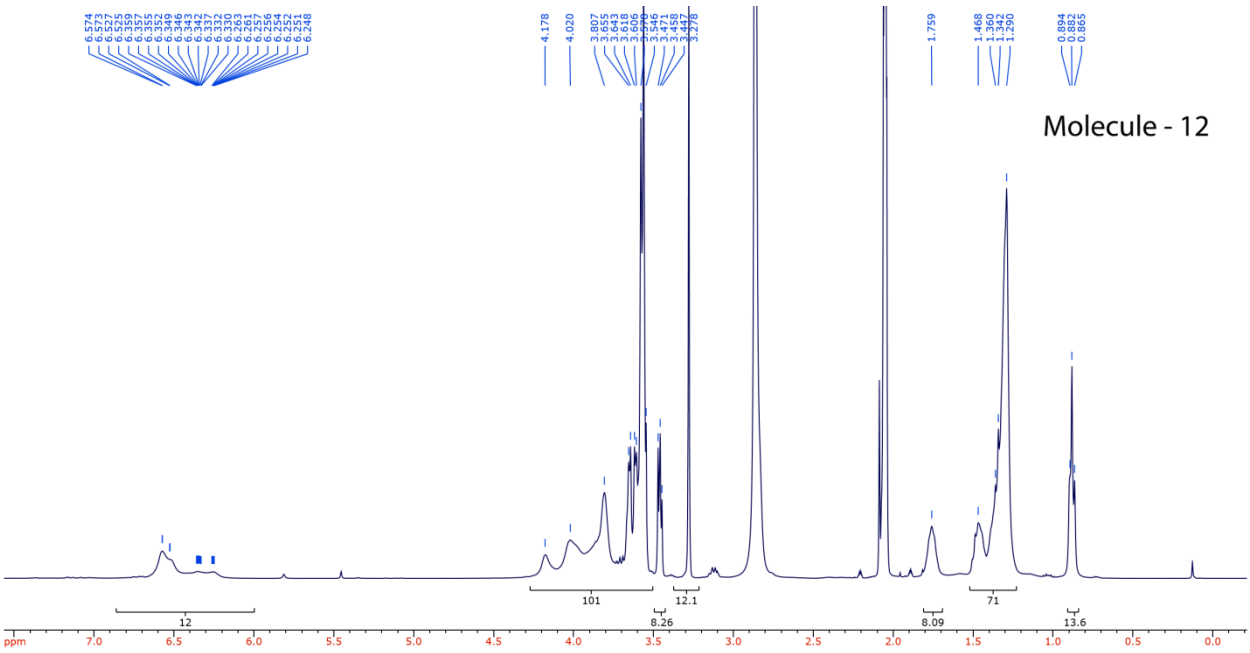

4.10 References

1. Blum, A. P.; Kammeyer, J. K.; Rush, A. M.; Callmann, C. E.; Hahn, M. E.; Gianneschi, N. C., Stimuli-Responsive Nanomaterials for Biomedical Applications. *J. Am. Chem. Soc.* **2015,** *137* (6), 2140-2154.

2. Stuart, M. A. C.; Huck, W. T. S.; Genzer, J.; Muller, M.; Ober, C.; Stamm, M.; Sukhorukov, G. B.; Szleifer, I.; Tsukruk, V. V.; Urban, M.; Winnik, F.; Zauscher, S.; Luzinov, I.; Minko, S., Emerging applications of stimuli-responsive polymer materials. *Nat Mater* **2010,** *9* (2), 101-113.

3. Liu, F.; Urban, M. W., Recent advances and challenges in designing stimuli-responsive polymers. *Prog. Polym. Sci.* **2010,** *35* (1–2), 3-23.

4. Ganta, S.; Devalapally, H.; Shahiwala, A.; Amiji, M., A review of stimuli-responsive nanocarriers for drug and gene delivery. *J. Controlled Release* **2008,** *126* (3), 187-204.

5. Special issue on stimuli responsive materials. *Special issue on stimuli responsive materials, Chem. Soc. Rev.* **2013,** (17), 7045-7486.

6. Cabral, H.; Nishiyama, N.; Kataoka, K., Supramolecular nanodevices: From design validation to theranostic nanomedicine. *Accounts Chem. Res.* **2011,** *44* (10), 999-1008.

7. Rijcken, C. J. F.; Soga, O.; Hennink, W. E.; Nostrum, C. F. v., Triggered destabilisation of polymeric micelles and vesicles by changing polymers polarity: An attractive tool for drug delivery. *J. Controlled Release* **2007,** *120* (3), 131-148.

8. Jackson, A. W.; Fulton, D. A., Making polymeric nanoparticles stimuli-responsive with dynamic covalent bonds. *Polym. Chem.* **2013,** *4* (1), 31-45.

9. Wei, P.; Cook, T. R.; Yan, X.; Huang, F.; Stang, P. J., A Discrete Amphiphilic Organoplatinum(II) Metallacycle with Tunable Lower Critical Solution Temperature Behavior. *Journal of the American Chemical Society* **2014,** *136* (44), 15497-15500.

10. Buller, J.; Laschewsky, A.; Lutz, J.-F.; Wischerhoff, E., Tuning the lower critical solution temperature of thermoresponsive polymers by biospecific recognition. *Polymer Chemistry* **2011,** *2* (7), 1486-1489.

11. Lutz, J.-F.; Akdemir, O.; Hoth, A., Point by point comparison of two thermosensitive polymers exhibiting a similar LCST: Is the age of poly(NIPAM) over? *J. Am. Chem. Soc.* **2006,** *128* (40), 13046-13047.

12. Corti, M.; Minero, C.; Degiorgio, V., Cloud point transition in nonionic micellar solutions. *J. Phys. Chem.* **1984,** *88* (2), 309-317.

13. Mitchell, D. J.; Tiddy, G. J. T.; Waring, L.; Bostock, T.; McDonald, M. P., Phase behaviour of polyoxyethylene surfactants with water. Mesophase structures and partial miscibility (cloud points). *J. Chem. Soc., Faraday Trans. 1 F.* **1983,** *79* (4), 975-1000.

14. Fujishige, S.; Kubota, K.; Ando, I., Phase transition of aqueous solutions of poly(N-isopropylacrylamide) and poly(N-isopropylmethacrylamide). *J. Phys. Chem.* **1989,** *93* (8), 3311-3313.

15. Heskins, M.; Guillet, J. E., Solution Properties of Poly(N-isopropylacrylamide). *Journal of Macromolecular Science: Part A - Chemistry* **1968,** *2* (8), 1441-1455.

16. Hocine, S.; Li, M.-H., Thermoresponsive self-assembled polymer colloids in water. *Soft Matter* **2013,** *9* (25), 5839-5861.

17. Hoffman, A. S., Applications of thermally reversible polymers and hydrogels in therapeutics and diagnostics. *Journal of Controlled Release* **1987,** *6* (1), 297-305.

18. Yu, X.; Yang, X.; Horte, S.; Kizhakkedathu, J. N.; Brooks, D. E., A pH and thermosensitive choline phosphate-based delivery platform targeted to the acidic tumor microenvironment. *Biomaterials* **2014,** *35* (1), 278-286.

19. Lutz, J. F., Polymerization of oligo(ethylene glycol) (meth)acrylates: Toward new generations of smart biocompatible materials. *J. Polym. Sci., Part A: Polym. Chem.* **2008,** *46* (11), 3459-3470.

20. Aathimanikandan, S. V.; Savariar, E. N.; Thayumanavan, S., Temperature-sensitive dendritic micelles. *J. Am. Chem. Soc.* **2005,** *127* (42), 14922-14929.

21. Vancoillie, G.; Frank, D.; Hoogenboom, R., Thermoresponsive poly(oligo ethylene glycol acrylates). *Progress in Polymer Science* **2014,** *39* (6), 1074-1095.

22. Lüsse, S.; Arnold, K., The Interaction of Poly(ethylene glycol) with Water Studied by 1H and 2H NMR Relaxation Time Measurements. *Macromolecules* **1996,** *29* (12), 4251-4257.

23. Inoue, T.; Matsuda, M.; Nibu, Y.; Misono, Y.; Suzuki, M., Phase Behavior of Heptaethylene Glycol Dodecyl Ether and Its Aqueous Mixture Revealed by DSC and FT-IR Spectroscopy. *Langmuir* **2001,** *17* (6), 1833-1840.

24. Hey, M. J.; Ilett, S. M., Poly(ethylene oxide) hydration studied by differential scanning calorimetry. *J. Chem. Soc., Faraday Trans.* **1991,** *87* (22), 3671-3675.

25. Fuller, J. M.; Raghupathi, K. R.; Ramireddy, R. R.; Subrahmanyam, A. V.; Yesilyurt, V.; Thayumanavan, S., Temperature-sensitive transitions below LCST in amphiphilic dendritic assemblies: host-guest implications. *J. Am. Chem. Soc.* **2013,** *135* (24), 8947-8954.

26. Eberhardt, E. S.; Raines, R. T., Amide-Amide and Amide-Water Hydrogen Bonds: Implications for Protein Folding and Stability. *J. Am. Chem. Soc.* **1994,** *116* (5), 2149-2150.

27. Gellman, S. H.; Dado, G. P.; Liang, G. B.; Adams, B. R., Conformation-directing effects of a single intramolecular amide-amide hydrogen bond: variable-temperature NMR and IR studies on a homologous diamide series. *J. Am. Chem. Soc.* **1991,** *113* (4), 1164-1173.

28. Pace, C. N.; Shirley, B. A.; McNutt, M.; Gajiwala, K., Forces contributing to the conformational stability of proteins. *Faseb J.* **1996,** *10* (1), 75-83.

29. Dixon, D. A.; Dobbs, K. D.; Valentini, J. J., Amide-Water and Amide-Amide Hydrogen Bond Strengths. *J. Phys. Chem.* **1994,** *98* (51), 13435-13439.

30. Doig, A. J.; Williams, D. H., Binding energy of an amide-amide hydrogen bond in aqueous and nonpolar solvents. *J. Am. Chem. Soc.* **1992,** *114* (1), 338-343.

31. Johansson, A.; Kollman, P.; Rothenberg, S.; McKelvey, J., Hydrogen bonding ability of the amide group. *J. Am. Chem. Soc.* **1974,** *96* (12), 3794-3800.

32. Jiwpanich, S.; Ryu, J.-H.; Bickerton, S.; Thayumanavan, S., Noncovalent Encapsulation Stabilities in Supramolecular Nanoassemblies. *J. Am. Chem. Soc.* **2010,** *132* (31), 10683-10685.

CHAPTER 5
SUMMARY AND FUTURE DIRECTIONS

5.1 Summary

Stimuli-responsive systems based on self-assembled aggregates such as micelles, liposomes, and thin films offer a robust and versatile platform in a broad range of applications such as sensing, diagnostics, and drug delivery.[1-3] The molecular features which influence the self-assembly and stimuli responsive nature of these systems are extensively studied.[4-6] However most of these systems are based on polymeric systems; while polymers offer several advantages such as low CAC's, good colloidal stability, and high loading capacity they do not allow for the study of fundamental structure property relationships owing to their inherent dispersity. The broad objective of this thesis was to present and analyze unique stimuli responsive micelle assemblies based on dendron and oligomer amphiphiles. This choice of these amphiphiles gives us a unique opportunity to understand the fundamental structure property relationships which influence the stimuli responsive properties. Chapter 1 focus on introducing self-assembling stimuli responsive systems and our versatile molecular design strategy based on micelle equilibrium and amphiphile HLB.

In Chapter 2,[7] we presented an enzyme responsive amphiphilic dendron which forms micelle type assemblies in aqueous solution and releases encapsulated hydrophobic guest molecules in response to a specific enzyme stimulus. By conjugating a pro-fluorophore to the enzyme substrate on the dendron we were

able to monitor the enzymatic reaction firsthand, and were also able to correlate this to the ensued guest release (after effect of enzyme reaction). Additionally, the photo-crosslinking feature incorporated into these dendrons was used to tune the extent of guest molecule release through variable crosslinking (stabilization) of aggregates. This crosslinking strategy has more importantly enabled us to also study the role of micelle-unimer equilibrium in enzyme response. Here the enzymatic response was found to be inversely related to the stability of aggregates.

LCST is a well-established phase change phenomenon observed in temperature responsive systems containing polyethylene glycol (PEG). In Chapter 3,[8] we studied the temperature sensitive amphiphilic dendron assembly below its LCST and have discovered that there exists another temperature responsive phenomenon (sub-LCST) where the size of aggregates changes by an order of magnitude. This sub-LCST was then investigated for its effect on guest encapsulation stability and unimer-aggregate equilibrium. It was found that the smaller aggregates (temperature below sub-LCST) exhibited poor guest encapsulation stability, and a dynamic unimer-aggregate exchange in comparison to the larger aggregates (temperature above sub-LCST and below LCST). Though the LCST feature was observed in amphiphilic dendrons of all generations (variable amphiphilic units), the sub-LCST feature was interestingly found to be exclusive only to generation one dendron (three amphiphilic units).

In Chapter 4,[9] the molecular design features responsible for the unique sub-LCST phenomenon in amphiphilic dendron were investigated with a series of PEG

containing amphiphiles. It was found that the presence of PEG is not the sole criterion for the sub-LCST feature nor was the trimeric architecture of the amphiphile akin to the dendron amphiphile. The sub-LCST feature was found to be due to the rigidity of the amphiphile which was validated by several molecular designs with trimeric as well as tetrameric architecture. Interestingly it was also found that the intramolecular hydrogen bonding in the amphiphile backbone can also induce this rigidity. The interesting molecular design findings are now applied to develop biocompatible molecular designs (peptide amphiphiles) which have a scope in temperature responsive delivery of encapsulated guests at lower temperatures.

5.2 Future Directions

5.2.1 Aggregate – Unimer Equilibrium Pathways: A Case study of Enzyme Responsive Assemblies

Micelles, due to their widespread applications such as in detergents, wetting agents, foaming agents, drug delivery vehicles, etc., have acquired considerable attention. A significant amount of research has been done to study the intricacies of the micelle formation itself, and factors which might affect the micelles formed. Though there are seemingly different viewpoints about the mechanism of micelle formation, it is widely accepted that once formed, the micelles always coexist with their unimeric entities.[7,10-11] The coexisting unimers and micelles are thought to be in thermodynamic equilibrium, suitably adjusting their equilibrium depending on the external perturbations. Small molecule surfactants are widely used to study the behavior of micelles; though important, they do not address the questions in the

realm where polymers are predominantly the molecules of interest. Dendrimers due to their large molecular weights mimic polymers; at the same time due to their uniformly disperse nature they can also be treated like surfactants to conduct fundamental studies. In this work we propose to study one aspect of the micelles i.e. unimer-micelle equilibrium. We are specifically interested in the nature of equilibrium/s existing between the unimers and micelles. These studies will be conducted in the context of enzyme responsive dendrimers.

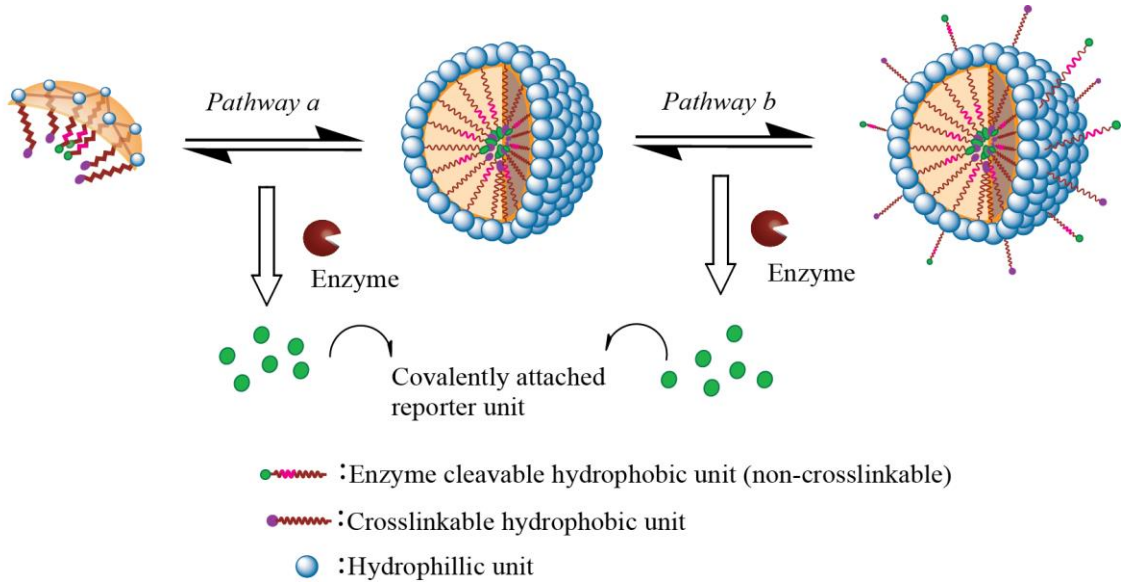

Figure 5.1. Pictorial representation of two different equilibrium states of micellar aggregates, and concurrent enzymatic cleavage of substrate available through each pathway.

In section 2 we have demonstrated the presence of monomer-aggregate equilibrium by controllably crosslinking the micelle type aggregates with the aid of photochemical reactions. However considering the dynamic nature of these micelles in the aqueous solutions it is reasonable to expect at least another pathway for enzyme to access the substrate (Figure 5.1/*pathway-b*). We presumed of a

possibility where the hydrophobic unit presents itself to the hydrophilic medium while the micelle is still intact. In such a scenario the hydrophobic unit will be exposed to non-favorable aqueous (hydrophilic) environment transiently, before it is forced to get back into the micellar interior where the solovophobic interactions are favored. During this brief period, the presence of an enzyme in aqueous bulk would access the substrate and cause the cleavage. This will be studied with the molecular design shown in Scheme 5.1.

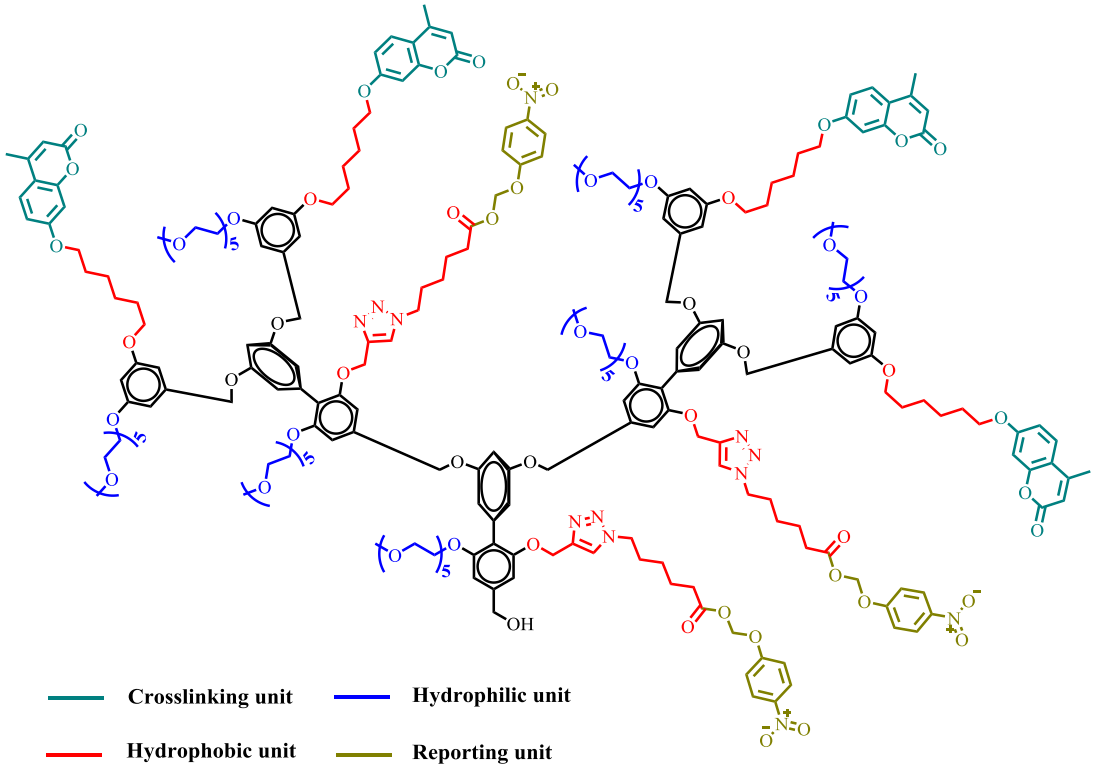

Scheme 5.1. Molecular design of G2 dendron(molecule **9**).

5.2.1.1 Molecular Design, Synthesis, and Proposed Enzymatic Studies

We hypothesize that there are two possible pathways involved in the enzymatic reaction on lipophilic substrate of amphiphilic dendrons: i) unimer-aggregate equilibrium (*pathway a*), where enzyme reacts with unimeric dendron; ii) transient presentation of substrate to the enzyme (*pathway b*), here the enzyme reacts with substrate present on intact aggregate (Figure 5.1). We have already realized the existence of *pathway a* in the previous chapter. In this work we are interested in i) studying *pathway b* separately, and ii) assessing the contributions

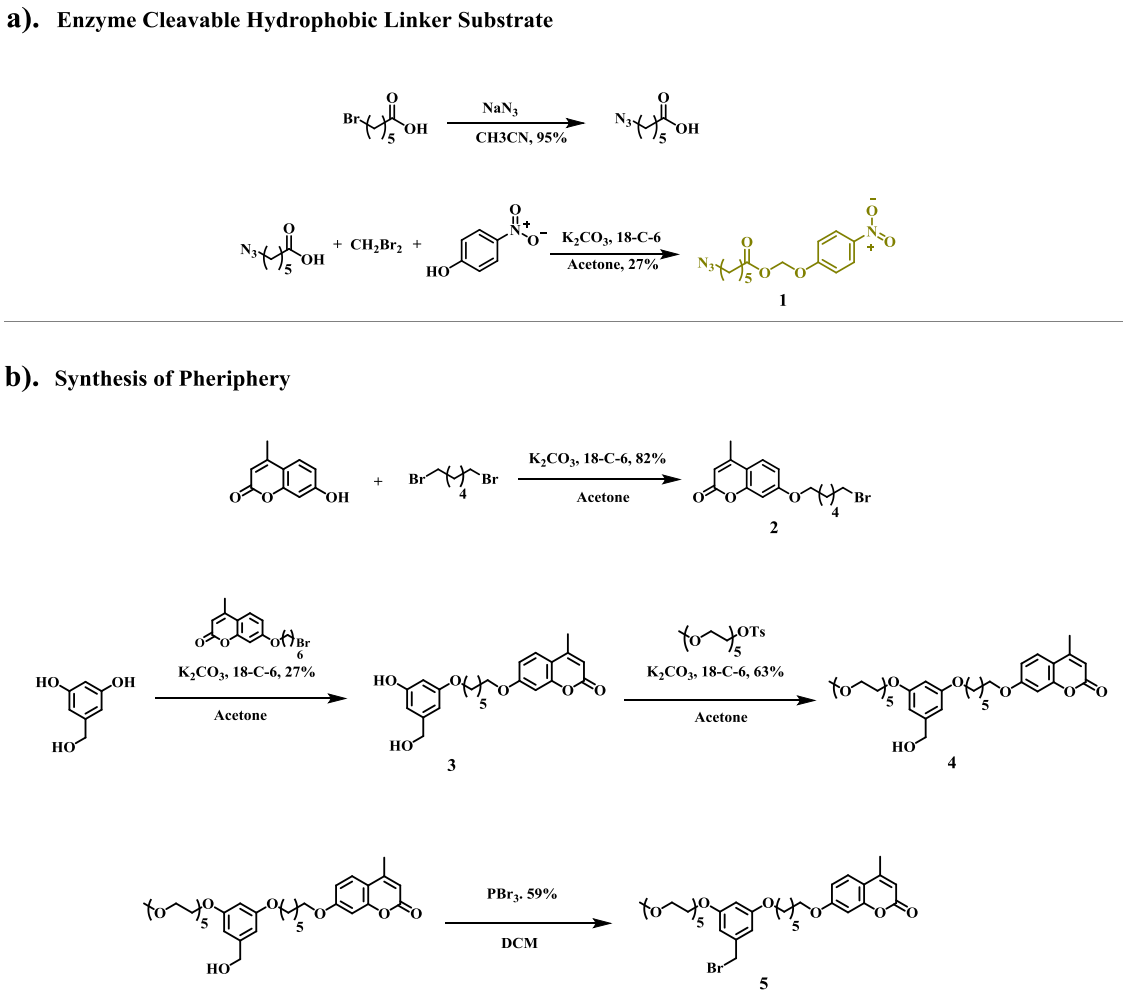

Scheme 5.2. Synthesis of enzyme cleavable linker (a), and periphery (b) of G2 dendron.

from *pathway a,* and *pathway b* to the enzymatic reaction. To achieve this, it is essential for the molecular design to be such that contribution from each of these pathways can be studied exclusively. To solely observe the *pathway b* it is essential to stabilize the formed micellar aggregates so as to eliminate the possibility of monomeric dendrons in solution; however this stabilization (crosslinking) should still allow the substrates to be in equilibrium through *pathway b*. To

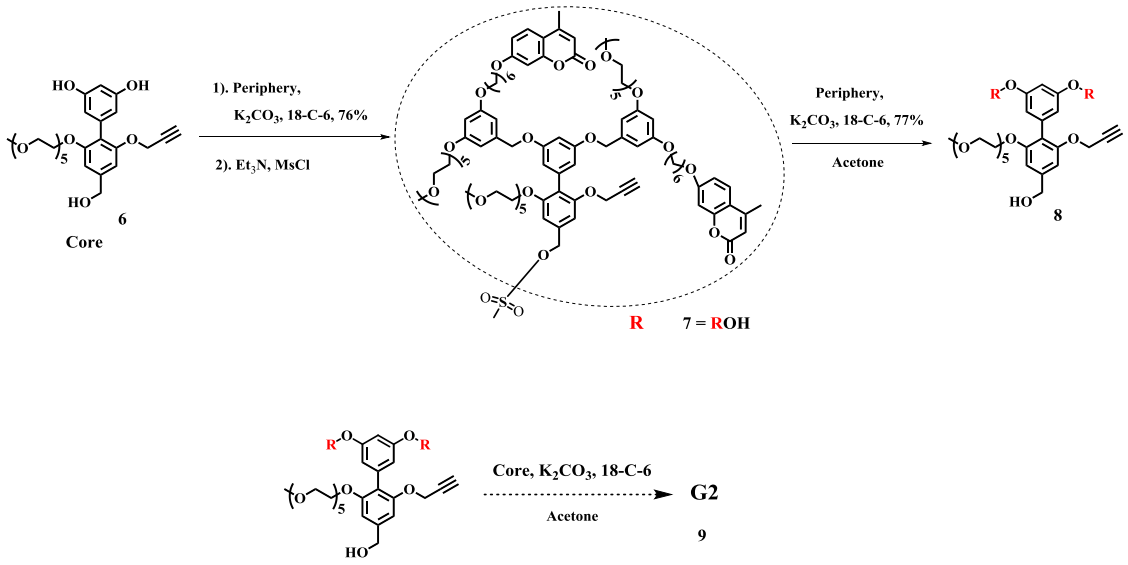

Scheme 5.3. Synthesis of G2 using periphery (**5**), core (**6**), and enzyme substrate (**1**).

achieve this, dendron **9** is designed such that its lipophilic units comprise of 57 % crosslinkable coumarin units and 43 % non crosslinkable enzyme sensitive reporting units. This design allows 43 % of enzyme sensitive units to be in equilibrium through *pathway b* even when all the coumarin units are crosslinked. It should be noted that a G2 dendron is chosen instead of a G1 dendron, because the G2 dendron will provide more flexibility for functional group modifications with 7 modifiable units as opposed to 3 units offered by the G1 dendron. The proposed G2

dendrimer **9** is synthesized by a modular approach (Scheme 5.2 and 5.3). The core, **6**, and the periphery, **5** were reacted under potassium carbonate conditions to achieve the G1 molecule **7**, which was then mesylated at the benzylic position and then reacted with molecule **6** to achieve a G2 precursor with propargyl units on core and two intermediate layers (Scheme 5.3). This molecule when reacted with molecule **1** under click chemistry conditions should result in dendrimer **9**. However click chemistry with copper sulfate and sodium ascorbate conditions in several solvents (THF/H_2O, DCM, DMSO) were unsuccessful, and further optimization of click reaction is necessary for achieving molecule **9**.

The enzyme responsive nature of the dendron will be tested by treating the dendron solution with PLE and monitoring the increase in nitrophenol absorbance at 400 nm. Please note that the enzymatic response is studied only through the release of covalently tethered nitrophenol, as monitoring the guest molecule release will not yield any additional information about the equilibrium. As demonstrated in Chapter 2, extensive photocrosslinking of aggregates will eliminate the possibility of dendron existing in unimeric form. However with current molecular design 43 % of the lipophilic units are non-crosslinkable enzyme cleavable functionalities, which are expected to be in equilibrium with the bulk aqueous solution through *pathway b* even after crosslinking of coumarin units. Therefore by exclusively studying the release characteristics of the crosslinked and un-crosslinked aggregates, we would be able to test if there is indeed any such equilibrium existing as *pathway b*. *Experimental design:* Dendrimer solution with concentration above CAC will be prepared in HEPES buffer at pH 7.4. This solution will be divided into half and one of

them crosslinked under UV at 365 nm wavelength. The crosslinked (*case a*) and uncrosslinked (*case b*) solutions will be treated with equal amounts of the enzyme porcine liver esterase and the absorbance of nitrophenol at 400 nm will be monitored with time. It is expected that *case b* shows more release than *case a*. This difference will give us a qualitative estimate of the contributions from *pathway a*, and accordingly *pathway b.*

Finally, if we are indeed able to qualitatively differentiate each of the pathways, we propose to study the kinetics of enzymatic reaction in each of these pathways using stopped-flow technique. This will be done by determining the rate of product (nitrophenol) formation in the crosslinked (*pathway b*) and non-crosslinked systems (*pathway a & b*). This project when accomplished will give us a fundamental understanding of the micelle equilibrium, which will provide insights into the rational molecular design of sensors and delivery vehicles based on micelles.

5.2.2 Photo-responsive Amphiphilic Assemblies; Role of Amphiphile Composition on Guest Release Kinetics

Photo responsive systems are a promising class of stimuli responsive systems where an external stimulus (light source) is used to trigger a molecular release at the targeted site. This method has several advantages in the context of targeted drug delivery such as i) non-invasive stimulus, ii) remote and accurate control of stimulus (light)directed to a specific target site with good resolution, ii) control of the dosage as a function of light exposure, etc. The design of these systems

largely constitute of two methods i) encapsulation of photo responsive moiety in the amphiphile assembly,[12,13] and ii) Incorporation of photo responsive moiety as a hydrophilic or hydrophobic functionality of the amphiphile.[14,15] Herein we use the later method and incorporated a light responsive functionality as the hydrophobic moiety of the amphiphile. This group undergoes irreversible transformation upon light exposure and therefore should result in a significant change in HLB prompting the release of encapsulated guest molecules.

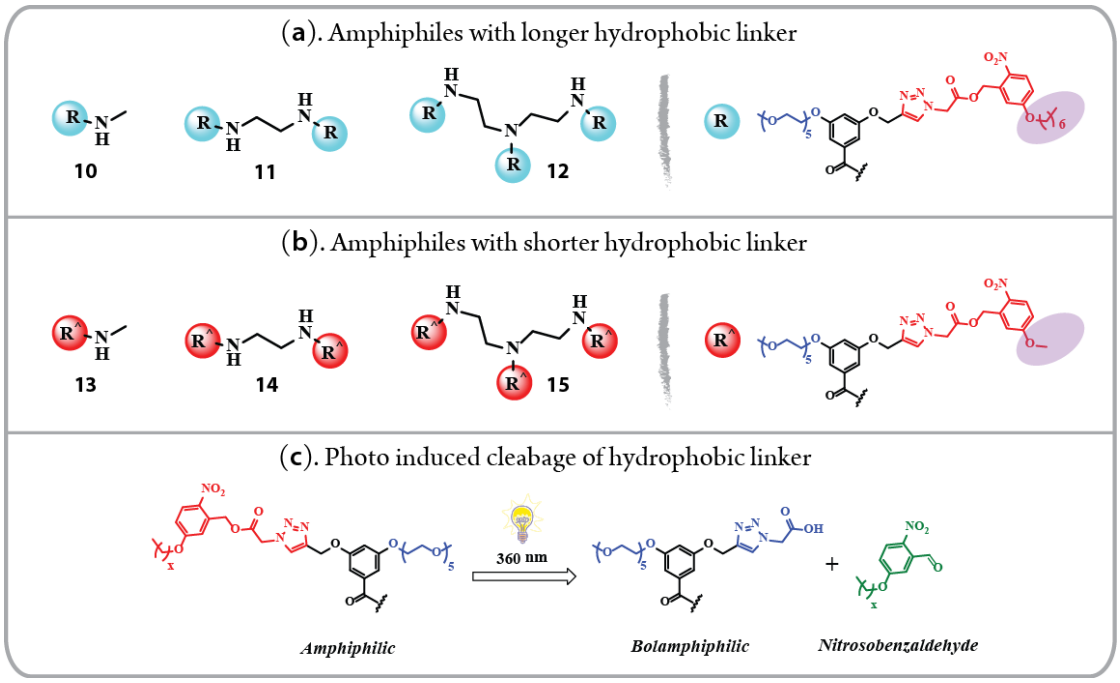

Scheme 5.4 Schematic of oligomers with variations in the oligomer length (a & b) and hydrophobic chain length (a *vs* b). Light induced cleavage of hydrophobic unit of amphiphile (c).

Though several studies have demonstrated the light induced release of guest molecules in small molecules as well as polymeric amphiphile systems, there has been very limited focus on understanding the kinetics of molecular release as

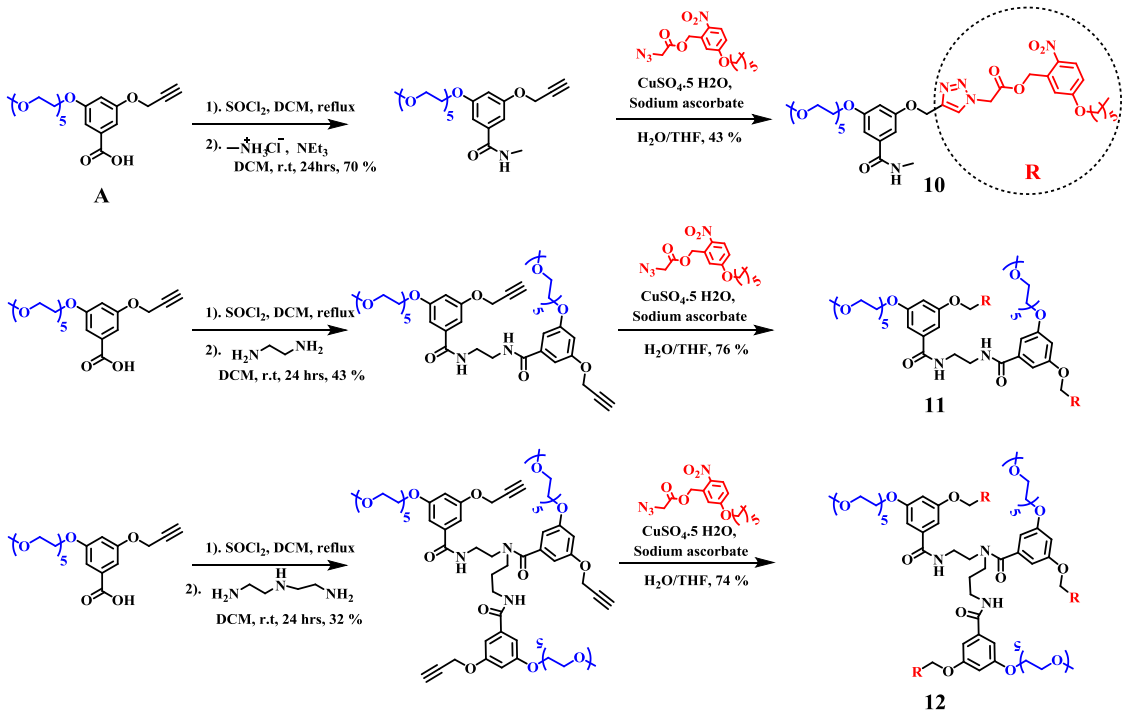

Scheme 5.5. Synthesis of light responsive oligomers with a longer hydrophobic linker.

function of amphiphile design. In this project we propose to study this aspect by investigating a series of photo responsive oligomers with rational molecular designs. Our objective is to essentially decipher both i) the role of amphiphile length (molecular weight) as well as the ii) effect of hydrophilic to hydrophobic group ratio within each amphiphile. The molecular design of corresponding amphiphiles is shown in Scheme 5.4. The amphiphiles are designed such that upon exposure to light (360 nm) the photo-responsive nitro benzyl ester cleaves to release nitrosobenzaldehyde and also generate a carboxylic group on the hydrophobic arm of the oligomer (Figure 5.4c). This should result in an oligomer which is hydrophilic on both ends, and therefore significantly altering its assembly properties. In addition to this, the generation of nitrosobenzaldehyde can also be monitored by a

characteristic peak at ~360 nm using UV-Vis spectroscopy; which is a direct response to light induced cleavage.

The synthesis of the oligomers is achieved by converting the acid precursor **A** to an acid chloride followed by an amide coupling with a corresponding amine. The oligomeric precursors thus obtained are then reacted with the nitrobenzyl ester subtrates under click chemistry conditions to obtain a series of light responsive oligomers (Sheme 5.5 and 5.6). All the oligomers were synthesized and characterized, except the molecule **14**. Exceptionally none of the oligomers in scheme 5.4 were soluble in soluble in water in any proportion, except molecule **13** which had partial solubility. The solubility of these oligomers was indeed very surprising as a dendron (reported earlier by our group) with three same amphiphilic units but a different backbone was soluble in water and formed micelle type aggregates.[9] Though we do not have comprehensive evidence at this point, we believe that this insoluble nature of the oligomers might be due to the presence of H-bonding amide backbone. The reason for this assertion is from the fact that methylated oligomers in Section 4 had significantly better solubility than the non-methylated counterparts.

It should be noted that the decrease in the length of hydrophobic component (Scheme 5.4b) in amphiphiles did not have a noticeable increase in solubility compared to the oligomers with longer hydrophobic units (Figure 5.4a). Based on our observations in section 4 we hypothesized that the methylation of secondary amides might increase the solubility. To test this hypothesis we synthesized

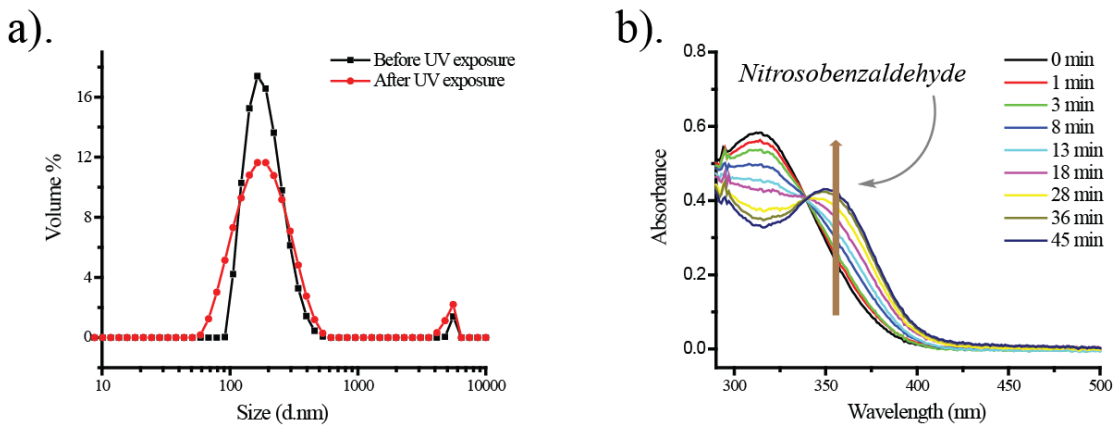

Figure 5.2 Characterization of molecule 16 assembly. Size analysis using DLS (a), and photo-induced nitrosobenzaldehyde release using UV-Vis spectroscopy

molecule **16** (Scheme 5.6) where the tertiary amide backbone does not hydrogen bond extensively; this simple transformation has resulted in a significant increase in solubility. The resultant molecule **16** also formed micelles in aqueous solution and also exhibited photo-responsive properties in the presence of light (Figure 5.2). Since the modification of amide backbone (13 to 16) has increased the water solubility of the amphiphile, we propose to synthesize all the other oligomers with exclusively tertiary amide backbone. Incase this modification does not improve the water solubility of all the oligomers we propose to increase the length of hydrophilic PEG component. Finally, photo-induced guest release studies as a function of oligomer length and amphiphile composition is expected to provide fundamental insights into the design of photo-responsive systems.

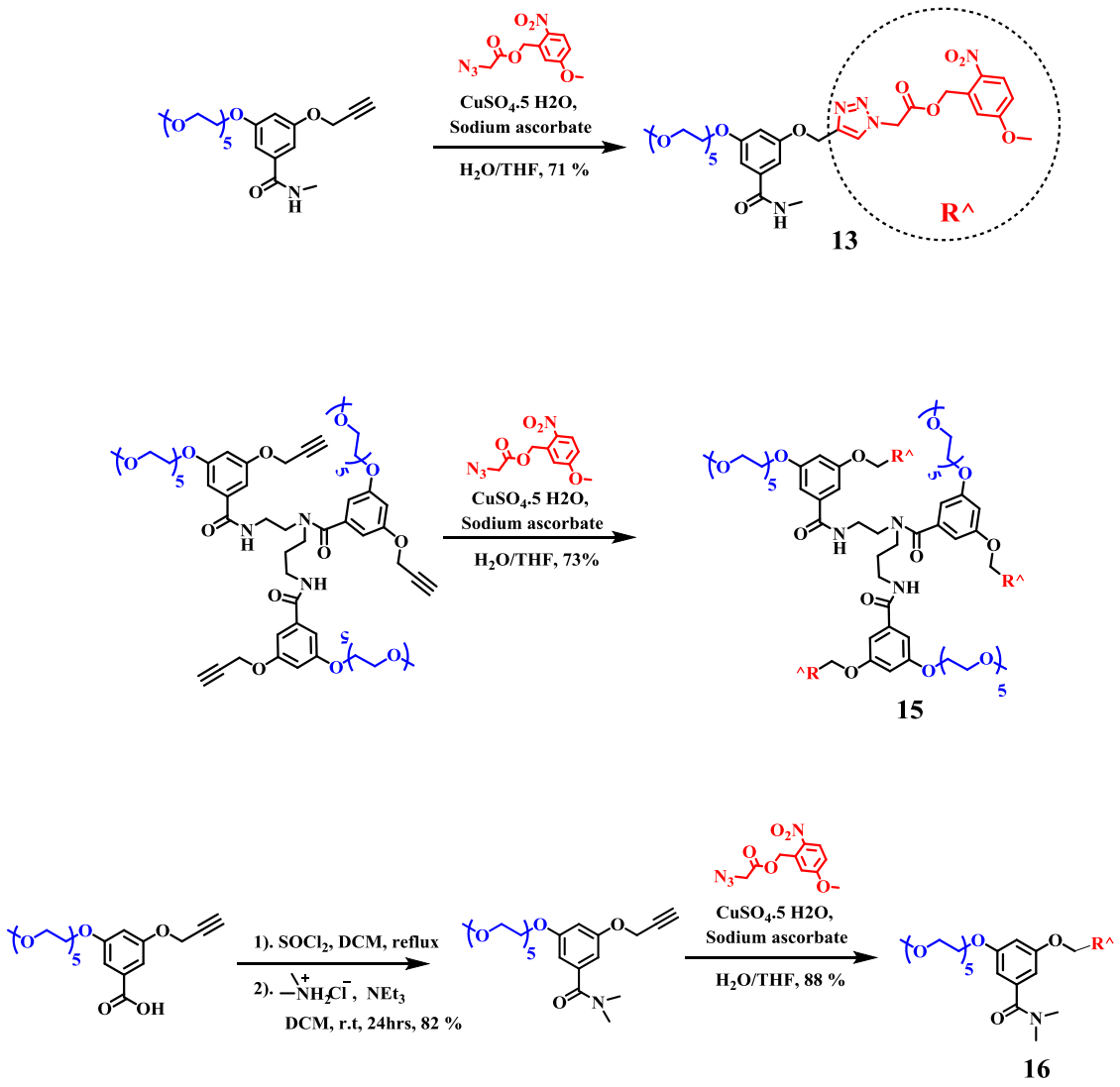

Scheme 5.6. Synthesis of light responsive oligomers with a shorter hydrophobic linker, and molecule **16** with tertiary amide backbone.

5.3 Experimental Methods

5.3.1 Synthesis and Characterization

All chemicals and reagents were purchased from commercial sources and were used as received, unless otherwise mentioned. Compounds **6**[16] and **A**[9] were synthesized following previously reported procedures. H-NMR spectra were

recorded on 400 MHz Bruker NMR spectrometer using the residual proton resonance of the solvent as the internal standard. Chemical shifts are reported in parts per million (ppm). When peak multiplicities are given the following abbreviations are used: s, singlet; d, doublet; t, triplet; m, multiplet. ^{13}C-NMR spectra were proton decoupled and measured on a 500 MHz Bruker spectrometer with 125 MHz frequency by using carbon signal of the deuterated solvent as the internal standard.

5.3.1.1 Molecule 1

^{1}H-NMR (400 MHz; Acetone-d_6): δ 7.63 (d, *J* = 8.8 Hz, 4H), 7.01-6.84 (m, 15H), 6.69-6.60 (m, 16H), 6.45 (s, 4H), 6.09 (d, *J* = 0.8 Hz, 4H), 5.08 (d, *J* = 41.6 Hz, 12H), 4.70-4.66 (m, 7H), 4.14-4.00 (m, 33H), 3.81-3.42 (m, 131H), 3.25 (s, 20H), 3.03 (t, *J* = 2.3 Hz, 1H), 2.97 (t, *J* = 2.2 Hz, 1H), 2.40 (s, 12H), 1.89-1.79 (m, 18H), 1.65-1.49 (m, 20H), 0.88 (t, *J* = 5.1 Hz, 6H).

5.3.1.2 Molecule 2

^{1}H-NMR (400 MHz; $CDCl_3$): δ 7.49 (d, *J* = 8.8 Hz, 1H), 6.85 (dd, *J* = 8.8, 2.5 Hz, 1H), 6.80 (d, *J* = 2.4 Hz, 1H), 6.13 (d, *J* = 1.0 Hz, 1H), 4.02 (t, *J* = 6.4 Hz, 2H), 3.43 (t, *J* = 6.7 Hz, 2H), 1.92-1.82 (m, 4H), 1.52 (t, *J* = 3.7 Hz, 4H).

5.3.1.3 Molecule 3

^{1}H-NMR (400 MHz; DMSO-d_6): δ 9.23 (s, 1H), 7.61 (d, *J* = 8.9 Hz, 1H), 6.91-6.88 (m, 2H), 6.25 (d, *J* = 2.5 Hz, 2H), 6.14-6.09 (m, 2H), 5.02 (t, *J* = 5.9 Hz, 1H), 4.29 (d, *J* = 5.8 Hz, 2H), 4.03 (t, *J* = 6.5 Hz, 2H), 3.82 (t, *J* = 6.4 Hz, 2H), 2.33 (d, *J* = 1.0 Hz, 3H), 1.78-1.69 (m, 4H), 1.41 (t, *J* = 3.4 Hz, 4H).

5.3.1.4 Molecule 4

^{1}H-NMR (400 MHz; Acetone-d_6): δ 7.67 (d, *J* = 8.8 Hz, 1H), 6.94 (dd, *J* = 8.8, 2.5 Hz, 1H), 6.87 (d, *J* = 2.5 Hz, 1H), 6.54 (d, *J* = 2.3 Hz, 2H), 6.37 (t, *J* = 2.2 Hz, 1H), 6.12 (d, *J* = 1.1 Hz, 1H), 4.55 (d, *J* = 5.8 Hz, 2H), 4.17-4.09 (m, 4H), 3.99 (d, *J* = 6.4 Hz, 2H), 3.80 (t, *J* = 4.8 Hz, 2H), 3.66-3.54 (m, 14H), 3.45 (t, *J* = 4.8 Hz, 2H), 3.28 (s, 3H), 2.44 (d, *J* = 1.2 Hz, 3H), 1.89-1.79 (m, 4H), 1.58 (t, *J* = 3.7 Hz, 4H).

5.3.1.5 Molecule 5

^{1}H-NMR (400 MHz; Acetone-d_6): δ 7.67 (d, *J* = 8.8 Hz, 1H), 6.94 (dd, *J* = 8.8, 2.5 Hz, 1H), 6.87 (d, *J* = 2.5 Hz, 1H), 6.63 (t, *J* = 1.8 Hz, 2H), 6.46 (t, *J* = 2.2 Hz, 1H), 6.12 (d, *J* = 1.2 Hz, 1H), 4.55 (s, 2H), 4.17-4.11 (m, 4H), 4.02 (t, *J* = 6.4 Hz, 2H), 3.81 (t, *J* = 4.8 Hz, 2H), 3.66-3.53 (m, 14H), 3.47-3.44 (m, 2H), 3.28 (s, 3H), 2.44 (d, *J* = 1.2 Hz, 3H), 1.89-1.80 (m, 4H), 1.59 (t, *J* = 3.7 Hz, 4H).

5.3.1.6 Molecule 7

^{1}H-NMR (400 MHz; Acetone-d_6): δ 7.64 (d, *J* = 8.8 Hz, 2H), 6.94-6.59 (m, 13H), 6.45 (s, 2H), 6.11 (s, 2H), 5.05 (s, 4H), 4.67-4.64 (m, 4H), 4.15-4.00 (m, 14H), 3.80 (t, *J* = 4.6 Hz, 4H), 3.64-3.44 (m, 52H), 3.26 (d, *J* = 4.3 Hz, 9H), 3.01 (s, 1H), 2.42 (s, 6H), 1.87-1.80 (m, 8H), 1.58 (s, 8H).

5.3.1.7 Molecule 8

^{1}H-NMR (400 MHz; Acetone-d_6): δ 7.63 (d, *J* = 8.8 Hz, 4H), 7.01-6.84 (m, 15H), 6.69-6.60 (m, 16H), 6.45 (s, 4H), 6.09 (d, *J* = 0.8 Hz, 4H), 5.08 (d, *J* = 41.6 Hz, 12H), 4.70-4.66 (m, 7H), 4.14-4.00 (m, 33H), 3.81-3.42 (m, 131H), 3.25 (s, 20H), 3.03

(t, *J* = 2.3 Hz, 1H), 2.97 (t, *J* = 2.2 Hz, 1H), 2.40 (s, 12H), 1.89-1.79 (m, 18H), 1.65-1.49 (m, 20H), 0.88 (t, *J* = 5.1 Hz, 6H). MALDI-ToF m/z 4011.813 ($C_{217}H_{288}N3O_{68}$+Na^+ requires 4007.609).

5.3.1.8 Molecule 10

^{1}H-NMR (400 MHz; Acetone-d_6): δ 8.22-8.20 (m, 2H), 7.63 (bs, 1H), 7.13-7.05 (m, 4H), 6.76 (s, 1H), 5.62 (d, *J* = 21.7 Hz, 4H), 5.26 (s, 2H), 4.17 (t, *J* = 6.5 Hz, 4H), 3.82 (s, 2H), 3.65-3.55 (m, 14H), 3.46 (d, *J* = 5.0 Hz, 2H), 3.27 (s, 3H), 2.87 (d, *J* = 4.5 Hz, 3H), 1.83 (quintet, *J* = 7.1 Hz, 2H), 1.52-1.29 (m, 8H), 0.90 (t, *J* = 6.2 Hz, 3H).

5.3.1.9 Molecule 11

^{1}H-NMR (400 MHz; Acetone-d_6): δ 8.22-8.06 (m, 5H), 7.16-7.07 (m, 8H), 6.75 (s, 2H), 5.61 (d, *J* = 21.0 Hz, 8H), 5.25 (s, 3H), 4.18-4.13 (m, 8H), 3.80 (t, *J* = 4.6 Hz, 4H), 3.64-3.54 (m, 32H), 3.45-3.43 (m, 4H), 3.26 (s, 6H), 1.84-1.78 (m, 4H), 1.50-1.48 (m, 4H), 1.37-1.29 (m, 12H), 0.89 (t, *J* = 6.6 Hz, 6H).

5.3.1.10 Molecule 12

^{1}H-NMR (400 MHz; Acetone-d_6): δ 8.21-7.97 (m, 8H), 7.16-7.04 (m, 10H), 6.72 (d, *J* = 1.9 Hz, 2H), 6.49 (d, *J* = 2.5 Hz, 2H), 6.37 (s, 1H), 5.63-5.54 (m, 12H), 5.22 (s, 4H), 4.95 (s, 2H), 4.18-4.09 (m, 12H), 3.85-3.54 (m, 60H), 3.45-3.43 (m, 6H), 3.26-3.25 (m, 9H), 1.86-1.78 (m, 8H), 1.49 (t, *J* = 3.8 Hz, 6H), 1.37-1.29 (m, 16H), 0.89 (t, *J* = 6.8 Hz, 9H).

5.3.1.11 Molecule 13

^{1}H-NMR (400 MHz; Acetone-d_6): δ 8.24-8.21 (m, 2H), 7.64 (bs, 1H), 7.13-7.05 (m, 4H), 6.77 (s, 1H), 5.65 (s, 2H), 5.60 (s, 2H), 5.26 (s, 2H), 4.16 (t, *J* = 4.6 Hz, 2H), 3.97 (s, 3H), 3.82 (t, *J* = 4.6 Hz, 2H), 3.66-3.54 (m, 14H), 3.45 (t, *J* = 4.7 Hz, 2H), 3.27 (s, 3H), 2.87 (d, *J* = 4.5 Hz, 3H).

5.3.1.12 Molecule 15

^{1}H-NMR (400 MHz; Acetone-d_6): δ 8.21-7.97 (m, 8H), 7.16-7.04 (m, 10H), 6.72 (d, *J* = 1.9 Hz, 2H), 6.49 (d, *J* = 2.5 Hz, 2H), 6.37 (s, 1H), 5.63-5.54 (m, 12H), 5.22 (s, 4H), 4.95 (s, 2H), 4.18-4.09 (m, 12H), 3.85-3.54 (m, 60H), 3.45-3.43 (m, 6H), 3.26-3.25 (m, 9H), 1.86-1.78 (m, 8H), 1.49 (t, *J* = 3.8 Hz, 6H), 1.37-1.29 (m, 16H), 0.89 (t, *J* = 6.8 Hz, 9H).

5.3.1.13 Molecule 16

^{1}H-NMR (400 MHz; $CDCl_3$): δ 8.24 (d, *J* = 9.0 Hz, 1H), 7.82 (s, 1H), 6.97-6.92 (m, 2H), 6.62-6.58 (m, 3H), 5.68 (s, 2H), 5.33 (s, 2H), 5.24 (s, 2H), 4.11 (t, *J* = 4.7 Hz, 2H), 3.85 (t, *J* = 4.7 Hz, 2H), 3.74-3.64 (m, 16H), 3.56 (dd, *J* = 5.7, 3.5 Hz, 2H), 3.39 (s, 3H), 3.11 (s, 3H), 2.97 (s, 3H).

5.4 NMR Spectra

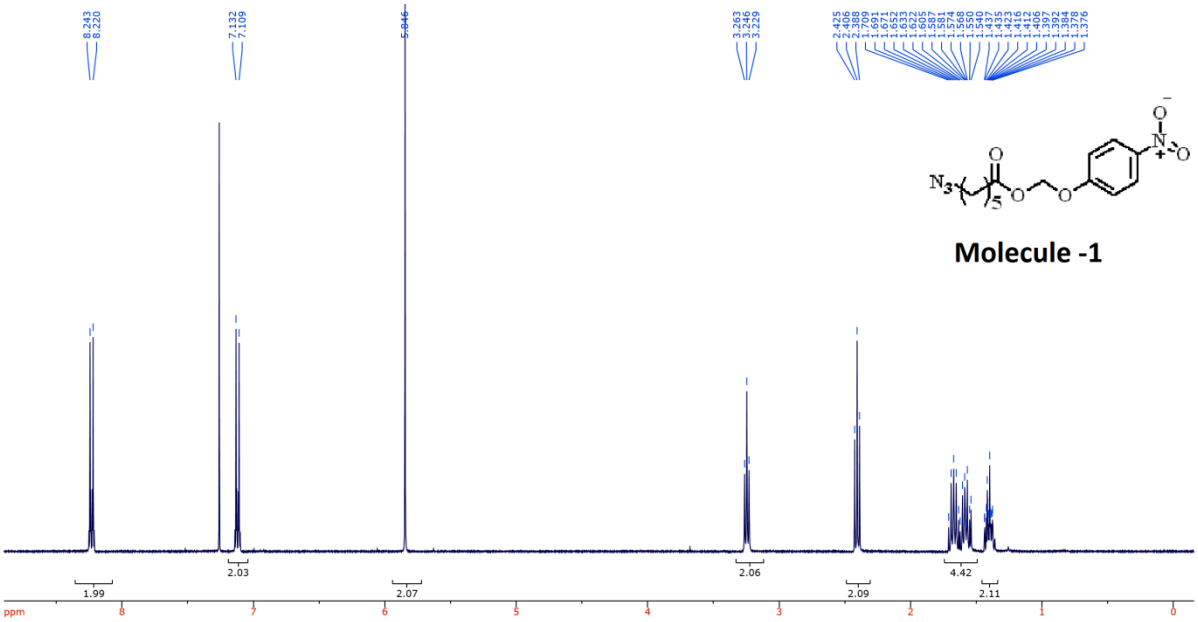

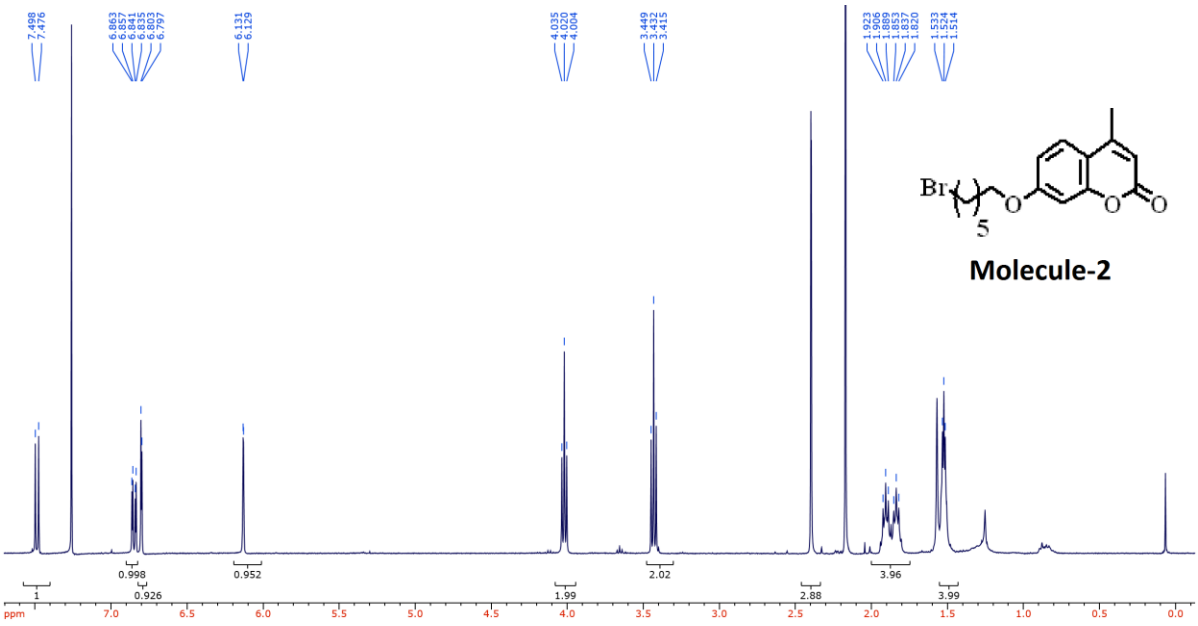

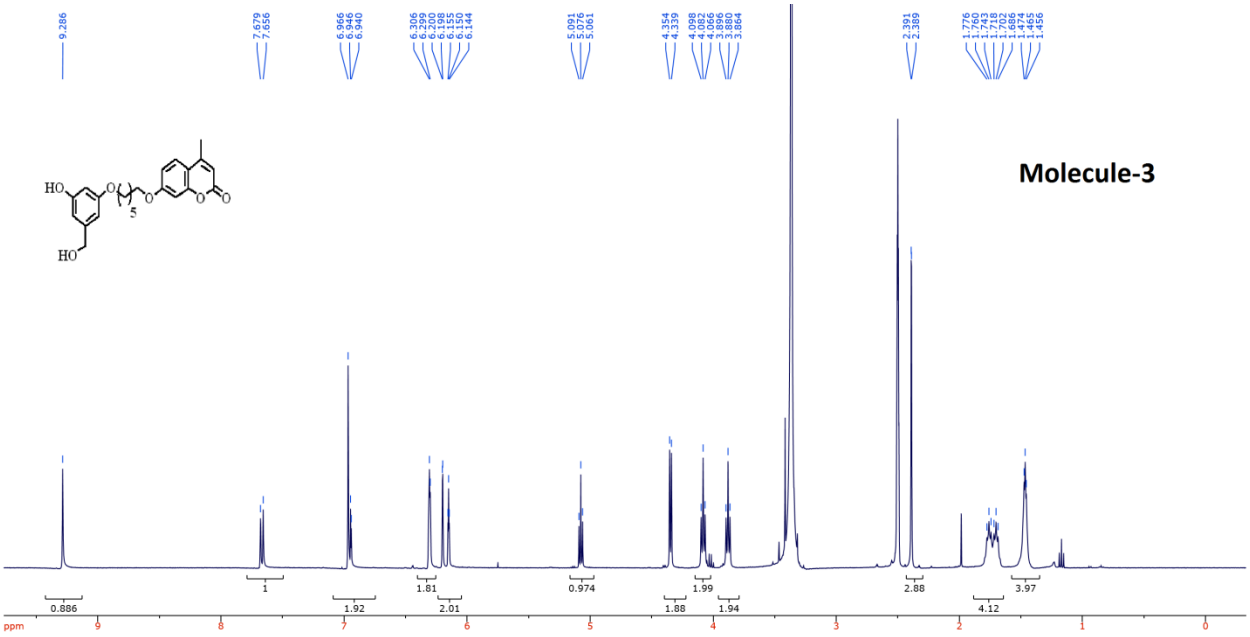
Molecule-3

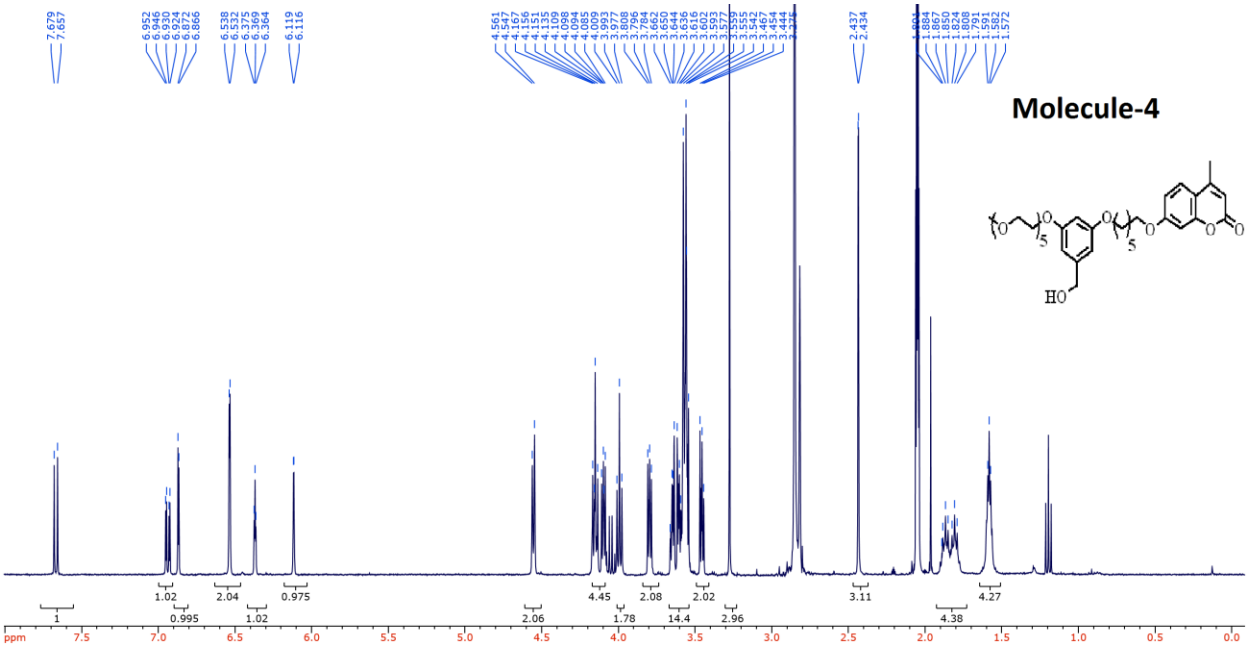
Molecule-4

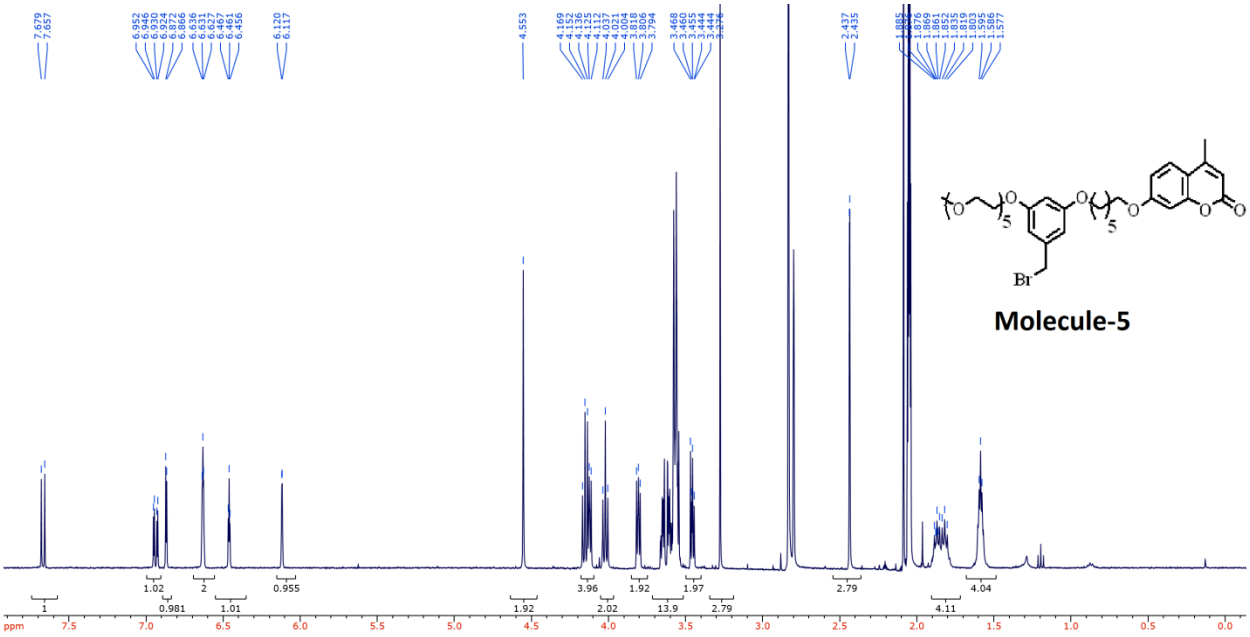
Molecule-5

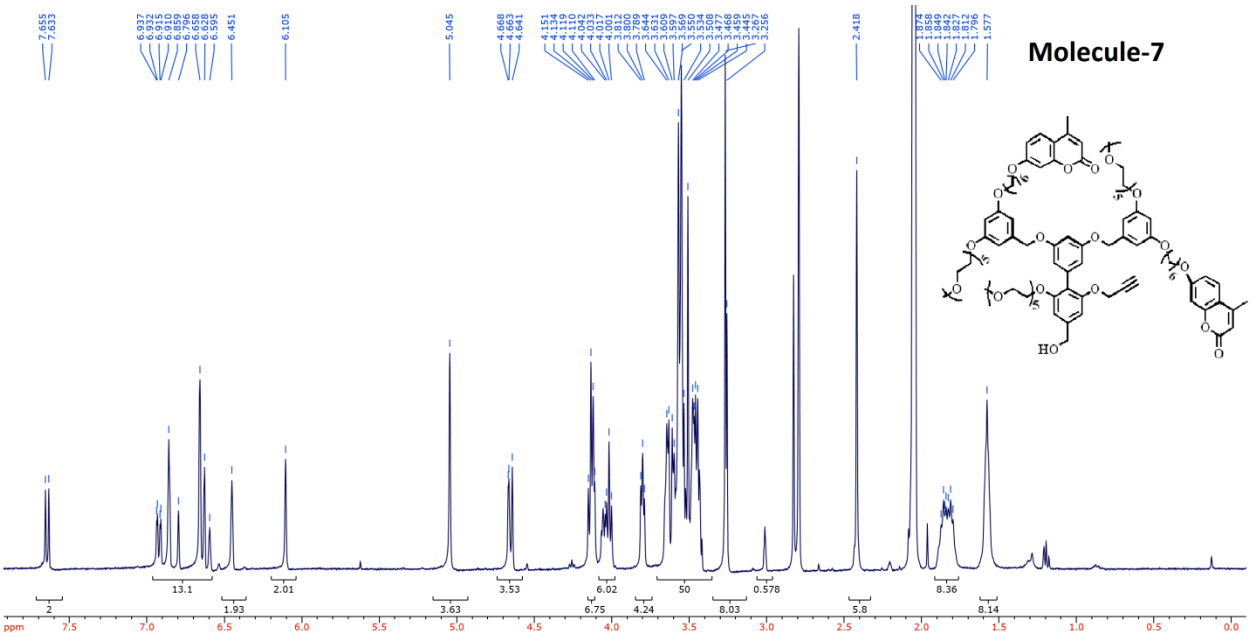
Molecule-7

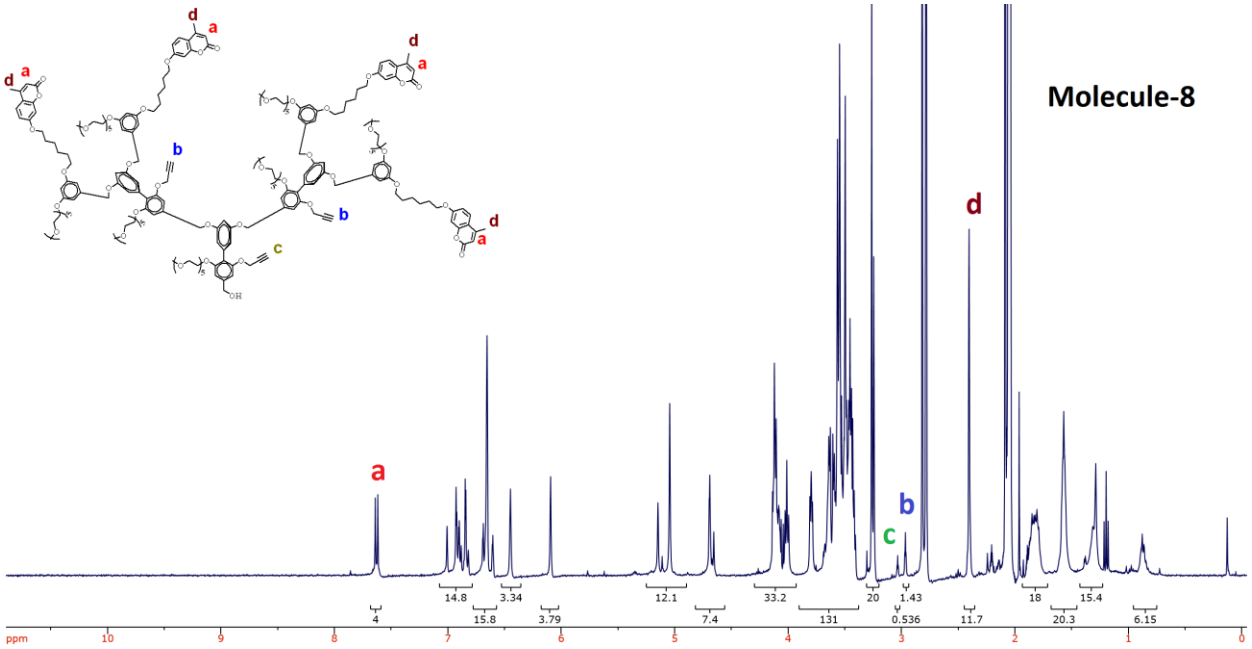
Molecule-8
a
b
c
d
14.8
3.34
15.8
3.79
12.1
7.4
33.2
131
20
1.43
0.536
11.7
18
15.4
20.3
6.15
4
ppm

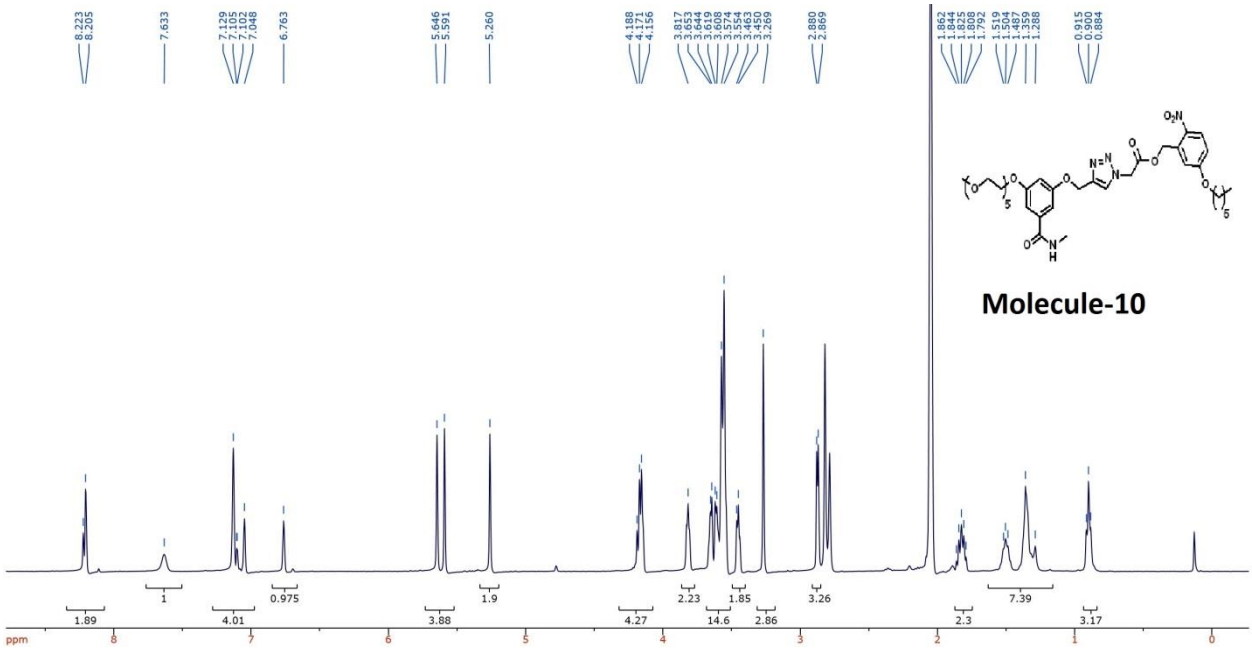
Molecule-10
1.89
1
4.01
0.975
3.88
1.9
4.27
2.23
14.6
1.85
2.86
3.26
2.3
7.39
3.17
ppm

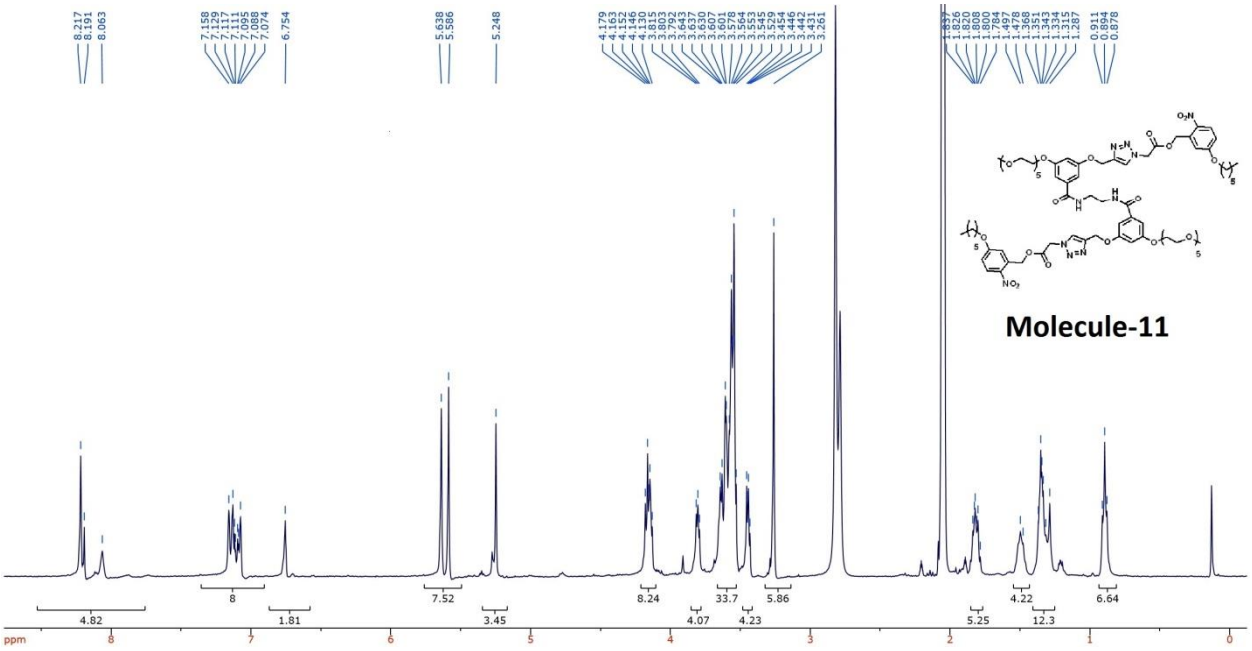
Molecule-11

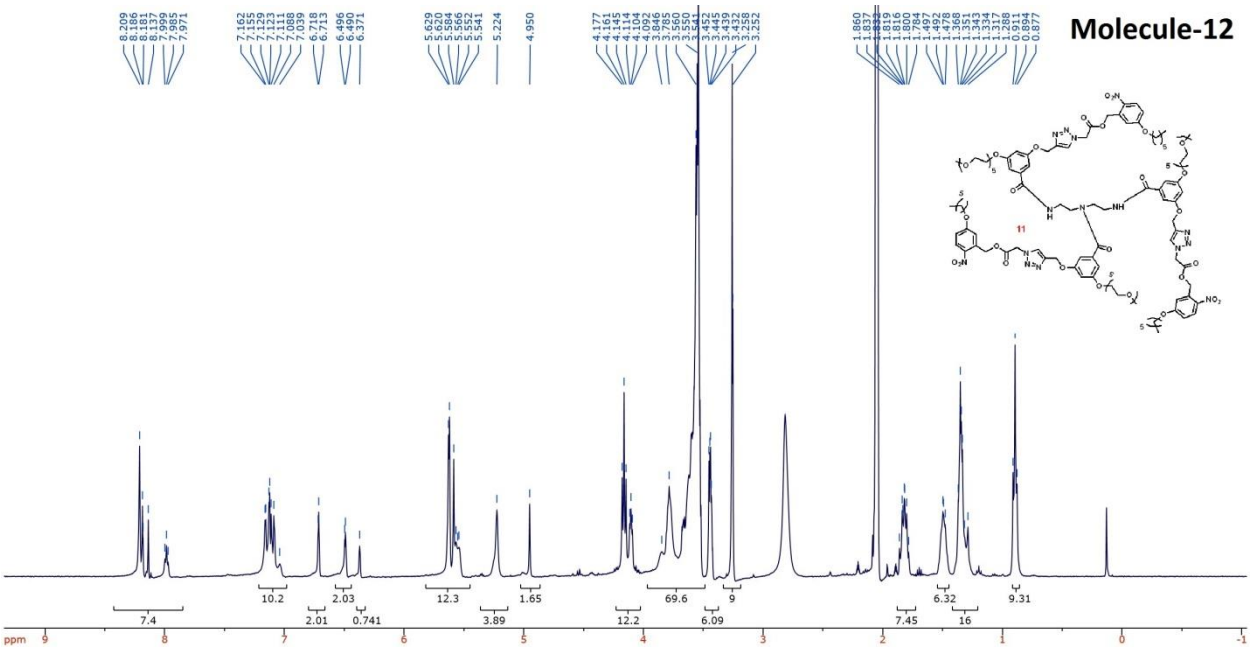
Molecule-12

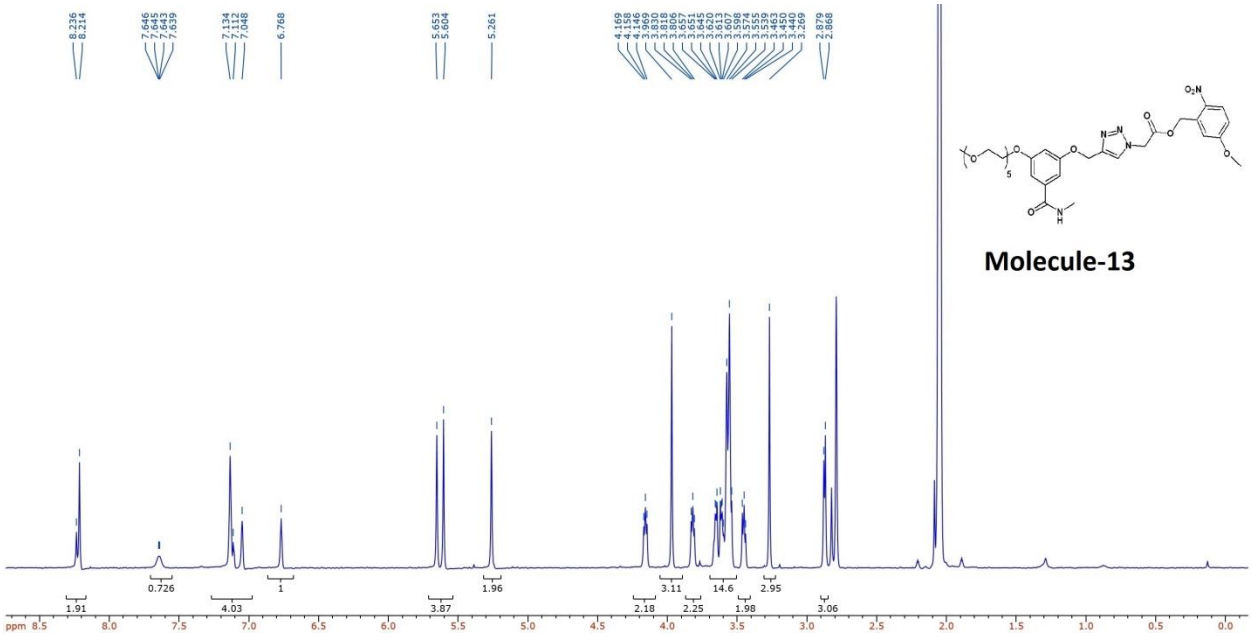

Molecule-13

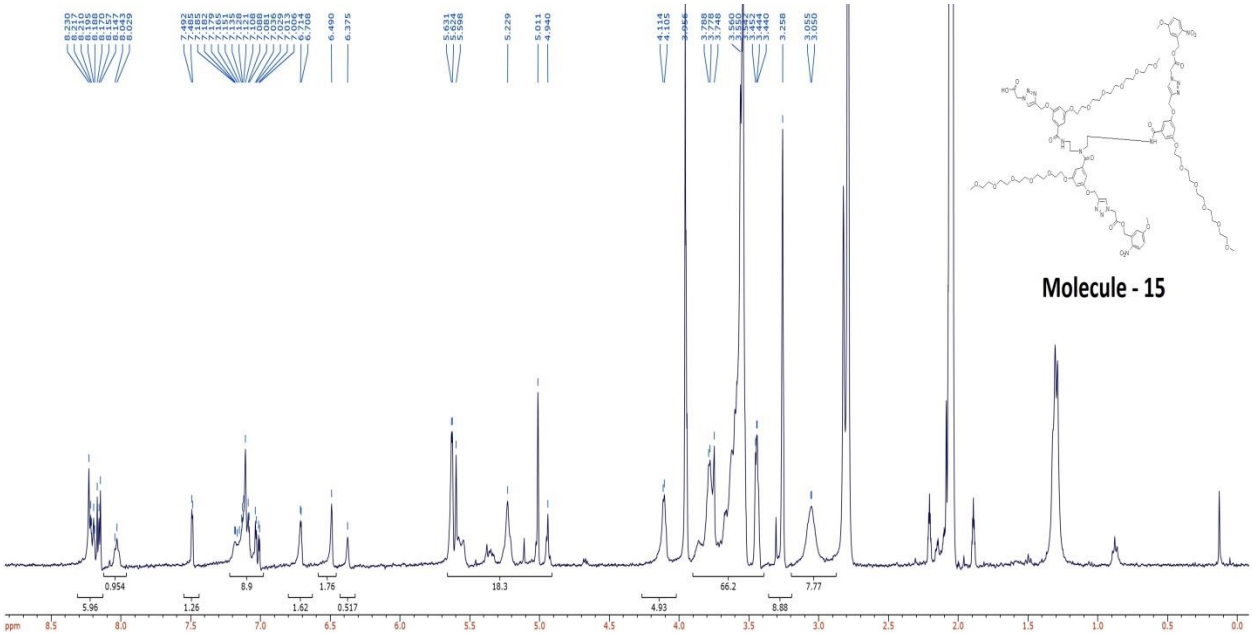

Molecule - 15

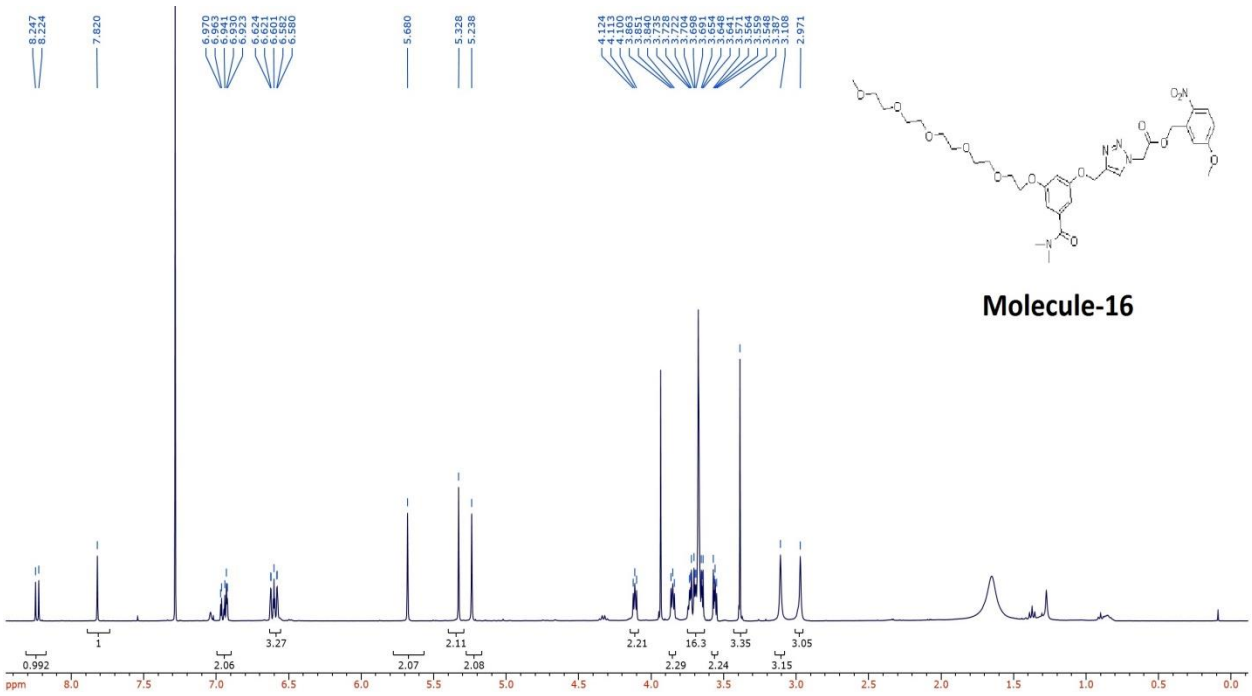

5.5 References

1. Song, J.; Cheng, Q.; Zhu, S. M.; Stevens, R. C., "Smart" materials for biosensing devices: Cell-mimicking supramolecular assemblies and colorimetric detection of pathogenic agents. *Biomed. Microdevices* **2002,** *4* (3), 213-221.

2. Nystrom, A. M.; Wooley, K. L., The importance of Chemistry in Creating Well-Defined Nanoscopic Embedded Therapeutics: Devices Capable of the Dual Functions of Imaging and Therapy. *Accounts Chem. Res.* **2011,** *44* (10), 969-978.

3. Jeong, B.; Bae, Y. H.; Lee, D. S.; Kim, S. W., Biodegradable block copolymers as injectable drug-delivery systems. *Nature* **1997,** *388* (6645), 860-862.

4. Israelachvili, J. N.; Mitchell, D. J.; Ninham, B. W., Theory of self-assembly of hydrocarbon amphiphiles into micelles and bilayers. *J. Chem. Soc. Faraday Trans II.* **1976,** *72*, 1525-1568.

5. Evans, D. F.; Ninham, B. W., Molecular forces in the self-organization of amphiphiles. *J. Phys. Chem.* **1986,** *90* (2), 226-234.

6. Fleischer, G., Micellization in Aqueous-Solution of a Poly(Ethylene Oxide) Poly(Propylene Oxide) Poly(Ethylene Oxide) Triblock Copolymer

Investigated with Pulsed Field Gradient Nmr. *J. Phys. Chem.* **1993,** *97* (2), 517-521.

7. Raghupathi, K. R.; Azagarsamy, M. A.; Thayumanavan, S., Guest release control in enzyme-sensitive amphiphilic dendrimer-based nanoparticles through photochemical crosslinking. *Chem. Eur. J.* **2011,** *17* (42), 11752-11760.

8. Fuller, J. M.; Raghupathi, K. R.; Ramireddy, R. R.; Subrahmanyam, A. V.; Yesilyurt, V.; Thayumanavan, S., Temperature-sensitive transitions below LCST in amphiphilic dendritic assemblies: Host–guest implications. *J. Am. Chem. Soc.* **2013,** *135* (24), 8947-8954

9. Raghupathi, K. R.; Sridhar, U.; Byrne, K.; Raghupathi, K.; Thayumanavan, S., Influence of backbone conformational rigidity in temperature-sensitive amphiphilic supramolecular assemblies. *J. Am. Chem. Soc.* **2015,** *137* (16), 5308-5311.

10. Hvidt, S.; Joergensen, E. B.; Brown, W.; Schillen, K., Micellization and Gelation of Aqueous Solutions of a Triblock Copolymer Studied by Rheological Techniques and Scanning Calorimetry. *J. Phys. Chem.* **1994,** *98* (47), 12320-12328.

11. Tanford, C., Theory of micelle formation in aqueous solutions. *J. Phys. Chem.* **1974,** *78* (24), 2469-2479.

12. Nishiyama, N.; Morimoto, Y.; Jang, W.-D.; Kataoka, K., Design and development of dendrimer photosensitizer-incorporated polymeric micelles for enhanced photodynamic therapy. *Adv. Drug Delivery Rev.* **2009,** *61* (4), 327-338.

13. Battah, S. H.; Chee, C.-E.; Nakanishi, H.; Gerscher, S.; MacRobert, A. J.; Edwards, C., Synthesis and Biological Studies of 5-Aminolevulinic Acid-Containing Dendrimers for Photodynamic Therapy. *Bioconjugate Chem.* **2001,** *12* (6), 980-988.

14. Park, C.; Lim, J.; Yun, M.; Kim, C., Photoinduced Release of Guest Molecules by Supramolecular Transformation of Self-Assembled Aggregates Derived from Dendrons. *Angew. Chem. Int. Ed.* **2008,** *47* (16), 2959-2963.

15. Yesilyurt, V.; Ramireddy, R.; Thayumanavan, S., Photoregulated release of noncovalent guests from dendritic amphiphilic nanocontainers. *Angew. Chem. Int. Ed.* **2011,** *50* (13), 3038-3042.

16. Azagarsamy, M. A.; Sokkalingam, P.; Thayumanavan, S., Enzyme-triggered disassembly of dendrimer-based amphiphilic nanocontainers. *J. Am. Chem. Soc.* **2009,** *131* (40), 14184-14185.

BIBLIOGRAPHY

Aathimanikandan, S. V.; Savariar, E. N.; Thayumanavan, S., Temperature-sensitive dendritic micelles. *J. Am. Chem. Soc.* **2005,** *127* (42), 14922-14929.

Alexis, F.; Pridgen, E.; Molnar, L. K.; Farokhzad, O. C., Factors affecting the clearance and biodistribution of polymeric nanoparticles. *Mol. Pharmaceutics* **2008,** *5* (4), 505-515.

Allen, T. M.; Cullis, P. R., Drug delivery systems: Entering the mainstream. *Science* **2004,** *303* (5665), 1818-1822.

Alvarez-Lorenzo, C.; Bromberg, L.; Concheiro, A., Light-sensitive Intelligent Drug Delivery Systems. *Photochem. Photobiol.* **2009,** *85* (4), 848-860.

Ambade, A. V.; Aathimanikandan, S. V.; Van der Poll, D.; Thayumanavan, S., Smaller building blocks form larger assemblies: Aggregation behavior of biaryl-based dendritic facial amphiphiles. *J. Org. Chem.* **2007,** *72* (22), 8167-8174.

Ambade, A. V.; Savariar, E. N.; Thayumanavan, S., Dendrimeric micelles for controlled drug release and targeted delivery. *Mol. Pharmaceutics.* **2005,** *2* (4), 264-272.

Amir, R. J.; Shabat, D., Domino dendrimers. In *Polymer Therapeutics I: Polymers as Drugs, Conjugates and Gene Delivery Systems*, **2006**; Vol. 192, pp 59-94.

Amir, R. J.; Shabat, D., Self-immolative dendrimer biodegradability by multi-enzymatic triggering. *Chem. Commun.* **2004,** (14), 1614-1615.

Amir, R. J.; Zhong, S.; Pochan, D. J.; Hawker, C. J., Enzymatically Triggered Self-Assembly of Block Copolymers. *J. Am. Chem. Soc.* **2009,** *131* (39), 13949-13951.

Astruc, D.; Boisselier, E.; Ornelas, C., Dendrimers designed for functions: From physical, photophysical, and supramolecular properties to applications in sensing, catalysis, molecular electronics, photonics, and nanomedicine. *Chem. Rev.* **2010,** *110* (4), 1857-1959.

Avital-Shmilovici, M.; Shabat, D., Self-immolative dendrimers: A distinctive approach to molecular amplification. *Soft Matter* **2010,** *6* (6), 1073-1080.

Azagarsamy, M. A.; Krishnamoorthy, K.; Sivanandan, K.; Thayumanavan, S., Site-Specific Installation and Study of Electroactive Units in Every Layer of Dendrons. *J. Org. Chem.* **2009,** *74* (24), 9475-9485.

Azagarsamy, M. A.; Sokkalingam, P.; Thayumanavan, S., Enzyme-triggered disassembly of dendrimer-based amphiphilic nanocontainers. *J. Am. Chem. Soc.* **2009,** *131* (40), 14184-14185.

Azagarsamy, M. A.; Yesilyurt, V.; Thayumanavan, S., Disassembly of dendritic micellar containers due to protein binding. *J. Am. Chem. Soc.* **2010,** *132* (13), 4550-4551.

Babin, J.; Pelletier, M.; Lepage, M.; Allard, J. F.; Morris, D.; Zhao, Y., A New Two-Photon-Sensitive Block Copolymer Nanocarrier. *Angew. Chem. Int. Ed.* **2009,** *48* (18), 3329-3332.

Bachelder, E. M.; Beaudette, T. T.; Broaders, K. E.; Dashe, J.; Frechet, J. M. J., Acetal-derivatized dextran: An acid-responsive biodegradable material for therapeutic applications. *J. Am. Chem. Soc.* **2008,** *130* (32), 10494-10495.

Bae, Y.; Fukushima, S.; Harada, A.; Kataoka, K., Design of environment-sensitive supramolecular assemblies for intracellular drug delivery: Polymeric micelles that are responsive to intracellular pH change. *Angew. Chem. Int. Ed.* **2003,** *42* (38), 4640-4643.

Bae, Y.; Kataoka, K., Intelligent polymeric micelles from functional poly(ethylene glycol)-poly(amino acid) block copolymers. *Adv. Drug Delivery Rev.* **2009,** *61* (10), 768-784.

Balzani, V.; Credi, A.; Raymo, F. M.; Stoddart, J. F., Artificial Molecular Machines. *Angew. Chem. Int. Ed.* **2000,** *39* (19), 3348-3391.

Banerjee, I.; Pangule, R. C.; Kane, R. S., Antifouling Coatings: Recent Developments in the Design of Surfaces That Prevent Fouling by Proteins, Bacteria, and Marine Organisms. *Adv. Mater.* **2011,** *23* (6), 690-718.

Battah, S. H.; Chee, C.-E.; Nakanishi, H.; Gerscher, S.; MacRobert, A. J.; Edwards, C., Synthesis and Biological Studies of 5-Aminolevulinic Acid-Containing Dendrimers for Photodynamic Therapy. *Bioconjugate Chem.* **2001,** *12* (6), 980-988.

Becer, C. R.; Hahn, S.; Fijten, M. W. M.; Thijs, H. M. L.; Hoogenboom, R.; Schubert, U. S., Libraries of Methacrylic Acid and Oligo(ethylene glycol) Methacrylate Copolymers with LCST Behavior. *J. Polym. Sci., Part A: Polym. Chem.* **2008,** *46* (21), 7138-7147.

Beer, P. D.; Gale, P. A., Anion recognition and sensing: The state of the art and future perspectives. *Angew. Chem. Int. Ed.* **2001,** *40* (3), 486-516.

Bensel, N.; Reymond, M. T.; Reymond, J. L., Pivalase catalytic antibodies: Towards abzymatic activation of prodrugs. *Chem. Eur. J.* **2001,** *7* (21), 4604-4612.

Benvin, A. L.; Creeger, Y.; Fisher, G. W.; Ballou, B.; Waggoner, A. S.; Armitage, B. A., Fluorescent DNA Nanotags: Supramolecular Fluorescent Labels Based on Intercalating Dye Arrays Assembled on Nanostructured DNA Templates. *J. Am. Chem. Soc.* **2007,** *129* (7), 2025-2034.

Bergbreiter, D. E.; Caraway, J. W., Thermoresponsive Polymer-Bound Substrates. *J. Am. Chem. Soc.* **1996,** *118* (25), 6092-6093.

Bergbreiter, D. E.; Case, B. L.; Liu, Y.-S.; Caraway, J. W., Poly(N-isopropylacrylamide) Soluble Polymer Supports in Catalysis and Synthesis. *Macromolecules* **1998,** *31* (18), 6053-6062.

Bharathi, P.; Zhao, H. D.; Thayumanavan, S., Toward globular macromolecules with functionalized interiors: Design and synthesis of dendrons with an interesting twist. *Org. Lett.* **2001,** *3* (12), 1961-1964.

Blum, A. P.; Kammeyer, J. K.; Rush, A. M.; Callmann, C. E.; Hahn, M. E.; Gianneschi, N. C., Stimuli-Responsive Nanomaterials for Biomedical Applications. *J. Am. Chem. Soc.* **2015,** *137* (6), 2140-2154.

Bosma, A. Y.; Ulijn, R. V.; McConnell, G.; Girkin, J.; Halling, P. J.; Flitsch, S. L., Using two photon microscopy to quantify enzymatic reaction rates on polymer beads. *Chem Commun.* **2003,** (22), 2790-2791.

Boutris, C.; Chatzi, E. G.; Kiparissides, C., Characterization of the LCST behaviour of aqueous poly(N-isopropylacrylamide) solutions by thermal and cloud point techniques. *Polymer* **1997,** *38* (10), 2567-2570.

Buller, J.; Laschewsky, A.; Lutz, J.-F.; Wischerhoff, E., Tuning the lower critical solution temperature of thermoresponsive polymers by biospecific recognition. *Polymer Chemistry* **2011,** *2* (7), 1486-1489.

Cabral, H.; Nishiyama, N.; Kataoka, K., Supramolecular nanodevices: From design validation to theranostic nanomedicine. *Accounts Chem. Res.* **2011,** *44* (10), 999-1008.

Carlmark, A.; Hawker, C. J.; Hult, A.; Malkoch, M., New methodologies in the construction of dendritic materials. *Chem. Soc. Rev.* **2009,** *38* (2), 352-362.

Chen, H.; Yuan, L.; Song, W.; Wu, Z. K.; Li, D., Biocompatible polymer materials: Role of protein-surface interactions. *Prog. Polym. Sci.* **2008,** *33* (11), 1059-1087.

Chen, W.; Meng, F. H.; Li, F.; Ji, S. J.; Zhong, Z. Y., pH-Responsive Biodegradable Micelles Based on Acid-Labile Polycarbonate Hydrophobe: Synthesis and Triggered Drug Release. *Biomacromolecules* **2009,** *10* (7), 1727-1735.

Chen, Y.; Chen, K. H., Synthesis and reversible photocleavage of novel polyurethanes containing coumarin dimer components. *J. Polym. Sci., Part A: Polym. Chem* **1997,** *35* (4), 613-624.

Chen, Y.; Chou, C. F., Reversible photodimerization of coumarin derivatives disersed in poly (vinyl acetate). *J. Polym. Sci., Part A: Polym. Chem* **1995,** *33* (16), 2705-2714.

Chilkoti, A.; Dreher, M. R.; Meyer, D. E.; Raucher, D., Targeted drug delivery by thermally responsive polymers. *Adv. Drug Delivery Rev.* **2002,** *54* (5), 613-630.

Choi, S. H.; Lodge, T. P.; Bates, F. S., Mechanism of Molecular Exchange in Diblock Copolymer Micelles: Hypersensitivity to Core Chain Length. *Phys. Rev. Lett.* **2010,** *104* (4).

Chujo, Y.; Sada, K.; Saegusa, T., A novel nonionic hydrogel from 2-methyl-2-oxazoline, 3 polyoxazoline having a coumarin as a pendant group - synthesis and photogelation. *Macromolecules* **1990,** *23* (10), 2693-2697.

Chung, J. E.; Yokoyama, M.; Yamato, M.; Aoyagi, T.; Sakurai, Y.; Okano, T., Thermo-responsive drug delivery from polymeric micelles constructed using block copolymers of poly(N-isopropylacrylamide) and poly(butylmethacrylate). *J. Controlled Release* **1999,** *62* (1–2), 115-127.

Corti, M.; Minero, C.; Degiorgio, V., Cloud point transition in nonionic micellar solutions. *J. Phys. Chem.* **1984,** *88* (2), 309-317.

de Groot, F. M. H.; Albrecht, C.; Koekkoek, R.; Beusker, P. H.; Scheeren, H. W., "Cascade-release dendrimers" liberate all end groups upon a single triggering event in the dendritic core. *Angew. Chem. Int. Ed.* **2003,** *42* (37), 4490-4494.

Dewhirst, M. W.; Viglianti, B. L.; Lora-Michiels, M.; Hanson, M.; Hoopes, P. J., Basic principles of thermal dosimetry and thermal thresholds for tissue damage from hyperthermia. *Int. J. Hyperthermia.* **2003,** *19* (3), 267-294.

Dixon, D. A.; Dobbs, K. D.; Valentini, J. J., Amide-Water and Amide-Amide Hydrogen Bond Strengths. *J. Phys. Chem.* **1994,** *98* (51), 13435-13439.

Doig, A. J.; Williams, D. H., Binding energy of an amide-amide hydrogen bond in aqueous and nonpolar solvents. *J. Am. Chem. Soc.* **1992,** *114* (1), 338-343.

Donald A. Tomalia, J. B. C., Ulrik Boas, *Dendrimers, Dendrons, and Dendritic Polymers: Discovery, Applications, and the Future*. 1 ed.; Cambridge University Press: New York, United States of America, 2012; p 420.

Eberhardt, E. S.; Raines, R. T., Amide-Amide and Amide-Water Hydrogen Bonds: Implications for Protein Folding and Stability. *J. Am. Chem. Soc.* **1994,** *116* (5), 2149-2150.

Evans, D. F.; Ninham, B. W., Molecular forces in the self-organization of amphiphiles. *J. Phys. Chem.* **1986,** *90* (2), 226-234.

Farokhzad, O. C.; Langer, R., Impact of Nanotechnology on Drug Delivery. *ACS Nano* **2009,** *3* (1), 16-20.

Fischer, M.; Vögtle, F., Dendrimers: From design to application—A progress report. *Angew. Chem. Int. Ed.* **1999,** *38* (7), 884-905.

Fleischer, G., Micellization in Aqueous-Solution of a Poly(Ethylene Oxide) Poly(Propylene Oxide) Poly(Ethylene Oxide) Triblock Copolymer Investigated with Pulsed Field Gradient Nmr. *J. Phys. Chem.* **1993,** *97* (2), 517-521.

Frechet, J. T., Donald, *Dendrimers and Other Dendritic Polymers*. John Wiley & Sons Ltd: Hoboken, N. J., 2001; p 688.

Fujishige, S.; Kubota, K.; Ando, I., Phase transition of aqueous solutions of poly(N-isopropylacrylamide) and poly(N-isopropylmethacrylamide). *J. Phys. Chem.* **1989,** *93* (8), 3311-3313.

Fuller, J. M.; Raghupathi, K. R.; Ramireddy, R. R.; Subrahmanyam, A. V.; Yesilyurt, V.; Thayumanavan, S., Temperature-sensitive transitions below LCST in amphiphilic dendritic assemblies: host-guest implications. *J. Am. Chem. Soc.* **2013,** *135* (24), 8947-8954.

Ganta, S.; Devalapally, H.; Shahiwala, A.; Amiji, M., A review of stimuli-responsive nanocarriers for drug and gene delivery. *J. Controlled Release* **2008,** *126* (3), 187-204.

Gellman, S. H.; Dado, G. P.; Liang, G. B.; Adams, B. R., Conformation-directing effects of a single intramolecular amide-amide hydrogen bond: variable-temperature NMR and IR studies on a homologous diamide series. *J. Am. Chem. Soc.* **1991,** *113* (4), 1164-1173.

George R. Newkome, C. N. M., Fritz Vögtle., *Dendrimers and Dendrons: Concepts, Syntheses, Applications.* Wiley-VCH: 2001; p 635.

Ghosh, S.; Yesilyurt, V.; Savariar, E. N.; Irvin, K.; Thayumanavan, S., Redox, Ionic Strength, and pH Sensitive Supramolecular Polymer Assemblies. *J. Polym. Sci., Part A: Polym. Chem* **2009,** *47* (4), 1052-1060.

Gillies, E. R.; Frechet, J. M. J., pH-responsive copolymer assemblies for controlled release of doxorubicin. *Bioconjugate Chem.* **2005,** *16* (2), 361-368.

Gillies, E. R.; Jonsson, T. B.; Fréchet, J. M. J., Stimuli-responsive supramolecular assemblies of linear-dendritic copolymers. *J. Am. Chem. Soc.* **2004,** *126* (38), 11936-11943.

Gnanaguru, K.; Ramasubbu, N.; Venkatesan, K.; Ramamurthy, V., A Study on the Photochemical Dimerization of Coumarins in the Solid-State. *J. Org. Chem.* **1985,** *50* (13), 2337-2346.

Gohy, J. F.; Hofmeier, H.; Alexeev, A.; Schubert, U. S., Aqueous micelles from supramolecular graft copolymers. *Macromol. Chem. Phys.* **2003,** *204* (12), 1524-1530.

Gomez-Escudero, A.; Azagarsamy, M. A.; Theddu, N.; Vachet, R. W.; Thayumanavan, S., Selective peptide binding using facially amphiphilic dendrimers. *J. Am. Chem. Soc.* **2008,** *130* (33), 11156-11163.

González, D. C.; Savariar, E. N.; Thayumanavan, S., Fluorescence Patterns from Supramolecular Polymer Assembly and Disassembly for Sensing Metallo- and Nonmetalloproteins. *J. Am. Chem. Soc.* **2009,** *131* (22), 7708-7716.

Goodwin, A. P.; Mynar, J. L.; Ma, Y. Z.; Fleming, G. R.; Frechet, J. M. J., Synthetic micelle sensitive to IR light via a two-photon process. *J. Am. Chem. Soc.* **2005,** *127* (28), 9952-9953.

Grayson, S. M.; Frechet, J. M. J., Convergent dendrons and dendrimers: from synthesis to applications. *Chem. Rev.* **2001,** *101* (12), 3819-3867.

Hammouda, B.; Ho, D.; Kline, S., SANS from Poly(ethylene oxide)/Water Systems. *Macromolecules* **2002,** *35* (22), 8578-8585.

Hawker, C. J.; Wooley, K. L.; Frechet, J. M. J., Unimolecular Micelles and Globular Amphiphiles - Dendritic Macromolecules as Novel Recyclable Solubilization Agents. *J. Chem. Soc., Perkin Trans. 1* **1993,** (12), 1287-1297.

He, J.; Tong, X.; Zhao, Y., Photoresponsive Nanogels Based on Photocontrollable Cross-Links. *Macromolecules* **2009,** *42* (13), 4845-4852.

Hecht, S.; Frechet, J. M. J., Dendritic encapsulation of function: Applying nature's site isolation principle from biomimetics to materials science. *Angew. Chem. Int. Ed.* **2001,** *40* (1), 74-91.

Helms, B.; Mynar, J. L.; Hawker, C. J.; Frechet, J. M. J., Dendronized linear polymers via "click chemistry". *J. Am. Chem. Soc.* **2004,** *126* (46), 15020-15021.

Heskins, M.; Guillet, J. E., Solution Properties of Poly(N-isopropylacrylamide). *Journal of Macromolecular Science: Part A - Chemistry* **1968,** *2* (8), 1441-1455.

Hey, M. J.; Ilett, S. M., Poly(ethylene oxide) hydration studied by differential scanning calorimetry. *J. Chem. Soc., Faraday Trans.* **1991,** *87* (22), 3671-3675.

Hocine, S.; Li, M.-H., Thermoresponsive self-assembled polymer colloids in water. *Soft Matter* **2013,** *9* (25), 5839-5861.

Hoffman, A. S., Applications of thermally reversible polymers and hydrogels in therapeutics and diagnostics. *Journal of Controlled Release* **1987,** *6* (1), 297-305.

Hvidt, S.; Joergensen, E. B.; Brown, W.; Schillen, K., Micellization and Gelation of Aqueous Solutions of a Triblock Copolymer Studied by Rheological Techniques and Scanning Calorimetry. *J. Phys. Chem.* **1994,** *98* (47), 12320-12328.

Inoue, T.; Matsuda, M.; Nibu, Y.; Misono, Y.; Suzuki, M., Phase Behavior of Heptaethylene Glycol Dodecyl Ether and Its Aqueous Mixture Revealed by DSC and FT-IR Spectroscopy. *Langmuir* **2001,** *17* (6), 1833-1840.

Israelachvili, J. N.; Mitchell, D. J.; Ninham, B. W., Theory of self-assembly of hydrocarbon amphiphiles into micelles and bilayers. *J. Chem. Soc. Faraday Trans II.* **1976,** *72*, 1525-1568.

Jackson, A. W.; Fulton, D. A., Making polymeric nanoparticles stimuli-responsive with dynamic covalent bonds. *Polym. Chem.* **2013,** *4* (1), 31-45.

Jeong, B.; Bae, Y. H.; Lee, D. S.; Kim, S. W., Biodegradable block copolymers as injectable drug-delivery systems. *Nature* **1997,** *388* (6645), 860-862.

Jeong, Y.; Joo, M. K.; Bahk, K. H.; Choi, Y. Y.; Kim, H. T.; Kim, W. K.; Lee, H. J.; Sohn, Y. S.; Jeong, B., Enzymatically degradable temperature-sensitive polypeptide as a new in-situ gelling biomaterial. *J. Controlled Release.* **2009,** *137* (1), 25-30.

Jiang, J. Q.; Tong, X.; Zhao, Y., A new design for light-breakable polymer micelles. *J. Am. Chem. Soc.* **2005,** *127* (23), 8290-8291.

Jiwpanich, S.; Ryu, J.-H.; Bickerton, S.; Thayumanavan, S., Noncovalent Encapsulation Stabilities in Supramolecular Nanoassemblies. *J. Am. Chem. Soc.* **2010,** *132* (31), 10683-10685.

Johansson, A.; Kollman, P.; Rothenberg, S.; McKelvey, J., Hydrogen bonding ability of the amide group. *J. Am. Chem. Soc.* **1974,** *96* (12), 3794-3800.

Jones, M.-C.; Leroux, J.-C., Polymeric micelles – a new generation of colloidal drug carriers. *Eur. J. Pharm. Biopharm.* **1999,** *48* (2), 101-111.

Kabanov, A. V.; Nazarova, I. R.; Astafieva, I. V.; Batrakova, E. V.; Alakhov, V. Y.; Yaroslavov, A. A.; Kabanov, V. A., Micelle Formation and Solubilization of Fluorescent-Probes in Poly(Oxyethylene-B-Oxypropylene-B-Oxyethylene) Solutions. *Macromolecules* **1995,** *28* (7), 2303-2314.

Kataoka, K.; Kwon, G. S.; Yokoyama, M.; Okano, T.; Sakurai, Y., Block-Copolymer Micelles as Vehicles for Drug Delivery. *J. Controlled Release.* **1993,** *24* (1-3), 119-132.

Kataoka, K.; Miyazaki, H.; Okano, T.; Sakurai, Y., Sensitive glucose-induced change of the lower critical solution temperature of poly[N,N-(dimethylacrylamide)-co-3-(acrylamido)-phenylboronic acid] in physiological saline. *Macromolecules* **1994,** *27* (4), 1061-1062.

Kennedy, J. E., High-intensity focused ultrasound in the treatment of solid tumours. *Nat Rev Cancer* **2005,** *5* (4), 321-327.

Kim, E.; Kim, D.; Jung, H.; Lee, J.; Paul, S.; Selvapalam, N.; Yang, Y.; Lim, N.; Park, C. G.; Kim, K., Facile, Template-Free Synthesis of Stimuli-Responsive Polymer Nanocapsules for Targeted Drug Delivery. *Angew. Chem. Int. Ed.* **2010,** *49* (26), 4405-4408.

Kimura, M.; Kato, M.; Muto, T.; Hanabusa, K.; Shirai, H., Temperature-Sensitive Dendritic Hosts: Synthesis, Characterization, and Control of Catalytic Activity. *Macromolecules* **2000,** *33* (4), 1117-1119.

Klaikherd, A.; Nagamani, C.; Thayumanavan, S., Multi-Stimuli Sensitive Amphiphilic Block Copolymer Assemblies. *J. Am. Chem. Soc.* **2009,** *131* (13), 4830-4838.

Klein, H. L., The consequences of Rad51 overexpression for normal and tumor cells. *DNA Repair* **2008,** *7* (5), 686-693.

Knop, K.; Hoogenboom, R.; Fischer, D.; Schubert, U. S., Poly(ethylene glycol) in Drug Delivery: Pros and Cons as Well as Potential Alternatives. *Angew. Chem. Int. Ed.* **2010,** *49* (36), 6288-6308.

Koopmans, C.; Ritter, H., Color Change of N-Isopropylacrylamide Copolymer Bearing Reichardts Dye as Optical Sensor for Lower Critical Solution Temperature and for Host−Guest Interaction with β-Cyclodextrin. *J. Am. Chem. Soc.* **2007,** *129* (12), 3502-3503.

Liu, F.; Urban, M. W., Recent advances and challenges in designing stimuli-responsive polymers. *Prog. Polym. Sci.* **2010,** *35* (1–2), 3-23.

Liu, M. J.; Kono, K.; Frechet, J. M. J., Water-soluble dendritic unimolecular micelles: Their potential as drug delivery agents. *J. Controlled Release.* **2000,** *65* (1-2), 121-131.

Liu, T.; Liu, S., Responsive Polymers-Based Dual Fluorescent Chemosensors for Zn2+ Ions and Temperatures Working in Purely Aqueous Media. *Anal. Chem.* **2011,** *83* (7), 2775-2785.

Liu, Y. C.; Le Ny, A. L. M.; Schmidt, J.; Talmon, Y.; Chmelka, B. F.; Lee, C. T., Photo-Assisted Gene Delivery Using Light-Responsive Catanionic Vesicles. *Langmuir* **2009,** *25* (10), 5713-5724.

Lu, J.; Choi, E.; Tamanoi, F.; Zink, J. I., Light-activated nanoimpeller-controlled drug release in cancer cells. *Small* **2008,** *4* (4), 421-426.

Lüsse, S.; Arnold, K., The Interaction of Poly(ethylene glycol) with Water Studied by 1H and 2H NMR Relaxation Time Measurements. *Macromolecules* **1996,** *29* (12), 4251-4257.

Lutz, J. F., Polymerization of oligo(ethylene glycol) (meth)acrylates: Toward new generations of smart biocompatible materials. *J. Polym. Sci., Part A: Polym. Chem.* **2008,** *46* (11), 3459-3470.

Lutz, J.-F., Thermo-Switchable Materials Prepared Using the OEGMA-Platform. *Adv. Mater.* **2011,** *23* (19), 2237-2243.

Lutz, J.-F.; Akdemir, O.; Hoth, A., Point by point comparison of two thermosensitive polymers exhibiting a similar LCST: Is the age of poly(NIPAM) over ? *J. Am. Chem. Soc.* **2006,** *128* (40), 13046-13047.

Maeda, H.; Bharate, G. Y.; Daruwalla, J., Polymeric drugs for efficient tumor-targeted drug delivery based on EPR-effect. *European Journal of Pharmaceutics and Biopharmaceutics* **2009,** *71* (3), 409-419.

Maeda, H.; Wu, J.; Sawa, T.; Matsumura, Y.; Hori, K., Tumor vascular permeability and the EPR effect in macromolecular therapeutics: a review. *J. Controlled Release.* **2000,** *65* (1-2), 271-284.

Medina, S. H.; El-Sayed, M. E. H., Dendrimers as Carriers for Delivery of Chemotherapeutic Agents. *Chemical Reviews* **2009,** *109* (7), 3141-3157.

Mitchell, D. J.; Ninham, B. W., Micelles, vesicles and microemulsions. *J. Chem. Soc., Faraday Transactions 2.* **1981,** *77* (4), 601-629.

Mitchell, D. J.; Tiddy, G. J. T.; Waring, L.; Bostock, T.; McDonald, M. P., Phase behaviour of polyoxyethylene surfactants with water. Mesophase structures and partial miscibility (cloud points). *J. Chem. Soc., Faraday Trans. 1 F.* **1983,** *79* (4), 975-1000.

Moseley, P. L., Heat shock proteins and heat adaptation of the whole organism. *J. Appl. Physiol.* **1997,** *83* (5), 1413-1417.

Muthuramu, K.; Ramamurthy, V., Photo-Dimerization of Coumarin in Aqueous and Micellar Media. *J. Org. Chem.* **1982,** *47* (20), 3976-3979.

Muthuramu, K.; Ramamurthy, V., Selectivity in Chemical-Reactions in Micellar Media - Photodimerization of Substituted Coumarins in Micelles. *Indian J. Chem., Sect B* **1984,** *23* (6), 502-508.

Newkome, G. R.; Moorefield, C. N.; Baker, G. R.; Johnson, A. L.; Behera, R. K., Chemistry of Micelles .11. Alkane Cascade Polymers Possessing Micellar Topology - Micellanoic Acid-Derivatives. *Angew. Chem. Int. Ed.* **1991,** *30* (9), 1176-1178.

Niederhafner, P.; Sebestik, J.; Jezek, J., Glycopeptide dendrimers. Part II. *J. Pept. Sci.* **2008,** *14* (1), 44-65.

Nir, E.; Michalet, X.; Hamadani, K. M.; Laurence, T. A.; Neuhauser, D.; Kovchegov, Y.; Weiss, S., Shot-noise limited single-molecule FRET histograms: Comparison between theory and experiments. *J. Phys. Chem. B* **2006,** *110* (44), 22103-22124.

Nishiyama, N.; Morimoto, Y.; Jang, W.-D.; Kataoka, K., Design and development of dendrimer photosensitizer-incorporated polymeric micelles for enhanced photodynamic therapy. *Adv. Drug Delivery Rev.* **2009,** *61* (4), 327-338.

Nystrom, A. M.; Wooley, K. L., The importance of Chemistry in Creating Well-Defined Nanoscopic Embedded Therapeutics: Devices Capable of the Dual Functions of Imaging and Therapy. *Accounts Chem. Res.* **2011,** *44* (10), 969-978.

Oh, K. T.; Bronich, T. K.; Kabanov, A. V., Micellar formulations for drug delivery based on mixtures of hydrophobic and hydrophilic Pluronic((R)) block copolymers. *J. Controlled Release.* **2004,** *94* (2-3), 411-422.

Otsuka, H.; Nagasaki, Y.; Kataoka, K., PEGylated nanoparticles for biological and pharmaceutical applications. *Adv. Drug Delivery Rev.* **2003,** *55* (3), 403-419.

Pace, C. N.; Shirley, B. A.; McNutt, M.; Gajiwala, K., Forces contributing to the conformational stability of proteins. *Faseb J.* **1996,** *10* (1), 75-83.

Park, C.; Lim, J.; Yun, M.; Kim, C., Photoinduced Release of Guest Molecules by Supramolecular Transformation of Self-Assembled Aggregates Derived from Dendrons. *Angew. Chem. Int. Ed.* **2008,** *47* (16), 2959-2963.

Peer, D.; Karp, J. M.; Hong, S.; FaroKhzad, O. C.; Margalit, R.; Langer, R., Nanocarriers as an emerging platform for cancer therapy. *Nat. Nanotechnol.* **2007,** *2* (12), 751-760.

Qin, S.; Geng, Y.; Discher, D. E.; Yang, S., Temperature-controlled assembly and release from polymer vesicles of poly(ethylene oxide)-block-poly(N-isopropylacrylamide). *Adv. Mater.* **2006,** *18* (21), 2905-2909.

R. Ramireddy, R.; Raghupathi, K. R.; Torres, D. A.; Thayumanavan, S., Stimuli sensitive amphiphilic dendrimers. *New J. Chem.* **2012,** *36* (2), 340-349.

Rackaitis, M.; Strawhecker, K.; Manias, E., Water-soluble polymers with tunable temperature sensitivity: Solution behavior. *J. Polym. Sci., Part B: Polym. Phys.* **2002,** *40* (19), 2339-2342.

Raghupathi, K. R.; Azagarsamy, M. A.; Thayumanavan, S., Guest release control in enzyme-sensitive amphiphilic dendrimer-based nanoparticles through photochemical crosslinking. *Chem. Eur. J.* **2011,** *17* (42), 11752-11760.

Raghupathi, K. R.; Sridhar, U.; Byrne, K.; Raghupathi, K.; Thayumanavan, S., Influence of backbone conformational rigidity in temperature-sensitive amphiphilic supramolecular assemblies. *J. Am. Chem. Soc.* **2015,** *137* (16), 5308-5311.

Rijcken, C. J. F.; Soga, O.; Hennink, W. E.; Nostrum, C. F. v., Triggered destabilisation of polymeric micelles and vesicles by changing polymers polarity: An attractive tool for drug delivery. *J. Controlled Release* **2007,** *120* (3), 131-148.

Ruel-Gariépy, E.; Leroux, J.-C., In situ-forming hydrogels—review of temperature-sensitive systems. *Eur. J. Pharm. Biopharm.* **2004,** *58* (2), 409-426.

Saavedra, J. E.; Shami, P. J.; Wang, L. Y.; Davies, K. M.; Booth, M. N.; Citro, M. L.; Keefer, L. K., Esterase-sensitive nitric oxide donors of the diazeniumdiolate family: In vitro antileukemic activity. *J. Med. Chem.* **2000,** *43* (2), 261-269.

Samantaray, S.; Sharma, R.; Chattopadhyaya, T. K.; Gupta, S. D.; Ralhan, R., Increased expression of MMP-2 and MMP-9 in esophageal squamous cell carcinoma. *J. Cancer. Res. Clin.* **2004,** *130* (1), 37-44.

Sasaki, K.; Medan, M. S.; Azuma, T.; Kawabata, K.-i.; Shimoda, M.; Umemura, S.-i., Effect of Echo-Guided High-Intensity Focused Ultrasound Ablation on Localized Experimental Tumors. *J Vet Med Sci.* **2006,** *68* (10), 1069-1074.

Savariar, E. N.; Aathimanikandan, S. V.; Thayumanavan, S., Supramolecular assemblies from amphiphilic homopolymers: Testing the scope. *J. Am. Chem. Soc.* **2006,** *128* (50), 16224-16230.

Schmaljohann, D., Thermo- and pH-responsive polymers in drug delivery. *Adv. Drug Delivery Rev.* **2006,** *58* (15), 1655-1670.

Schott, H., Hydrophilic-lipophilic balance, solubility parameter, and oil-water partition coefficient as universal parameters of nonionic surfactants. *J. Pharm. Sci.* **1995,** *84* (10), 1215-1222.

Song, J.; Cheng, Q.; Zhu, S. M.; Stevens, R. C., "Smart" materials for biosensing devices: Cell-mimicking supramolecular assemblies and colorimetric detection of pathogenic agents. *Biomed. Microdevices* **2002,** *4* (3), 213-221.

Special issue on stimuli responsive materials. *Special issue on stimuli responsive materials, Chem. Soc. Rev.* **2013,** (17), 7045-7486.

Stuart, M. A. C.; Huck, W. T. S.; Genzer, J.; Muller, M.; Ober, C.; Stamm, M.; Sukhorukov, G. B.; Szleifer, I.; Tsukruk, V. V.; Urban, M.; Winnik, F.; Zauscher, S.; Luzinov, I.; Minko, S., Emerging applications of stimuli-responsive polymer materials. *Nat Mater* **2010,** *9* (2), 101-113.

Tanford, C., Theory of micelle formation in aqueous solutions. *J. Phys. Chem.* **1974,** *78* (24), 2469-2479.

Thayumanavan, S.; Bharathi, P.; Sivanandan, K.; Vutukuri, D. R., Towards dendrimers as biomimetic macromolecules. *CompteC. R. Chimie.* **2003,** *6* (8-10), 767-778.

Thornton, P. D.; McConnell, G.; Ulijn, R. V., Enzyme responsive polymer hydrogel beads. *Chem Commun.* **2005,** (47), 5913-5915.

Torchilin, V. P., Structure and design of polymeric surfactant-based drug delivery systems. *Journal of Controlled Release* **2001,** *73* (2-3), 137-172.

Trenor, S. R.; Shultz, A. R.; Love, B. J.; Long, T. E., Coumarins in polymers: From light harvesting to photo-cross-linkable tissue scaffolds. *Chem. Rev.* **2004,** *104* (6), 3059-3077.

Ulijn, R. V., Enzyme-responsive materials: a new class of smart biomaterials. *J. Mater. Chem.* **2006,** *16* (23), 2217-2225.

Uttamapinant, C.; White, K. A.; Baruah, H.; Thompson, S.; Fernandez-Suarez, M.; Puthenveetil, S.; Ting, A. Y., A fluorophore ligase for site-specific protein labeling inside living cells. *PNAS* **2010,** *107* (24), 10914-10919.

Vancoillie, G.; Frank, D.; Hoogenboom, R., Thermoresponsive poly(oligo ethylene glycol acrylates). *Progress in Polymer Science* **2014,** *39* (6), 1074-1095.

Vutukuri, D. R.; Basu, S.; Thayumanavan, S., Dendrimers with Both Polar and Apolar Nanocontainer Characteristics. *J. Am. Chem. Soc.* **2004,** *126* (48), 15636-15637.

Wang, L. P.; Yang, X. F.; Zhao, M. L., A 4-Methylumbelliferone-based Fluorescent Probe for the Sensitive Detection of Captopril. *J. Fluoresc.* **2009,** *19* (4), 593-599.

Wang, Q.; Chittaboina, S.; Barnhill, H. N., Advances in 1,3-dipolar cycloaddition reaction of azides and alkynes - A prototype of "click" chemistry. *Lett. Org. Chem.* **2005,** *2* (4), 293-301.

Waton, G.; Michels, B.; Zana, R., Dynamics of Micelles of Polyethyleneoxide-Polypropyleneoxide-Polyethyleneoxide Block Copolymers in Aqueous Solutions. *J. Colloid Interface Sci.* **1999,** *212* (2), 593-596.

Wei, P.; Cook, T. R.; Yan, X.; Huang, F.; Stang, P. J., A Discrete Amphiphilic Organoplatinum(II) Metallacycle with Tunable Lower Critical Solution Temperature Behavior. *Journal of the American Chemical Society* **2014,** *136* (44), 15497-15500.

Wilson, K. E.; Langdon, S. P.; Lessells, A. M.; Miller, W. R., Expression of the extracellular matrix protein tenascin in malignant and benign ovarian tumours. *Br. J. Cancer.* **1996,** *74* (7), 999-1004.

Yamaguchi, S.; Matsumoto, S.; Ishizuka, K.; Iko, Y.; Tabata, K. V.; Arata, H. F.; Fujita, H.; Noji, H.; Hamachi, I., Thermally responsive supramolecular nanomeshes for on/off switching of the rotary motion of F-1-ATPase at the single-molecule level. *Chem. Eur. J.* **2008,** *14* (6), 1891-1896.

Yang, X. F.; Wang, L. P.; Zhao, M. L.; Qi, H. P.; Wu, Y., A 4-Methylumbelliferone-based Fluorescent Probe for Sodium New Houttuyfonate. *Chin. J. Chem.* **2010,** *28* (8), 1469-1474.

Yebra, D. M.; Kiil, S.; Dam-Johansen, K., Antifouling technology - past, present and future steps towards efficient and environmentally friendly antifouling coatings. *Prog. Org. Coat.* **2004,** *50* (2), 75-104.

Yesilyurt, V.; Ramireddy, R.; Thayumanavan, S., Photoregulated Release of Noncovalent Guests from Dendritic Amphiphilic Nanocontainers. *Angew. Chem.-Int. Edit.* **2011,** *50* (13), 3038-3042.

You, J.; Shao, R. P.; Wei, X.; Gupta, S.; Li, C., Near-Infrared Light Triggers Release of Paclitaxel from Biodegradable Microspheres: Photothermal Effect and Enhanced Antitumor Activity. *Small* **2010,** *6* (9), 1022-1031.

Yu, X.; Yang, X.; Horte, S.; Kizhakkedathu, J. N.; Brooks, D. E., A pH and thermosensitive choline phosphate-based delivery platform targeted to the acidic tumor microenvironment. *Biomaterials* **2014,** *35* (1), 278-286.

Yuan, Q.; Zhang, Y. F.; Chen, T.; Lu, D. Q.; Zhao, Z. L.; Zhang, X. B.; Li, Z. X.; Yan, C. H.; Tan, W. H., Photon-Manipulated Drug Release from a Mesoporous Nanocontainer Controlled by Azobenzene-Modified Nucleic Acid. *Acs Nano* **2012,** *6* (7), 6337-6344.

Zhang, S., Fabrication of novel biomaterials through molecular self-assembly. *Nat Biotech* **2003,** *21* (10), 1171-1178.

Zhong, S.; Cui, H. G.; Chen, Z. Y.; Wooley, K. L.; Pochan, D. J., Helix self-assembly through the coiling of cylindrical micelles. *Soft Matter* **2008,** *4* (1), 90-93.